Multi-omic analysis of the aging mouse brain

Dissertation

For the award of the degree

“Doctor rerum naturalium”

of the Georg-August-Universität Göttingen

within the doctoral program

Cellular and Molecular Physiology of the Brain

of the Georg-August University School of Science (GAUSS)

submitted by

Verena Klüver

from Augsburg, Germany

Göttingen 2021

Members of the Thesis Advisory Committee

Prof. Dr. Silvio Rizzoli
Department of Neuro- and Sensory Physiology, University Medical Center Göttingen

Prof. Dr. Klaus-Armin Nave
Neurogenetics, Max Planck Institute for Experimental Medicine

Prof. Dr. Ralf Heinrich
Cellular Neurobiology, University of Göttingen

Members of the Examination Board

Referee: Dr. Eugenio F. Fornasiero
Department of Neuro- and Sensory Physiology, University Medical Center Göttingen

2nd Referee: Prof. Dr. Thomas Dresbach
Department of Anatomy and Embryology, University Medical Center Göttingen

Prof. Dr. Silvio Rizzoli
Department of Neuro- and Sensory Physiology, University Medical Center Göttingen

Further members of the Examination Board

Prof. Dr. Ralf Heinrich
Cellular Neurobiology, University of Göttingen

Prof. Dr. Klaus-Armin Nave
Neurogenetics, Max Planck Institute for Experimental Medicine

Prof. Dr. Dörthe Katschinski
Department of Cardiovascular Physiology, University Medical Center Göttingen

Date of oral examination: 16.12.2021

Contents

1 | Summary 7
2 | Introduction 8
2.1 | Genetic and epigenetic instability 10
2.2 | Mitochondrial dysfunction 12
2.3 | Signaling and energy metabolism 13
2.4 | Inflammation and immune activation 15
2.5 | Protein homeostasis 15
2.6 | Challenges in understanding brain aging and aims of this work 18
3 | Materials and Methods 20
4 | Results 25
4.1 | Transcriptomics 27
4.2 | Proteomic description of physiological aging in the mouse brain 35
4.2.1 | Total fraction 36
4.2.2 | Correlations between RNA and protein levels are minimal 46
4.2.3 | Insoluble fraction 48
4.3 | Proteomic description of brain aging in mouse models 51
4.3.1 | SAMP8 52
4.3.2 | Zfand2b: KO of proteostasis factor AIRAPL 53
4.3.3 | Line 61: overexpression of human α-synuclein 55
4.3.4 | HM2: overexpression of human α-synuclein mutants A30P and A53T 56
4.3.5 | APPPS1: human transgene expression of mutated APP and PSEN1 57
4.3.6 | m*Cat*-mice: overexpressing human catalase in mitochondria 59
4.3.7 | AntiOx-mice: antioxidant diet 60
4.3.8 | Ucp2-mice: KO of uncoupling protein 2 61
4.3.9 | LAKI: homozygous knock-in of mutated Lmna to model HGPS 64
4.3.10 | Zmpste24: KO of the lamin A processing protease 66
4.3.11 | Environmental enrichment 67
4.3.12 | Male and female WT mice 67
4.4 | Combined analysis 69
4.4.1 | Core protein changes 69
4.4.2 | Changes in functional groups of proteins 70
5 | Discussion 74
5.1 | Gene expression changes are pronounced in early aging 74
5.2 | Nuclear transcription implicates specific rearrangements in synaptic, mitochondrial, and ribosomal processes 75

5.3 | Physiological aging shows modest, but relevant protein abundance changes 75
5.3.1 | Evidence for altered protein homeostasis in brain aging 76
5.3.2 | Strong alterations in cytoskeleton and -associated proteins 77
5.3.3 | Neuron growth and network homeostasis 78
5.3.4 | Altered energy metabolism and declining detoxification systems 78
5.4 | Aging-specific enrichment of insoluble proteins 79
5.4.1 | Aggregation of specific ribosomal proteins with age 80
5.4.2 | Underlying mechanisms for age-related protein aggregation are diverse 80
5.4.3 | Altered aggregation status influences energy homeostasis across cellular networks, affecting neuronal activity 81
5.5 | Aging signatures vary between different models of aging 82
5.5.1 | Core and accessory pathways of aging in mouse models 82
5.5.2 | Composite modeling of physiological brain aging using mouse models 85
5.6 | Conclusion and outlook 86
6 | References 90
7 | List of abbreviations 113
8 | Acknowledgements ..... **Error! Bookmark not defined.**
9 | Curiculum Vitae ..... **Error! Bookmark not defined.**

1 | Summary

Brain function is highly dependent on a well-regulated, harmonic interaction of a multitude of cellular and molecular pathways. During aging, many of these pathways undergo progressive changes, leading to gradual deterioration of brain health and ultimately cognitive abilities. While neurodegenerative events likely occur throughout one's lifetime, detrimental effects often only become apparent with high age, when homeostatic mechanisms finally fail to uphold full functionality. Aging is therefore the highest risk factor to develop dementia and neurodegenerative diseases, such as Alzheimer's or Parkinson's. With the increasing lifespan of humans, such defects become prominent, and dementia is predicted to affect 152 million people worldwide by 2050, almost tripling current numbers.

Several hallmarks of aging in general have been suggested. These include 1) alterations at the level of the genome, with DNA instability, chromatin modifications and nuclear architecture dysfunction. 2) Declining mitochondrial function and increasing levels of cellular oxidative stress. 3) Impaired intercellular signaling and shifting energy metabolism. 4) Widespread inflammation and activation of immune responses. And lastly, 5) dysregulation of protein homeostasis (proteostasis), with declining protein degradation capacity, stoichiometric imbalance of protein complexes, and protein aggregation. To what extent these alterations affect the brain and neuronal function is mainly studied in animal models, as human studies are limited to imaging and other non-invasive techniques or postmortem tissue analysis. Small rodents, especially mice, offer a high similarity in genetics, as well as in nervous system anatomy and function, combined with easy handling and relatively short lifespan. The genetic tools to manipulate single genes or pathways are becoming increasingly sophisticated, as are large-scale analysis methods to describe changes in transcriptomics, proteomics and other -omics levels. Nevertheless, the differentiation of organismal aging versus brain aging and the difficulty of defining core versus accessory alterations still hinders a detailed understanding of aging processes in the brain.

In this work, I provide a systematic investigation of aging in the mouse brain. I use RNA sequencing and liquid chromatography-mass spectrometry to study several subcellular fractions of the brain. Physiologically aged wildtype mice, 6, 12, and 24 months of age, are thoroughly described regarding total and nuclear transcript abundance, as well as total, soluble and insoluble protein content. Qualitative and quantitative measurements of more than 20,000 genes and 8700 protein groups implicate the expected mitochondrial function decline, neurodegeneration, protein aggregation and immune activation, but also ribosomal and intermediate filament-based reorganizations in the aging process. Further, 12 mouse models of aging, neurodegenerative disease, dietary supplementation, or environmental enrichment are analyzed in parallel to gain insight into their proteomic landscape and aging signatures, specific to the brain. An overall comparison between physiological aging and aging modeled in a range of different mice reveals overlapping, but also separate pathways being the main drivers of (phenotypical) aging. The collection of data presented here sheds light on some previously undiscovered or underappreciated concepts and serves as valuable database for the scientific community. Together with additional experiments and considerations prompted by this study, we will ultimately achieve a better definition of brain aging and perspectives for medically postponing or preventing cognitive decline.

2 | Introduction

Aging, the gradual, time-dependent decline of physiological functions and deterioration of bodily performance is a basic feature of life. While we intuitively comprehend its concept, it is composed of several complex physiological changes that remain poorly understood. Impairments of hearing, vision, cardiovascular and motor capabilities, immune competency, or cognitive acuity are common challenges posed by time and age. Naturally, aging thus has major socio-economic consequences and shapes human societies (Chiao et al., 2014). Numerous interventions have been developed to counteract or ameliorate age-related impairments, extending human lifespan progressively. With this increasing lifespan, defects of the brain, which often become symptomatic only at high age, became more and more apparent and acute. Aging is the greatest risk factor for neuropathology, with neurodegenerative diseases (NDDs) like Alzheimer's disease (AD) or Parkinson's disease (PD), manifesting in the elderly with rising proportion. The prevalence of dementia increases exponentially after 60 years of age (Niccoli and Partridge, 2012), with more than one third of people age 85 or older having Alzheimer's dementia (numbers from the US population; Alzheimer's Association, 2020). With an increasingly aged population, the number of people suffering from dementia and requiring constant care will double to triple by 2050 (Alzheimer's Association, 2020; Prince et al., 2016). A detailed understanding of the molecular process of brain aging is however still missing to date and our ability to prevent the deterioration of brain function is superficial and incomplete.

Brain aging is associated with deteriorating attention, impaired memory formation, and diminished motor functions, which can be assessed with non-invasive techniques like magnetic resonance imaging or with cognitive and behavioral tests (Kondo et al., 2015; Salthouse, 2010). The severity of symptoms is however often difficult to evaluate objectively and uniformly. For obvious practical and ethical reasons, tissue-based cellular and molecular data cannot be obtained from humans during the course of brain aging. Comparatively few molecular studies of human brain aging are thus available, and the large majority are based on postmortem tissues. Not only is the proper preservation of postmortem samples a major challenge, but it also means that early stages of cognitive decline and neuropathology likely get overlooked. It is however especially in these early, asymptomatic stages of cognitive decline that it might be crucial to understand the pathological transformations and intervene pharmacologically or non-pharmacologically, to keep the effects of brain aging at guard (Sperling et al., 2014).

What do we know about brain aging? The early belief that a general loss of neurons and other brain cells with age is responsible for cognitive decline has recently been corrected and replaced by the knowledge that morphological alterations and more subtle cellular rearrangements (Yankner et al., 2008) are relevant for functional deterioration (**Figure 1**). They include the loss of dendritic spines and dendritic tree complexity, altered spine density, axonal swellings and dystrophic neuronal morphology, and the appearance of intracellular granules, fibrils or lipofuscin deposits (Pannese, 2011; Uylings and Brabander, 2002). These morphological changes are highly region-specific, though (Burke and Barnes, 2006) and often controversial. Hippocampal dendritic branching for example has been described as both increased (Buell and Coleman, 1979) and decreased (Ypsilanti et al., 2008) in aged humans, while neocortical dendritic trees are more likely to indeed undergo reduction (Brabander et al., 1998). Cerebellar Purkinje cell number does decline with age (Andersen et al., 2003; Woodruff-Pak et al., 2010; Woodruff-Pak, 2006), in this case likely linking cell number reduction and impaired motor functions in the elderly (Glisky, 2007). Neuronal networks are also influenced by an altered

excitatory-inhibitory balance (Rozycka and Liguz-Lecznar, 2017), gene expression that affects neurogenesis and synaptic function (Loerch et al., 2008), membrane cholesterol and sphingolipids that change synaptic activity by rigidifying membranes (Shinitzky, 1987) and a general glucose hypometabolism with decreased expression of glycolysis enzymes and glucose transporters (Camandola and Mattson, 2017). Neural stem cells, located in the dentate gyrus of the hippocampus and the subventricular zone of the lateral ventricles, proliferate and differentiate throughout life, but with declining capacity and decreasing number (Encinas et al., 2011; Lupo et al., 2019; Molofsky et al., 2006; Zhang et al., 2017b). Other brain cell types are also affected by age. Altered oligodendrocyte morphology, gene expression, precursor recruitment and differentiation are correlated with a gradual demyelination and loss of myelin remodeling with age (Hill et al., 2018; Sim et al., 2002; Soreq et al., 2017). Such decompaction or loss of myelin disturbs neuronal communication and synchrony, thus limiting cognitive functions (Peters, 2002; Zatorre et al., 2012). Lastly, gliosis and a low-grade chronic pro-inflammatory state are typical hallmarks of human brain aging (Santoro et al., 2018; Sierra et al., 2007). Astrocytes often show hypertrophic morphology, increased expression of synapse elimination genes, and altered glutamate homeostasis (Boisvert et al., 2018; Bronson et al., 1993; Santos et al., 2018). Microglia are increasingly reactive, with altered inflammation and migration phenotype (Harry, 2013; Schuitemaker et al., 2012). Innate immune gene expression is upregulated with age (Cribbs et al., 2012) and senescent cells exhibit a pro-inflammatory secretion profile (Santoro et al., 2018), changing the cellular environment and eliciting inflammatory responses in return.

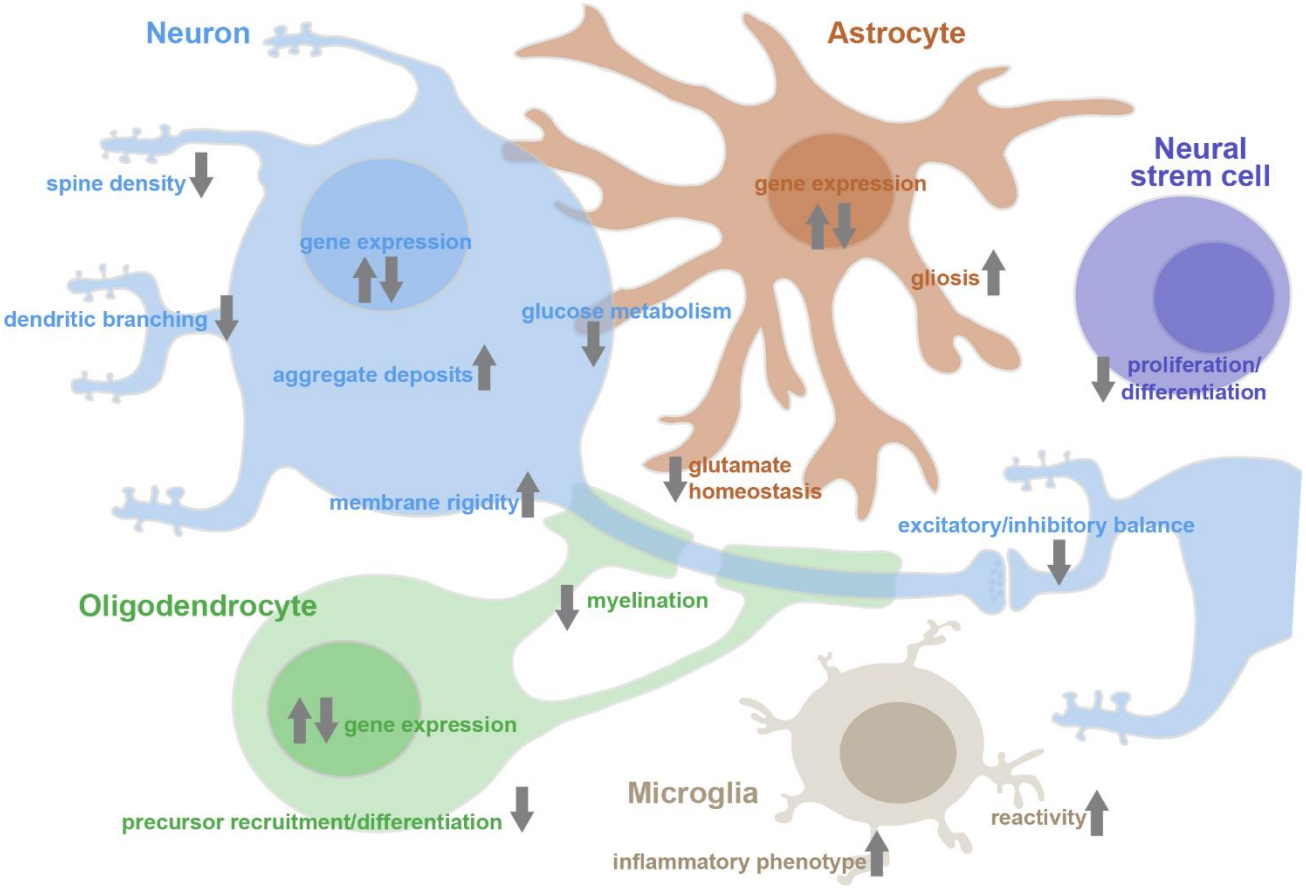

Figure 1 Age-related cellular and molecular changes in the brain. Schematic representation of neurons, oligodendrocytes, astrocytes, microglia, and neural stem cells with their respective alterations observed in aged brains. Arrows indicate direction of change, which is however highly region specific and, in the case of gene expression, multilayered.

With the brain being such a complex organ, showing multi-layered and interdependent cellular and molecular changes with age, the study of relatively simple model organisms is indispensable. Aging in general has been and still is extensively modeled in yeast, worms and fruit flies to identify pathway interactions and single gene or protein impact (Kenyon, 2010; Kenyon et al., 1993). Due to obvious anatomical differences however, the relevance of these models for the study of brain aging is limited. Small rodents, especially mice, combine a high level of similarity to the human brain with high fertility, easy breeding, small size, and short lifespan. Mice also allow a tight control of genetic and environmental variables, which is essential for the reproducibility of results. A vast availability of inbred and outbred strains, as well as numerous tools for genetic manipulation, available mutant mouse lines and the animal's ability to learn simple behavioral tasks has made the mouse the favorite small mammal to study brain aging, with ~90% of the available scientific literature on this subject consisting of mouse data (Kluever and Fornasiero, 2021).

A direct translation of results and insights gained from animal models to humans is always difficult and warrants caution. Especially in the aging field, it is often tricky to discern aging phenotypes from disease phenotypes, meaning signs of sickness are easily interpreted as signs of aging. In the case of genetic manipulations, the impact of that manipulation on general health needs to be considered as well. Further, the timing and strength of knock out (KO), knock in (KI) or transgene expression (tg) are crucial. Developmental defects need to be well separated from age-related defects when the manipulation takes effect already at or even before birth. Defining a hierarchy of events is the major challenge and most likely not well simulated by an abrupt modification of a single gene. However, by modifying specific genes, groups of interconnected pathways can be described, commonalities can be found, and essential mechanisms of aging can be identified. These lines of evidence can be further supported by studying not only genetic mouse models, but physiological, wildtype (WT) aging in parallel. For the brain specifically, the added difficulty is to discern the consequences of whole organism aging and aspects that pertain to brain function. Phenotypic signs of aging, like hair graying or skin lesions and even regenerative tissue aging (cardiovascular decline, renal dysfunction, etc.), are often disconnected from cognitive decline and any major signs of brain aging. Among the many mouse models used to study aging (Ackert-Bicknell et al., 2015; Flurkey et al., 2007; Folgueras et al., 2018; Kõks et al., 2016), the minority have been developed to investigate the brain specifically (Bilkei-Gorzo, 2014; Heng et al., 2017; Kluever and Fornasiero, 2021).

Several 'core aging pathways' have emerged by combining animal studies with human large-scale population studies and genome-wide association studies. These pathways, acting in parallel, often overlapping and intersecting, can be summarized in five categories (Kluever and Fornasiero, 2021) and will be described in the following sections. They are: 1) genetic and epigenetic instability; 2) mitochondrial dysfunction; 3) altered intercellular signaling, including hormonal stimuli and energy consumption regulation; 4) inflammation and immune activation; and 5) protein homeostasis (proteostasis) defects. See also **Figure 2** for a schematic summary.

2.1 | Genetic and epigenetic instability

The basic building plan for each cell is stored in its DNA and extended information is provided by the epigenetic code. Reliable preservation and transmission of this fundamental information is therefore vital. Aging however affects DNA integrity and changes the landscape of epigenetic markers. Exposure to ultraviolet light or reactive

molecular species from within the cell can damage DNA bases, inducing double strand breaks, base dimerizations, crosslinking or single base exchanges (Hoeijmakers, 2009). Prolonged exposure to exo- or endogenous stressors, as naturally occurring with age, thus lead to errors accumulating while the cell's mechanisms try to repair the damages (Vermeij et al., 2016). Also in human neuronal cells, such a correlation between somatic mutations and age could be confirmed (Lodato et al., 2018). Several mouse models with impaired DNA-repair mechanisms further strengthen the connection of lacking genomic repair and typical brain aging signs, such as motor neuron loss, increased inflammation, mislocalization of synaptic proteins and abnormal mitochondrial function (Graaf et al., 2013; Sepe et al., 2016; Waard et al., 2010). Genomic structure is additionally preserved by telomeres, the protective, repetitive DNA structures at the ends of chromosomes. Telomere shortening, occurring with cell division, is also observed in neurons and glia, leading to a senescent-like phenotype (Ain et al., 2018; Jurk et al., 2012). Telomerase-deficient mouse models with reduced telomere length develop increased DNA damage, decreased neurogenesis and defects in brain-function related behavioral tasks (Whittemore et al., 2019; Zhou et al., 2017).

DNA is kept stable and accessible for transcription by wrapping and packaging around histones, octameric protein complexes that can be modulated to allow or restrict transcription of specific DNA stretches. Modifications of histone residues and direct DNA modifications thus serve as epigenetic regulation layer, defining when and where DNA can be transcribed (Lardenoije et al., 2015). The landscape of epigenetic modifications changes in aged tissues and histone deacetylases might provide a window of possible aging-intervention, as targeted inhibition or KO of these histone remodeling proteins has been shown to enhance neuroprotection and cognitive function in models of neurodegeneration (Benito et al., 2015), as well as in physiological aging (Guan et al., 2009).

Lastly, genomic integrity is preserved by the nuclear architecture itself. In the human Hutchinson-Gilford-Progeria Syndrome (HGPS), a defect of the nuclear lamina leads to aberrant nuclei structure with growth retardation after birth, muscular dystrophy, cardiomyopathy, and drastically shortened lifespan (Dechat et al., 2008; Hennekam, 2006). Mouse models have been developed to mimic the defect in the nuclear envelope. One of them, referred to as LAKI in this work, is a KI of the point mutation in the prelamin-A/C (*LMNA*) gene identified in human HGPS patients, which prevents the correct processing of this protein (Osorio et al., 2011). Another model is the KO of the processing enzyme, zinc metalloproteinase ZMPSTE24 (Varela et al., 2005). While both of these models mimic the human syndrome very reliably, it is unclear, whether and to what extent the brain is affected and suffering from this lamin defect as little to no functional defects have been observed (Baek et al., 2015; Jung et al., 2012; Yang et al., 2015).

The nuclear envelope is further responsible for correct segregation of cellular compartments and transport of RNA and other macromolecules through nuclear pores. Pore complex proteins are amongst the longest-lived proteins (Fornasiero et al., 2018; Savas et al., 2012) and thus prone to damage accumulation, structural deterioration, and leaky permeability (D'Angelo et al., 2009). Nuclear transport receptors and pore proteins show age-related decline in numbers or density and complex assembly is heavily dependent on correct stoichiometry of its components (Ding and Sepehrimanesh, 2021). If brought out of balance by posttranscriptional modifications or damage accumulation, nuclear pore complexes not only can no longer perform their function of regulated transport, but orphan proteins themselves are aggregation prone and likely damaging other structures (Cho and Hetzer, 2020). Nucleocytoplasmic transport is further implicated in gene expression regulation and transcriptional buffer activity by retaining RNA transcripts (Bahar Halpern et al., 2015). Just like

pore proteins, RNA-binding proteins that transport transcripts from one compartment to the other, are likely age-dysregulated (Ding and Sepehrimanesh, 2021). Impaired nucleocytoplasmic transport has also been identified in several NDDs (Li and Lagier-Tourenne, 2018).

2.2 | Mitochondrial dysfunction

Erroneous nucleic acid or protein modifications and damage pose major threats to cellular and organismal homeostasis. One of the endogenous causes of such unwanted alterations are the already mentioned reactive molecular species, i.e., reactive oxygen or nitrogen species (ROS and RNS, respectively), which are produced as a byproduct of ATP production during cellular respiration in mitochondria (Schriner et al., 2005). Long-term increased presence of ROS oxidizes and damages DNA, proteins, and lipids (Houtkooper et al., 2011). In a vicious cycle, mitochondrial function itself becomes impaired which leads to inefficient respiration and even more ROS release into the cell (Cui et al., 2012). Mitochondrial DNA (mtDNA) is especially vulnerable, due to its close proximity to the origin of ROS, the lack of protective histones and less-efficient repair mechanisms, compared to nuclear DNA. mtDNA mutation load was thus suggested as hallmark and possible biomarker of aging. While mouse models of defective mtDNA maintenance (referred to as 'mtDNA mutator mice') indeed show high numbers of mtDNA mutations and several aging phenotypes (Sörensen et al., 2001; Trifunovic et al., 2004), a reduction of lifespan is only observed with very pronounced mutation load that is not found in normal human aging (Khrapko et al., 2006; Kujoth et al., 2005).

Nevertheless, mitochondrial respiration is clearly affected in aging. The respiratory complexes which contain mitochondrially encoded subunits (complex I and IV) are the first to suffer in mtDNA mutator mice (Sörensen et al., 2001; Trifunovic et al., 2004) and several electron transport genes are decreased in aged nematodes, fruit flies, mice and humans (Zahn et al., 2007). To rescue mitochondrial membrane potential deficits and reduce ROS production, cells can uncouple mitochondria to allow proton flow into the matrix without going through complex V first. This however decreases energy production and increases oxygen consumption (Andrews and Horvath, 2009). A mouse model that lacks this protective uncoupling protein (Ucp2) shows increased ROS production, inflammatory interleukin (IL)-1β upregulation, activated microglia and decreased lifespan (Arsenijevic et al., 2000; Hirose et al., 2016). Other oxidative stress response mechanisms are also often found to be increased with age, especially reactive species scavenging enzymes (Barth et al., 2019; Nowotny et al., 2014; Yankner et al., 2008). One such scavenging enzyme is catalase (Cat) and upon mitochondria-targeted overexpression of the human form in mice, it prolongs the lifespan of modified mice by inactivating hydrogen peroxide (H_2O_2) and protecting mitochondria from oxidative damage (Mao et al., 2012; Schriner et al., 2005). These mCat mice are however unique in their clear beneficial effects. Overexpression of a different antioxidant enzyme, copper zinc superoxide dismutase, or the overexpression of Cat in peroxisomes does not extend lifespan in mice (Huang et al., 2000; Pérez et al., 2009b). Similarly, the effect of antioxidant diets has been shown to be effective in some cases in mice (Liu et al., 2002; Park et al., 2009), but also non-effective in mice and humans (Bjelakovic et al., 2012; Flurkey et al., 2007). Lastly, many studies argue for a protective role of mild ROS exposure, as it could lead to long term shifts in mitochondrial efficiency and generally enhanced antioxidant defense mechanisms which could be especially beneficial in the brain (Bilkei-Gorzo, 2014; Ristow and Zarse, 2010; Schulz et al., 2007).

2.3 | Signaling and energy metabolism

The pathways of cellular energetic control are tightly connected to mitochondrial function and are interconnected to intercellular, often hormonal, signaling. This category of age-related changes is possibly one of the most complex, with well-studied signaling cascades, animal models and seemingly easy intervention through dietary regimes and available pharmacological modulators. It is however also a category, where effects often lack a clear molecular explanation and results can be contradictory.

Before genetic tools to manipulate animal models were established, aging studies were often conducted on mouse strains that showed spontaneous differences in lifespan or that were selectively bred to show accelerated or delayed aging. An overview of different lifespans of WT mice is provided by the Jackson Aging Center (Yuan et al., 2009). Extensive breeding efforts were undertaken by Takeda and colleagues to develop senescence-prone mouse lines (SAMP) and senescence-resistant lines (SAMR), each line showing their own signature of accelerated or delayed aging (Takeda et al., 1981). Among these lines, the SAMP10 and SAMP8 mice display brain aging phenotypes, manifesting in glial activation, reduced complexity of dendritic trees, spine and synapse number decline and pronounced learning and memory defects (Miyamoto, 1997; Shimada et al., 2003; Shimada and Hasegawa-Ishii, 2011; Takeda, 2009). Signs of NDDs were also found in SAMP8 mice, such as increased amyloid beta peptide levels, neurotoxic oligomers or hyperphosphorylated tau (Dobarro et al., 2013; Grinan-Ferre et al., 2018), although plaque, neurofibrillary tangle or inclusion body formation are absent in these mice (Akiguchi et al., 2017). The severity of learning defects in these mice was shown to correlate with impaired glucose metabolism and gradual decline of mitochondrial function after 2 months of age (Ohta et al., 1996). Glycolysis, tricarboxylic acid cycle (TCA) and other energy pathways were preferentially affected in aged SAMP8 mice in a later study of brain metabolites (Currais et al., 2019).

Beyond that, the so called ‘dwarf mice’ were probably one of the first models used to investigate aging in the context of body size, energy demands and hormonal regulation of growth. George Snell discovered mice with a spontaneous recessive autosomal mutation that drastically reduces body size (Snell, 1929); these mice are now known as ‘Snell dwarf’ mice. The loss-of-function mutation of homeobox transcription factor, pituitary factor 1 (Pit1), was later identified to be causative of the dwarf-phenotype. With the defective differentiation of pituitary cells, biosynthesis of growth hormone (GH), prolactin (PRL) and thyroid-stimulating hormone (TSH) is abrogated, and animals show heavily reduced levels of insulin-like growth factor 1 (IGF-1). Most importantly, the Snell dwarf mice show an extension of lifespan of up to 40-50% (Flurkey et al., 2002). Similarly, the small Laron mice and Ames dwarf mice have genetic alterations in GH-receptor (GH-R) and adenohypophyseal development, respectively, and show increased lifespan (Brown-Borg and Bartke, 2012).

A reduction of hypothalamic control or pituitary function affecting GH levels, which in turn stimulates IGF-1, thus influences organism development, growth, metabolism, and energy expenditure. Lifespan is also extended in a model of brain-specific KO of IGF-1-R (Kappeler et al., 2008), exemplifying that these hormonal modifications not only take effect in peripheral organs and tissues, but also in the brain. When a reduction of metabolic rate or growth via IGF-1(R) downregulation prolongs life, then its upregulation should have the opposite effect. This is the case in a mouse model where IGF-1-R levels are increased tenfold by having knocked out its translocation and degradation regulator arsenite-inducible RNA-associated protein-like (AIRAPL), encoded by the *Zfand2b* gene (Osorio et al., 2016).

Both IGF and insulin are produced locally in the brain (Bondy and Lee, 1993; Kuwabara et al., 2011) and both have specific neuronal functions. Insulin is believed to act as a neuroprotective factor and the loss of the hormone or insulin receptor (IR) might precede AD (Felice et al., 2014) and PD (Bassil et al., 2014). Declining levels of IR have been shown to occur during physiological aging (Zaia and Piantanelli, 2000). Further downstream of GH, IGF or IR are the key energy sensing regulators of the cell, adenosine monophosphate-activated protein kinase (AMPK) and mechanistic/mammalian target of rapamycin (mTOR). mTOR is mostly known as an autophagy inhibitor, favoring anabolic pathways, while AMPK favors catabolic mechanisms (Salminen and Kaarniranta, 2012). These central modulators are prominent targets for pharmacological intervention using small molecule agonists (e.g., metformin for AMPK) or antagonists (e.g. rapamycin for mTOR), which have been successfully applied to prolong the lifespan of mice (Harrison et al., 2009; Martin-Montalvo et al., 2013), although not universally in small rodents (Smith et al., 2010). In the above-mentioned senescence accelerated SAMP8 mice, metformin was shown to ameliorate endoplasmic reticulum (ER) stress and improve cognitive performance (Liu et al., 2020).

While these pharmacological interventions have a very specific target with far-reaching consequences, both dietary- and exercise-based paradigms affect a wide range of parameters which ultimately lead to the most significant and reproducible amelioration of age-related deterioration and lifespan extension (Fontana et al., 2010; Masoro, 2005; McCay et al., 1935; Most et al., 2017). Exercise has been shown to be beneficial for brain health and cognition in several species (Berchtold et al., 2010; Rhyu et al., 2010), including humans (Chirles et al., 2017), by stimulating, among others, brain-derived neurotrophic factor (BDNF; Adlard et al., 2004). Exercise thus decreases neuroinflammation, increases synaptic plasticity and neurogenesis and stimulates mitochondria biogenesis (Dallagnol et al., 2017; Speisman et al., 2013; Steiner et al., 2011; Stranahan et al., 2010), all beneficial also in NDD models (Choi et al., 2018; Lau et al., 2011), as well as in mtDNA mutator (Ross et al., 2019; Safdar et al., 2015) and SAMP8 mice (Dong et al., 2018). Many of the positive effects of exercise-regimes can also be found following environmental enrichment (EE) of mice. EE provides physical, social and cognitive stimuli, which elicit hypothalamic pituitary-adrenal axis adaptations. Increased BDNF circulation, expression of synaptic proteins, elevated neuronal extension branching, cell proliferation and promoted angiogenesis are just some of the described consequences (Nithianantharajah and Hannan, 2006).

Dietary restriction (DR), such as reducing calorie intake, intermittent fasting, or ketogenic diets, change the metabolic landscape of organisms. Subsequently reduced levels of insulin and insulin related signaling (Kenyon, 2010) or increased autophagy (Egan et al., 2011) link DR back to the molecular hubs surrounding AMPK. Transcriptional adaptations favor neuroprotective factors and chaperones, strengthening mitochondrial function and protein homeostasis (Amigo et al., 2017; Lee et al., 2000; Lee et al., 1999; Wood et al., 2015; Yu and Mattson, 1999). DR also shifts the main energy source from carbohydrates to fatty acids (Bruss et al., 2010; Roberts et al., 2017), where oxidation bypasses electron transfer of complex I, thus minimizing local ROS production (Guarente, 2008; Kushnareva et al., 2002). While this mechanism likely plays a bigger role in peripheral tissues due to neurons' limited use of fatty acid oxidation (Panov et al., 2014), the DR-upregulated peripheral and brain produced ketone bodies (Romano et al., 2017) contribute to the brain's energy supply, strengthen antioxidant glutathione peroxidase activity and synaptic function (Brandhorst et al., 2015; Cahill, JR, 2006; Ziegler et al., 2003). The effects of diet and exercise, while not always leading to a guaranteed lifespan extension per se (Liao et al., 2010), still clearly improve several aspects of physiological function, which otherwise would decline with age.

DR and exercise can also be seen as mild stressors, to which an organism responds by optimizing its metabolic processes and energy consumption. A very fine line then separates beneficial adaptations from detrimental ones and the effect becomes highly dependent on the extent and duration of stress. Excessive DR in humans leads to osteoporosis, infertility, or amenorrhea (Dirks and Leeuwenburgh, 2006) and physical activity in the elderly can be associated with mortality (Lee and Skerrett, 2001). Likewise, dwarf mice, while living longer, have delayed or absent sexual maturation (Bartke and Brown-Borg, 2004). In nematodes, it was even shown that DR improves stress resistance and survival of the first generation, but that their offspring has reduced fitness and increased mortality risk (Ivimey-Cook et al., 2021; Mautz et al., 2020). A thorough, transgenerational assessment of different metabolic paradigms, whether pharmacological, genetic, activity-related, or dietary, is therefore warranted.

2.4 | Inflammation and immune activation

A low level of chronic tissue inflammation is a common feature of aging, caused by constant creation of toxic and bio-reactive byproducts in biosynthetic pathways and subsequent gradual modification and damage of molecules (Barth et al., 2019; Cellerino and Ori, 2017; Green et al., 2011; Lee et al., 2000; Podtelezhnikov et al., 2011). In the brain, this 'inflammageing' phenotype (Franceschi and Campisi, 2014) becomes noticeable by dystrophic microglia cells, which become hyperreactive and unable to mount adequate immune responses with advancing age (Hart et al., 2012). Immune cell populations (dendritic cells and T-cells) become more abundant, as do circulating inflammatory cytokines (Hammond et al., 2019; Stichel and Luebbert, 2007). Senescent cells contribute to this increase of pro-inflammatory factors by acquiring senescence-associated secretory phenotypes (Chinta et al., 2015). The blood-brain-barrier, which guards the passage of peripheral molecules and signals into the brain, becomes increasingly leaky with age, which is correlated with cognitive decline (Erickson and Banks, 2019; Montagne et al., 2015). Immune activation and gliosis are often observed in the vicinity of damaged neurons or extracellular aggregates. While there is little doubt that immune reactions and inflammatory signals are generally upregulated in aged organisms, whether these are beneficial, detrimental, or both (in temporal sequence), is disputed (Garaschuk et al., 2018; Johnson et al., 2020; Santoro et al., 2018).

2.5 | Protein homeostasis

A common hallmark of several NDDs is the formation of protein deposits and aggregates. This encompasses amyloid beta peptides, hyperphosphorylated tau protein, α-synuclein, TAR DNA-binding protein 43 (TDP43) and huntingtin (Jucker and Walker, 2013). Notably, these aggregates are found before signs of neuropathology become apparent and increase from young to old age (Braak and Del Tredici, 2011; Elobeid et al., 2016). Similar to the previously described accumulation of DNA damages, proteins are likely to undergo a manifold of unwanted or unregulated modifications, some of which lead to protein misfolding and aggregation. And just like the involvement of immune reactions to the benefit or detriment of overall organism health with age is debated, so is the exact role of protein segregation, deposit formation and aggregation. On one hand, 'sequestering' and concentrated localization of reactive or non-functional proteins could protect the intracellular environment. On

the other hand, aggregates lead to stress responses, impaired transport and degradation pathways and might sequester still healthy proteins into inaccessible structures (Currais et al., 2017; Lindner and Demarez, 2009).

Irrespective of their precise role in aging and neuropathology, protein aggregates are considered a sign of aging and implicate protein homeostasis, or proteostasis, as aging mechanism. Protein synthesis, folding, trafficking and degradation need to be finely balanced, but can derail individually or collectively, as is the case in NDDs or prion protein diseases, as well as in physiological aging (Cuervo and Dice, 2000; Kaushik and Cuervo, 2015). A positive correlation of lifespan and translation fidelity (Ke et al., 2017) as well as of lifespan and efficient proteostasis (Pérez et al., 2009a; Treaster et al., 2014) has been described.

Protein synthesis has been described to undergo age-related decline, but most likely, this is not equally true for all tissues and organs (Finch and Morgan, 1990; Schimanski and Barnes, 2010; Ward, 2000). In the brain, ribosomal disorganization and altered stoichiometry has been implicated in the aging process (Kelmer Sacramento et al., 2020; Yu et al., 2020). During and after the process of protein synthesis at ribosomes, chaperones ensure proper protein folding. However, transcript and protein levels of chaperones decline with age, so does their enzymatic activity, which is often ATP dependent (Brehme et al., 2014; Naidoo et al., 2008; Nuss et al., 2008; Paz Gavilán et al., 2006). Hydroxylation, chlorination, oxidation, peroxidation, or the appearance of advanced glycation end products (AGEs) on proteins can further render these modified structures unrecognizable for chaperones (Kaushik and Cuervo, 2015; Munch et al., 2012; Xiao et al., 2020). Unguarded, these structurally and functionally altered species then lead to crosslinking, aggregation, and inflammation (Horie et al., 1997; Nowotny et al., 2014). The unfolded protein response (UPR) is elicited upon ER and general proteostasis stress and upregulates, among others, chaperone production (Hetz et al., 2020). Upon artificial downregulation of UPR function, cognitive and motor ability declined, while the opposite effect was observed upon upregulation in genetic mouse models (Cabral-Miranda et al., 2020).

For protein degradation, lysosomal and ubiquitin-proteasome pathways complement each other (Kaushik and Cuervo, 2015). Misfolded proteins or entire organelles (e.g., mitochondria) can be degraded by lysosomal autophagy and genetic KO of autophagic proteins leads to severe neuropathology and reduced lifespan in mice (Komatsu et al., 2006). Lysosomal failure in cells can be detected by the presence of auto-fluorescent lipofuscin deposits, which are hallmarks of aged neurons (Brunk and Ericsson, 1972; Terman and Brunk, 1998). Maintenance of a low luminal pH within lysosomes is essential for their function, yet ATPases and K^+-channels show diminished reliability in aging and NDD (Jinn et al., 2017; Sulzer et al., 2008). Levels of autophagy-regulating and -related transcripts, intersecting with cellular metabolic pathways and the AMPK-mTOR axis, tend to decrease with age (Lee et al., 2000) and their upregulation was shown to prolong the median survival of mice (Fernández et al., 2018). In the ubiquitin-proteasome system, ubiquitin can be covalently linked to proteins by E1, E2 and E3 enzymes, thus marking them for delivery to and degradation in the proteasome. Not only abundance, but also diminished enzymatic activity of degrading enzymes is implicated in the aging process. Proteasomal efficiency declines with age (Keller et al., 2000; Vilchez et al., 2012) and aberrant ubiquitin ligation mechanisms are linked to NDD (Lucking et al., 2000; Min et al., 2008; Shimura et al., 2001). Inclusions with ubiquitin conjugates are characteristic of aged neurons (Gray et al., 2003) and aggregated protein fractions from aged mice livers show a high degree of ubiquitianted proteins (Basisty et al., 2018).

Ubiquitin monomers can be linked in homo- or heterotypic polyubiquitin chains, depending on which of the seven lysine residues is used for linkage (French et al., 2021). Different poly-ubiquitination patterns, serve as

intracellular signals beyond degradation (Grillari et al., 2006). The ‘classical’ K48 linkage signals degradation, while the K63 ubiquitination acts mainly in other processes such as endocytosis, mitochondrial and ribosomal function or DNA repair. K6 linkage has even been described as negative proteasomal effector (Shang et al., 2005). Similarly, small ubiquitin like modifiers (SUMOs) are emerging as functional modifiers in aged organisms by influencing activity, localization and interaction of their targets. They have been described in the context of stress responses, including autophagy and cellular senescence, as well as in telomere regulation in NDD and physiological aging (Princz and Tavernarakis, 2017; Vijayakumaran and Pountney, 2018). Further, the activity of other signaling molecules, involved in a plethora of cellular functions including proteostasis, is often regulated through reversible phosphorylation. Calcium/calmodulin-dependent protein kinases for examples show different activity and phosphorylation states with age (Ori et al., 2015) and phospho-proteomic results implicate calcium signaling pathways in AD progression (Bai et al., 2020).

With protein aggregation being so closely linked to NDDs, many mouse models have been designed to study their origin, impact, and extent in more detail. For an overview see Kluever and Fornasiero, 2021 or http://www.alzforum.org. AD hallmarks include extracellular amyloid plaques and intracellular aggregates of hyperphosphorylated tau protein. Aggregation-prone amyloid beta (Aβ) peptides are produced by enzymatic cleavage of amyloid precursor protein (App). Genetic lines mimicking AD mostly harbor modifications affecting App itself or App processing enzymes presenilin 1 (Psen1) and beta-secretase 1 (Bace1). Intracellular tau protein can also be modified by targeting its gene, microtubule associated protein tau (Mapt). In order to create phenoptyes that resemble human pathology, combinations of multiple genetic mutations are often used. For example, the APPPS1 mouse carries a combination of *App* (KM670/671NL) and *Psen1* (L166P) mutations that are found in human AD patients (Radde et al., 2006). Expression of the human transgene *App* is increased three times compared to endogenous mouse expression. Amyloid plaques become apparent from six weeks of age onwards, but no fibrillar tau inclusion were found. Animals are cognitively impaired from 7 months.

For PD, characteristic diminished dopaminergic signaling and α-synuclein aggregation with Lewy body formation can be modeled by altering α-synuclein (Snca) expression levels. The mouse line called ‘Line 61’ overexpresses human α-synuclein under the Thy1 promoter (Rockenstein et al., 2002), reproducing altered dopamine release, Snca-pathology, motor impairments and inflammation. They do not show loss of dopaminergic neurons, though. The HM2 model harbors two mutations in *Snca*: A30P and A53T (Richfield et al., 2002). Loss of dopaminergic neurons in the substantia nigra, low dopamine levels and motor coordination defects are the consequence. Lewy body-like inclusions are not observed.

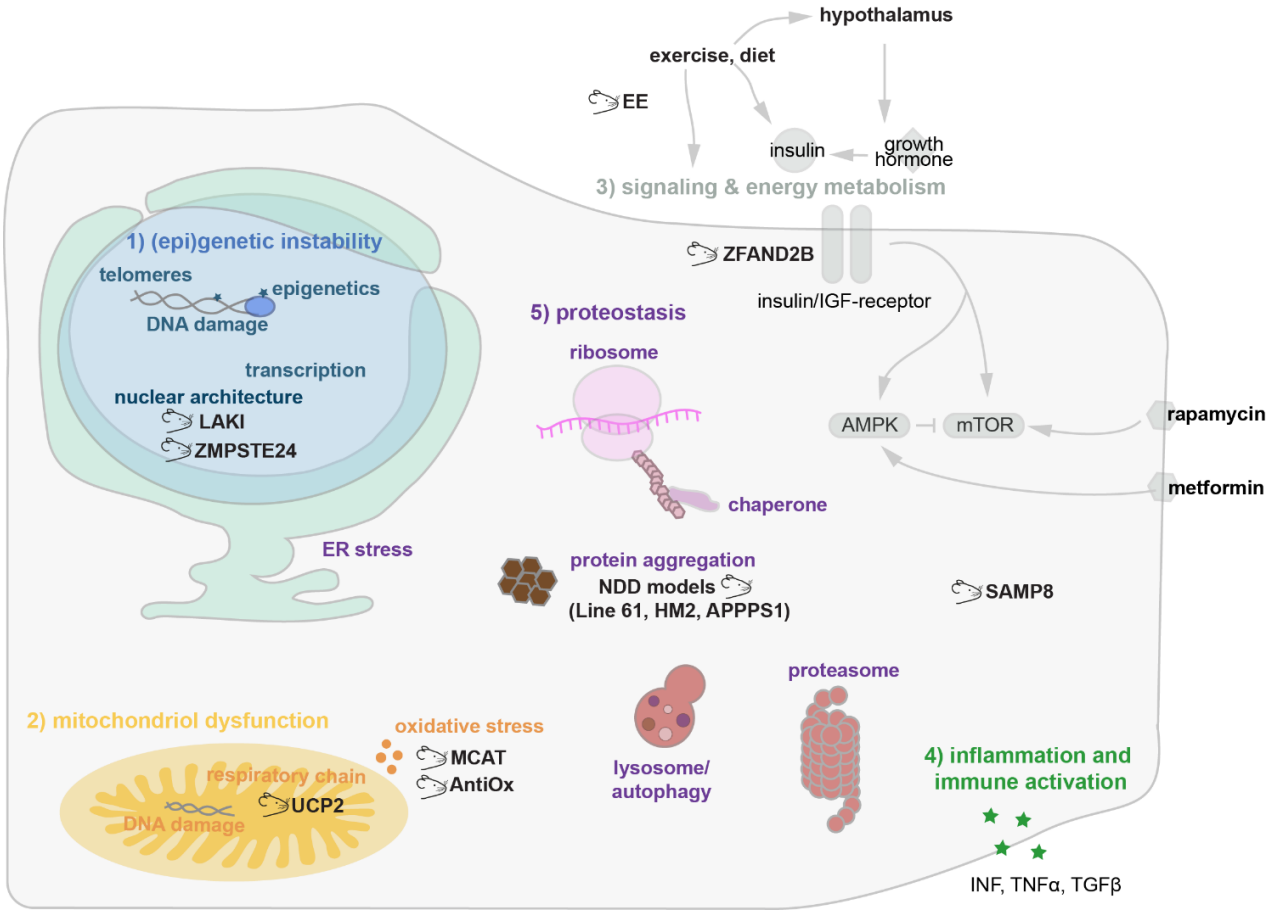

Figure 2 Overview of cellular aging pathways. The scheme shows some of the most important molecular pathways altered during brain aging and indicates the 11 mouse models used in this work (mouse symbol and name). See introduction for details. AntiOx: cohort of mice fed with an antioxidant-supplemented diet, AMPK: adenosine monophosphate-activated protein kinase, IGF: insulin-like growth factor, INF: interferon, mTOR: mechanistic/mammalian target of rapamycin, TGF: transforming growth factor, TNF: tumor necrosis factor.

2.6 | Challenges in understanding brain aging and aims of this work

Insights into the molecular processes of aging and brain aging have been facilitated by technical developments in the fields of genetic manipulation, high-throughput analyses of RNA and protein, including single-cell and modification investigations, and the increasing initiative to share large datasets online. Nevertheless, the study of physiological aging with large-scale measurements has shown that RNA expression changes are modest, as are protein abundance changes (Cellerino and Ori, 2017; Lee et al., 2000; Walther and Mann, 2011; Yu et al., 2020). One of the first proteomic studies of aged mouse brains using mass spectrometry (MS) found only 3% of all quantified proteins to change by more than one third (Walther and Mann, 2011). A more recent study even shows that statistically significant changes range around only 20% difference (Yu et al., 2020).

Sufficient sample number is indispensable when changes are subtle. Inter-individual differences further complicate a significant identification of age-affected transcripts or proteins (Cellerino and Ori, 2017). Gene expression heterogeneity in human brains has been described as greater in individuals age 45-71 years, in comparison to the group of <42 as well as the group >73 (Lu et al., 2004). Similarly, epigenetic signatures in brains of individuals >75 years are more homogeneous than those of younger groups (Oh et al., 2016). To my knowledge, no such human brain multi-age comparison has been performed on protein level, but in mice, protein abundances become more variable after 17 months of age (Mao et al., 2010). In animal models, it is therefore

essential to consider the specific age-windows that are under investigation. For example, comparing the gene expression of young adult 2 months old mice with aged 22 months old mice might capture differences that are due to ongoing development and brain-specific synaptic rearrangements rather than old age (Jiang et al., 2001). Preferably, at least three timepoints should be studied, capturing early, late and long continuing changes (Baker and Peleg, 2017; Kluever and Fornasiero, 2021; Oh et al., 2016).

Early observations of rodent lifespans were often divergent due to differences in housing conditions and general health of the animals. While regulations on these parameters have become stricter, the addition of simple behavioral or blood-based tests would benefit any major study of aging to exclude underlying and misleading conditions. Ideally, as many layers of homeostatic regulation would be measured in parallel. That could include transcript (including non-coding RNA) and protein levels as well as modifications, metabolic measurements, protein lifetimes and enzymatic activity assays. Translation from animal models to humans needs to be carefully evaluated, especially taking into account that singular genetic modifications likely are a poor representation of the many interconnected pathways that lead to aging under physiological conditions. The models of AD and PD mentioned in the previous paragraph are a good example of fragmented and limited modeling of human pathology and aging in mice and *vice versa*. Nevertheless, regulation across pathways, rather than by single proteins, has been shown to be relatively conserved between species (Zahn et al., 2007) and the hallmarks of aging described here so far exemplify how several lines and methods of studies contribute to pinpoint molecular changes occurring during aging more and more.

In this work, I set out to thoroughly describe physiological aging in wildtype C57BL/6 mice, one of the most common mouse strains used in science. I did this by preparing sub-cellular fractions ('total' and 'nuclear') and solubility-based fractions ('total', 'soluble' and 'insoluble') of the brain for mRNA sequencing and protein liquid chromatography–mass spectrometry (LC-MS), respectively, resulting in the quantification of more than 20,000 transcripts and 8700 proteins. This combination of two large-scale omics approaches enabled me to look at the complex processes underlying aging from at least two perspectives and to answer the following questions:

First, how does the transcriptomic landscape change with aging in the brain? And second, what is the influence of total and nuclear-localized RNA on this landscape? Third, what are the physiological proteomic rearrangements in the aging brain, meaning what constitutes as 'normal' brain aging? Fourth, are there groups of proteins that undergo an age-related redistribution between a soluble and an aggregated state?

Adding to this extensive set of fundamental data on physiological aging of the brain, in itself unique and a valuable asset for the scientific community, I studied the proteome of 12 other mouse models of aging, dietary supplementation or environmental enrichment. Consequently, fifth, which protein abundance and solubility changes are observed in the brains of mouse models of aging? While each cohort provides important information about several pathways previously implicated in aging, my goal was to examine these cohorts for common underlying mechanisms of brain aging, for proteins or groups of proteins that represent a set of core changes. So finally, sixth, which parameters of physiological aging are represented in the examined mouse models and what can we learn from different signatures of aging?

Overall, the results presented here constitute one of the largest collections of transcriptomic and proteomic brain data from physiological aging and different mouse models of aging that was acquired in parallel and that can be searched and built upon to gain a deeper and more meaningful understanding of brain aging. This will be invaluable to develop new strategies to study and possibly change the course of brain aging.

3 | Materials and Methods

Mouse cohorts

All locally performed animal experiments were approved by the local authority, the Lower Saxony State Office for Consumer Protection and Food Safety (Niedersächsisches Landesamt für Verbraucherschutz und Lebensmittelsicherheit). SAMP8 and SAMR1 mice were obtained from Coral Sanfeliu Pujol, Institute of Biomedical Research of Barcelona. NDD models Line 61 and HM2 were provided by Tiago Outeiro, University Medical Center Göttingen, APPPS1 mice by Andre Fischer, German Center for Neurodegenerative Diseases Göttingen. mCat and AntiOx mice were provided by Michael Müller, University Medical Center Göttingen. Ucp2 KO mice were obtained from Saleh Ibrahim, University of Luebeck. HGPS models LAKI and Zmpste24 KO were provided by Carlos López-Otín, Universidad de Oviedo. Environmentally enriched mice and aged female and male animals were provided by Hannelore Ehrenreich, Max-Planck-Institute of Experimental Medicine, Göttingen. All models were obtained with respective littermate controls.

Antioxidant diet for the cohort of AntiOx mice was composed following López-Erauskin et al., 2011. Briefly, regular mouse diet (V11124-0, SSNIFF) was supplemented with 250 mg/kg diet α-lipoic acid, 2.5 g/kg diet N-acetyl cysteine and 125 mg/kg diet vitamin E. Food was provided *ad libitum*.

Environmental enrichment was performed in the group of Hannelore Ehrenreich, Max-Planck-Institute of Experimental Medicine, Göttingen. Briefly, mice were put into enriched housing environment at the age of 19.5 months, remained there for 16 weeks and were placed back into normal housing for 6 weeks before sacrifice. Control animals remained in normal housing conditions throughout.

Mouse basic behavior and motor abilities assessment

Open field hole board and rotarod test were performed for the cohort of physiological aging mice. Briefly, motor coordination was assessed using a mouse RotaRod (Ugo Basile) on three consecutive days. The speed of the rotating drums (non-skid surface, 30 mm diameter) was increased from 5 to 50 rpm and the time until fall for each animal was recorded. To assess motor activity and exploration, mice were placed in the center of an open field (45 cm x 45 cm) with 16 holes (25 mm diameter) and their movements tracked for 5 min using a grid of 16 infrared beams and the ActiTrack 2.7.13 (Panlab, Harvard Apparatus) software.

Brain sample preparation

Brain samples in-house were collected by euthanizing mice by cervical dislocation, removing the brain on ice and snap-freezing in liquid nitrogen. Samples sent by collaborators were similarly obtained and shipped on dry ice. All samples were kept at -80° C until use. From the frozen brains, the olfactory bulbs were removed, and one hemisphere was taken for preparing the lysate. The fractionation protocol was optimized based on Bandopadhyay, 2016, and personal communication with collaborators. Hemispheres were washed in 320 mM sucrose buffer to remove blood and superficial vessels and then homogenized in 2 mL of 320 mM sucrose buffer containing protease inhibitors (cOmplete, Roche) and phosphatase inhibitors (PhosSTOP, Roche). Homogenization was performed using a Teflon pestle, ten strokes at 900rpm. 10X RIPA lysis and extraction buffer (ThermoFisher) was added to obtain a final concentration of 1X RIPA. After addition of Benzonase (Merck), samples were mixed on a rotation mixer for 30 min at RT. After this extraction and lysis, samples were centrifuged at 2000 g at 4° C to clear cell debris. The supernatant was collected in a fresh tube and 20% SDS

was added to obtain a final concentration of 5% SDS. Samples rotated again for 30 min at RT, 400µl were collected for the 'total' fraction, the rest was ultracentrifuged at 100,000 g for 30 min at RT. The supernatant was collected ('soluble' fraction), the pellet was resuspended in 5% SDS and put on a shaker for 30 min and 800 rpm, with rigorous pipet-mixing in between, to dissolve ('insoluble' fraction). BCA-assay protein estimation was performed for all samples.

Trypsin digestion and SP3 cleanup

Appropriate volumes were taken to obtain 50µg protein for SP3 cleanup of the sample (Hughes et al., 2019) and trypsin digestion. Samples were boiled at 95° C with RapiGest SF (Waters), reduced with DTT (Sigma-Aldrich) and alkylated with IAA (Sigma-Aldrich) while shaking at 600 rpm. RapiGest was diluted before addition of the magnetic carboxylate modified beads (Sera-Mag SpeedBeads; GE Healthcare). SP3 cleanup followed the protocol by Hughes et al., 2019, with slight adaptations. Briefly, 25 µg of beads were used for 50µg of protein, ethanol to 50% concentration was added to induce binding to the beads and 80% ethanol was used for subsequent washes using a magnetic rack. Remaining ethanol was removed and 200 µl of digestion solution was added (1 µg of trypsin in 100 mM ammonium bicarbonate buffer). Samples were sonicated briefly and incubated shaking at 37° C over night. The next day, samples were centrifuged, separated on a magnet and the supernatant was collected and dried in a SpeedVac vacuum concentrator (Eppendorf).

Peptide Library

To create a peptide library for spectral matching (Meier et al., 2018), digested peptides from the total, soluble and insoluble fraction from different animals and mouse models were mixed. To improve subsequent LC-MS analysis depth, these mixes were separated offline by high pH reverse phase chromatography and collected in 10 or 20 concatenated fractions using an Agilent 1100 HPLC system, a Waters XBridge BEH C18 column and an in-house built fraction collector rotating every minute. Flow rate was set to 60µl/min. Buffer A (hydrophilic; 10 mM ammonia in water) and buffer B (hydrophobic, 10mM ammonia in 80% ACN) were used to create a linear gradient up to 70% B. The collected fractions were again dried in a SpeedVac and later resuspended in loading buffer suitable for LC-MS/MS (0.05% TFA, 5% ACN in water).

LC-MS

For LC-MS, all samples were resuspended in loading buffer (0.05% TFA, 5% ACN in water), sonicated and roughly 1 µg of peptide was injected two times per sample (technical replicate) in an online UltiMate 3000 RSLCnano HPLC system coupled to a Q Exactive HF. Peptides were desalted on a reverse phase C18 pre-column and separated over 88 min in a 30 cm ReproSil-Pur C18 AQ 1.9 µm reversed phase resin analytical column. MS data was either acquired with a standard data-dependent method by scanning precursors from 350 to 1600 Da at 60,000 resolution at *m/z* 200 and automated gain control (AGC) to $3x10^6$. Top 30 precursor ions for MS2 were acquired at a resolution of 15,000 at m/z 200 with maximum IT of 50 ms and AGC of $1x10^6$; or with the BoxCar method using MaxQuant Live (Meier et al., 2018). Resolution for MS1 was set to 120,000 in m/z range 300 to 1650, maximum IT at 250 and AGC target to $3x10^6$. MS2 was collected at 15,000 resolution, maximum IT of 28 and $1x10^6$ AGC target. Preset BoxCar settings were applied with 3 Scans, 12 BoxCar Boxes and 1 Thomson overlap. All mass spectrometry measurements were acquired in collaboration with the Bioanalytical Mass Spectrometry group at the Max Planck Institute for Biophysical Chemistry, Göttingen, led by Henning Urlaub.

Raw MS-data analysis

Mass spectra were searched in MaxQuant 1.6.17.0 using BoxCar as search mode and using the high pH reverse phase fractionated sample data as peptide library. Label free quantification (LFQ) was performed. The mouse reference proteome was downloaded from Uniprot in August 2020. Search parameters are as follows and were chosen in reference to Meier et al., 2018. The option 'match between runs' was enabled (with 0.5 min window after retention time alignment) and 'LFQ min ratio' set to 1. MS-MS was not required for LFQ. False-discovery rate (FDR) on peptide and protein level match was set to 0.01. Methionine oxidation and N-terminal acetylation were set as variable modifications, carbamidomethylation as fixed. First search tolerance was 20 ppm, main search tolerance 4.5 ppm. Seven amino acids were set as minimum peptide length and 4600 Da as maximum peptide mass.

Filtering

Technical replicates, that had an inter-replicate correlation $r \leq 0.79$ and were outliers in hierarchical clustering (based on Pearson's *r*) and/or principal component analysis (PCA), were removed before further analysis. Both replicates of total_AIRAPL_3 did not meet quality criteria and were discarded. Further, I noticed that the mouse called APP_2 did not seem to overexpress the protein APP and was therefore excluded from analysis. Only proteins with a minimum of fifty percent of valid values for each group (mutant/control) based on the biological replicate were retained for further analyses. The following contaminating blood proteins were excluded from the analysis: Hbb-b1, Hbb-b2, Hba, Hbb-y, Hbb-bh1, Hbz, Hbb-bh0, and Alb. The filtered dataset was quantile normalized to correct for systematic shifts and to make the samples comparable.

Analyses

All analyses were performed with Perseus 1.6.14.0, Microsoft Excel, Graphpad Prism 9, R 4.0.4 and Python 3.8.1. Figures were compiled using Adobe Illustrator.

Differential protein expression was calculated using limma v3.46 (Ritchie et al., 2015), a R Bioconductor package, which assumes a prior variance for all samples. DEqMS v1.10.0 (Zhu et al., 2020) function 'SpectraCounteBayes()' was applied over the limma fitted model, to correct the variance by quantified number of peptides. LFQ measurements and differential protein expression results can be found in **Supplementary Table 1.**

The age-specific enrichment of proteins in the insoluble fraction was calculated in Perseus, using ANOVA testing, S0 set to 0.1, permutation-based FDR correction with 250 randomizations and FDR cutoff at 0.05. The ratio of soluble to total fraction abundance was subtracted before to correct any possible fractionation biases.

For gene ontology (GO) analysis, Web-based Gene Set Analysis Toolkit (WebGestalt; Liao et al., 2019) geneset enrichment analysis (GSEA) or overrepresentation analysis (ORA) was always performed with the respective fraction full background list of all quantified proteins and limited to the top 10 FDR hits. Significant protein-protein interaction network analysis (STRING; Szklarczyk et al., 2019) categories were chosen as meaningful 'core' and representative pathways when their annotated proteins made up and explained a major proportion of the network that remained after filtering for 'high confidence interaction score (0.7)' and after removal of disconnected nodes.

RNA isolation

For RNA isolation, hemispheres from the 'physiological aging' cohort were used. Note that these were the corresponding hemispheres for the same animals from which protein data was collected. The fractionation protocol to obtain total and nuclear fraction is based on Gagnon et al., 2014 and Song et al., 2006. Brain tissue was washed briefly in 320 mM sucrose buffer (320 mM sucrose, 5 mM HEPES pH7.4) and homogenized with a Teflon pestle (10 strokes at 900 rpm) in 2mL of sucrose buffer supplemented with RNase inhibitor. Lysate was strained through a 100µm cell strainer, washed with 2mL 2x hypotonic lysis buffer (HLB; 10 mM Tris pH 7.5, 10 mM NaCl, 2 mM $MgCl_2$, 0.3% NP-40 and 10% glycerol), vortexed briefly and kept on ice for 10min. 500µl were taken for 'total' RNA, mixed with 800 µl Trizol LS and kept at -80°C overnight. The remaining lysate was filled to 7 mL volume with HLB, centrifuged at 4° C, 1000g for 3 min. 2 mL of the supernatant was taken as cytosolic fraction at kept at -20°C. Remaining supernatant was discarded and the raw nuclear pellet was washed two more times in HLB followed by 2 min centrifugation at 1000 g. After removal of supernatant, the pellet was resuspended in 1.8 M sucrose buffer (1.8 M sucrose, 50 mM Tris pH7.5, 1 mM $MgCl_2$) and transferred to an ultracentrifugation tube. After ultracentrifugation at 4° C, 70,900 g for 60 min, the upper phase was removed, and the pellet ('nuclear') washed and resuspended in 320 mM sucrose buffer. 800 µl Trizol LS was added, and samples were kept at -80° C at least overnight. The Qiagen RNeasy mini kit was used for RNA extraction following the manufacture's protocol. RNA was always kept on ice and stored at -80° C.

RT-qPCR

Samples of RNA were taken to perform reverse transcription (RT) PCR and quantitative (q) PCR. First-strand cDNA was synthesized using SuperScript IV (ThermoFisher) following manufacturer's protocol and qPCR was performed on an Agilent Mx3000P with SYBR Green (Roche) and ROX reference dye (Agilent). Readout Ct values were normalized to those of 18S.

Target	Primer sequence
18S	F: CTTAGAGGGACAAGTGGCG R: ACGCTGAGCCAGTCAGTGTA
Malat1	F: GAGAGCAGAGCAGCGTAGAG R: TATCTGCGATTTCCTCGGGC
mt-Co1	F: CAGACCGCAACCTAAACACA R: TTCTGGGTGCCCAAAGAAT

Western Blot

For verification of successful subcellular fractionation, before addition of Trizol LS, some lysate was kept separate for protein assessment. Protein quantity was determined using Pierce BCA Protein Assay and 20 µg of protein were boiled with Laemmli sample buffer and loaded onto SDS Gels. After transfer, membranes were stained overnight at 4° C with primary anti-α-Tubulin antibody (Proteintech) or anti-Lamin A/C antibody (Proteintech) in milk-TBST buffer. Secondary anti-rabbit 800CW antibody was incubated the next day for 1 h at RT and detection was performed with a Licor Odyssey CLx.

RNA sequencing

Before sequencing, RNA samples were checked for their quality with an Agilent 2100 Bioanalyzer and the Agilent RNA 6000 Nano Kit. Sample 'total_24-3' showed degradation and was excluded, all others passed quality check. Both total and nuclear fraction underwent mRNA sequencing with HiSeq4000, 50bp read length, performed by the Transcriptome and Genome Analysis Laboratory headed by Gabriela Salinas, Göttingen. Sample 'total_24-1' was identified as outlier and excluded during the bioinformatic analysis. Counts were normalized using the R package DESeq2 and used for differential expression analysis. For determination of relative nuclear enrichment of transcripts, nuclear expression counts were normalized by the median ratio nuc/total for each sample individually to minimize effects of sample preparation and global enrichment shifts. Normalized nuclear transcript counts and their enrichment could then be compared between samples and age groups. For RNA-sequencing results see **Supplementary Table 1**.

Supplementary Data

Due to the extent of supplementary data tables, files will not be printed, but are available online. All supplementary tables can be found under the following link. The password is 'ThesisKluever'

https://owncloud.gwdg.de/index.php/s/nPRvruliSKmRuvg

Supplementary Table 1: all protein and RNA abundances and categorizations used in this study
Supplementary Table 2: mouse sample overview
Supplementary Table 3: RNA GO analyses and direction category annotation
Supplementary Table 4: GO analysis of age-regulated nuclear fraction enrichment
Supplementary Table 5: proteomic results and GO analyses of physiologically aged mice
Supplementary Table 6: correlation between RNA and protein abundance
Supplementary Table 7: quality control and age-specific enrichment of insoluble proteins
Supplementary Table 8: proteomic results and GO analyses of SAMP8 mice
Supplementary Table 9: proteomic results and GO analyses of Zfand2b mice
Supplementary Table 10: proteomic results and GO analyses of Line 61 mice
Supplementary Table 11: proteomic results and GO analyses of HM2 mice
Supplementary Table 12: proteomic results and GO analyses of APPPS1 mice
Supplementary Table 13: proteomic results and GO analyses of mCat mice
Supplementary Table 14: proteomic results and GO analyses of AntiOx mice
Supplementary Table 15: proteomic results and GO analyses of Ucp2 mice
Supplementary Table 16: proteomic results and GO analyses of LAKI mice
Supplementary Table 17: proteomic results and GO analyses of Zmpste24 mice
Supplementary Table 18: proteomic results and GO analyses of EE mice
Supplementary Table 19: proteomic results and GO analyses of female and male aged mice

4 | Results

Aging and aging phenotypes are studied in in a wide variety of species and animal models. I concentrate on the widely used common mouse (*Mus musculus*) to examine several omics-layers of brain aging. To gather a comprehensive dataset on several (brain) aging characteristics, we performed mRNA-sequencing of two subcellular fractions from physiologically aged male WT-mice (C57BL/6J, also known as BL6J) and LC-MS from three solubility-based fractions from overall 13 cohorts of mice, each modeling an assumed aspect of aging. I collected 11 mouse models of aging, dietary supplementation, or environmental enrichment. Together with my cohort of physiologically aged WT mice of 6, 12, and 24 months of age (representing young adult, mature adult, and aged animal, respectively), as well as a cohort of aged males and females, my work provides an extensive database of brain aging data. The mouse models used (see **Supplementary Table 2** for a list and details of all animals) are non-genetic, KO, KI or tg in origin and either model (a phenotype) of aging or represent a possible anti-aging intervention (**Figure 3a**).

For the cohort of physiologically aged mice, I performed basic motor ability and behavior tests to exclude any sick or noticeably out of line behaving individuals. The rotarod test showed no significant differences in motoric functions across ages and no within-group outliers. In an open field hole board, one animal of the 12-month group was identified as outlier in the assessment of time spent in the peripheral zone (~40% more time spent; robust regression and outlier removal (ROUT) test, Q=1%) and the group of 6 months old mice spent significantly more time in the center zone than the group of 24 months aged mice (ANOVA p=0.0294). Other parameters, like distance travelled, velocity and number and duration of nose pokes were not significantly different between groups or within. Young animals of 6 months of age weighed significantly less than both their older counterparts, no significant difference between 12- and 24-months old animals was observed although a trend was present. Daily food consumption was not significantly different between ages.

First, with nuclear shuttling and RNA localization being implicated in aging, I optimized a protocol to isolate nuclear RNA from my physiologically aged cohort. Briefly, this includes hypotonic lysis buffer and a sucrose-cushion ultracentrifugation, for details see **Figure 3b** and **Methods**. Nuclear RNA as well as total RNA was sequenced, measuring more than 20,000 transcripts. Second, proteins of different solubility were extracted from hemispheres of all 13 cohorts of mice. Protein aggregation is a hallmark of brain aging and occurs in varying degree and strength of the aggregates. I isolated SDS-insoluble fractions of aggregates that resist 5% SDS concentration (Kelmer Sacramento et al., 2020; Reis-Rodrigues et al., 2012). Because even the smallest amounts of SDS interfere with MS-protein identification, it was important to optimize a protocol to clear the samples of the detergent. After trying several methods, including precipitation and size-exclusion columns, the recently published single-pot, solid-phase-enhanced sample preparation (SP3; Hughes et al., 2019) delivered consistently well-cleared samples and was fully compatible with my workflow (**Figure 3c**). In order to reduce machine runtime while maximizing protein quantification in LC-MS, I set up and applied the BoxCar acquisition method, which optimizes mean ion injection time by filling multiple narrow mass-to-charge segments (Meier et al., 2018). This allowed us to run more than 300 samples with duplicate technical replicates without any prior offline pre-fractionation while maintaining a high number of identifications. The acquired spectra from BoxCar runs were matched with spectra from an extensive peptide library that I created by offline basic reverse phase HPLC pre-fractionation of pooled samples from all cohorts and solubility fractions. All samples were run on the same Orbitrap LC-MS with the BoxCar acquisition method, matched to an extensive peptide library, and

analyzed together with MaxQuant for highest comparability. This meticulously tested and optimized sample preparation and measurement method reduced LC-MS machine acquisition time alone by ~20-fold, without which the study of the vast number of samples used here would not have been feasible. Overall, I could identify and label-free quantify (LFQ) more than 150,000 peptides and 8700 protein groups.

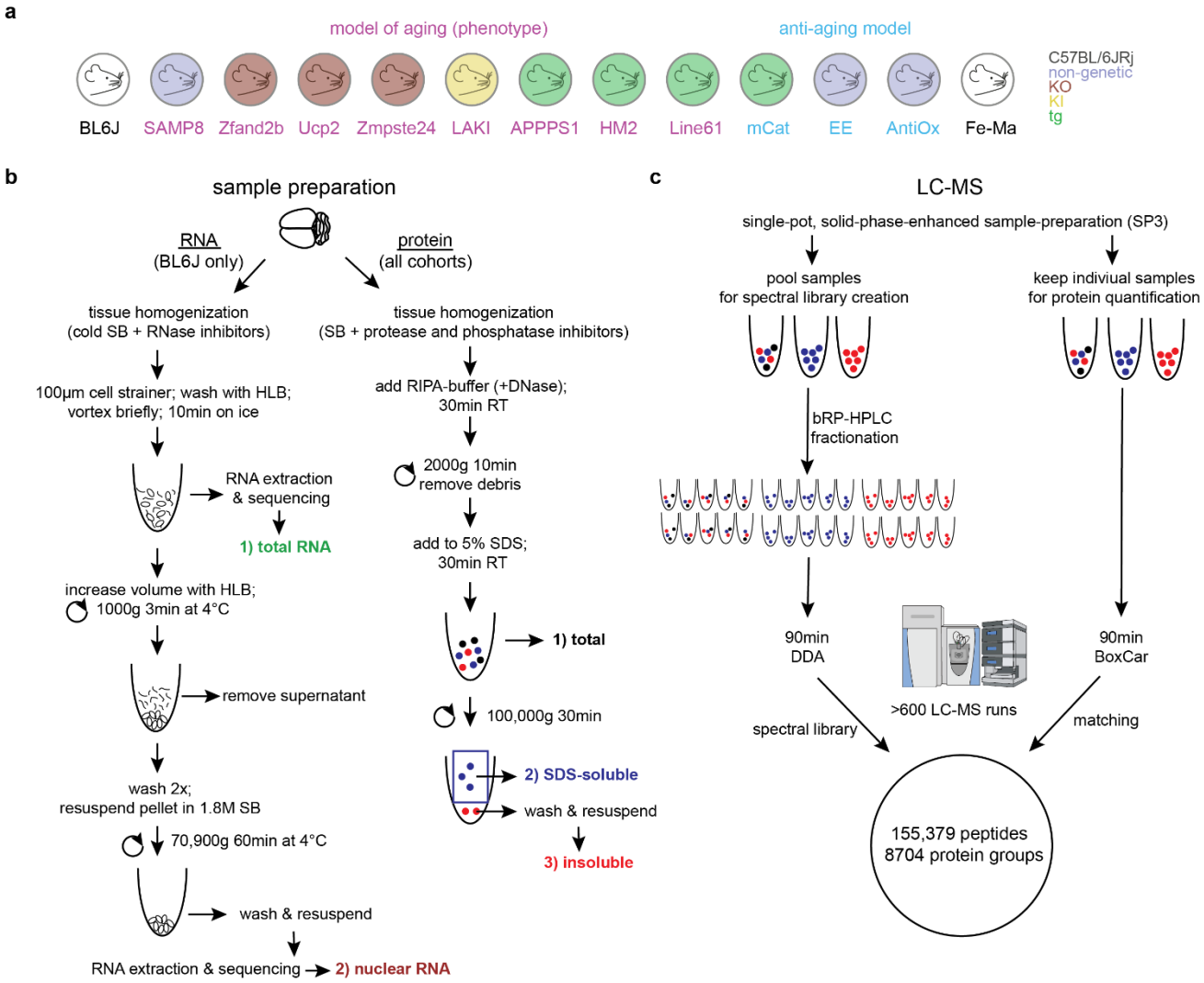

Figure 3 Sample and workflow overview. **a** 13 cohorts of mice were used this study. I compared wildtype BL6J mice of three different ages (6, 12 and 24 months) with models of aging (names indicated in pink) and mice with anti-aging phenotypes or interventions (names in blue). The color in the circle surrounding the mouse head indicates whether the model is non-genetic (light purple), knock out (KO; red), knock in (KI; yellow), transgenic (tg; green) or wildtype (no color, white). **b** RNA and protein sample preparation. For each individual mouse brain, the olfactory bulbs were removed, and half brains were separately processed for either RNA or protein fractionation. All cohorts of mouse samples were processed for protein measurement by homogenization in sucrose buffer (SB), supplemented with protease and phosphatase inhibitors. After addition of RIPA-buffer and DNase, samples were centrifuged to separate debris. SDS was added to obtain a final concentration of 5%. After solubilization, a sample taken here is subsequently called the 'total' fraction. The solution was ultracentrifuged to separate the SDS-soluble fraction from an SDS-insoluble pellet. The pellet was washed and resuspended mechanically in 5% SDS solution to result in the 'insoluble' fraction. For RNA preparation, only the physiological cohort of WT BL6 mice was used. Tissue was homogenized in SB buffer, supplemented with RNase-inhibitors, strained, washed with hypotonic lysis buffer (HLB) and taken as 'total' fraction after incubation. To isolate a pure nuclear fraction, the sample was washed and centrifuged several times and finally ultracentrifuged. The remaining nuclear pellet was resuspended, and all RNA samples were further processed for RNA-isolation and sequencing. **c** Liquid-chromatography mass spectrometry (LC-MS) analysis of all protein samples. SDS was cleared from the samples by single-pot, solid-phase enhanced sample preparation (SP3). Samples of the same solubility fraction were pooled for subsequent basic reverse phase high pressure liquid-chromatography (bRP-HPLC). Resulting fractions were pooled in a concatenated manner into 10 or 20 samples each. 90-minute data-dependent acquisition (DDA) was used to build a spectral library. Individual samples from all solubility fractions were run in BoxCar mode and their spectra matched to the generated library. These more than 600 LC-MS runs resulted in the identification and LFQ quantification of 155,379 peptides and 8704 protein groups.

Since my main focus is on the proteome of the aging brain, I will first briefly describe the findings from my mRNA sequencing but then move on to discuss in detail the changes between 6-, 12-, and 24-months old wildtype mice on the protein level. In the third part of this work, I will describe the changes for each mouse model of aging and conclude by presenting an overarching analysis that broadens our understanding of brain aging.

4.1 | Transcriptomics

I first set out to describe differences of the nuclear and total transcriptome of WT mice brains of the ages of 6, 12, and 24 months. Hemispheres were lysed on ice in the presence of RNA-inhibitors and a series of washes and centrifugations resulted in a total and a nuclear fraction (see **Figure 3b** and **Methods** for details), from which I extracted RNA. The quality of my fractionation was assessed with real-time quantitative PCR (RT-qPCR) and western blot. For RT-qPCR, I used primers specific for the strictly nuclear long non-coding RNA *Malat1* (Bernard et al., 2010) and the cytosolic, mitochondrially translated *mt-Co1*. Both transcripts were enriched in their respective fraction, with *mt-Co1* being barely detectable in the nuclear fraction (**Figure 4a**). I also assessed the proteins from my subcellular fractions via western blot and antibodies against the cytosolic α-Tubulin and the nuclear envelope protein Lamin A/C. Again, analysis confirms correct enrichment of each protein and high nuclear fraction purity (**Figure 4b**). mRNA sequencing was then performed on an Illumina HiSeq4000 by the Transcriptome and Genome Analysis Laboratory, Göttingen. Comparison of my sequencing data with published data from single-cell integrated nuclear RNA and cytoplasmic RNA sequencing (SINC-seq; Abdelmoez et al., 2018) as well as the RNALocate database (Zhang et al., 2017a) again confirms the quality of my fractionation and sequencing results (**Figure 4c, d**). Transcripts annotated as 'nuclear' in either of these previously published works are highly enriched in the nuclear fraction acquired here, whereas transcripts annotated as 'cytoplasmic' are de-enriched.

Principal component analysis of my sequencing results shows a slightly clearer separation between the age-groups in the total fraction (compared with the nuclear fraction), with the samples of 12- and 24-months old animals clustering closer together and the 6 months old animals clustering by themselves **(Figure 5a, b**). Stronger differences between the ages can also be seen in the number of differentially expressed (DE) transcripts, which is higher in the total fraction (**Figure 5c, d, e**). Notably, DE transcripts are more prominent between 6 and 12 months (10265 DE genes in the total fraction) than between 12 and 24 months (1546 DE genes in the total fraction; **Figure 5e** and **Supplementary Table 1**). The total transcriptomic landscape might thus change more in early adult life, rather than from middle- to old-age. In the late comparison, changes in the nuclear fraction (measured by their number and range of adjusted *p*-values; *padj*) are relatively similar to those in the total fraction (**Figure 5f**).

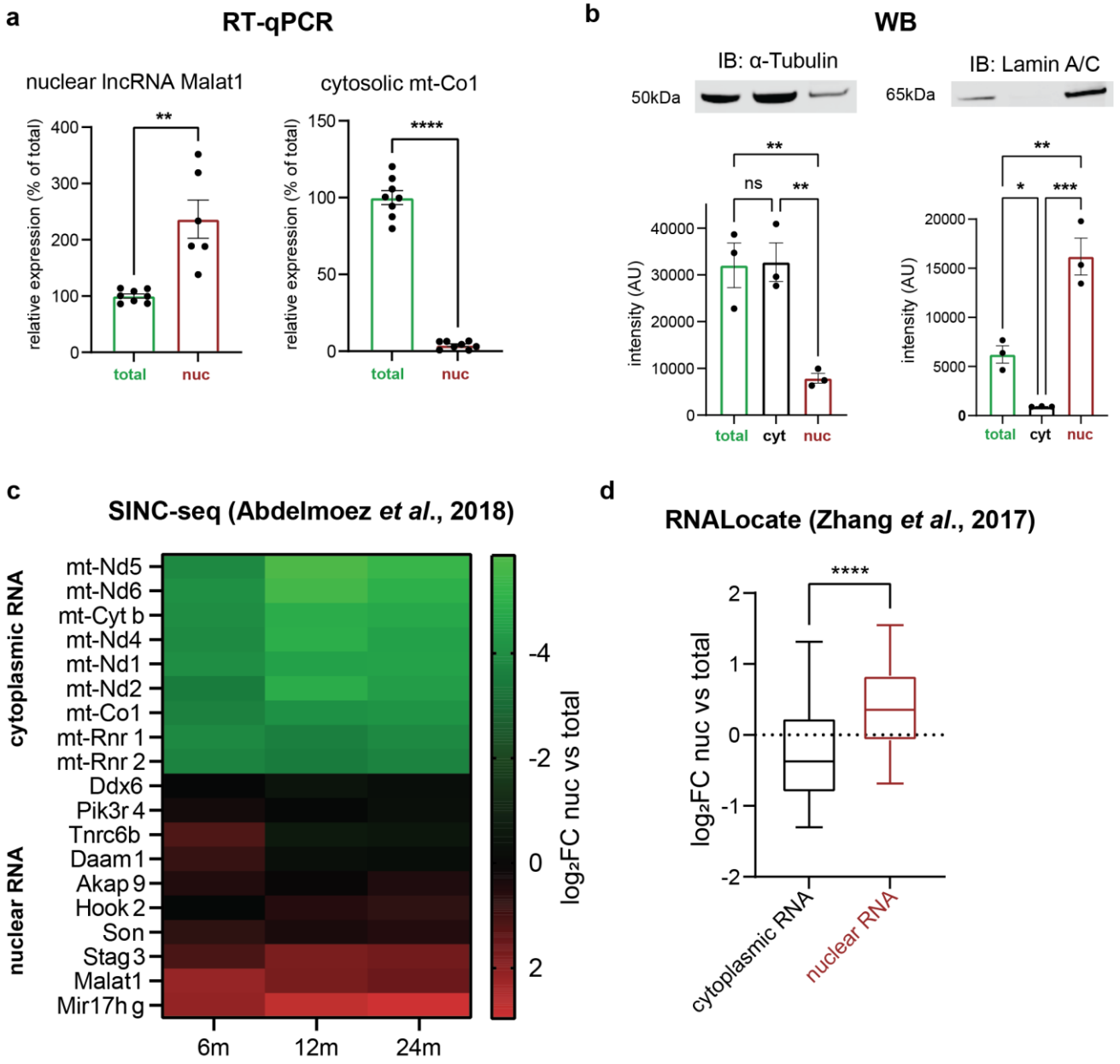

Figure 4 Quality control of subcellular fractionation for RNA-Isolation and subsequent sequencing. **a** Reverse-transcription qualitative PCR (RT-qPCR) confirms enrichment of nuclear transcript *Malat1* in the nuclear fraction (nuc). Reversely, cytosolic *mt-Co1* is strongly depleted in the nuclear fraction. Unpaired t-test with Welch correction; n=6 technical replicates from 3 biological samples. **b** Western blot analysis of cytosolic protein α-Tubulin, which is depleted in the nuclear fraction (nuc), and nuclear lamin Lamin A/C, which is depleted in the cytosolic fraction (Cyt) and relatively enriched in Nuc. Ordinary one-way ANOVA with Turkey correction; n=3 biological replicates. **c** Comparison of nuclear vs total enrichment (log_2FC Nuc vs Total) of my data with single-cell integrated nuclear RNA and cytoplasmic RNA sequencing (SINC-seq, Abdelmoez et al., 2018) showing that transcripts identified by SINC-seq as nuclear are indeed enriched in the nucleus in my dataset and cytoplasmic transcripts are de-enriched. **d** Comparison with annotations from RNALocate, a web-accessible database providing subcellular RNA localization (Zhang et al., 2017a). Fold changes of nuclear enrichment (log_2FC Nuc vs Total) are significantly higher, meaning nuclear enrichment, among transcripts that are annotated as 'nuclear RNA'. Unpaired t-test with Welch correction of 1465 and 2259 transcripts with cytoplasmic and nuclear annotation, respectively. Boxplots show median, 25th to 75th percentile as box and 5th to 95th percentile as whiskers. * p<0.5, ** p<0.01, *** p<0.001, **** p<0.0001.

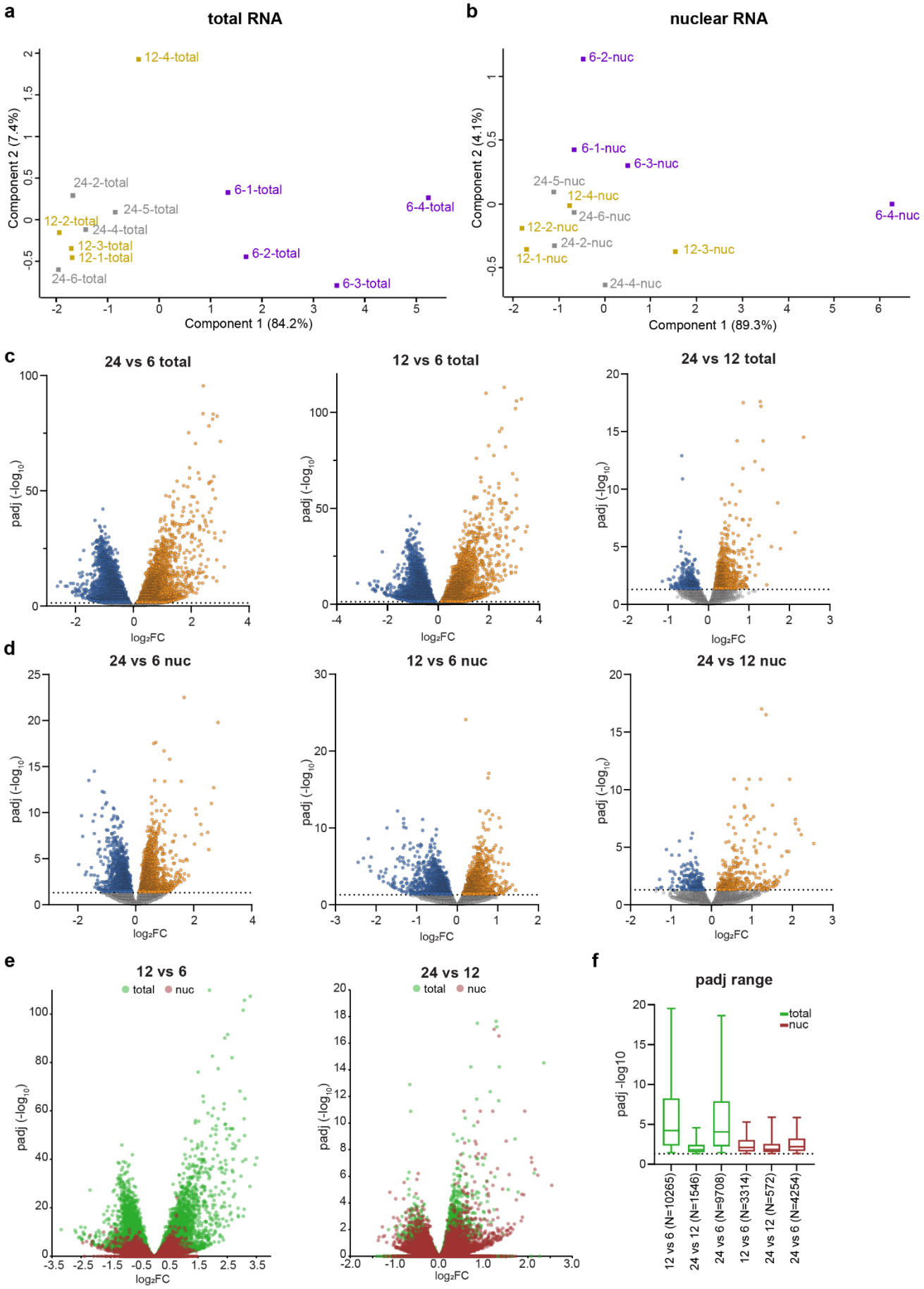

Figure 5 Comparison of total and nuclear RNA sequencing data from the brains of 6-, 12-, and 24-months old mice. **a, b** Principal component analysis (PCA) for age samples of total and nuclear RNA, respectively. Age groups are color coded for visibility. Samples cluster closer according to their age groups in the total RNA. **c**, **d** Volcano plots showing all differentially

expressed genes in any of the three possible age comparisons for total and nuclear RNA, respectively. Downregulated genes in blue, upregulated in orange. Dotted line represents *padj* cutoff at 0.05. **e** Combined volcano plots of total and nuclear RNA DE genes showing a higher magnitude of changes at the early age comparison and in the total fraction. Note also the higher scales in both x- and y-axis in the early comparison. **f** Range of significant *padj*-values across all comparisons confirms more highly significant hits in early (12 vs 6) and long (24 vs 6) comparison, especially in the total fraction. Total fraction in green, nuclear fraction in red. Boxplots show median, 25th to 75th percentile as box and 5th to 95th percentile as whiskers.

I next used gene ontology (GO) annotation to gain insights into which functional classes of transcripts change with age in the mouse brain (**Figure 6** and **Supplementary Table 3**). Gene-set enrichment analysis (GSEA) shows that, in the total fraction, synapse organization and transmission related genes are upregulated, while genes connected to mitochondria organization and detoxification are downregulated in the long comparison 24 vs 6 (**Figure 6a**). These top GO annotations are found again in the early comparison, 12 vs 6. In contrast, in the late comparison, 24 vs 12, several immune-related annotations are enriched in the upregulated transcripts and synaptic transmission is downregulated. This apparent contradiction in both up- and downregulation of synaptic genes is explained by firstly, the high number of member genes within these GO categories, which can mean that different transcripts are up- and downregulated, but all are annotated as 'synaptic'. Secondly, with the extent of early changes being higher (see **Figure 5**), drastic early downregulations might obscure mild late upregulations, which are then not picked up in the long overall comparison.

In the nuclear fraction, with early and late changes being more comparable in number and extent, the long comparison GO annotations resemble a composite of early and late enriched and de-enriched categories (**Figure 6b**). Developmental transcripts, relating to 'regulation of tube size', 'feeding behavior', 'response to estrogen' or 'pattern specification process' are decreasing from 6 to 12 months. Ammonium and neurotransmitter transport are additionally downregulated early. Immune response genes are late upregulated in the nucleus, genes related to vesicle localization are downregulated (the only significant GO annotation in the late downregulated genes). Most of these annotations are also found in the long comparison, with the addition of decreasing transcripts regulating 'protein folding'. No GO annotations were significantly enriched in the early upregulated genes (12 vs 6).

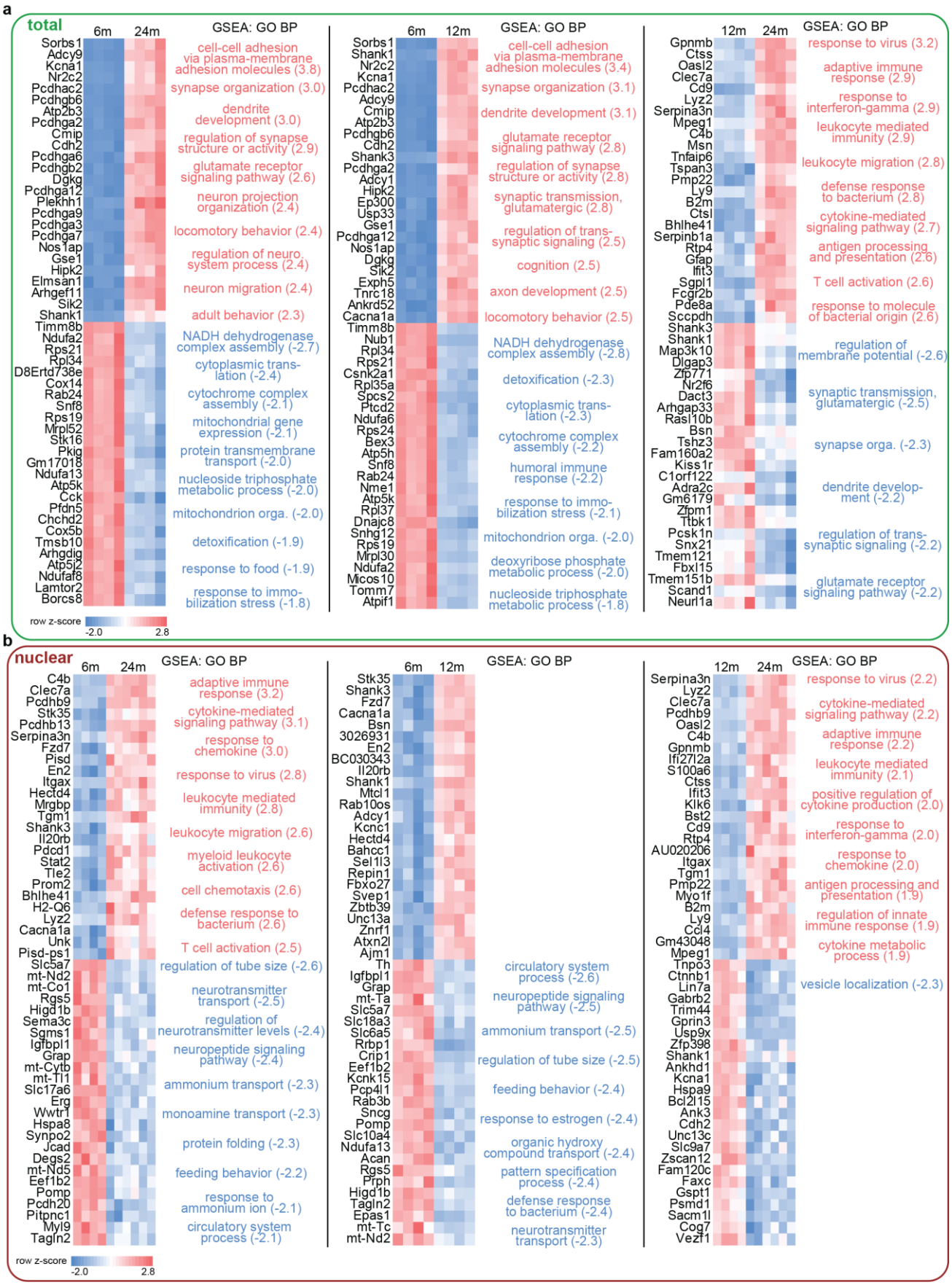

Figure 6 Summary of transcript abundance changes in total (**a**) and nuclear (**b**) RNA. Heatmaps show the top 25 most significant up- and downregulated genes in each comparison. Next to each heatmap is the overall GO biological process (BP) analysis using GSEA of the complete list of *padj*-significant genes. All GO terms have FDR<0.05. Note the similarities in genes and GO annotations of the early (12 vs 6) and long (24 vs 6) comparison of the total fraction, relating to the high magnitude of early changes shown in **Figure 3**.

I assessed the ‘early’ and ‘late’ changes in significant DE transcripts more closely by categorizing them depending on their directionality, meaning whether they were up- or downregulated by at least 20% in any age-comparison (**Supplementary Table 3**). The pie-charts in **Figure 7a, b** summarize these results. 15.7% of DE transcripts remain overall unchanged in the total fraction; the highest proportion of DE transcripts (59.7%) are found between 6 and 12 months (early up and early down). In contrast, only 6% of DE transcripts change between 12 and 24 months (late up and late down). 15.8% of transcripts ‘change their direction’ between 6 and 24 months, meaning that they are up- or downregulated in one comparison and reversely in the other. Only 4.5% show a continuous direction change (meaning they are up- or downregulated in both early and late comparison). In the nuclear fraction, 33.1% of DE transcripts remain unchanged, with early changing transcripts making up 45%. Compared to the relatively smaller percentage of early changes with respect to the total fraction, the nuclear late changing fraction is slightly higher with 9.4%. 8.9% of DE transcripts change their direction, only 3.8% show continuous change. **Figure 7 c-j** shows the line profiles of all genes sorted into either of the direction categories together with the most significantly enriched GO biological process (BP) annotation. These annotations strengthen the theory of particularly strong changes overshadowing the smaller ones. The line profiles of early upregulated ‘synapse organization’ transcripts (**Figure 7c**) also show a relatively wide range of late downregulations, which are identified by GSEA (**Figure 6a**). Interestingly, late downregulation of ‘synapse organization’ is especially apparent in the nuclear fraction (**Figure 7g**), as is ‘cognition’ in the nuclear continuously downregulated genes (**Figure 7h**). Immune response-related genes are prominently early and continuously upregulated in both total and nuclear RNA fraction (**Figure 7d, e**). ‘Leukocyte migration’ transcripts show a more unique ‘down-up’ pattern (**Figure 7i**). The decline of mitochondrial and ATP-biosynthetic process associated genes is also apparent in both total and nuclear fraction (**Figure 7f**). Lastly, the regulation of membrane potential and intercellular adhesion is found to increase early and decrease late (up-down; **Figure 7j**).

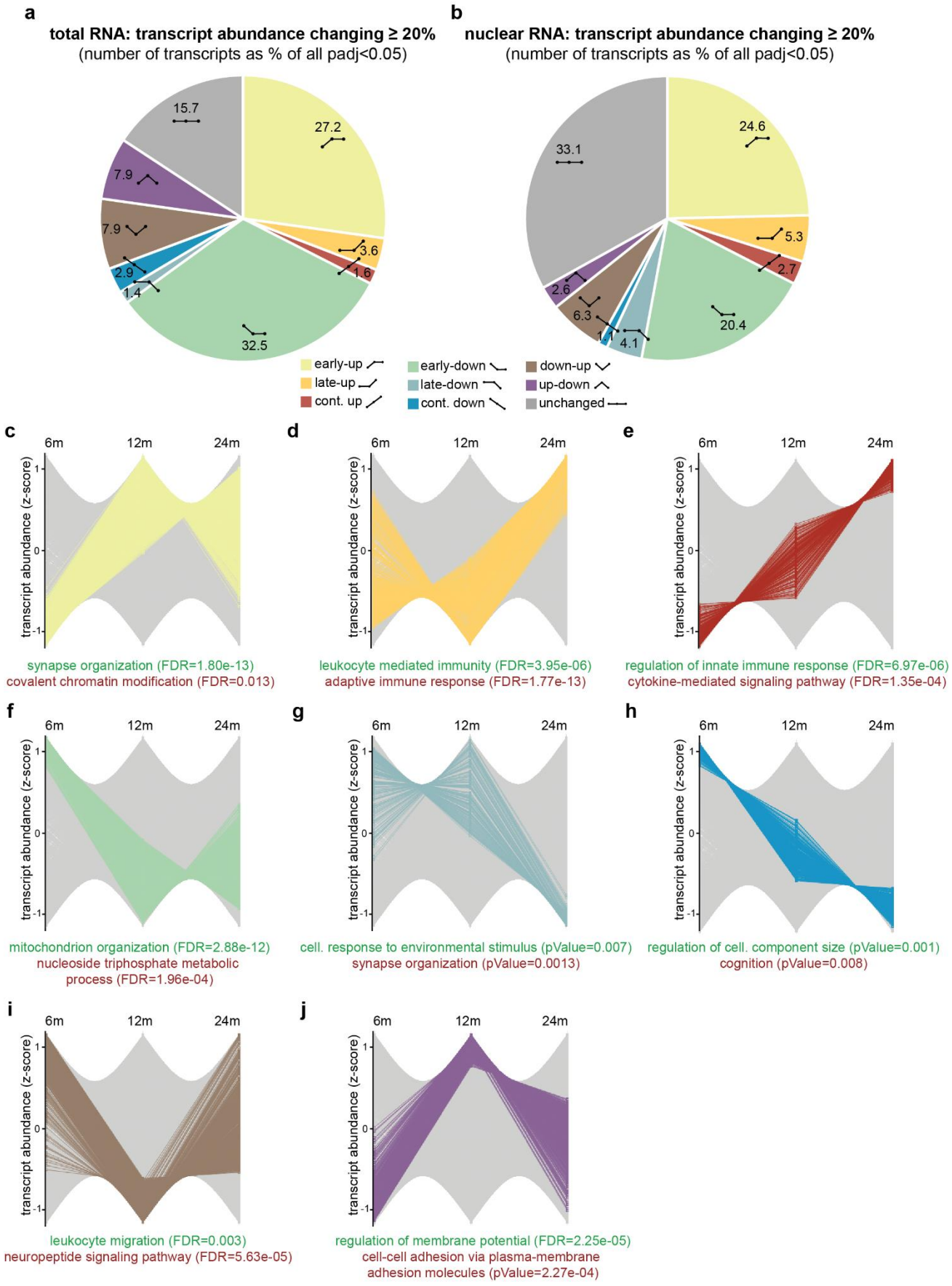

Figure 7 Transcript abundance changes in total and nuclear fraction across the three ages**. a, b** Pie charts showing the distribution of transcripts changed more than 20% in abundance and *padj*<0.05 significant between the different ages for total RNA (**a**) and nuclear RNA (**b**). **c-j** Line profiles showing the direction changes across ages as row z-score normalized transcript abundance per category. Top significant GO BP categories, identified by overrepresentation analysis (ORA), for total RNA (green) and nuclear RNA (red) are mentioned below each direction category graph.

Correct RNA processing and localization is vital to maintain cellular homeostasis. I was interested, whether certain functional classes of transcripts would change their relative abundance between total and nuclear fraction. This could either be caused by specific up- or downregulation of transcription in the nucleus that cannot be seen in the total fraction due to fast turnover or transport 'dilution', or by specific shuttling mechanisms that retain or release nuclear transcripts into the cytosol. The 'nuclear fraction' is calculated by building the ratio between nuclear and total transcript abundance (for details see **Methods**). I performed gene ontology overrepresentation analysis (ORA) of relative decreasing or increasing (irrespective of whether the change occurs early or late) nuclear fraction transcripts. A decreasing nuclear fraction, as I found it for many synaptic GO categories, means that relatively less transcripts are found in the nucleus with age (**Figure 8a**). The reverse is true for ribosomal and ribosome-related transcripts, which lead the increasing nuclear fraction annotations (**Figure 8b**). Additionally, mitochondrial and spliceosomal transcripts are also increasingly found in the relative nuclear fraction with age (**Supplementary Table 4**).

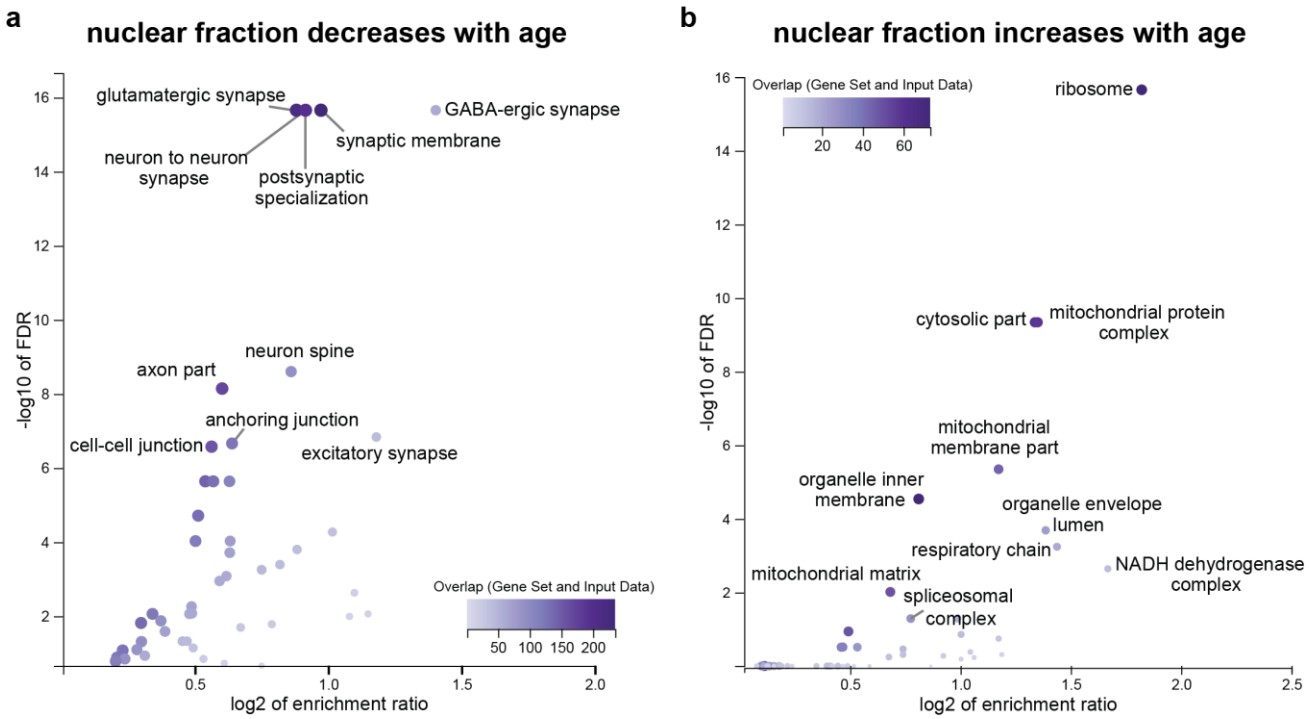

Figure 8 Gene ontology cellular component overrepresentation analysis (ORA) of relative nuclear fraction RNA changes between 6 and 24 months. **a** Transcripts with decreasing nuclear fraction with age and *padj*<0.05 are enriched in terms relating to 'neuron' and 'synapse'. **b** Transcripts with increasing nuclear fraction with age and *padj*<0.05 are enriched in terms relating to 'ribosome' and 'mitochondria'.

Overall, the transcriptomic landscape of the brain changes with age, with greater extent in early aging (between 6 and 12 months). Immune activation, mitochondrial function and synaptic activity are heavily implicated in these gene expression changes. Nuclear transcript levels change more equally throughout aging and show a decreased abundance of genes regulating synaptic organization and activity. Combined, a rearrangement of spatial transcript distribution becomes apparent, with, on one side, neuronal and synaptic RNAs being less enriched in the nucleus with age. On the other side, ribosome and mitochondria organizing RNAs increase in nuclear enrichment.

4.2 | Proteomic description of physiological aging in the mouse brain

The study of brain aging is notoriously difficult, both in humans and in animal models, albeit with obvious advantages for animal models. I wanted to examine the brain proteome of physiologically aged mice of the commonly used strain C57BL/6J at three ages: young adult 6 months, mature adult 12 months, and aged 24 months old male mice. We and others strongly believe in the importance of at least comparing three timepoints, with properly aged animals for the question at hand (Baker and Peleg, 2017; Kluever and Fornasiero, 2021; Li et al., 2011). I additionally separated the brain proteins according to their solubility by using 5% SDS fractionation. The BoxCar method and MaxQuant-based LFQ quantification resulted in the measurement of ~5300 proteins in the total fraction. PCA analysis shows clustering of the averaged age-groups according to their solubility fraction, with the greatest variation between ages seen in the insoluble fraction, especially at 24 months (**Figure 9a**). In the total fraction, differences between ages were small, in line with previous proteomic brain studies (Cellerino and Ori, 2017; Walther and Mann, 2011). Abundance measurements covered several magnitudes and were quantile normalized to allow inter-group comparisons (**Figure 9b**). Correlation coefficients between samples was higher within solubility groups, with insoluble fractions showing the greatest differences (**Figure 9c**). I found no significant differences in protein abundance comparisons between age groups that could be assigned to astrocytes, microglia, neurons, or oligodendrocytes specifically, neither in the total, nor in the insoluble fraction (**Figure 9d**, using the classification provided by Sharma et al., 2015).

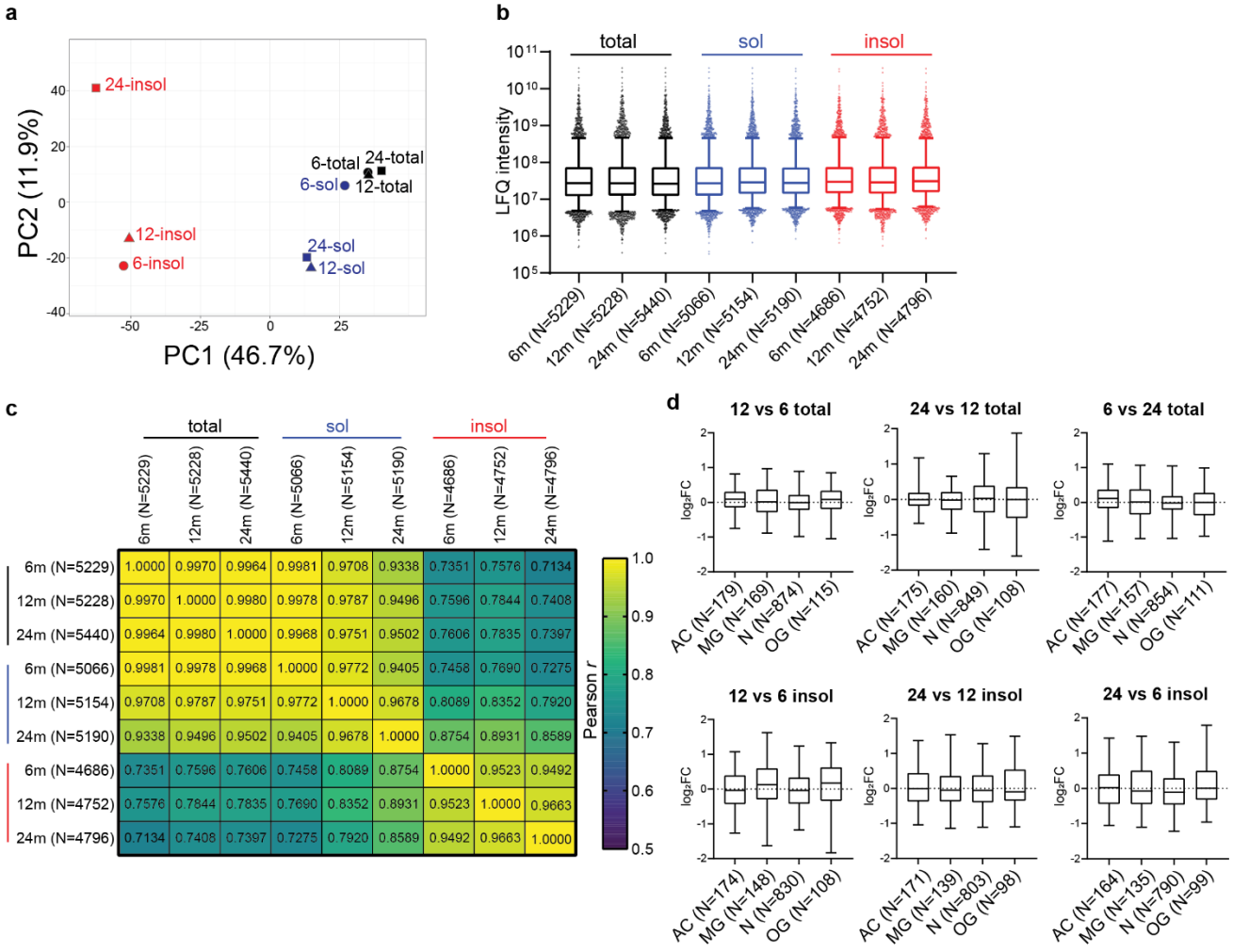

Figure 9 Proteomic results from physiologically aged mice. **a** Distribution of age- and solubility-groups from LC-MS results. PCA-plot shows main clustering according to solubility. **b** Boxplots showing the dynamic range of abundance measurements

(LFQ intensity) per averaged age group, after quantile normalization. **c** Correlation matrix based on Pearson correlation between all averaged age and solubility groups. **d** Between astrocytes (AC), microglia (MG), neurons (N) and oligodendrocytes (OG), no cell type-specific proteins are overall significantly enriched or de-enriched with age. All Tukey-ANOVA comparisons are non-significant. Boxplots show median, 25th to 75th percentile as box and 5th to 95th percentile as whiskers.

4.2.1 | Total fraction

For statistical analysis, there is no unified consensus on the best methodology for mass spectrometry data. Methods have been adapted from other types of data, like RNA-sequencing, but few consider the specifics of MS-data structure. One of these specifics is the variance of the number of peptides used for protein quantification. DEqMS is a method that has been designed to take this into account and calculate differential protein abundances more accurately (Zhu et al., 2020). After multiple comparison correction using the DEqMS method, 31 proteins are found significantly changed between 6 and 24 months in the total fraction (**Figure 10c** and **Supplementary Table 5)**.

The most significant upregulation is observed for glial fibrillary acidic protein (Gfap), which is slightly more abundant at 6 compared to 12 months, but then strongly increases in 24 months aged brains. 27 proteins change significantly between 6 and 12 months (**Figure 10a**) and 37 proteins between 12 and 24 months (**Figure 10b**). I performed gene ontology overrepresentation analysis (ORA) for all proteins of the different comparisons with non-adjusted p<0.05 (**Figure 10d, e** and **Supplementary Table 5**). In the early comparison (12 vs 6 months), ‘antibiotic metabolic process’ and ‘cofactor metabolic process’ are significantly (FDR<0.05) enriched among the upregulated proteins; ‘intermediate filament-based process’ is enriched among the downregulated proteins. In the late comparison (24 vs 12 months), ‘intermediate filament-based process’ is then enriched among the upregulated proteins. Several metabolic process GOs are significantly enriched among the downregulated proteins, including ‘antibiotic metabolic process’ and ‘cofactor metabolic process’, which were upregulated early. Additionally, ‘tricarboxylic acid metabolic process’, ‘generation of precursor metabolites and energy’, ‘pyridine-containing compound metabolic process’, ‘nucleobase-containing small molecule biosynthetic process’ and others are enriched. Few, often overlapping, proteins are responsible for these enrichments and no FDR-significant enrichments were found for the comparison of 6 to 24 months old mice.

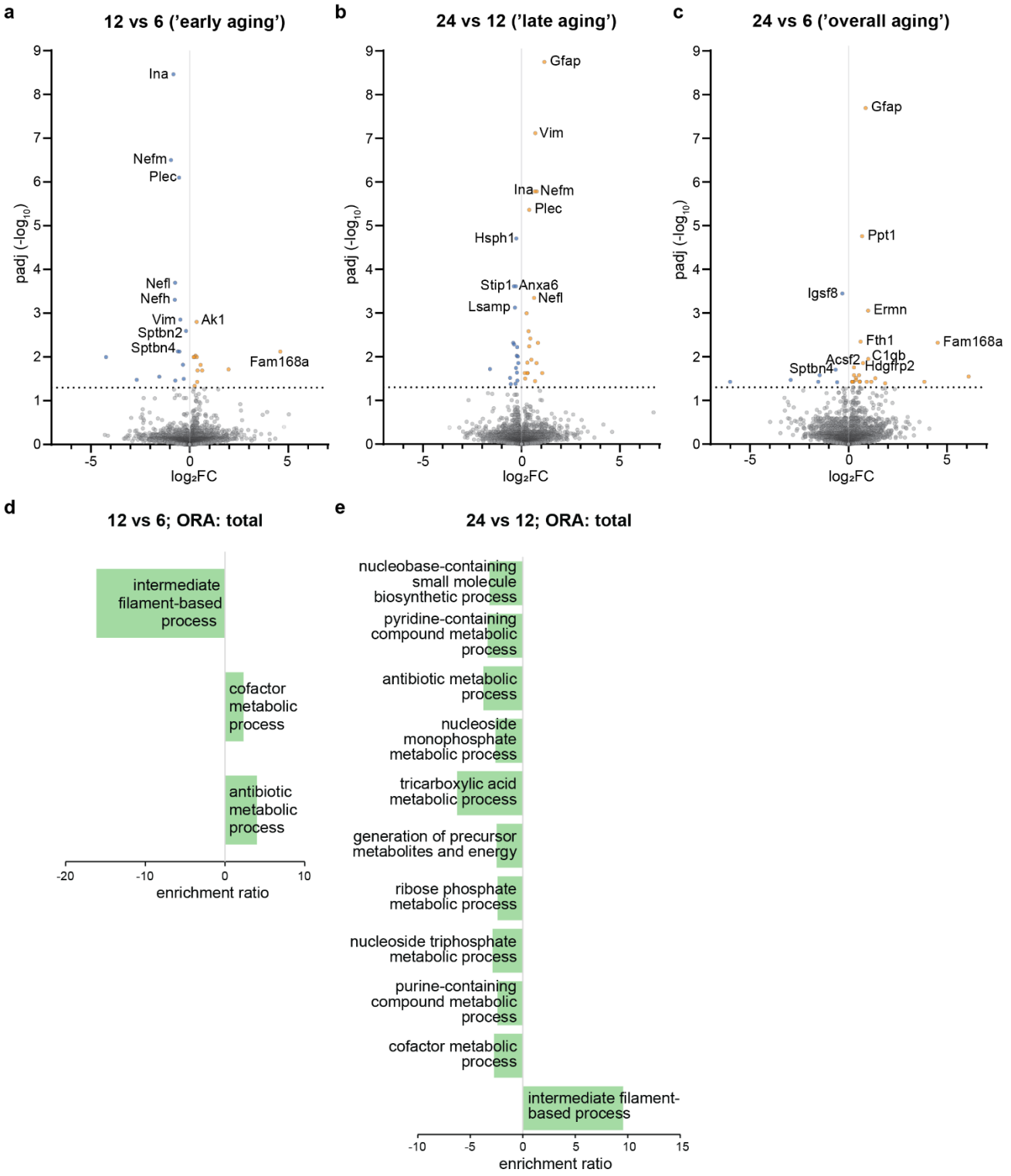

Figure 10 Overview of differentially expressed proteins in physiologically aged mice. a**-c** Volcano plots, indicating *padj* (as -log10) and log2FC between the different ages in the total fraction. Signifcant proteins indicated in orange (upregulated) and blue (downregulated), horizontal line is *padj*-value cutoff at 0.05. **d** and **e** WebGestalt ORA analysis of the non-adjusted *p*-value significant proteins that are upregulated (positive enrichment ratio) or downregulated (negative enrichment ratio) in the early comparison (12- vs 6- months; **d**) and in the late comparison (24 vs 12 months; **e**) fraction. GO categories are all FDR<0.05 and sorted with the most significant on top.

All significant proteins in any of the three possible age comparisons are listed in **Figure 11**. Several intermediate filaments stand out with decreased levels at 12 months, being significant in both early and late comparison but not from 6 to 24 months. These include the light, medium and heavy neurofilament polypeptides (Nefl, Nefm, Nefh), vimentin (Vim), plectin (Plec) and α-internexin (Ina). GO BP category 'intermediate filament-based process' is therefore significantly enriched in both the early and late comparison (**Figure 10d, e**) Among the exclusively late downregulated proteins, I found protein folding and stress response proteins, like heat shock protein HSP 90-beta (Hsp90ab1), heat shock protein 4 (Hspa4), heat shock protein 105 kDa (Hsph1), activator of 90 kDa heat shock protein ATPase homolog 1 (Ahsa1), co-chaperone peptidyl-prolyl cis-trans isomerase D (Ppid) and calnexin (Canx).

Because GO annotations are not necessarily specific for protein function in the brain and their usefulness is limited in datasets with few significant results, I used custom functional annotations in addition. Such manually curated categorizations have proven useful before (Fornasiero et al., 2018; Kwon et al., 2012; Souza et al., 2018) and often provide the groundwork for large biomedical resources (Oughtred et al., 2021; Rath et al., 2021) eventually. The annotations made here were based on protein information obtained from Uniprot and STRING databases, taking into consideration known functions and roles specifically in the brain (opposed to other organs, where proteins might have different functions) as well as their timing (known roles in aging vs development). More than 4200 proteins were manually annotated this way (see **Supplementary Table 1**). With these brain-specific curated functional categories, I was able to identify protein classes that were more affected in brain aging than others, both in up- and downregulation (**Figure 12**).

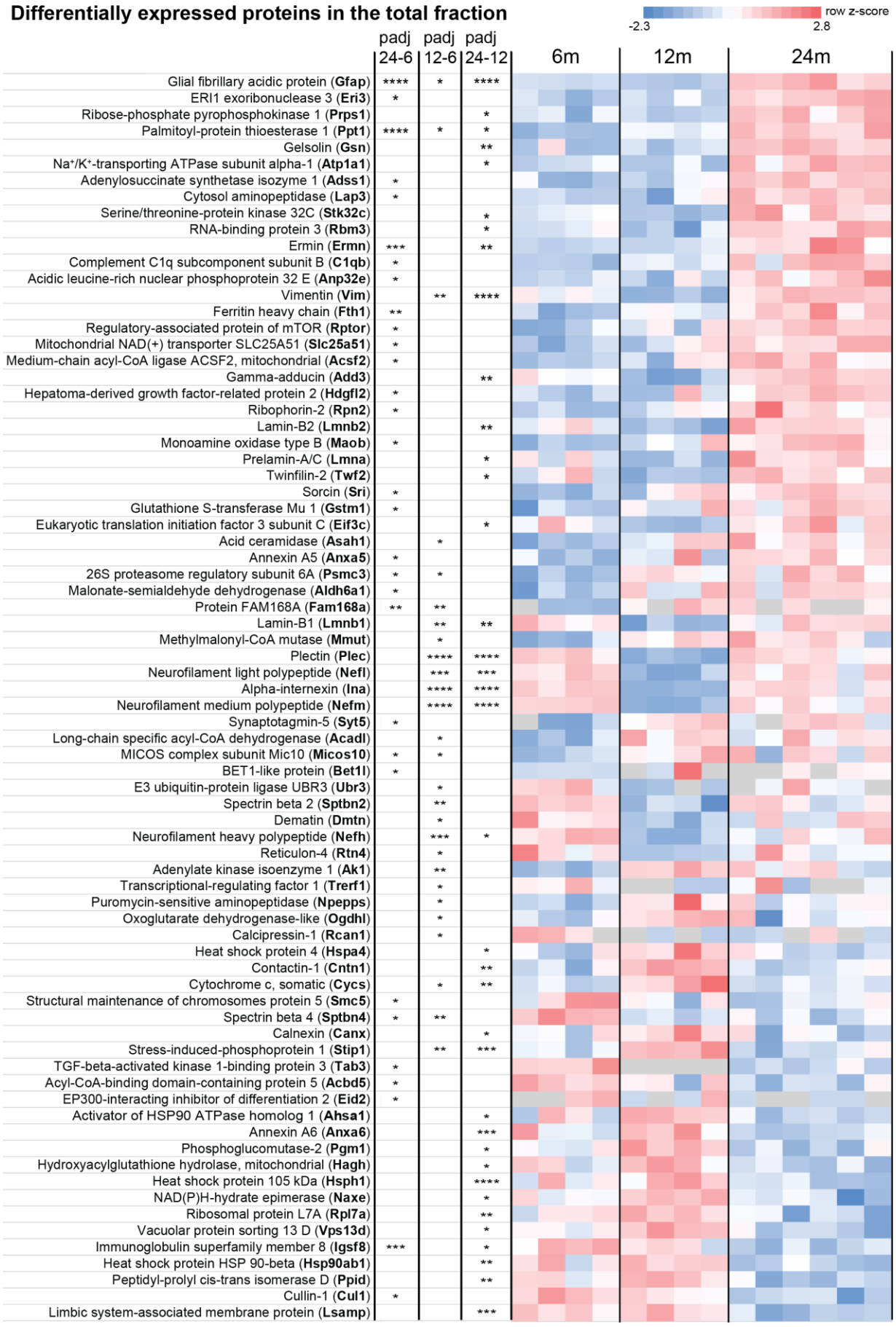

Figure 11 Heatmap showing all proteins significantly changed in the total fraction in any of the age-comparisons. Columns show the DEqMS adjusted *p*-value significances and all biological replicates. LFQ protein abundances are z-score normalized for illustration purposes, grey fields represent missing values; * $p<0.5$, ** $p<0.01$, *** $p<0.001$, **** $p<0.0001$.

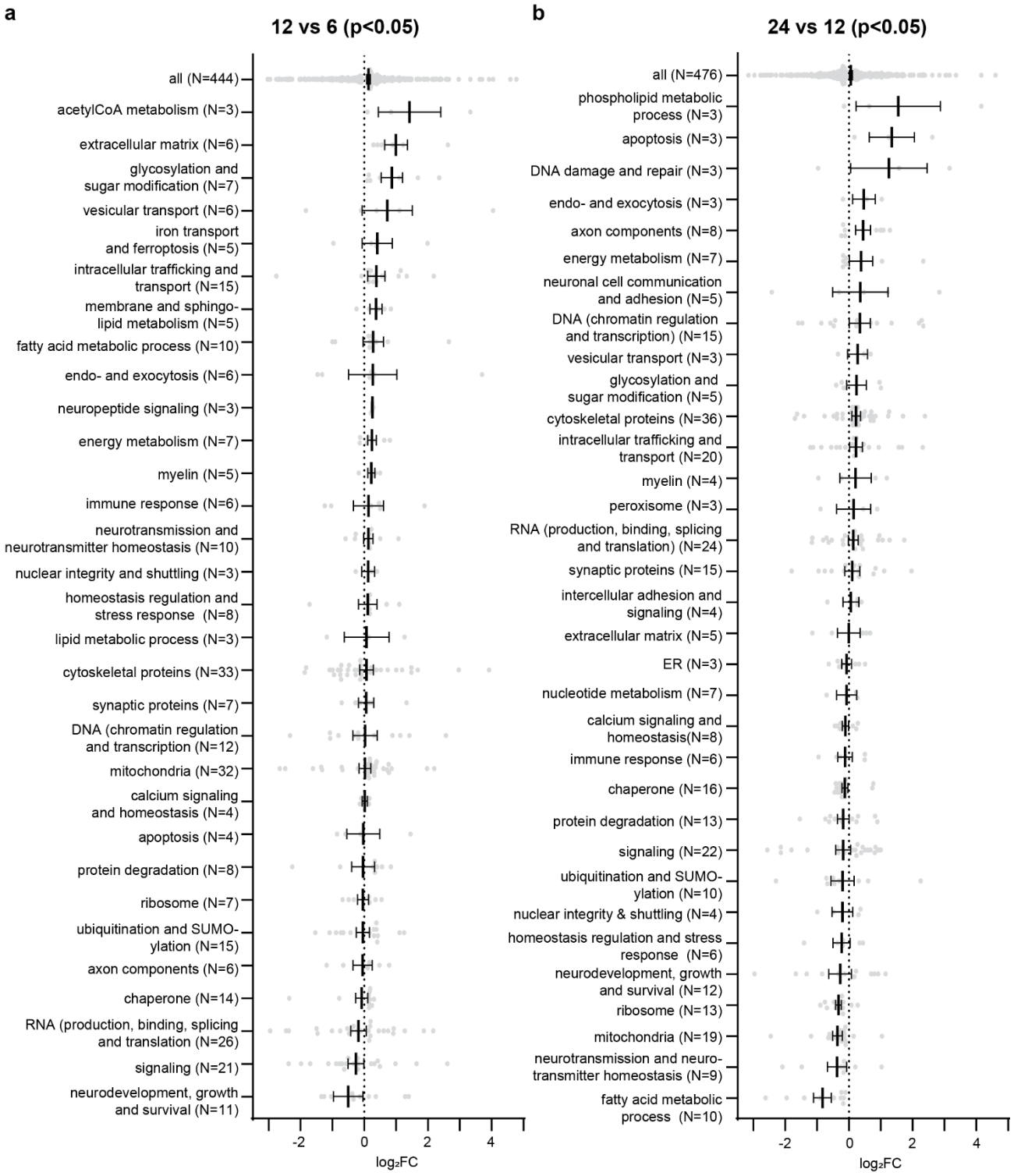

Figure 12 Proteins with significant abundance changes in physiologically aged mouse brains, sorted into functional categories (DEqMS p<0.05, minimum of 3 protein members per category). **a** Early aging comparison 12 vs 6 months, **b** late aging comparison 24 vs 12 months. N gives the number of proteins belonging to each category. Each dot represents a single protein log_2FC. Line and error bars represent mean ± SEM.

Only proteins with DEqMS *p*<0.05 and at least 3 protein members per category were taken into account. 'AcetylCoA metabolism' (with strong upregulation of pantothenate kinase 1, catalyzing the rate determining step in CoA synthesis), 'extracellular matrix' (e.g., serine protease HTRA1 which degrades fibronectins and proteoglycans) and 'glycosylation and sugar modification' (e.g., fucosyltransferase 9) lead the early (12 vs 6) upregulated protein categories, while 'neurodevelopment, growth and survival' (e.g., central nervous system development involved calcipressin-1), 'signaling' (e.g., phosphoinositide 5-phosphatase) and RNA-related

processes (e.g., spliceosome component NHP2-like protein 1) are early downregulated, possibly connected to ceasing maturation processes (**Figure 12a**). In the late comparison (24 vs 12), 'phospholipid metabolic process' (e.g., phosphatidylserine synthase 1), 'apoptosis' (e.g., apoptosis regulator BAX) and 'DNA damage and repair' (e.g., telomerase-binding protein EST1A) proteins are upregulated, whereas 'fatty acid metabolic process' (e.g., elongation of very long chain fatty acids protein 5), 'neurotransmission and neurotransmitter homeostasis' (e.g., voltage-dependent sodium channel protein type 1 subunit alpha) and mitochondrial proteins (e.g., mitochondrial elongation factor G, which is important for mitochondrial protein synthesis) are downregulated (**Figure 12b**).

As proteins show diverse abundance patterns across ages, I subdivided all quantified proteins into categories based on their trajectory across age groups (direction categories; **Figure 13** and **Supplementary Table 1**). Irrespective of significances, 41.6% of proteins show no abundance changes beyond 20% and only 2.8% and 1.6% show continuous up- or downregulation, respectively (**Figure 13a**). Instead, I found more proteins changing from one age to the next while staying relatively stable in the other interval. 9.5 % of measured proteins increase early, for example adenylate kinase isoenzyme 1 (Ak1), which catalyzes the phosphate transfer between ATP and AMP and is thus involved in cellular energy homeostasis (**Figure 13b**). Late upregulated proteins (10.5%) include Gfap, which is significantly increased in the late and in the long comparison (**Figure 13c**). Lysosomal enzyme palmitoyl-protein thioesterase 1 (Ppt1) is involved in the lysosomal degradation of lipid modified proteins and one of the few proteins with significant upregulation all age comparisons (**Figure 13d**). Early downregulated proteins make up 6.2% and include actin-binding spectrin beta chain (Sptbn4; **Figure 13e**). Involved in protein folding and co-chaperone of Hsp90, peptidyl-prolyl cis-trans isomerase D (Ppid) is one of the 4.9% late downregulated proteins (**Figure 13f**). Proteasome subunit beta type-6 (Psmb6), while only being significant in the long comparison, fits the trend of continuously decreasing proteins (**Figure 13g**). Proteins that decrease until 12 months and then increase again (12.2%) encompass the previously noticed neurofilaments, e.g., neurofilament medium polypeptide (Nefm; **Figure 13h**). Early up- and late downregulated proteins (10.7%) include the electron carrier somatic cytochrome c (Cycs; **Figure 13i**)

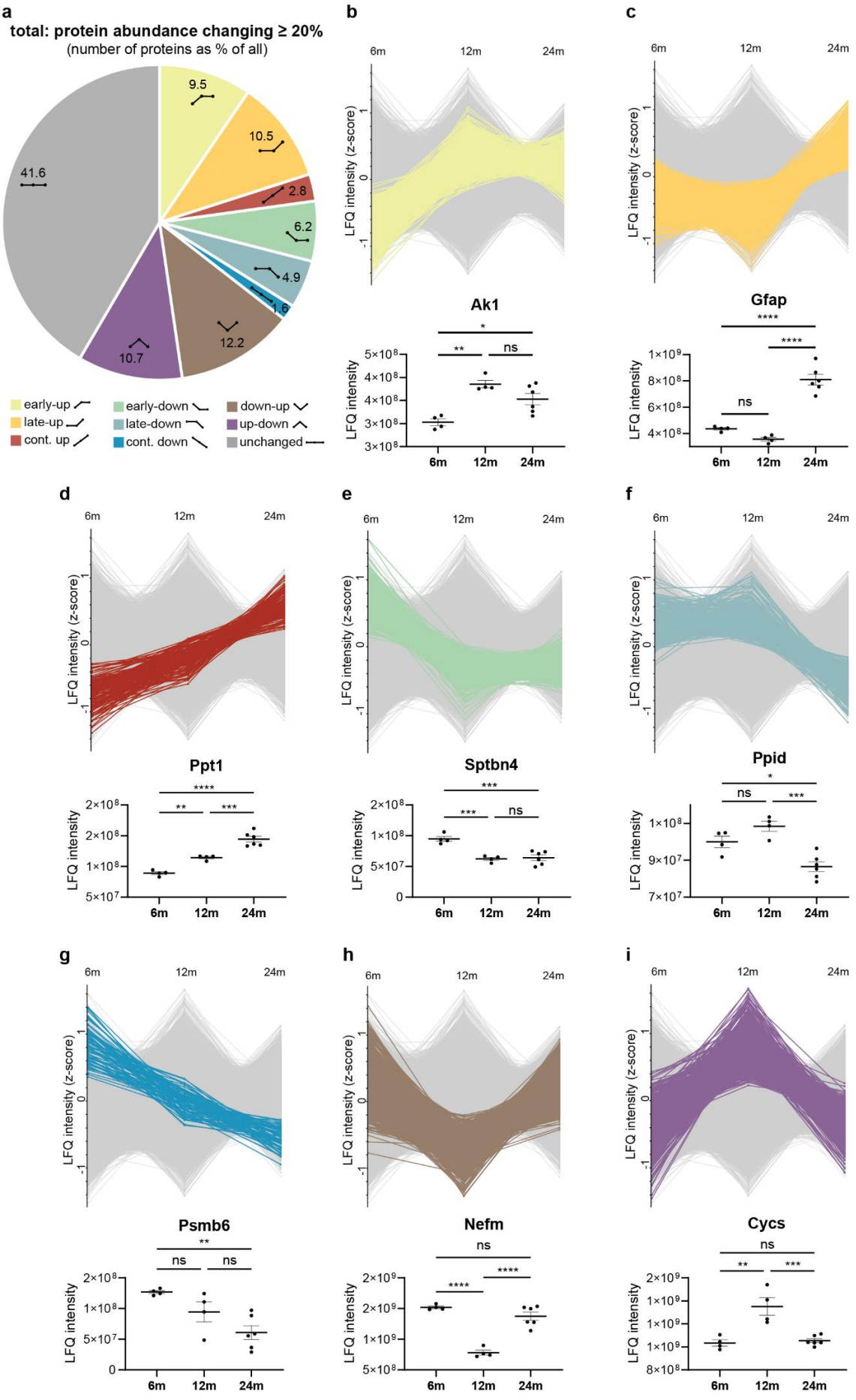

Figure 13 Proteins have different trajectories across age groups. **a** Pie chart showing the distribution of proteins changing at least 20% in either direction between the three ages, sorted into nine direction categories. **b-i** Line profiles of all age-

group average protein abundances per direction category, row z-score normalized, and exemplary proteins belonging to each direction category below. Points represent biological replicates (n=4-6); Tukey-corrected ANOVA; ns not significant, * p<0.5, ** p<0.01, **** p<0.0001. **b** Early upregulated proteins; **c** late upregulated proteins; **d** continuously upregulated proteins; **e** early downregulated proteins; **f** late downregulated proteins; **g** continuously downregulated proteins; **h** proteins decreasing early and then increasing again (down-up) and **i** proteins increasing early and then decreasing again (up-down).

Based on the overall distribution of protein abundances changing at least 20% with different trajectories (**Figure 13a**), I then examined whether any functional category of proteins has a relatively overrepresented direction change, for example a higher number of continuously upregulated proteins in a proportion that is not found overall (see **Figure 14** for exemplary calculation of 'relative distribution' and **Figure 15b**). **Figure 15** shows all functional categories with more than 50 protein members and their direction trajectory distributions, relative to the overall distribution.

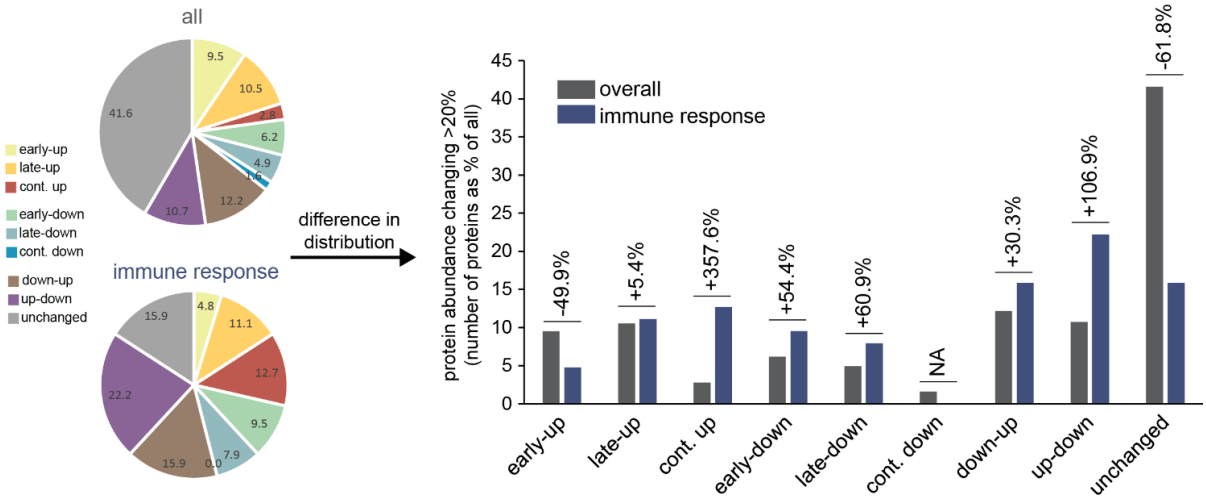

Figure 14 Exemplary transformation of protein direction distribution of the category 'immune response' into relative distribution values used in **Figure 15**. The numbers of proteins changing ≥20% in abundance in either direction category were collected for functional groups of proteins, see lower pie chart (immune response proteins). Each group's distribution was then compared with the overall distribution, upper pie chart and **Figure 13a**. The difference is used a 'relative distribution' value for summarizing **Figure 15**.

Extracellular matrix (ECM) and synapse associated proteins (synapse) have relatively more proteins late upregulated, energy- and neurotransmission-related proteins show fewer proteins with this directionality (**Figure 15a**). Proteins that are involved in immune regulation and response ('immune') have a direction trajectory distribution that differs greatly from the overall distribution (**Figure 15b**). Very few proteins are unchanged (36.5% of the general percentage), while a higher proportion is continuously upregulated (484.9% of the general percentage). Axon (guidance and morphology) proteins, chromatin, DNA, and transcription regulators as well as proteins involved in RNA, transcription and splicing processes also show the highest variation to the overall distribution in the category of continuously upregulated proteins, although other directionalities are overrepresented, too. Mitochondrial proteins show the strongest de-enrichment of continuously upregulated proteins, relatively more members remain unchanged over the three ages. In contrast, ribosomal proteins have a strong overrepresentation of late downregulated proteins and lack any continuously upregulated members (**Figure 15c**). Proteins of neurodevelopment, -growth and -survival also have higher proportions of late-downregulated members, followed by a high fraction of down-up expressed proteins. The groups of fatty acid metabolic regulators and proteins involved in the modification of glycosylation and sugars have relatively fewer members that are late-downregulated. The highest proportions of continuously downregulated proteins are found in the categories 'homeostasis regulation, stress response, detox', 'nuclear integrity and shuttling', 'calcium', 'protein degradation', 'intercellular adhesion and signaling' as well as 'intracellular trafficking and transport' (**Figure 15d**). Ubiquitin- and SUMOylation related proteins show higher relative enrichment of proteins

that are downregulated towards 12 and then upregulated towards 24 months (**Figure 15e**). Lastly, chaperones and cytoskeletal proteins most strongly deviate from the overall direction distribution by having relatively fewer proteins that are first up- and then downregulated (**Figure 15f**).

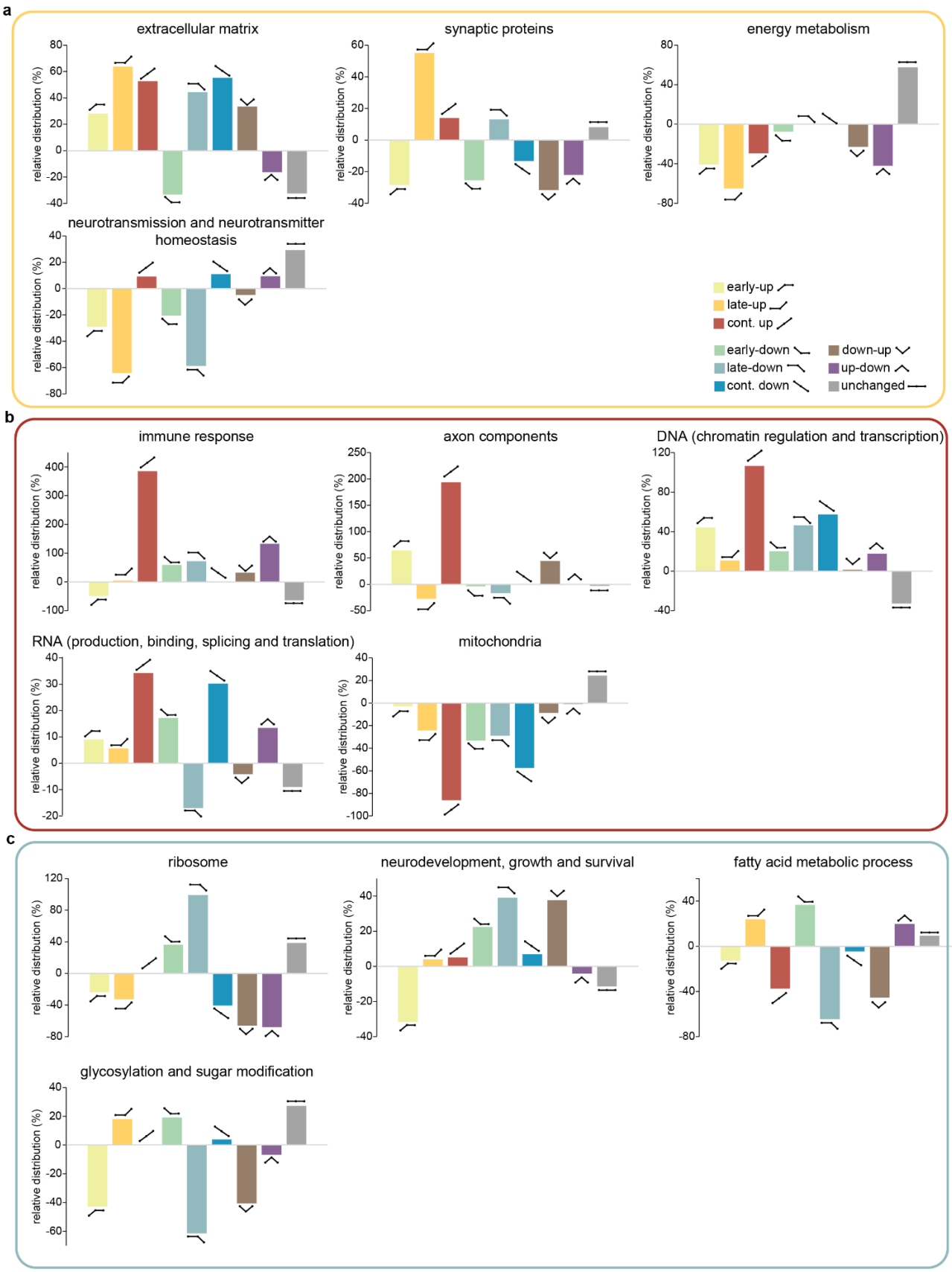

Figure 15 Proteins have different abundance trajectories between samples of 6-, 12-, and 24-months old WT mice. All quantified proteins have been sorted according to their change between the three ages, with a cutoff of 20% change. Bars

show the relative enrichment or de-enrichment of a certain direction-class compared to the overall distribution in % (see **Figure 6b**) and are summarized for functional categories with >50 protein members. Graphs are sorted in the figure (left to right) according to their highest deviation (positive or negative). **a-f** Functional protein classes with greatest deviation from the overall distribution per respective direction category, color coded by the surrounding frame.

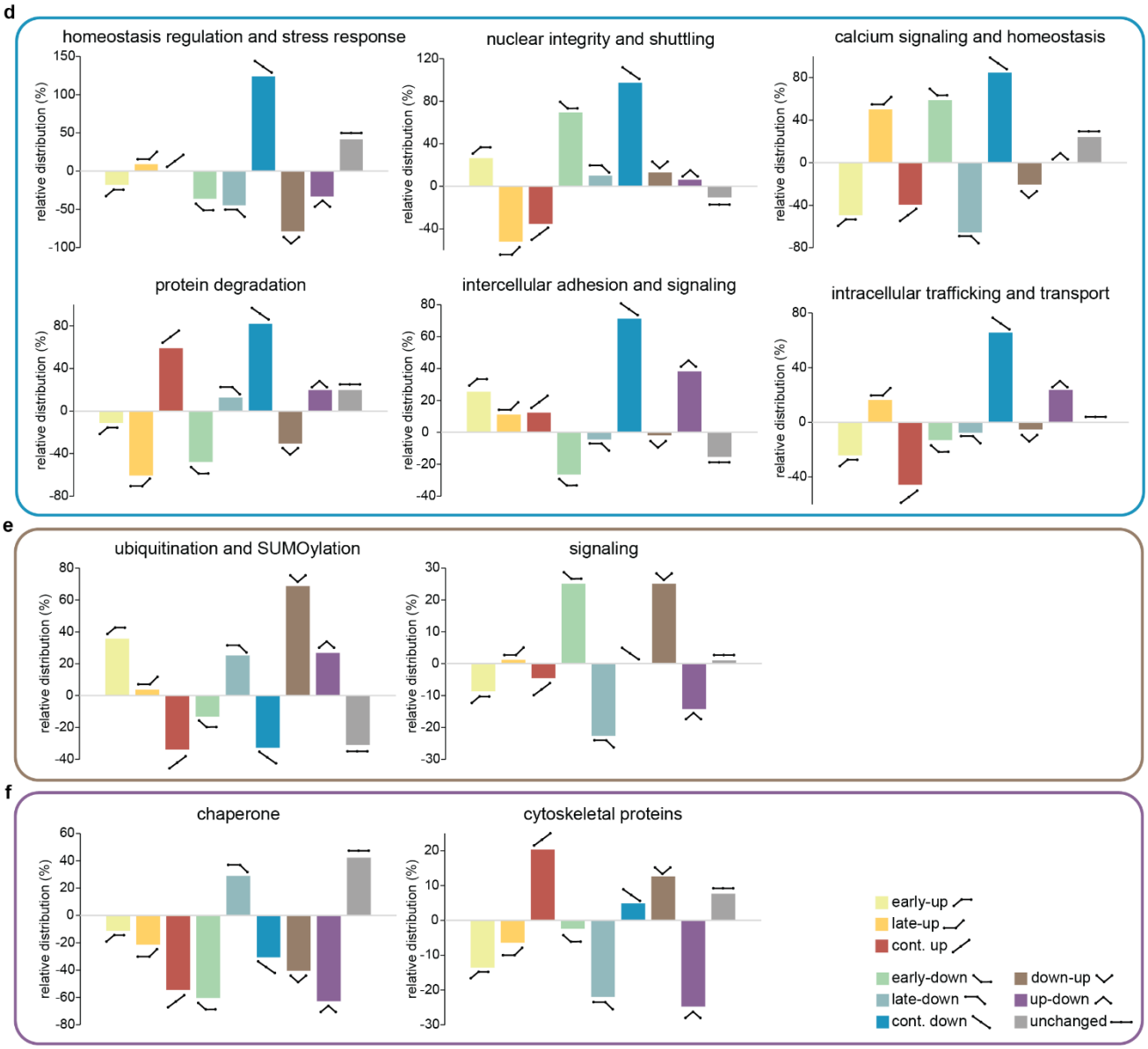

Figure 15 (continued)

These results, while multifaceted and complex in their interpretation, provide insights into the variation of proteins within a functional category as well as implication of that category for age-related processes. Further analyses based on my classifications can potentially elucidate complexes and networks of proteins that are regulated together or that influence each other, which were not noticed or connected previously.

4.2.2 | Correlations between RNA and protein levels are minimal

As correlations between RNA expression and protein abundance are generally small (Vogel and Marcotte, 2012), I was interested in whether either total or nuclear RNA might show higher correspondence to my total protein abundances and if any functional groups would emerge. I calculated the Pearson correlation of each protein that was found in all biological replicates of the total fraction in my physiological aging cohort with its respective RNA abundance in the total or nuclear fraction (row correlation across all biological ages of the three ages, 6-, 12-, and 24 months).

Overall, the thus obtained ~3300 row correlations were not significantly different between total and nuclear RNA and widely spread (t-test with Welch correction p=0.1544; **Figure 16a**). The proteins with the highest correlation of protein and RNA abundance (in both total and nuclear fraction) across all three ages are (among others) Gfap, Psmb6, Nefh and Nefl, with Pearson's r coefficients >0.6. Negatively correlated to both total and nuclear RNA are protein abundances of 26S proteasome regulatory subunit 6A (Psmc3), spectrin beta chain (Sptbn2) and Plec, to name a few. See **Figure 16b** and **Supplementary Table 6** for all correlations). Beyond single proteins being better correlated than others, no significant functional grouping was possible.

Further, the fold change differences of proteins between the early and late age comparisons (logFCs of 12 vs 6 and 24 vs 12) were not significantly correlated with fold changes observed in RNA levels (column correlation; **Figure 16c, d**). The marked exception are FCs between 24 and 6 months, which are very slightly but significantly correlated between protein and nuclear RNA (Pearson's r=0.04123, p=0.0042), but not with total RNA (r=-0.003068, p=0.8316).

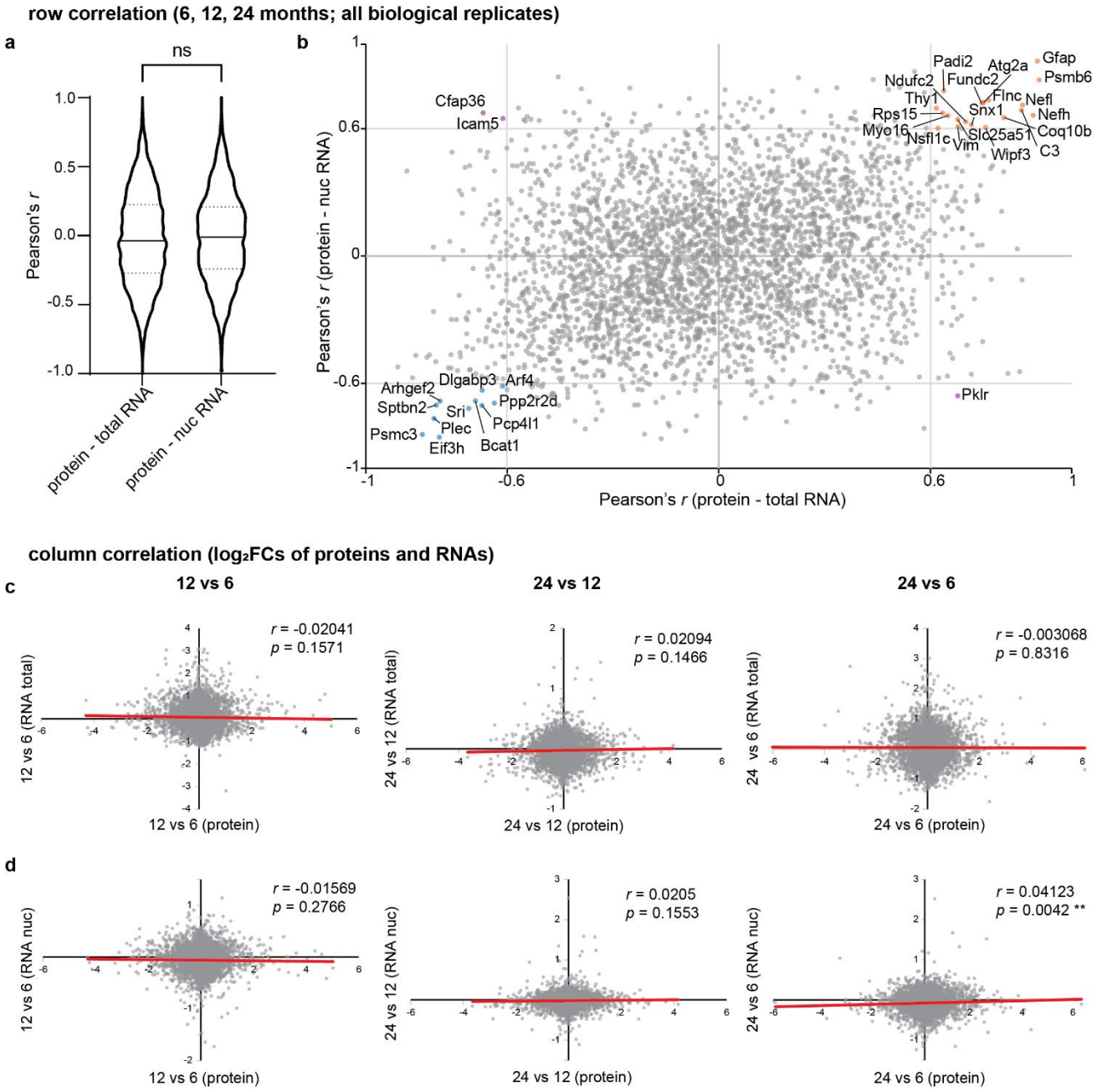

Figure 16 Correlations between RNA and protein abundances. **a** Row correlations were calculated using Pearson's *r* for all proteins that had measurements in every biological replicate across ages for protein abundance, total, and nuclear RNA abundance. Correlations are small and not differently distributed between total and nuclear RNA (Welch's t-test, p=0.1544). Violin plots show distribution of correlation values, middle line represents median, dashed lines represent quartiles. **b** Scatter plot of Pearson's *r* correlation values between protein and total RNA (x-axis) and between protein and nuclear RNA (y-axis) abundances. Colored in orange are proteins with correlation >0.6 in both total and nuclear RNA, colored in blue are correlation values <-0.6 for both comparisons. Purple points represent reverse signs of correlations between total and nuclear RNA and protein abundance (positive correlation in one fraction, negative in the other and *vice versa*). **c** and **d** Column correlations between logFCs of proteins and RNAs in early (12 vs 6), late (24 vs 12) or overall (24 vs 6) aging. **c** shows logFCs of protein and total RNA, **d** shows the logFCs of protein and nuclear RNA. Red line shows correlation between each set of values and Pearson's *r*, as well as *p*-value of correlation are indicated for each graph.

4.2.3 | Insoluble fraction

Next, I analyzed the protein abundance results from my insoluble fraction. While I quantify ~4700 proteins across all ages, their enrichment compared to the abundance in the total fraction changes considerably. **Figures 17a-c** show the number of proteins per enrichment score (ratio insol vs total) for proteins de-enriched or non-enriched (ratio 0-2), enriched (ratio 2-10) and highly enriched (ratio 10-50) per age. The extend of enrichment increases with advancing age and enriched proteins (ratio 2-50) are significantly more present in 12- and especially 24 months old animals (**Figure 17d**). Additionally, I compared my insoluble enrichment results from 24 months old animals with previously published results (Kelmer Sacramento et al., 2020) and found significant high correlation (Pearson's r=0.6236, p<0.0001) of overlapping proteins from both studies (**Figure 17e** and **Supplementary Table 7**). This correlation was even higher, when I compared my results to only those found significant in the study by Kelmer Sacramento et al. (Pearson's r=0.7899, p<0.0001; **Figure 17f**). Lastly, I found a small, but highly significant correlation of my insoluble enriched proteins to the solubility score, introduced by Määttä et al., 2020 (**Figure 17g**). The more negative the score, the more likely a protein is to aggregate after non-lethal heat shock in human cells.

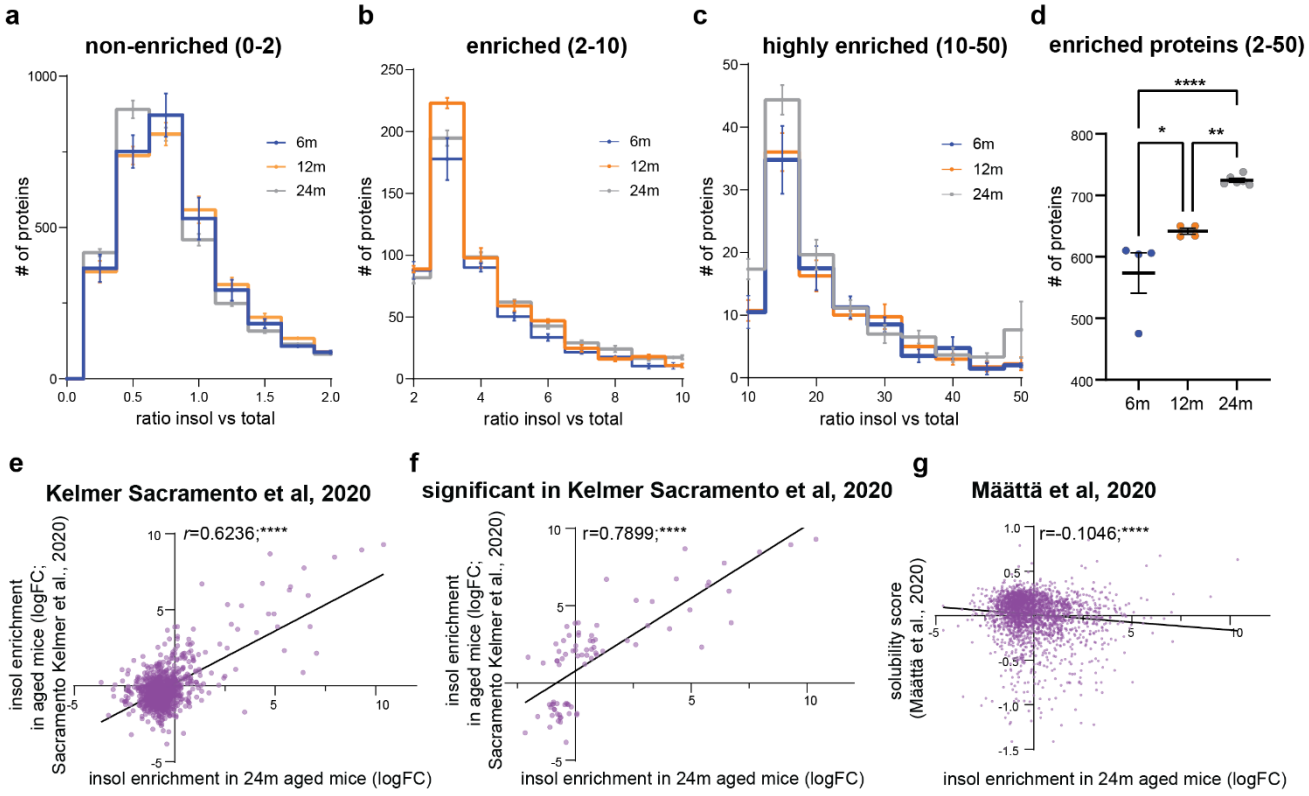

Figure 17 Increasing enrichment of insoluble proteins with age and correlations to previously publishes works. **a-c** Histograms showing the number of proteins that are non-enriched in the insoluble fraction (ratio insol vs total between 0 and 2; **a**), enriched (ratio between 2 and 10; **b**) and highly enriched (ratio 10-50; **c**) per age group. **d** Combined comparison of enriched and highly enriched proteins between 6, 12 and 24 months shows increasing insolubility of proteins with age. Ordinary one-way ANOVA with Tukey correction. **e, f** comparison of insoluble-enriched proteins between my study and the study by Kelmer Sacramento et al. **e** Shows the correlation of all common proteins and their insoluble enrichment at 24 months between the two studies, **f** shows the correlation between the significantly enriched proteins from the Kelmer Sacramento study and my data. **g** Correlation of my insoluble enrichment data to the protein solubility score introduced by Määttä at al., 2020. Note that increasing negative solubility score indicates higher aggregation propensity. Correlations are indicated as Pearson correlation coefficient. * p<0.5, ** p<0.01, **** p<0.0001.

DEqMS identifies several proteins significantly changed in the insoluble fraction with age, listed in **Figure 18a**. Annexin A11 (Anxa11), Gfap and ribosomal protein Rpl29 are prominently upregulated with age, while,

surprisingly, among others, alpha synuclein (Snca) is downregulated. The differential expression analyzed here does not however consider the relative enrichment vs the total fraction. I calculated the insoluble enrichment for each protein that had abundance measures in both total and insoluble fraction, corrected for possible enrichment also seen in the soluble fraction (see Methods for details) and performed ANOVA testing with permutation-based multiple comparison correction to find 18 proteins significantly changing their insoluble enrichment with age (**Figure 18b** and **Supplementary Table 7**).

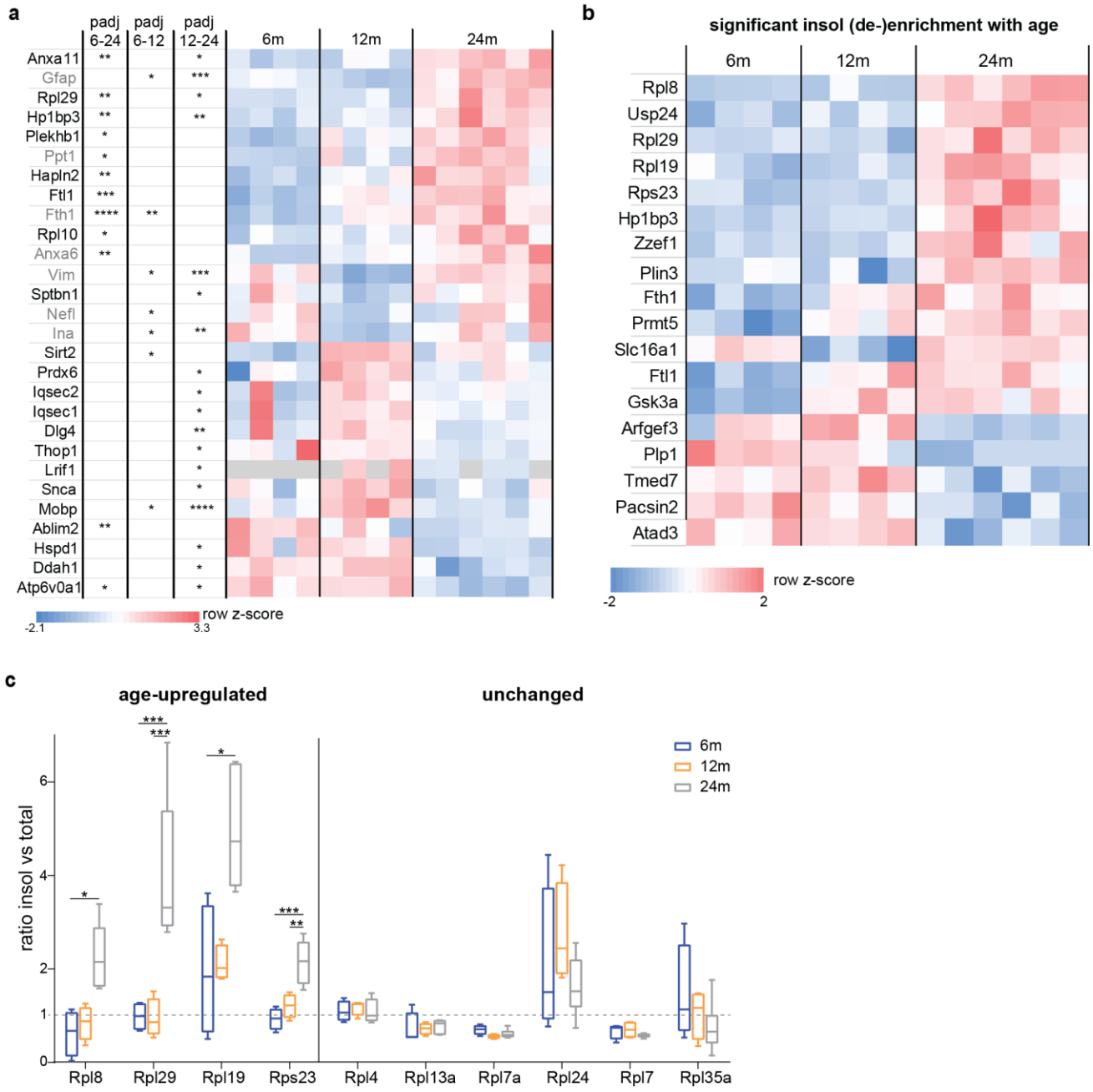

Figure 18 Differentially expressed protein in the insoluble fraction. **a** Heatmap showing all proteins significantly changed in the insoluble fraction in any of the age-comparisons. Columns show the DEqMS adjusted *p*-value significances and all biological replicates. Protein names in grey are also found significantly changed in the total fraction. Grey fields in the heatmaps indicate missing values. **b** Heatmap showing the 18 significantly changing proteins in terms of insoluble enrichment with age. **c** Some ribosomal components have specific age-upregulated enrichment in the insoluble fraction, others are unchanged or age-downregulated. Selection of ribosomal proteins based on own data and Kelmer Sacramento et al., 2020. Boxplots show median, 25th to 75th percentile as box and 5th to 95th percentile as whiskers, significance tested with ANOVA and Tukey multiple comparison correction. * p<0.5, ** p<0.01, *** p<0.001, **** p<0.0001

Ribosomal proteins Rpl8, Rpl29, Rpl19, Rps23 as well as ferritin light and heavy chain (Fth1 and Ftl1) are highly enriched in the insoluble fraction of 24 months old brains, as has been previously described (Kelmer Sacramento et al., 2020). Fth1 and Ftl1 enrichment are gradual and present already at 12 months. Monocarboxylate transporter 1 (Slc16a1) shows noticeably de-enrichment at 12 months. Brefeldin A-inhibited guanine nucleotide-exchange protein 3 (Arfgef3), myelin proteolipid protein (Plp1), transmembrane p24-trafficking protein 7 (Tmed7), protein kinase C and casein kinase substrate in neurons protein 2 (Pacsin2) and ATPase family AAA domain-containing protein 3 (Atad3) are insoluble-enriched until high age, where they become relatively more soluble.

I show here that the enrichment of some ribosomal components is exclusively found in the oldest animals. Other ribosomal proteins found significantly enriched in Kelmer Sacramento et al., 2020 however show little change in enrichment with age (Rpl4, Rpl13a, Rpl7a, Rpl24 and Rpl7) and Rpl35a even shows gradual de-enrichment from 6 to 12 months (**Figure 18c**). These insolubility changes with age can disrupt complex stoichiometries and affect a number of pathways, which will be discussed at the end of this work (section 5.4).

4.3 | Proteomic description of brain aging in mouse models

In addition to the description of physiological brain aging presented so far, I set out to study and compare the proteome of 12 other cohorts of mice which model aging. Notably, the average lifespan of mice differs already between inbred strains, ranging from ~8 months in female AKR/J to ~32 months in male WSB/EiJ (Yuan et al., 2009). The most widely used inbred strain C57BL/6J (BL6J), which I also use here for my cohort of physiological aging, has an average lifespan of ~28 months. Genetic modifications, altering the lifespan of animals, are also dependent on the background strain into which the modification was introduced. **Figure 19** summarizes the ages and lifespans of all cohorts used for this study with both their 'natural' life expectancy, as well as their lifespan after genetic, dietary or enrichment manipulation. Ages were chosen so that mice showed 'aging' defects without overwhelming damage load, meaning before severe pathological alterations would obscure underlying changes. All cohorts included littermate controls to which the model could be directly compared (**Supplementary Table 2**). Consistent quality of measurements was achieved by streamlined sample preparation and periodic assessment of mass spectrometric performance. All ~650 spectral files acquired by LC-MS, including the extensive spectral library that was prepared, were analyzed together using MaxQuant and the 'match between runs' feature. This allowed the calculation of ratios 'model vs control' for 7541 proteins, of which 5141 were measured in at least 6 cohorts. I here present the results for each cohort individually in brief, further analyses will be performed in our group and all data will be deposited to be publicly available at the PRIDE database.

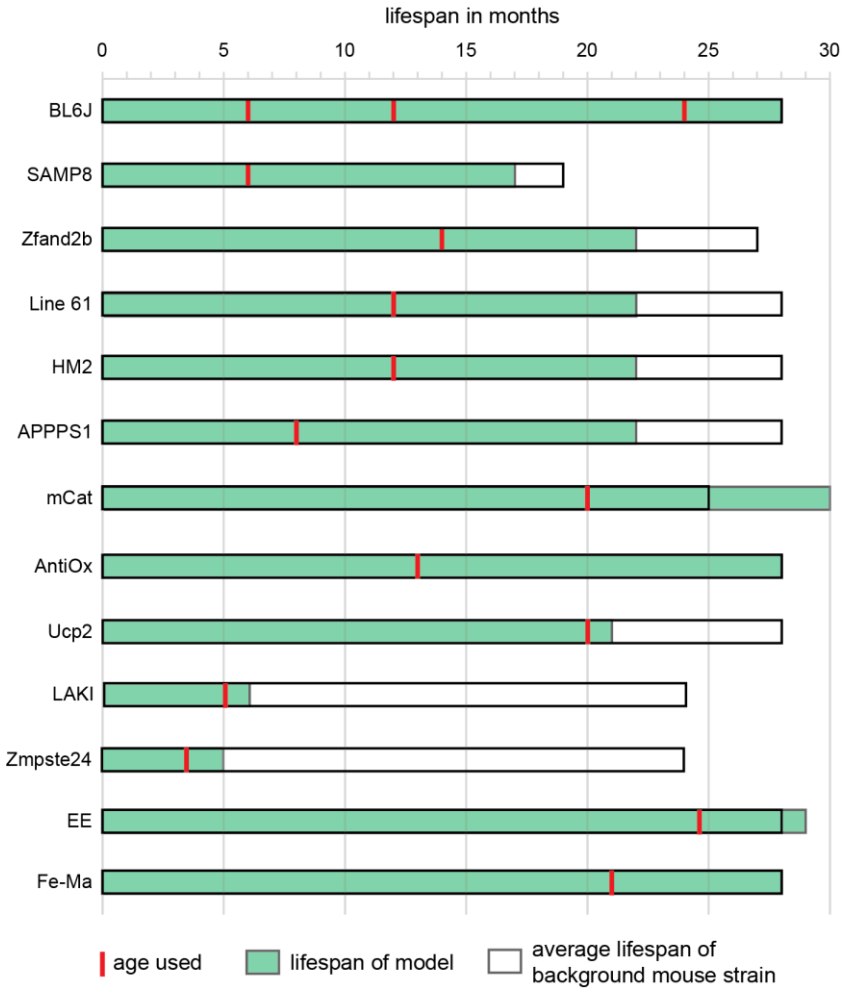

Figure 19 Overview of average lifespan and used ages of mouse model cohorts used in this study. General average lifespan of the specific mouse strain is indicated in white. If the model has extended or decreased lifespan, this is indicated in the

overlaid green. The red line marks the age used here. Age in months. Note that the mCat and EE models prolong their background strain lifespan. Data on lifespan was retrieved from the original publications for each model, which will be referenced in the respective following sections.

4.3.1 | SAMP8

Before the establishment of genetic models, several mouse lines were developed by selective breeding that showed a precocious or delayed aging phenotype. The senescence-accelerated mouse (SAM) lines developed by Takeda and colleagues (Takeda et al., 1981) are one example. Mouse lines presenting typical 'aging phenotypes' were called senescence-prone (SAMP), lines without aging signs senescence-resistant (SAMR). SAMP8 mice show several brain-related deteriorations and can thus model neurodegeneration and accelerated aging, likely tracing back to metabolic pathway alterations (Currais et al., 2019; Dobarro et al., 2013; Grinan-Ferre et al., 2018; Ohta et al., 1996; Takeda, 2009).

400 proteins are significantly different between 6 months old SAMP8 and SAMR1 mice in the total fraction (**Figure 20a** and **Supplementary Table 8**). 248 are upregulated, which ORA analysis identifies as enriched in the GO BP term 'pyridine-containing compound metabolic process' (**Figure 20b**). STRING protein-protein interaction networks functional enrichment analysis (from here on referred to as 'STRING analysis') of the top 100 significantly upregulated proteins further identifies the partly overlapping 'cellular respiration' (FDR=0.0036), 'cellular amino acid metabolic process' (FDR=0.0003) and 'generation of precursor metabolites and energy' (FDR=0.00043) with high confidence interaction scores (**Figure 20c**). Among the top 100 significantly downregulated proteins, 'myelin sheath' is the top hit (FDR=0.0095), with major myelin proteins Mog, Cnp and Plp1 moderately decreased (**Figure 20d**).

Interestingly, compared to the high number of differentially expressed proteins in the total fraction, only 4 proteins reach that threshold in the insoluble fraction (**Figure 20e**). These are the increased G-protein coupled receptor Gpr37l1, guanylate cyclase Gucy1a2, ribosomal Rps18 and decreased unconventional myosin Myo1d. 17 other ribosomal proteins are increased in the insoluble fraction among the proteins changed with non-adjusted *p*-value <0.05. This class of proteins is significantly enriched in ORA analysis (**Figure 20f**), together with NDD-categories 'Alzheimer disease', 'Huntington disease' and 'Parkinson disease', which include Snca, and several mitochondrial electron transport chain proteins implicated in disease.

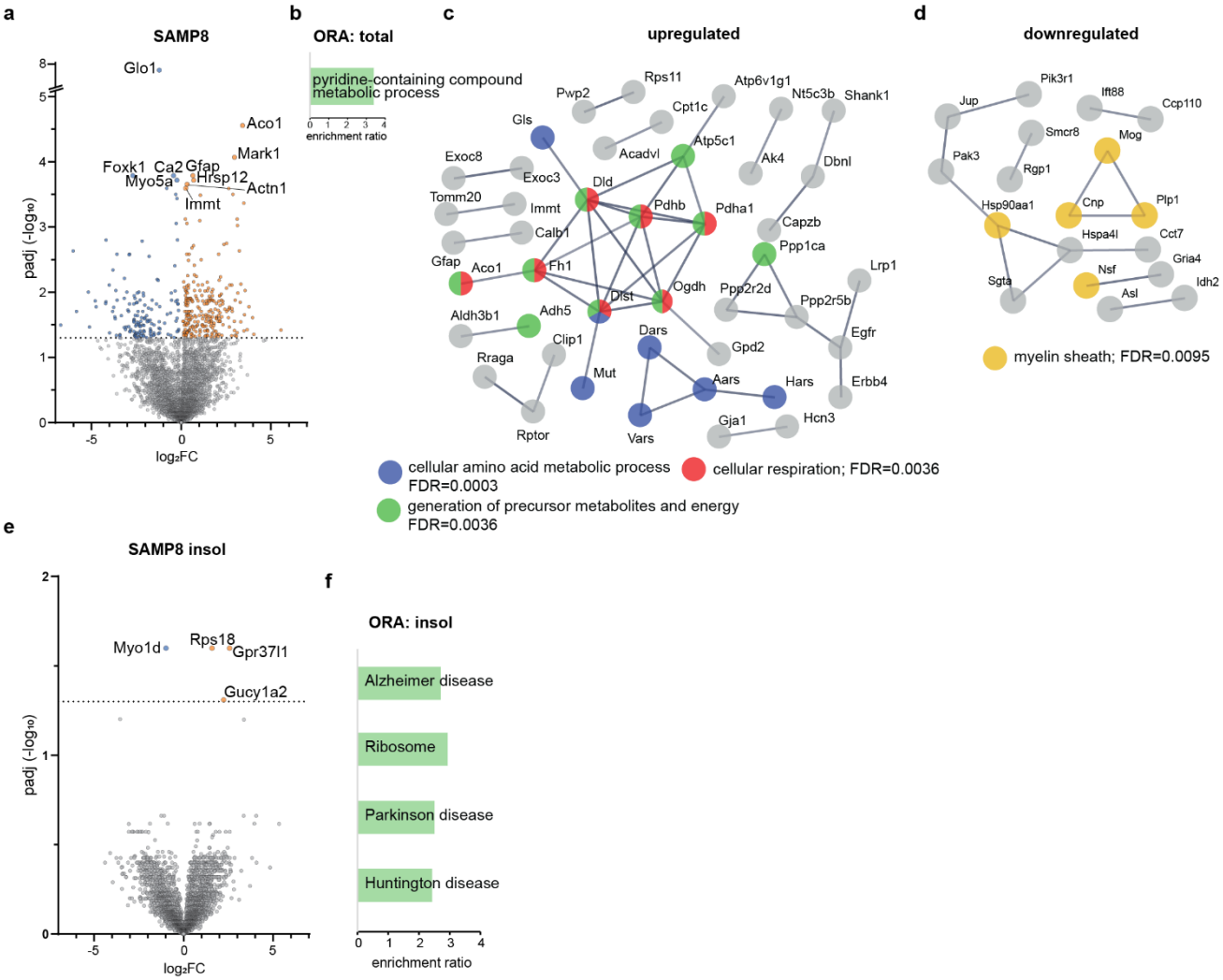

Figure 20 Overview of differentially expressed proteins in the SAMP8-mice (vs control SAMR1 mice). **a** and **e** Volcano plots, indicating *padj* (as -log10) and log2FC between model vs its own control in the total (**a**) and insol (**e**) fraction. Signifcant proteins indicated in orange (upregulated) and blue (downregulated); horizontal dotted line indicates *padj*-value cutoff at 0.05. **b** Significantly upregulated proteins in the total fraction with WebGestalt ORA analysis and **c** STRING functional enrichment network. **d** STRING functional enrichment network for downregulated proteins in the total fraction. Core GO or pathway annotations after high-confidence interaction score filtering are color-coded. **f** WebGestalt ORA analysis of the non-adjusted p significant upregulated proteins in the insoluble fraction. GO categories are all FDR<0.05 and sorted with the most significant on top.

4.3.2 | Zfand2b: KO of proteostasis factor AIRAPL

Proteostatic balance is closely linked to cellular and organismal health and heavily implicated in aging. In *C. elegans,* proteostasis impairment caused by inactivation of ER protein AIP-1, shortened the lifespan of the animal (Yun et al., 2008). Its ortholog AIRAPL (*Zfand2b*) seems to play a role in the insulin/insulin-like growth factor 1 (IGF1) pathway by regulating the translocation and degradation of IGF1 receptor (Osorio et al., 2016). It is therefore likely, that energy pathways and metabolism are altered, too. Zfand2b-KO-mice show reduced lifespan of 22 months compared to 27 months of controls (Osorio et al., 2016). My available samples of 14 months old mice represent a middle-aged to aged cohort.

I found 6 proteins significantly changed in the total fraction, the two moderately upregulated proteins are Proline-rich transmembrane protein 2 (Prrt2, component of the outer core AMPAR complex) and Lmna, the downregulated proteins show stronger differences (FC at least -1.5), three are RNA-processing related (RNA

helicase aquarius (Aqr), nucleolar and coiled-body phophoprotein 1 (Nolc1), and nuclear cap-binding protein subunit 1 (Ncbp1); **Figure 21a** and **Supplementary Table 9**).

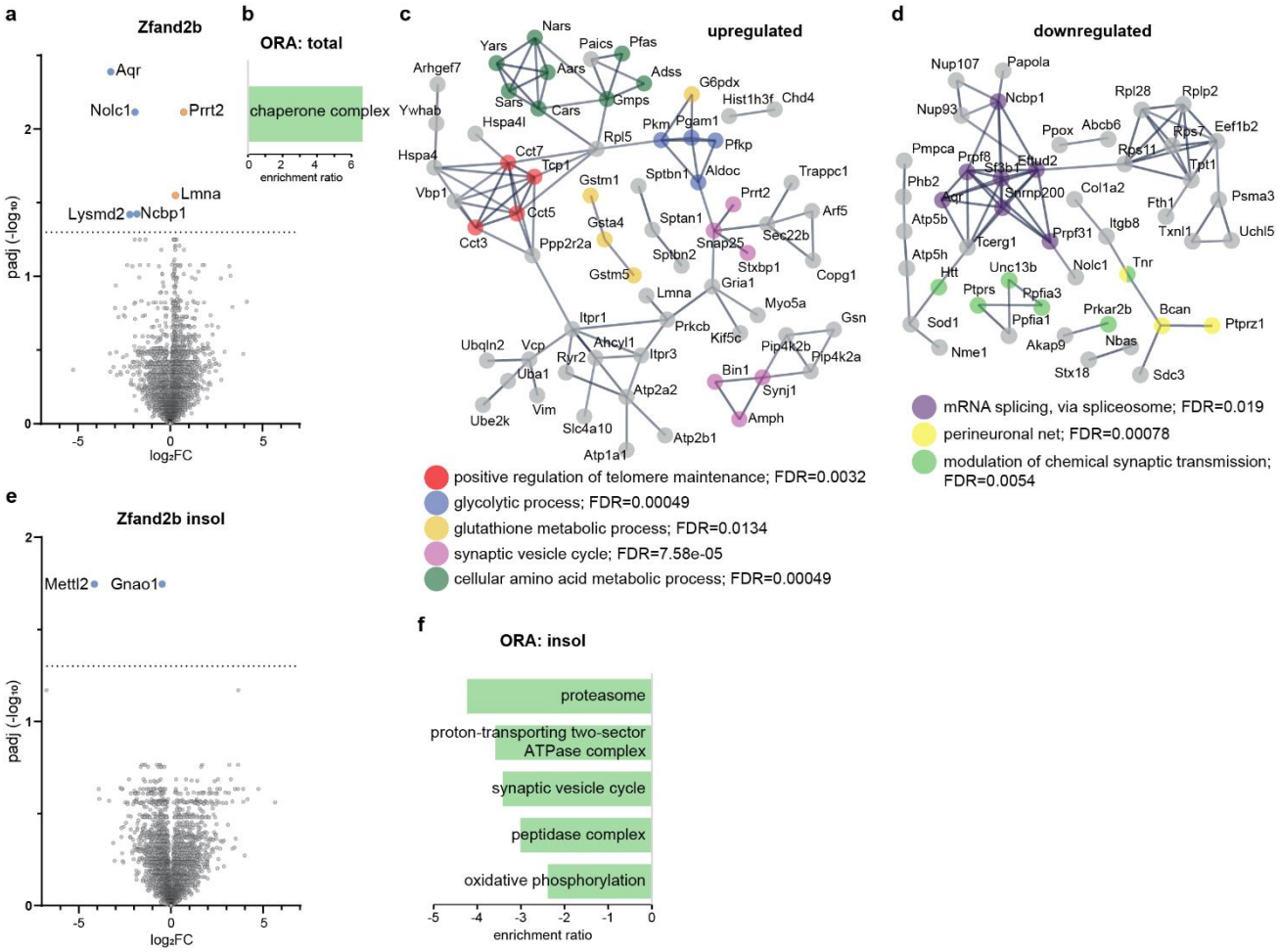

Figure 21 Overview of differentially expressed proteins in Zfand2b-mice. **a** and **e** Volcano plots, indicating *padj* (as -log10) and log2FC between model vs its own control in the total (**a**) and insol (**e**) fraction. Signifcant proteins indicated in orange (upregulated) and blue (downregulated); horizontal line is *padj*-value cutoff at 0.05. **b** WebGestalt ORA analysis of the upregulated, non-adjusted p significant proteins implicate increased levels on chaperone complex proteins in Zfand2b-mice. **c, d** STRING functional enrichment network for upregulated and downregulated proteins in the total fraction, respectively. Core GO annotations after high-confidence interaction score filtering are color-coded. **f** WebGestalt ORA analysis of the downregulated, non-adjusted *p* significant proteins in the insoluble fraction.

With the less strict cutoff of unadjusted *p*-value, 590 proteins are changed. The 427 upregulated proteins are enriched in the term ‘chaperone complex’, identified by ORA (GO cellular component (CC); **Figure 21b**). This enrichment is driven by upregulated chaperonin-containing T-complex (TRiC) members, of which 4 are among the top 100 significant upregulated proteins. Interestingly, STRING high confidence interaction score analysis of these top 100 links TriC to telomere maintenance. Other STRING functional enrichments among the top 100 upregulated proteins include ‘glycolytic process’ (FDR=0.00049), ‘glutathione metabolic process’ (FDR=0.0134), ‘synaptic vesicle cycle’ (FDR=7.58e-05) and ‘cellular amino acid metabolic process’ (FDR=0.00049; **Figure 21c**). Fewer proteins are downregulated, the top 100 of them (sorted by significance, $p<0.05$) mirror the splicing implication seen already in the *padj*-significant proteins. STRING analysis finds ‘mRNA splicing, via spliceosome’ (FDR=0.019), ‘modulation of chemical synapse transmission’ (FDR=0.0054) and the ‘perineuronal net’ (FDR=0.00078). Several ribosomal proteins are also mapped, but do not show functional enrichment (**Figure 21d**).

Only 2 proteins are significantly changed in the insoluble fraction of Zfand2b-KO mice. One is the strongly decreased tRNA methyltransferase Mettl2, the other is moderately decreased guanine nucleotide-binding Gnao1. After loosening the threshold cutoff to non-adjusted $p<0.05$ (533 proteins changed), no prominent GO or pathway enrichment among the upregulated proteins was identified. However, the 313 decreased proteins are enriched in GO CC 'peptidase complex', 'proton-transporting two-sector ATPase complex', KEGG 'proteasome', 'synaptic vesicle cycle' and 'oxidative phosphorylation' in ORA analysis (FDR<0.05).

4.3.3 | Line 61: overexpression of human α-synuclein

The mouse line called 'Line 61' overexpresses human α-synuclein under the Thy1 promoter at moderate levels and models PD in several aspects (Rockenstein et al., 2002). Although no neuron loss is observed in the substantia nigra (even at 22 months of age), dopamine levels decline after 8 months and strong α-Synuclein aggregates are detected already at 1 month of age. I examined animals of 12 months of age.

I found 92 significantly changed proteins (**Figure 22a**), the top significant hit compared to littermate controls being moderately upregulated Snca (characteristic for this mouse model; Rockenstein et al., 2002). 66 proteins were upregulated, without significant enrichment in any GO annotation among them. STRING analysis implicates them in the expected Kyoto Encyclopedia of Genes and Genomes (KEGG) classification 'Parkinson disease' (FDR=0.0378), as well as GO BP categories 'regulation of catalytic activity' (FDR=0.0063) and 'glucose metabolic process' (FDR=0.0140). For the 26 downregulated proteins, no FDR-significant GO or pathway annotation was found. Once I extended my analysis of the downregulated proteins to include those that were non-adjusted *p*-value significant, many synaptic vesicle-related proteins became apparent, including Snap25, Stxbp1, Syt5, Syn2, Syn3, Synj1 and others (**Figure 22b, c** and **Supplementary Table 10**).

As this model relies on the overexpression of Snca, I wanted to know which proteins have the highest correlation in terms of their abundance in mutant and WT mice. Among the significantly upregulated proteins, 15 proteins have a correlation Pearson's $r>0.83$ and $p<0.01$ (**Supplementary Table 10**), meaning that their abundance might be tightly linked to that of Snca. These include two components of the COP9 signalosome (Cops4 and Cops3), three (co-)chaperones (Fkbp4, Hspa4l and Hspd1), two ADP transmembrane transporters (Slc25a31 and Slc25a42) and the iron binding serrotransferin (Tf). The strongest negative correlation among the significant proteins had dynactin 6 (Dctn6), a member of the dynactin family, which is involved in Lewy body pathology (Shen et al., 2018). Dctn6 is followed by the two synapsins, Syn1 and Syn2, the serine hydrolase Rbbp9 and the GTPase Atl3, which functions in ER remodeling.

In the insoluble fraction, only 6 proteins are significantly different between mutant and WT mice after multiple comparison correction (**Figure 22d**). Only Cox6a1 and Gpd2, which is also upregulated in the total fraction, are upregulated. These proteins remain relatively more abundant in the mutant insoluble fraction also when looking at the insoluble enrichment (compared to the total fraction). Snca is the fourth most significantly upregulated protein when also considering the non-adjusted *p*-value. Among the top 100 (sorted by *p*-value significance) upregulated proteins in the insoluble fraction, 'oxidative phosphorylation' (FDR=0.0037), 'calcium ion transmembrane transport' (FDR=0.0196) and 'organonitrogen compound biosynthetic process' (FDR=0.0015) are functionally enriched in a STRING network analysis (**Figure 22e**). The top 100 downregulated proteins in

the insoluble fraction are enriched in ‘regulation of telomere maintenance’ (FDR=0.0291), ‘exocytosis’ (FDR=0.0454) and ‘regulation of neuron apoptotic process’ (FDR=0.0291; **Figure 22f**).

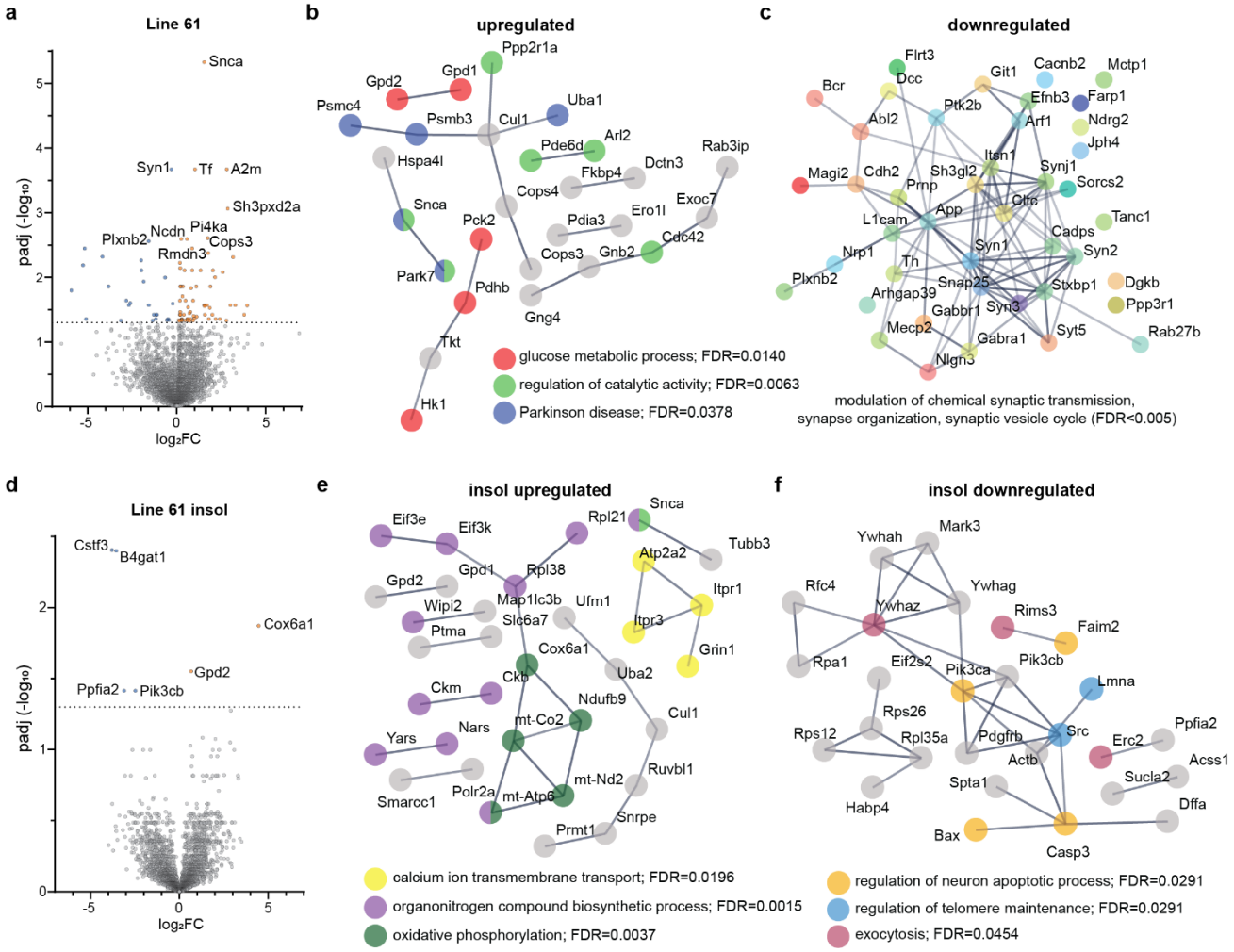

Figure 22 Overview of differentially expressed proteins in Line 61-mice. **a** and **d** Volcano plots, indicating *padj* (as -log10) and log2FC between model vs its own control in the total (**a**) and insol (**d**) fraction. Signifcant proteins indicated in orange (upregulated) and blue (downregulated); horizontal dotted line indicates *padj*-value cutoff at 0.05. **b** STRING functional enrichment network for upregulated proteins in the total fraction. Core GO or pathway annotations after high-confidence interaction score filtering are color-coded. **c** STRING network of synaptic proteins that are downregulated in Line 61-mice. **e** and **f** STRING functional enrichment network for up- and downregulated proteins, respectively, in the insoluble fraction. Core GO or pathway annotations after high-confidence interaction score filtering are color-coded.

4.3.4 | HM2: overexpression of human α-synuclein mutants A30P and A53T

The HM2-model expresses two mutant forms of human α-synuclein (A30P and A53T) under the Th1 promoter, thereby targeting it to dopaminergic neurons. Proteasome dysfunction, progressive dopaminergic neuron loss in the substantia nigra and consequent abnormalities in the dopaminergic system occur (Chen et al., 2006; Richfield et al., 2002). A more recent proteomic study of 6 months old HM2 mice confirmed these changes and additionally found altered mitochondrial function, oxidative and ER stress (Yan et al., 2017).

I found only 5 proteins significantly changed, all of them downregulated, in 12 months old HM2 mice compared to their controls (**Figure23a** and **Supplementary Table 11**). 475 proteins are changed with $p<0.05$, among them the upregulated Snca (FC=1.15; $p= 0.0004$). The 216 upregulated proteins are STRING GO BP annotated as, among other terms, ‘NLS-bearing protein import into nucleus’ (FDR=0.0138), ‘Golgi organization’

(FDR=0.0415) and ‘regulation of synapse organization’ (FDR=0.0402). The cellular component ‘postsynapse’ is also functionally enriched among the top 100 upregulated proteins, sorted by significance (**Figure 23b**). Proteins here include Snca, Htt, and Mtor. 259 proteins are downregulated, and STRING high confidence interaction score analysis identifies core GOs such as ‘leucine catabolic process’ (FDR=0.0274), ‘tRNA aminoacylation for protein translation’ (FDR=0.0338), ‘ribose phosphate biosynthetic process’ (FDR=3.32e-05), ‘lipid modification’ (FDR=0.0482), ‘enzyme regulator activity’ (FDR=0.0251), ‘U2-type catalytic step 2 spliceosome’ (FDR=0.0305) and 'proteasome complex’ (FDR=0.0111).

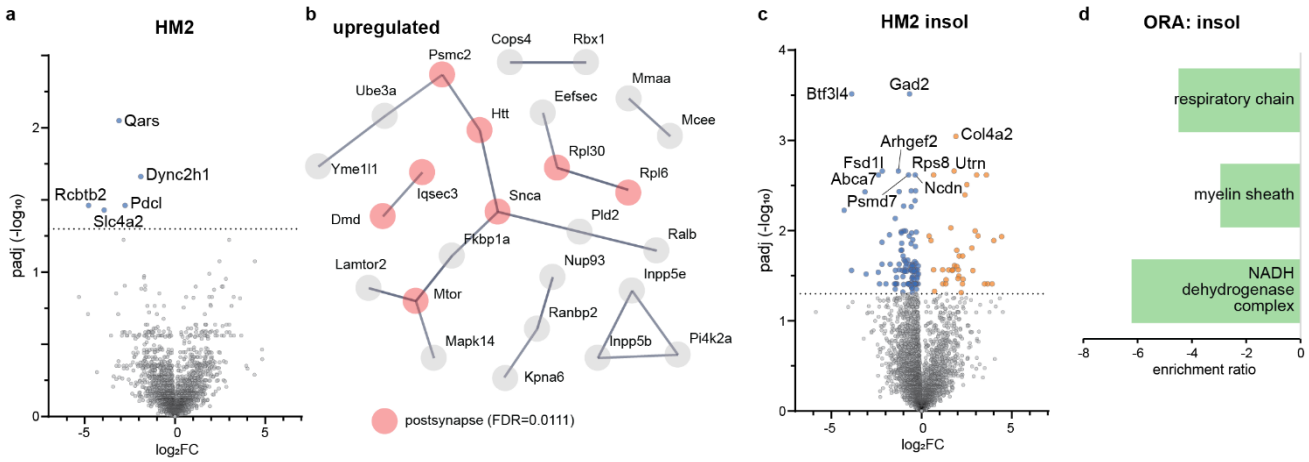

Figure 23 Overview of differentially expressed proteins in HM2-mice. **a** and **c** Volcano plots, indicating *padj* (as -log10) and log2FC between model vs its own control in the total (**a**) and insol (**c**) fraction. Signifcant proteins indicated in orange (upregulated) and blue (downregulated); horizontal line indicates *padj*-value cutoff at 0.05. **b** STRING functional enrichment network for the top 100 significantly upregulated proteins (p>0.05). Core GO annotation after high-confidence interaction score filtering is color-coded. **d** WebGestalt ORA analysis of the downregulated, *padj* significant proteins in the insoluble fraction.

In terms of Snca correlating proteins within all non-adjusted p<0.05 proteins, 6 proteins have a positive correlation Pearson’s r>0.83 and p<0.01. This is the COP9 signalosome member Cops4, the regulator of microtubule dynamics protein 3 (Rmdn3), which both also correlate well with Snca levels in the Line 61 model. Further, UDP-N-acetylhexosamine pyrophosphorylase-like protein 1 (Uap1l1), which is implicated in N-acetylglucosamine modifications of proteins, the tau protein binding S100b and microtubule organizing Cep170b correlate well. 21 proteins are anti-correlated with Snca, most strongly the RNA and protein methyltransferase Fbl, the scaffolding protein, required to maintain Golgi integrity, Akap9, and the signal transducer Stat3.

Interestingly, while I found few proteins changed in the insoluble fraction of the Line 61 mice, 151 proteins are adjusted p-value significant in the HM2 mice compared to their controls (**Figure 23c**). Among the 39 upregulated proteins, the four ribosomal proteins Rpl10, Rpl4, Rpl29 and Rps8 are found (STRING GO CC; ‘cytosolic ribosome’; FDR=0.0273). For the downregulated proteins in the insoluble fraction, WebGestalt ORA (GO CC) identifies the ‘respiratory chain’ with 6 ‘NADH dehydrogenase complex’ members and the ‘myelin sheath’ as FDR<0.05 significantly overrepresented (**Figure 23d**). This downregulation also holds true when looking at the insoluble enrichment for the proteins of both GO categories.

4.3.5| APPPS1: human transgene expression of mutated APP and PSEN1

APPPS1-mice, also known as APPPS1-21 mice, express the human Swedish mutation of APP (KM670/671NL) and PSEN1 (L166P) under the Thy1 promoter. They subsequently develop amyloid plaques, phosphorylated

tau-positive neuritic processes, but no fibrillar tau inclusions (Radde et al., 2006). Strong gliosis is another hallmark of this model (He et al., 2019; Malm et al., 2007).

I found 24 significantly changed proteins in almost 9 months old APPPS1-mice, all but one (monosaccharide transporter Slc2a3) upregulated and led by APP. The next highest upregulated proteins are Gfap, ApoE, C1qa and C1qb, Clu, Hexb, Htra1 and Cnn3, all with a FC>1 (**Figure 24a** and **Supplementary Table 12**).

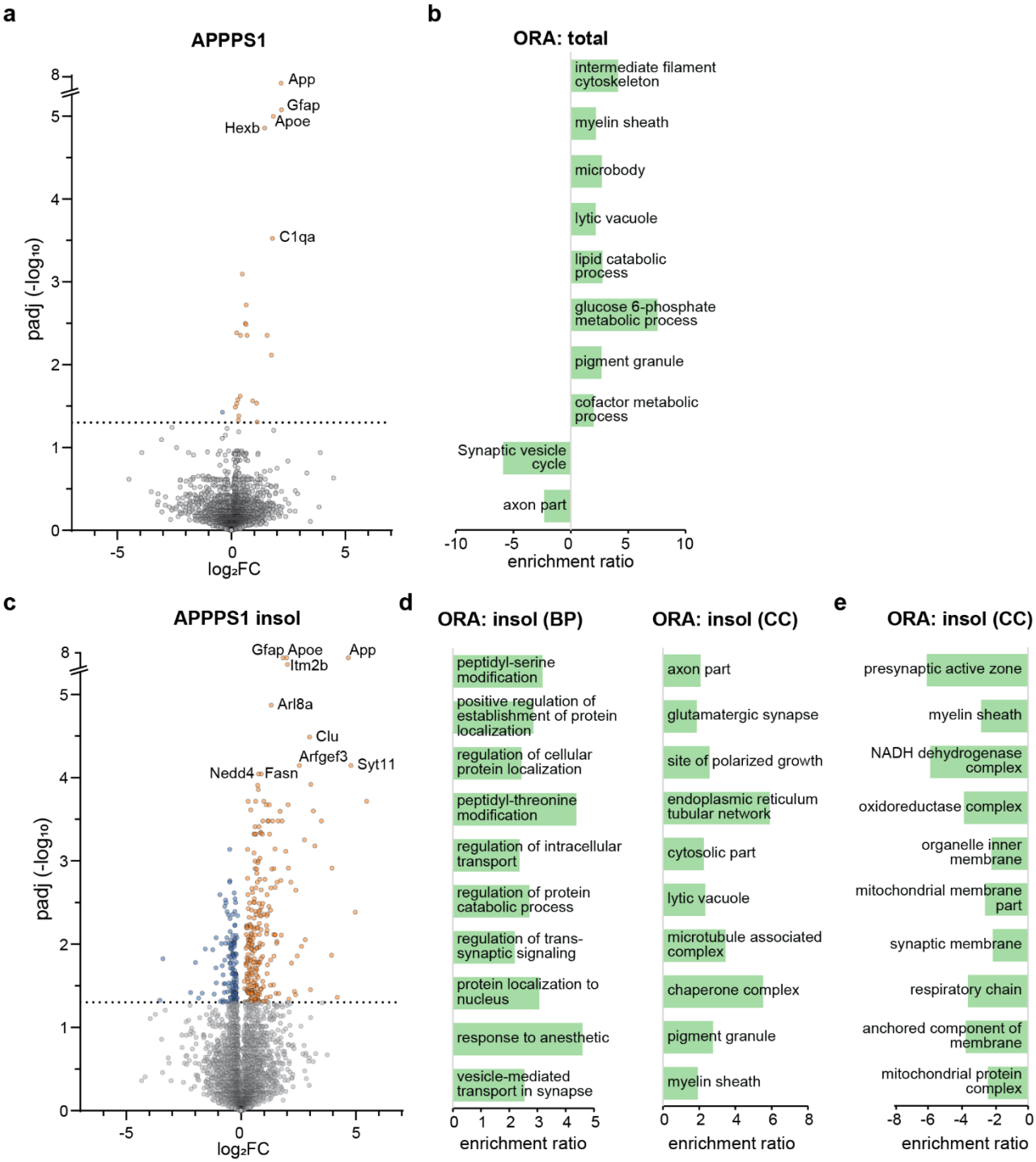

Figure 24 Overview of differentially expressed proteins in the APPPS1-mice. **a** and **c** Volcano plots, indicating *padj* (as -log10) and log2FC between model vs its own control in the total (**a**) and insol (**c**) fraction. Signifcant proteins indicated in orange (upregulated) and blue (downregulated); horizontal dotted line indicates *padj*-value cutoff at 0.05. **b** WebGestalt ORA analysis of the non-adjusted p significant proteins that are upregulated (positive enrichment ratio) or downregulated (negative enrichment ratio) in the total fraction. GO categories are both FDR<0.05 and sorted with the most significant on top. **d** and **e** WebGestalt ORA analysis of the significantly upregulated (**d**) and downregulated (**e**) proteins in the insoluble

fraction, separately for GO BP and GO CC annotation. GO categories are all FDR<0.05 and sorted with the most significant on top.

475 proteins are changed when I filter less strictly for $p<0.05$. Among the 313 upregulated proteins, GO BP terms 'glucose 6-phosphate metabolic process', 'lipid catabolic process' and 'cofactor metabolic process' are overrepresented, as well as GO CC terms 'intermediate filament cytoskeleton', 'microbody', 'pigment granule', 'myelin sheath' and 'lytic vacuole', all with FDR<0.05 in a WebGestalt ORA analysis. 'Synaptic vesicle cycle' (KEGG) and 'axon part' (GO CC) are overrepresented among the downregulated proteins (WebGestalt ORA, FDR<0.05; **Figure 24b**).

The protein that correlates best with the abundance pattern of App is synaptotagmin-binding cytoplasmic RNA interacting protein (Syncrip), which is an RNA-binding protein previously shown to interact with amyloid-β (Virok et al., 2011) and the RNA molecule BC200 (Duning et al., 2008). As such, it is believed to regulate local translation in dendrites. The second most correlated protein is the complement protein C1qa, which activates the complement pathway and has been shown to be present in amyloid plaques (Afagh et al., 1996). Further well correlating proteins (Pearson's $r>0.99$ and $p<0.001$) are β- hexosaminidase subunit beta and alpha (Hexb and Hexa), farnesyl pyrophosphate synthase (Fdps), and reactive intermediate imine deaminase A homolog (Rida). The protein most anti-correlated with App is citron rho-interacting kinase (Cit). See **Supplementary Table 12** for the full list.

A relatively high number of 408 proteins is significantly different in the insoluble fraction of APPPS1-mice compared with their controls (**Figure 24c**). 258 of these are upregulated, most strongly calsyntenin-3 (Clstn3), lactation elevated protein 1 (Lace1, also known as AFG1-like ATPase), synaptotagmin 11 (Syt11) and App, all with FC>4.5. Gene ontology ORA identifies the BP categories 'regulation of cellular protein localization', 'regulation of protein catabolic process', 'regulation of trans-synaptic signaling' and 'vesicle-mediated transport in synapse' as FDR-significantly enriched; CC terms 'glutamatergic synapse', 'microtubule associated complex', 'lytic vacuole', 'endoplasmic reticulum tubular network', 'chaperone complex' and 'myelin sheath' and are also enriched (**Figure 24d** and see **Supplementary Table 12** for the full list). Significantly downregulated proteins in the insoluble fraction are enriched in the GO CC categories 'presynaptic active zone', 'NADH dehydrogenase complex' and closely related categories. Interestingly, the GO 'myelin sheath' is implicated in both the up- and downregulated proteins (**Figure 24e**).

4.3.6 | m*Cat*-mice: overexpressing human catalase in mitochondria

To enhance the intracellular handling of ROS, several mouse models overexpressing the human radical scavenging enzyme Catalase have been developed. The catalase can be targeted to different cellular compartments, in the case of the m*Cat* mice, it is mitochondria. Catalase inactivates H_2O_2 and can locally protect mitochondria from oxidative damage, extending the lifespan of these animals by ~20% (4-5 months; Schriner et al., 2005). No such lifespan extension was observed in models ubiquitously overexpressing copper zinc superoxide dismutase (Huang et al., 2000) or when catalase was targeted to peroxisomes (Pérez et al., 2009b). Mitochondrially targeted catalase might therefore be unique in its effects. Another study, examining the role of mCat in the brain of AβPP (Tg2576 line) mice, found downregulated *App* and *Bace1* mRNA expression, reduced

Aβ-plaques, increased neuroprotective transcription and lower levels of oxidative DNA damage in m*Cat*/AβPP mice (Mao et al., 2012).

In my study, 13 proteins are significantly different between 20 months old m*Cat* and WT mice (**Figure 25a** and **Supplementary Table 13**). Among these, FUN14 domain-containing protein 1 (Fundc1), a mitophagy receptor, is the most upregulated.

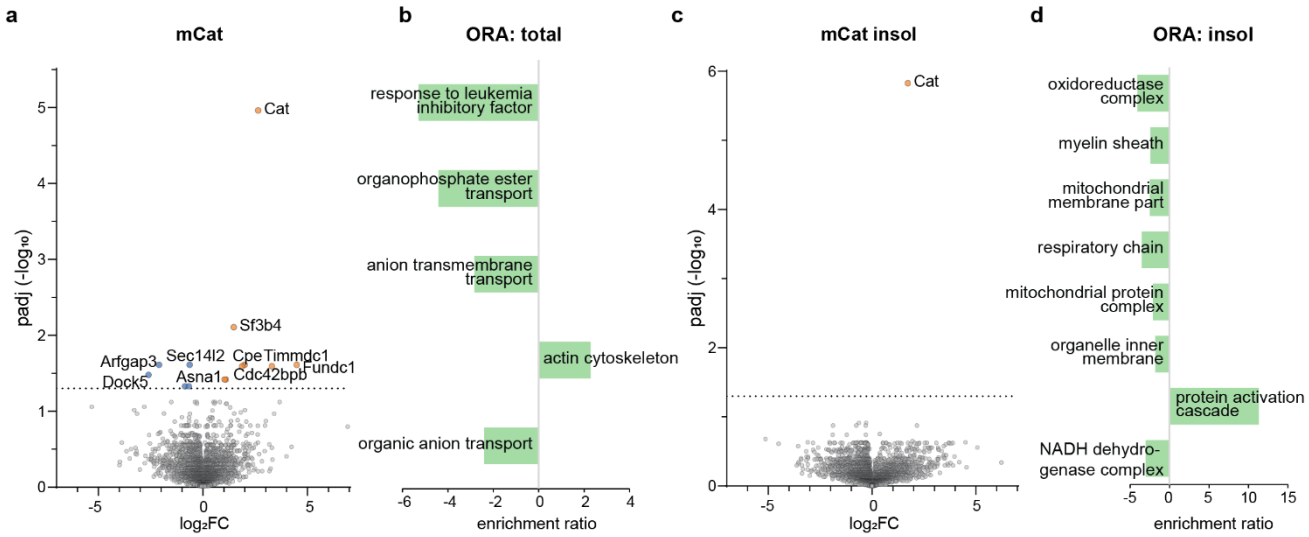

Figure 25 Overview of differentially expressed proteins in the mCAT-mice. **a** and **c** Volcano plots, indicating *padj* (as -log10) and log2FC between model vs its own control in the total (**a**) and insol (**c**) fraction. Signifcant proteins indicated in orange (upregulated) and blue (downregulated); horizontal dotted line indicates *padj*-value cutoff at 0.05. **b** and **d** WebGestalt ORA analysis of the non-adjusted p significant proteins that are upregulated (positive enrichment ratio) or downregulated (negative enrichment ratio) in the total (**b**) and insoluble (**d**) fraction. GO categories are all FDR<0.05 and sorted with the most significant on top.

The second most upregulated protein in m*Cat* mice is Timmdc1, a complex I assembly factor. 618 proteins are significantly different between mCat and WT mice in the total fraction once I filter less strictly for non-adjusted *p*<0.05. The 260 upregulated proteins are enriched in the GO CC term ‘actin cytoskeleton’ (FDR<0.05). The remaining downregulated proteins are enriched in GO BP terms ‘response to leukemia inhibitory factor’, ‘organophosphate ester transport’, ‘anion transmembrane transport’ and ‘organic anion transport’ (FDR<0.05), with several ATPases and solute carriers annotated (**Figure 25b**).

Interestingly, looking at my insoluble fraction, within the non-adjusted significant proteins, ‘protein activation cascade’ (GO BP, FDR<0.05; complement components and fibrinogens) is enriched in the upregulated proteins. Members of the ‘oxidoreductase complex’, the ‘respiratory chain’, the ‘NADH dehydrogenase complex’, the ‘mitochondrial membrane part’, the ‘myelin sheath’, the ‘mitochondrial protein complex’ and the ‘organelle inner membrane’ are overrepresented in the downregulated proteins (GO CC, FDR<0.05; **Figure 25c, d** and **Supplementary Table 13**).

4.3.7 | AntiOx-mice: antioxidant diet

I found 90 significantly altered proteins between 12 months old WT mice fed a standard mouse diet and 12 months old WT mice fed an antioxidant diet, supplemented with α-lipoic acid, N-acetyl cysteine, and vitamin E (**Figure 26a** and **Supplementary Table 14**). Antioxidant diets have been described to ameliorate axonal

degeneration (López-Erauskin et al., 2011), mitochondrial decay (Liu et al., 2002) and inflammation (Park et al., 2009). 61 proteins were upregulated, 17 are annotated with the GO CC term ‘mitochondrion’, 14 with the term ‘synapse’ (STRING FDR 0.0014 and 0.0116, respectively). The 29 downregulated proteins do not share considerable annotations. After less strict filtering to *p*<0.05, ‘mitochondrion’ remains the strongest defined cellular component that is enriched (STRING FDR=4.29e-07) within the top 100 upregulated genes (sorted by *p*-value), led by the highly upregulated complex I core subunit Mtnd3. The top 100 downregulated proteins are functionally enriched in GO BP term ‘synapse organization’ (STRING FDR=0.00017).

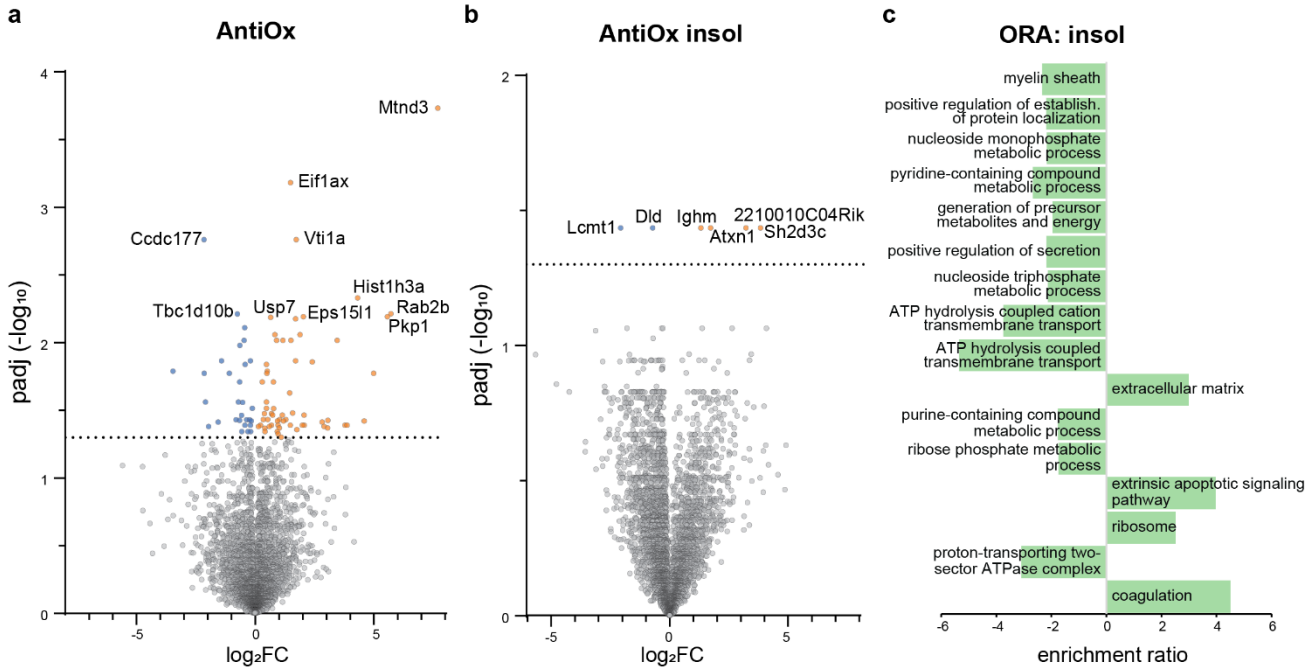

Figure 26 Overview of differentially expressed proteins in the AntiOx-mice. **a** and **b** Volcano plots, indicating *padj* (as -log10) and log2FC between model vs its own control in the total (**a**) and insol (**b**) fraction. Signifcant proteins indicated in orange (upregulated) and blue (downregulated); horizontal dotted line indicates *padj*-value cutoff at 0.05. **c** WebGestalt ORA analysis of the non-adjusted p significant proteins that are upregulated (positive enrichment ratio) or downregulated (negative enrichment ratio) in the insoluble fraction. GO categories are all FDR<0.05 and sorted with the most significant on top.

In the insoluble fraction, 6 proteins are significantly changed with *padj*<0.05, 764 with *p*<0.05 (**Figure 26b**). WebGestalt ORA identifies ‘extrinsic apoptotic signaling pathway’ and ‘coagulation’ enriched among the upregulated proteins (GO BP), as well as ‘extracellular matrix’ and ‘ribosome’ in GO CC annotation. The downregulated proteins are overrepresented in GO BP categories connected to ‘ATP hydrolysis coupled transport’, ‘pyridine. and purine-containing compound metabolic process’, ‘positive regulation of secretion’ and ‘positive regulation of establishment of protein localization’ and others (**Figure 26c**). Please see **Supplementary Table 14** for all terms and FDRs.

4.3.8 | Ucp2-mice: KO of uncoupling protein 2

In order to reduce ROS generation from mitochondria, cells can undergo mitochondrial “uncoupling”, meaning that protons can flow into the mitochondrial matrix, without relying on the function of complex V. While this decreases energy synthesis, it increases the mitochondrial membrane potential, leading to higher oxygen consumption and lowered ROS production (Andrews and Horvath, 2009). This has been proposed as protective mechanism and can be achieved through the action of uncoupling protein 2 (Ucp2). The mouse model lacking

this protein (Ucp2$^{-/-}$ or Ucp2 KO) presents shortened lifespan (decreased by ~24%; Hirose et al., 2016), increased ROS production and inflammatory microglia (Arsenijevic et al., 2000).

I found 464 significantly altered proteins between 20 months old WT and Ucp2-KO mice (**Figure 26a** and **Supplementary Table 15**). No FDR-significant GO enrichment was found, neither with up- or downregulated ORA, nor with GSEA. Remarkably, STRING analysis with high confidence interaction score revealed an overrepresentation of the following GO CC annotations in the upregulated proteins ($log_2FC>1$): 'glutamatergic synapse' (FDR=3.23e-06), 'vesicle coat' (FDR=0.0051), 'mitochondrial protein complex' (FDR=0.0113) and 'U2-type spliceosomal complex' (FDR=0.0322). Among the most downregulated proteins ($log_2FC<-1$), GO BP 'regulation of GTPase activity' (FDR=0.0018), 'protein transport' (FDR=0.0020) and the compartment 'mitochondrial protein complex' (FDR=0.0372) were overrepresented (**Figure 26b, c**).

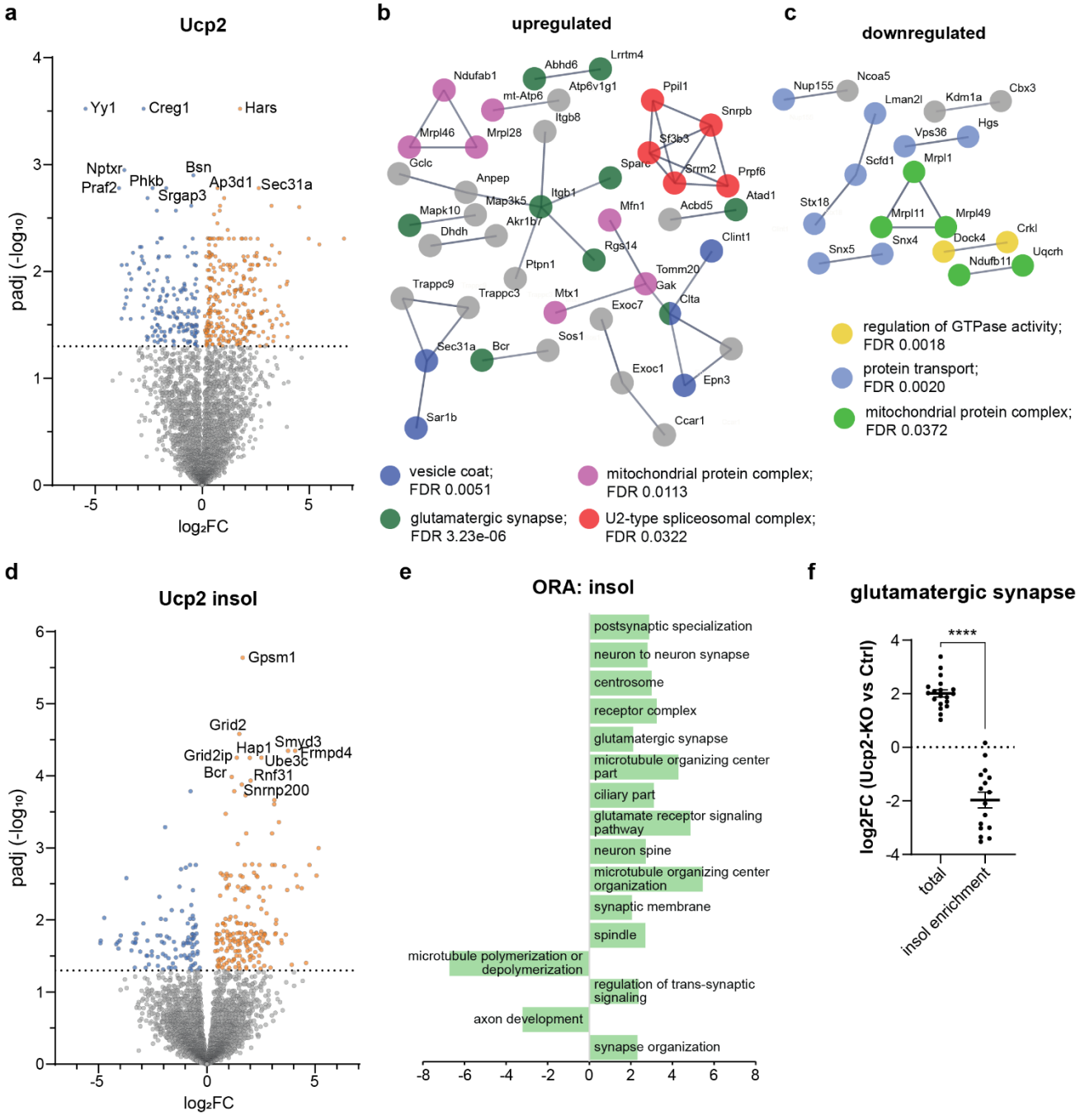

Figure 27 Overview of differentially expressed proteins in the Ucp2-mice. **a** and **d** Volcano plots, indicating *padj* (as -log10) and log2FC between model vs its own control in the total (**a**) and insol (**d**) fraction. Signifcant proteins indicated in orange

(upregulated) and blue (downregulated); horizontal dotted line indicates *padj*-value cutoff at 0.05. **b** and **c** STRING functional enrichment network for up- and downregulated proteins, respectively, in the total fraction. Core GO or pathway annotations after high-confidence interaction score filtering are color-coded. **e** WebGestalt ORA analysis of the significant proteins that are upregulated (positive enrichment ratio) or downregulated (negative enrichment ratio) in the insoluble fraction. GO categories are all FDR<0.05 and sorted with the most significant on top. **f** Proteins annotated as 'glutamatergic synapse' are upregulated in the total fraction and relatively downregulated in the insoluble fraction, pointing to a specific redistribution of these proteins rather than a general upregulation seen throughout the fractions. Unpaired t-test; **** *p*<0.0001.

Interestingly, upon comparison with the age-matched m*Cat*-mice (which supposedly have better handling and thus reduced ROS-damage), the proteins annotated in the above-mentioned up- or downregulated GO-categories are also the ones with the greatest differences to the expression FC in mCat-mice. FC in the mCat- and Ucp2-mice are significantly different for the representative proteins with high interaction score confidence shown in **Figure 28** (t-test *p*<0.05, except for 'regulation of GTPase activity' with *p*=0.089). Strong reverse trends are also seen in single proteins: the spliceosome core component Snrpb (Ucp2 FC=1.44, *padj*=0.009; mCat FC=-0.38, *p*=0.049) or the accessory subunit of complex I Ndufab1 (Ucp FC=2.42, *padj*=0.032; mCat FC=-3.65, *p*=0.025)

a

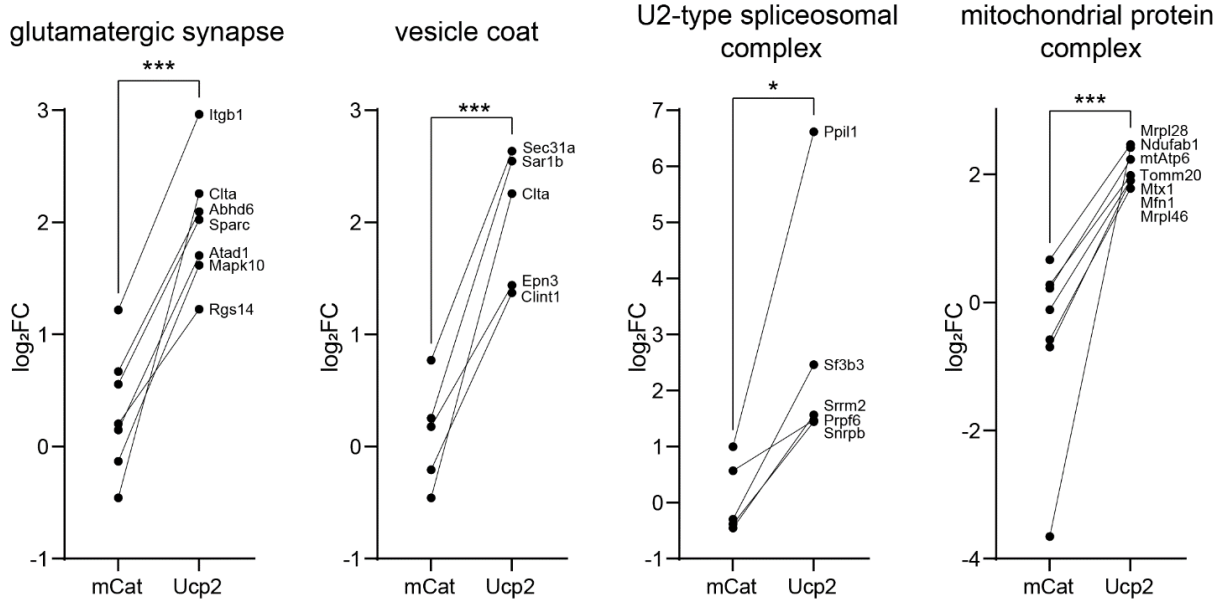

b

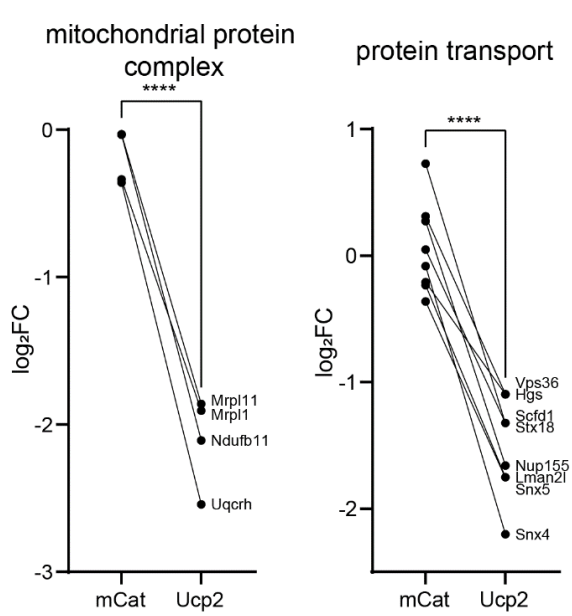

Figure 28 Comparison between age-matched mCat- and Ucp2-mice. Core proteins upregulated in Ucp2-mice (**a**) show significantly larger FCs compared to those observed in mCat-mice. Core downregulated proteins of the Ucp2-mice (**b**) show significantly more positive FCs in the mCat-mice. Unpaired t-test; * $p<0.05$, *** $p<0.001$, **** $p<0.0001$.

In the insoluble fraction, 'synapse organization' (FDR=0.040) and especially the 'glutamatergic synapse' (FDR=0.003) is among the enriched GO-terms (WebGestalt ORA) for proteins that are increasingly insoluble in Ucp2-KO mice (**Figure 27e**). Of note, while the GO-annotation is the same, the corresponding proteins differ from the total-upregulated ones, meaning that it is not a general upregulation of glutamatergic synapse proteins, but a specific rearrangement of components. 15 of the 19 proteins annotated as glutamatergic synapse in the total upregulated fraction are even decreased in their insoluble enrichment of Ucp2-KO mice compared to their controls (**Figure 27f)**. The downregulated proteins in the insoluble fraction are enriched in the GO-BP categories of 'microtubule polymerization or depolymerization' (FDR=0.014) and 'axon development' (FDR=0.031) with prominent members Snca, Mapt or ApoE, whose total levels are only changed marginally (FC between -0.11 and 0.19; **Supplementary Table 15**).

4.3.9 | LAKI: homozygous knock-in of mutated Lmna to model HGPS

The C- to T-transition at nucleotide 1824 is a specific mutation in the *LMNA* gene encoding lamin A found in human Hutchinson-Gilford progeria syndrome (HGPS) patients. While there is no amino acid substitution, this mutation activates a cryptic splicing donor site which leads to progerin (the truncated form of prelamin A) formation and accumulation at the nuclear envelope. The homozygous knock-in mouse to mimic human HGPS carries the mouse corresponding C- to T- transition at nucleotide 1827 instead of its wildtype *Lmna* gene and is also known as LAKI or $Lmna^{G609G/G609G}$ (Osorio et al., 2011). Fibroblasts from HGPS patients show increased DNA damage load, as do HGPS mouse models. Further, decreased serum levels of IGF-1 and GH have been found in LAKI mice (Osorio et al., 2011). While in the original publication, these mice have been described with a maximum lifespan of ~100 days, the current stock kept in the same institute is fed with wet food and lives considerably longer, up to 6 months. I received animals of 5 months of age that showed progeroid phenotypes but were still relatively healthy.

37 proteins are significantly changed in the LAKI-mice after multiple comparison correction (**Figure 29a** and **Supplementary Table 16**). 19 of them are upregulated, among them the most significant hit Lmna, albeit with a modest FC of 0.485. The 18 downregulated proteins include the chaperones HSP90 alpha and beta, as well as the HSP90 co-chaperone Chordc1.

Once I expanded the analysis to include the non-adjusted significant proteins, the 'DNA packaging complex' and 'nuclear chromatin' was FDR-significantly overrepresented in a WebGestalt ORA analysis of the 295 upregulated proteins (**Figure 29b**). This was confirmed in a STRING analysis, where high confidence interaction score GO BP and GO CC categories annotate the upregulated proteins as 'nuclear chromatin' (FDR=0.00018). Beyond that, proteins of the 'ionotropic glutamate receptor signaling pathway' (FDR=0.0053), 'fatty acid beta oxidation' (FDR=0.00031), 'glutathione metabolic process' (FDR=0.0019), 'regulation of RNA splicing' (FDR=1.68e-05), 'axo-dendritic transport' (FDR=0.0399) and the 'proteasome complex' (FDR=2.46e-05) are upregulated. Within the 239 downregulated proteins ($p<0.05$), STRING high confidence interaction score analysis highlights again 'chaperone mediated protein complex assembly' (FDR=0.0093) and shows that,

among others, the categories ‘axon extension’ (FDR=8.66e-06), ‘protein folding’ (FDR=9.04e-06), ‘nuclear envelope’ (FDR=0.0061) and ‘microtubule cytoskeleton’ (FDR=6.25e-06) are affected.

The best correlated proteins (non-adjusted p<0.05) to the expression of Lmna are two metabolic enzymes on the upregulated side (Idh2 and Aldoc, both with Pearson’s r>0.99, p<0.0001) and three chaperones (Hsp90aa1, Chordc1, Dnaja2; all with Pearson’s r<-0.97, p<0.001) on the negatively correlated side.

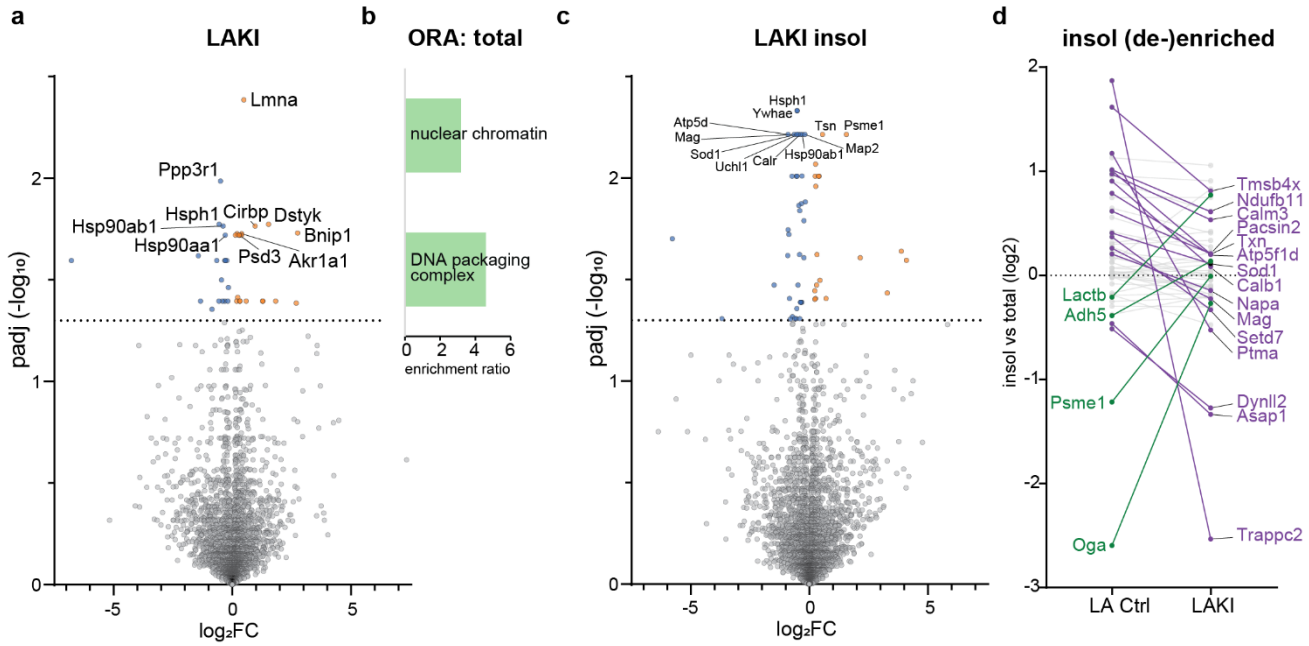

Figure 29 Overview of differentially expressed proteins in the LAKI-mice. **a** and **c** Volcano plots, indicating *padj* (as -log10) and log2FC between model vs its own control in the total (**a**) and insol (**c**) fraction. Signifcant proteins indicated in orange (upregulated) and blue (downregulated); horizontal dotted line indicates *padj*-value cutoff at 0.05. **b** WebGestalt ORA analysis of the non-adjusted p significant proteins that are upregulated (positive enrichment ratio) in the total fraction. GO categories are both FDR<0.05 and sorted with the most significant on top. **d** Relative enrichment or de-enrichment of proteins in the insoluble fraction vs their total levels shows that only a specific subset is actually insoluble-upregulated (green) or downregulated (purple), whereas many other proteins are changed in both total and insoluble fraction without specific redistribution between the fractions (grey).

In the insoluble fraction, 56 proteins are significantly changed, with 18 of them upregulated (**Figure 29c**). Upon extension of the analysis to include the p<0.05 upregulated proteins, the top 100 (sorted by significance) are functionally enriched in GO categories ‘monosaccharide biosynthetic process’ (FDR=0.0011), ‘tricarboxylic acid cycle’ (FDR=0.009), ‘regulation of RNA splicing’ (FDR=0.0052) and ‘proteasome complex’ (FDR=0.0015). The top 100 downregulated proteins are enriched in ‘SNARE complex disassembly’ (FDR=0.0232), ‘mitochondrial membrane organization’ (FDR=0.00028), ‘protein folding’ (FDR=4.48e-06), ‘axo-dendritic transport’ (FDR=0.0383) and ‘reactive oxygen species metabolic process’ (FDR=0.0152). Chaperones Hsp90aa1 and Hsp90ab1, which are at the center of downregulated networks, are downregulated in all solubility fractions, without any major shift between the fractions. The significant proteins of the insoluble fraction that do show redistribution are highlighted in **Figure 29d**.

4.3.10 | Zmpste24: KO of the lamin A processing protease

CAAX prenyl protease 1 homolog, encoded by *Zmpste24,* is the protease that cleaves the precursor of lamin A to create the mature protein which inserts into the nuclear membrane. In the human HGPS, the above-mentioned specific point mutation in exon 11 of *LMNA* is responsible for removing the Zmpste24 recognition site and thus for accumulation of aberrant lamin A. Zmpste24-KO mice model HGPS, show a very similar phenotype to LAKI mice (Varela et al., 2005) and have a reduced lifespan of 20 weeks (Pendás et al., 2002). I studied the brains of animals of 3.5 months of age.

Only 6 proteins are significantly changed in the Zmspte24-KO mice after multiple comparison correction in the total fraction (**Figure 30a** and **Supplementary Table 17**). The upregulated are (in descending FC order) lysophosphatidylcholine acyltransferase 1 (Lpcat1), RhoGEF kalirin (Kalrn) and dihydropyrimidinase-related protein 4 (Dpysl4). Downregulated is HSP90 alpha (Hsp90aa1), tyrosine-protein phosphatase non-receptor type 12 (Ptpn12) and prothymosin alpha (Ptma).

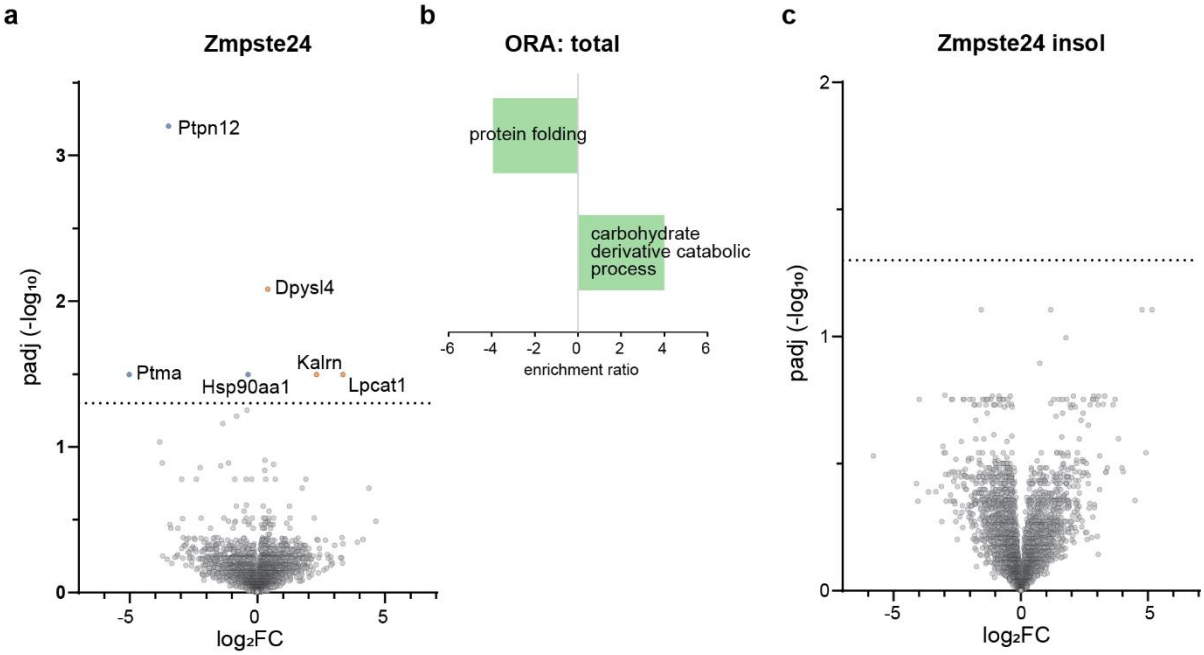

Figure 30 Overview of differentially expressed proteins in the Zmpste24-mice. **a** and **c** Volcano plots, indicating *padj* (as -log10) and log2FC between model vs its own control in the total (**a**) and insol (**c**) fraction. Signifcant proteins indicated in orange (upregulated) and blue (downregulated); horizontal dotted line indicates *padj*-value cutoff at 0.05. **b** WebGestalt ORA analysis of the non-adjusted p significant proteins that are upregulated (positive enrichment ratio) or downregulated (negative enrichment ratio) in the total fraction. GO categories are both FDR<0.05 and sorted with the most significant on top.

444 proteins are non-adjusted *p*-value significantly different between Zmpste24-KO and controls. The 265 upregulated proteins are enriched in the GO BP term 'carbohydrate derivative catabolic process' (WebGestalt ORA, FDR<0.05; **Figure 30b**). This is confirmed in the STRING analysis (FDR=0.0002) and additional core annotations include 'intermediate filament cytoskeleton organization' (FDR=0.00059), 'AP-2 adaptor complex' (FDR=0.0125), 'spliceosomal complex' (FDR=3.76e-05) and 'fatty acid metabolism' (FDR=0.0019). The 179 downregulated proteins are enriched in the GO BP 'protein folding' (WebGestalt ORA, FDR<0.05), with several chaperones decreasing in levels, similar to the LAKI-mice. Chaperones and 'protein folding' (FDR=2.47e-07), together with 'regulation of early endosome to late endosome transport' (FDR=0.0048), 'regulation of

proteasomal ubiquitin-dependent protein catabolic processes' (FDR=0.0215), 'ubiquitin binding' (FDR=0.00031) and the 'cytosolic ribosome' (FDR=0.0085) describe the downregulated proteins in STRING analysis.

No proteins are significantly changed in the insoluble fraction of Zmpste24-KO mice (**Figure 30c**). Among the upregulated top 100 non-adjusted *p*-value significant proteins, the 'fibrinogen complex' (FDR=0.0015), the 'complex of collagen trimers' (FDR=0.0097) and the 'spliceosomal complex' (FDR=0.0006) are functionally enriched. Within the top 100 downregulated proteins in the insoluble fraction, proteins of the 'synaptic vesicle cycle' (FDR=0.0371) and 'ATP metabolic process' (FDR=0.0298) are enriched.

4.3.11 | Environmental enrichment

Long-term environmental enrichment can extend lifespan and promote healthy aging (Arranz et al., 2010; McMurphy et al., 2018). The cohort of mice analyzed here underwent short-term housing enrichment for 16 weeks beginning at the age of 19.5 months.

I found no significant differences in the total fraction of enriched and non-enriched mice of 26 months of age (**Figure 31a** and **Supplementary Table 18**). In the insoluble fraction, there is a single downregulated protein, cytosolic phospholipase A2 epsilon (Pla2g4e; **Figure 31b**).

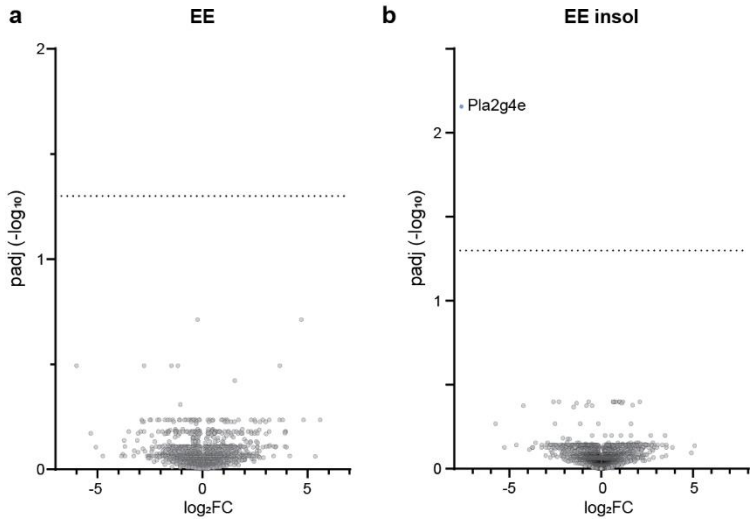

Figure 31 Overview of differentially expressed proteins in EE-mice. **a** and **b** Volcano plots, indicating *padj* (as -log10) and log2FC between model vs its own control in the total (**a**) and insol (**b**) fraction. Signifcant proteins indicated in orange (upregulated) and blue (downregulated); horizontal dotted line indicates *padj*-value cutoff at 0.05.

4.3.12 | Male and female WT mice

4 proteins are significantly different between the total fraction of aged female and male mice of 24 months of age (**Figure 32a** and **Supplementary Table 19**). These are female-upregulated nuclear receptor corepressor 2 (Ncor2), Gfap and choline transporter-like protein 1 (Slc44a1) and downregulated serine protease inhibitor A3K (Serpina3k). The top 100 female-upregulated proteins (sorted by *p*-value) are STRING functionally enriched in cellular components 'COP9 signalosome' (FDR=0.0275), 'myelin sheath' (FDR=2.22e-09) and 'intermediate filament' (FDR=0.0218). Among the top 100 male-upregulated proteins, 'IMP metabolic process'

(FDR=0.0369), ‘trans-synaptic signaling’ (FDR=0.0369) and ‘pyruvate dehydrogenase complex’ (FDR=0.0484) are functionally enriched (**Figure 32b, c**).

In the insoluble fraction, 4 different proteins were significantly different between aged female and male brains (solute carrier family 12 member 2 (Slc12a2), serine/threonine-protein phosphatase 2A subunit A alpha isoform (Ppp2r1a), FERM domain-containing protein 8 (Frmd8), and RNA binding protein fox-1 homolog 1 (Rbfox1); **Figure 32d**). GO ORA results show an enrichment of ‘myelin sheath’ proteins in the female upregulated insoluble fraction (FDR=0.0000188; **Figure 32e**), no FDR-significant enrichment is found in the male upregulated fraction.

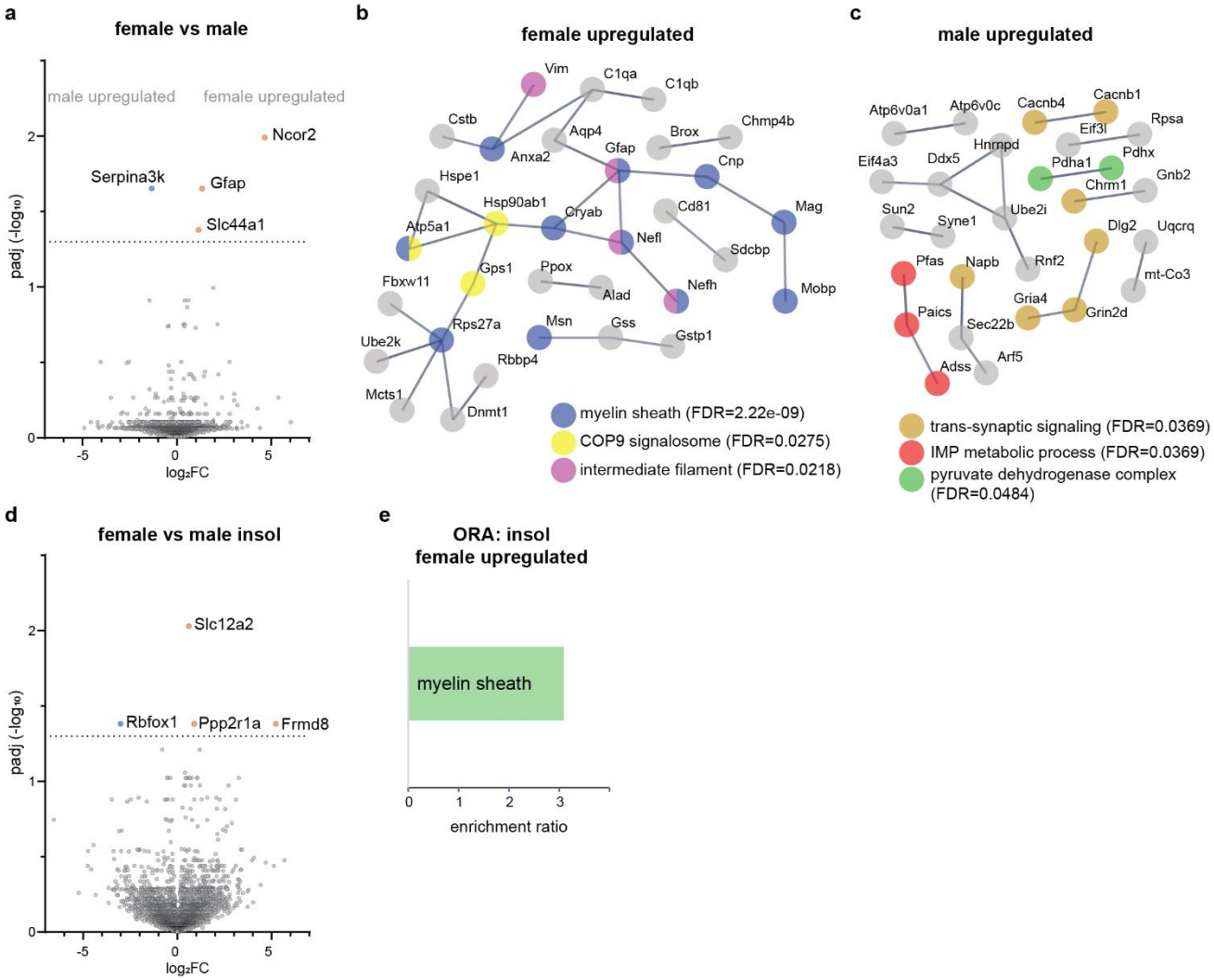

Figure 32 Overview of differentially expressed proteins between female and male mice. **a** and **d** Volcano plots, indicating *padj* (as -log10) and log2FC between model vs its own control in the total (**a**) and insol (**d**) fraction. Signifcant proteins indicated in orange (upregulated) and blue (downregulated); horizontal dotted line indicates *padj*-value cutoff at 0.05. **b** and **c** STRING functional enrichment network for female and male upregulated proteins, respectively, in the total fraction. Core GO or pathway annotations after high-confidence interaction score filtering are color-coded.

4.4 | Combined analysis

The study of brain aging in mouse models mostly concentrates on a specific genetic modification. Comparisons to physiological aging processes are done across studies, or in some cases when aged mutants and physiologically aged animals are matched to younger counterparts. I present here proteomic data from 13 cohorts of mice, each with their own control. This allows comparisons of respective changes as logFCs across cohorts, with all samples having undergone the same preparation and analysis, thus minimizing technical variability.

Changes in protein abundances with age are modest, but nevertheless can enable far-reaching consequences in single cells as well as neuronal network function. In order to find commonly affected proteins and molecular pathways, I grouped the analyzed cohorts roughly into 5 groups: physiological aging, metabolic aging (SAMP8 and Zfand2b), neurodegenerative aging (NDD models Line 61, HM2 and APPPS1), mitochondrial aging (mCat, AntiOx and Ucp2), and nuclear architecture related aging (LAKI and Zmpste24). The results presented in this section (and **Supplementary Table 1**) provide an overview and serve as starting points for further analyses, which can range from large bioinformatic, clustering-based approaches to the study of individual proteins of interest across different protein solubility and subcellular transcript fractions.

4.4.1 | Core protein changes

I was first interested in proteins that were found to change significantly in the majority of investigated cohorts. No protein had an adjusted *p*-value <0.05 in all intra-cohort comparisons. I then restricted my collection to include only the physiological late aging comparison (24 vs 12) and all genetic and dietary models but excluded the environmental enrichment groups and the female-male comparison (**Figure 33**). The latter two served more as internal controls, do not represent an aged vs non-aged comparison, and show the fewest significant changes. Among the 11 remaining cohorts, Gfap was significantly affected in 8 (**Figure 33a**). Strong upregulation was observed in physiological aging, the AD-model APPPS1 and SAMP8 (logFC>0.5). Zfand2b, HM2, Ucp2 and LAKI also showed significant upregulation, all hinting to processes of gliosis and inflammation. Interestingly, the mCat model shows significant downregulation of Gfap and stands out. A similar pattern is observed for the intermediate filament vimentin (**Figure 33b**). Intermediate filament associated plectin is significantly upregulated in physiological aging, SAMP8, all three NDD models, Ucp2 and Zmpste24. LAKI-mice notably show significant downregulation of Plec, a trend that is also found in the two mitochondrial antioxidant models (**Figure 33c**). Reversely, SUMO activating enzyme subunit 1 (Sae1) is decreased in most pro-aging models, significantly in physiological aging, SAMP8, HM2 and Zmpste24, but significantly increased in mCat and AntiOx-mice, as well as in Line 61 (**Figure 33d**). Glycerol-3-phosphate dehydrogenase, a mitochondrial enzyme that is also implicated in gluconeogenesis, is significantly increased in the metabolic models SAMP8 and Zfand2b, as well as in Line 61 and both nuclear envelope models (**Figure 33e**). Folding chaperone Hsp90-beta shows strong significant downregulation in physiological aging and both nuclear envelope models, while all other models show either non-significant or slightly upregulated (Zfand2b and Line 61) protein levels (**Figure 33f**). Oxysterol-binding protein-related protein 1 (Osbpl1a), which binds phospholipids and modulates late endocytic/lysosomal compartments is significantly downregulated in physiological aging and the three NDD models, while upregulation is observed in Zfand2b, AntiOx and Ucp2 (**Figure 33g**). The mitochondrial succinyl-

CoA:3-ketoacid coenzyme A transferase 1 (Oxct1) is a key enzyme of ketone body catabolism. It is significantly upregulated in both metabolic models, AntiOx-mice and to the highest degree in Zmpste24. HM2-mice show significant downregulation of this enzyme (**Figure 33h**). As last example, cytosol aminopeptidase Lap3 is significantly upregulated in physiological aging, Line 61, APPPS1 and AntiOx. mCat and the nuclear envelope models show the reverse (**Figure 33i**).

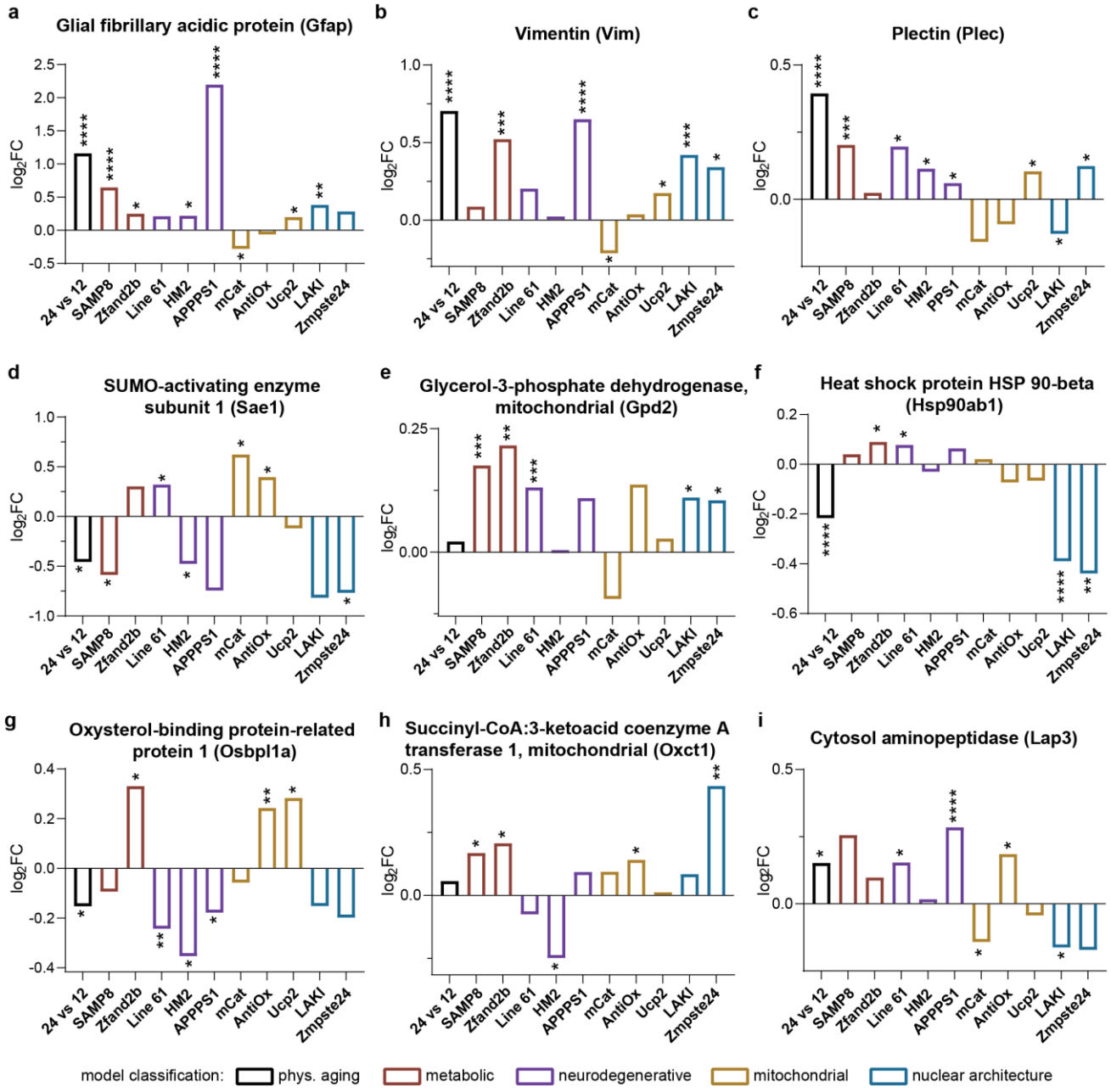

Figure 33 Proteins found significantly changed in at least 5 pro- or anti-aging models, including physiological aging 24 vs 12. Functional groups of models (metabolic in red, neurodegenerative in purple, mitochondrial in orange, or nuclear architecture in turquoise) often, but not always, show similar protein expression changes. Stars indicate DEqMS significance in the respective comparison of 24 vs 12 or of model vs littermate control; * p<0.05, ** p<0.01, *** p<0.001, **** p<0.0001.

4.4.2 | Changes in functional groups of proteins

Second, I tested whether any functional groups of proteins were significantly differently affected in one model than another. Overall, even within my manually annotated categories, that take brain-specific function into

account, proteins within a category mostly showed high variation of individual FCs, rendering the comparison of large categories not significant. Neurofilaments and associated cytoskeletal proteins (Nefm, Nefl, Nefh, Vim, Plec and Ina) were strongly implicated in physiological aging and my combined analysis shows that this observation significantly differentiates physiological aging from the other cohorts (**Figure 34a**). The late upregulation (24 vs 12) of neurofilaments is not modeled to the same extent and the mCat model resembles more the early phenotype of physiological aging (12 vs 6). The second striking group of proteins prominently affected in physiological aging are ribosomal proteins (Rpl and Rps; **Figure 34b**). The, on average, late downregulation of these proteins significantly differs from patterns observed in SAMP8, Line 61 and APPPS1. Zfand2b, AntiOx and Ucp2 also have upregulation trends, while the nuclear envelope models LAKI and Zmpste24 resemble physiological aging better in this regard.

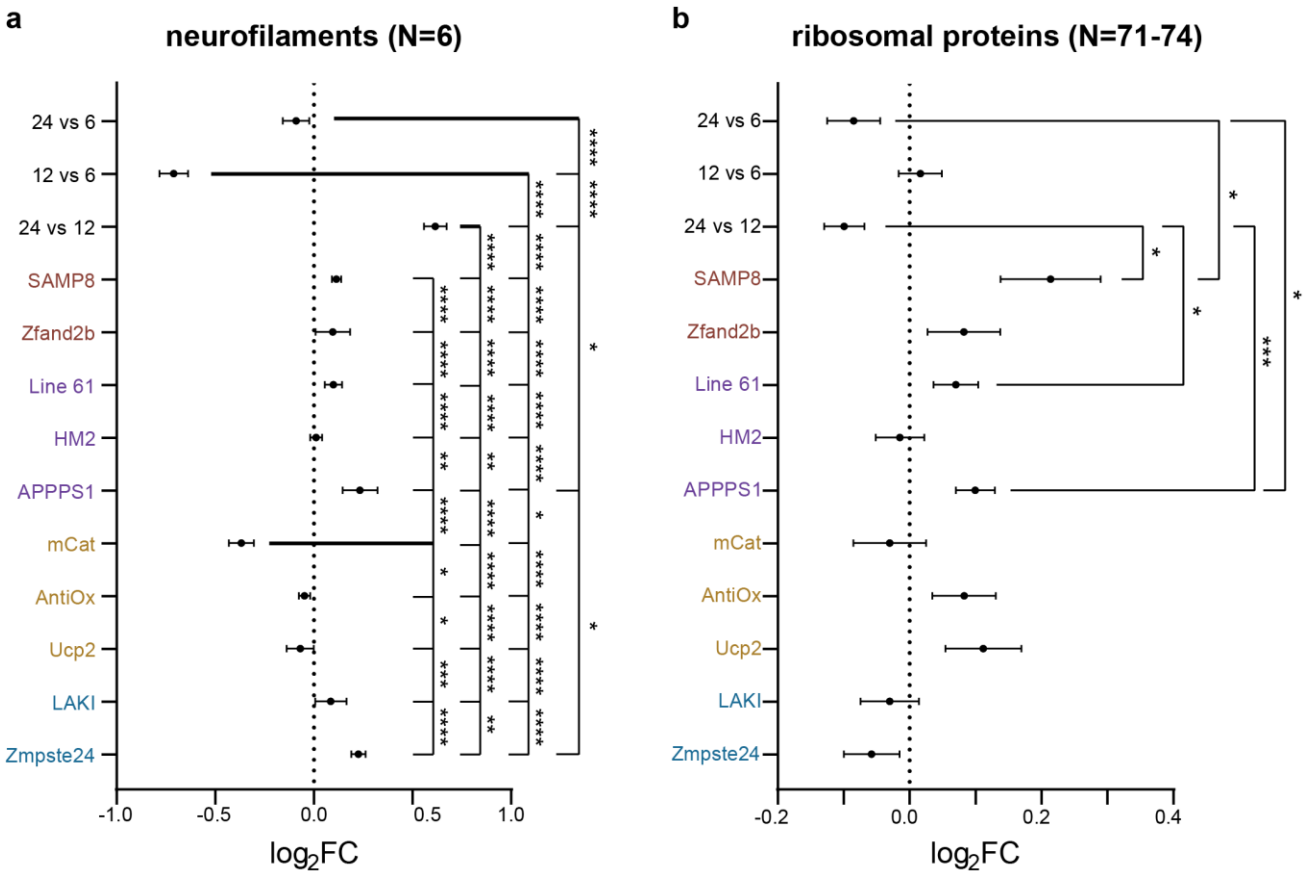

Figure 34 Across-cohort differences in protein abundance changes identify neurofilaments and ribosomal proteins as highly relevant for physiological aging. **a** Neurofilaments as a functional group of proteins change significantly different in physiological aging than in any of the aging models examined here. The mCat-mice also show significant differences to most other cohorts, similar to the early aging comparison 12 vs 6 months. **b** Ribosomal proteins (all Rpl and Rps proteins quantified in this study) show a decline in late physiological aging (24 vs 12 months) that differs significantly from several other models. N indicates the number of proteins sorted into this functional category and compared here, not all corresponding proteins were quantified in all cohorts. ANOVA testing with Brown-Forsythe correction when standard deviations were significantly different between groups, multiple testing was adjusted with Tukey (ordinary ANOVA) or Games-Howell correction. Thick lines indicate the cohort that is being tested against; * p<0.05, ** p<0.01, *** p<0.001, **** p<0.0001.

Vacuolar ATPases are responsible for acidifying intracellular compartments, most prominently they are essential to maintain lysosomal pH gradients. 11 subunits, both catalytic and accessory, of v-type proton ATPase and one solute carrier in the pH buffering system have been measured in my study (**Figure 35a**). On average, these proteins responsible for acidification are not majorly changed in physiological aging. They are however slightly upregulated in SAMP8 and strongly upregulated in Ucp2-mice, although with variation.

Significantly different to this upregulation is the downregulation in HM2. The other two NDD models, Line 61 and APPPS1, also show decreasesing trends.

Energetic defects would be expected in mitochondrial models of aging as well as in metabolic models. I grouped proteins with roles in sugar- and ketone-based energy metabolism, energy sensing and ATP-hydrolysis, comparing ~50 proteins between cohorts (**Figure 35b**). Again, physiological aging shows no average change in the abundance of these proteins. SAMP8 however have a marked decrease that is unique in my comparison. In contrast, Zfand2b, AntiOx and Zmpste24 have significantly differing upregulations.

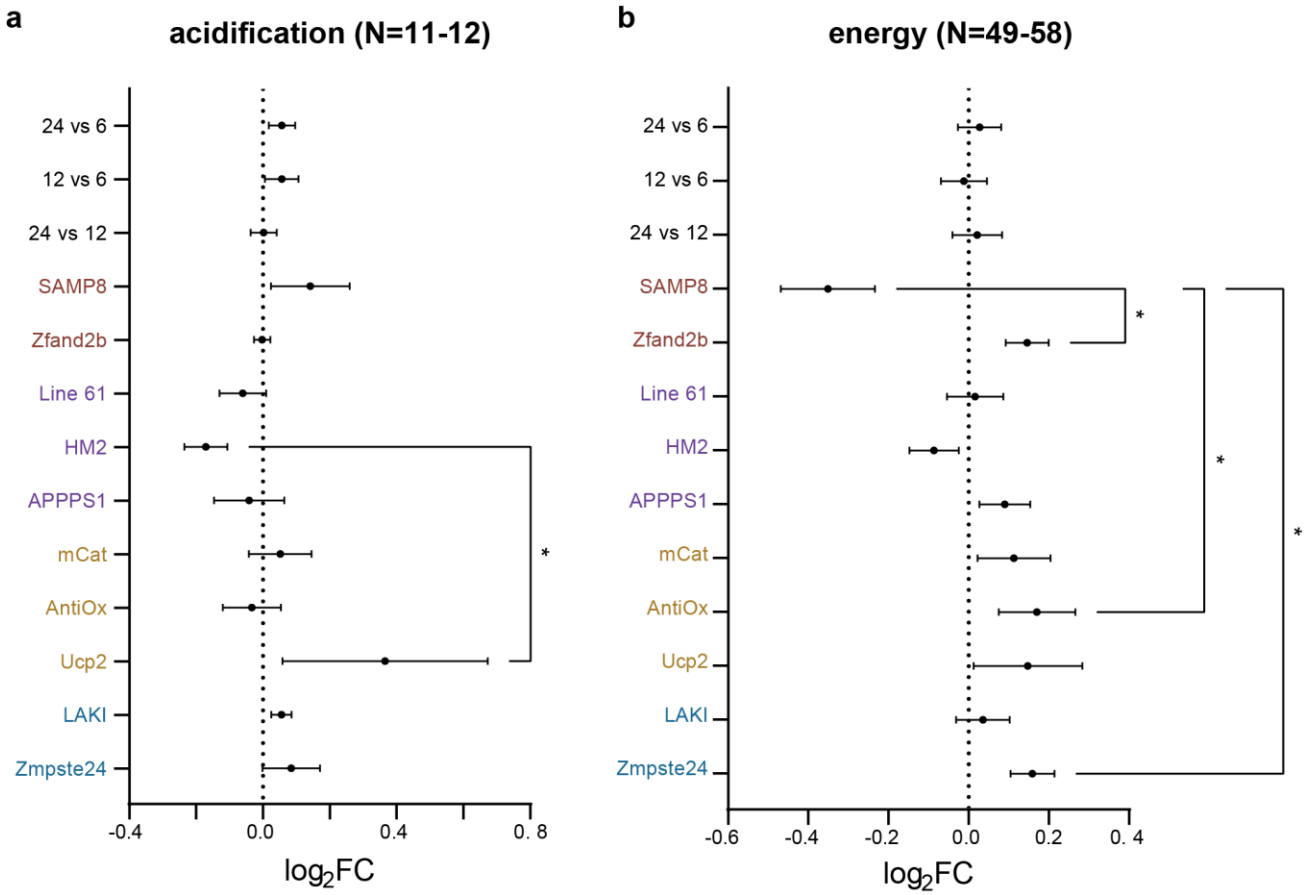

Figure 35 Across-cohort differences in protein abundance implicates altered acidification processes of intracellular structures in the Ucp2-mouse model (**a**). While only the comparison with the HM2 model of PD is significant, the range of upregulated proteins involved in acidification stands out. **b** Impaired energy homeostasis is implicated in the SAMP8 model of accelerated aging. N indicates the number of proteins sorted into this functional category and compared here, not all corresponding proteins were quantified in all cohorts. Ordinary one-way ANOVA testing, multiple testing was adjusted with Tukey correction in **a**; Brown-Forsythe ANOVA testing with Games-Howell correction for multiple testing in **b**. * p<0.05.

Lastly, the chaperone Hsp90 was already identified as core protein of aging in both nuclear lamina defect models (**Figure 33f**). Hsp90-alpha, Hsp90-beta and endoplasmin (Hsp90b1) are clearly decreased in both LAKI and Zmpste24 (**Figure 36a**). This significantly differentiates these models from all other included cohorts. Late physiological aging (24 vs 12) also shows decreased levels of these chaperones, while the early physiological aging comparison shows increased levels, more similar to Zfand2b and the three NDD models. The mitochondrial models are situated between the decreased levels of LAKI and Zmpste24 and the upregulations in the other cohorts.

The Cop9 signalosome complex consists of eight subunits and participates in ubiquitin-dependent proteolysis. Its components are decreased in LAKI, but not in Zmpste24 (**Figure 36b**). The late comparison in physiological

aged mice (24 vs 12) resemble this downregulation the most. 12 vs 6 however shows upregulated levels, as does SAMP8 and AntiOx, mostly though Line 61. The PD model abundance of Cop9 signalosome differs significantly from the one in LAKI.

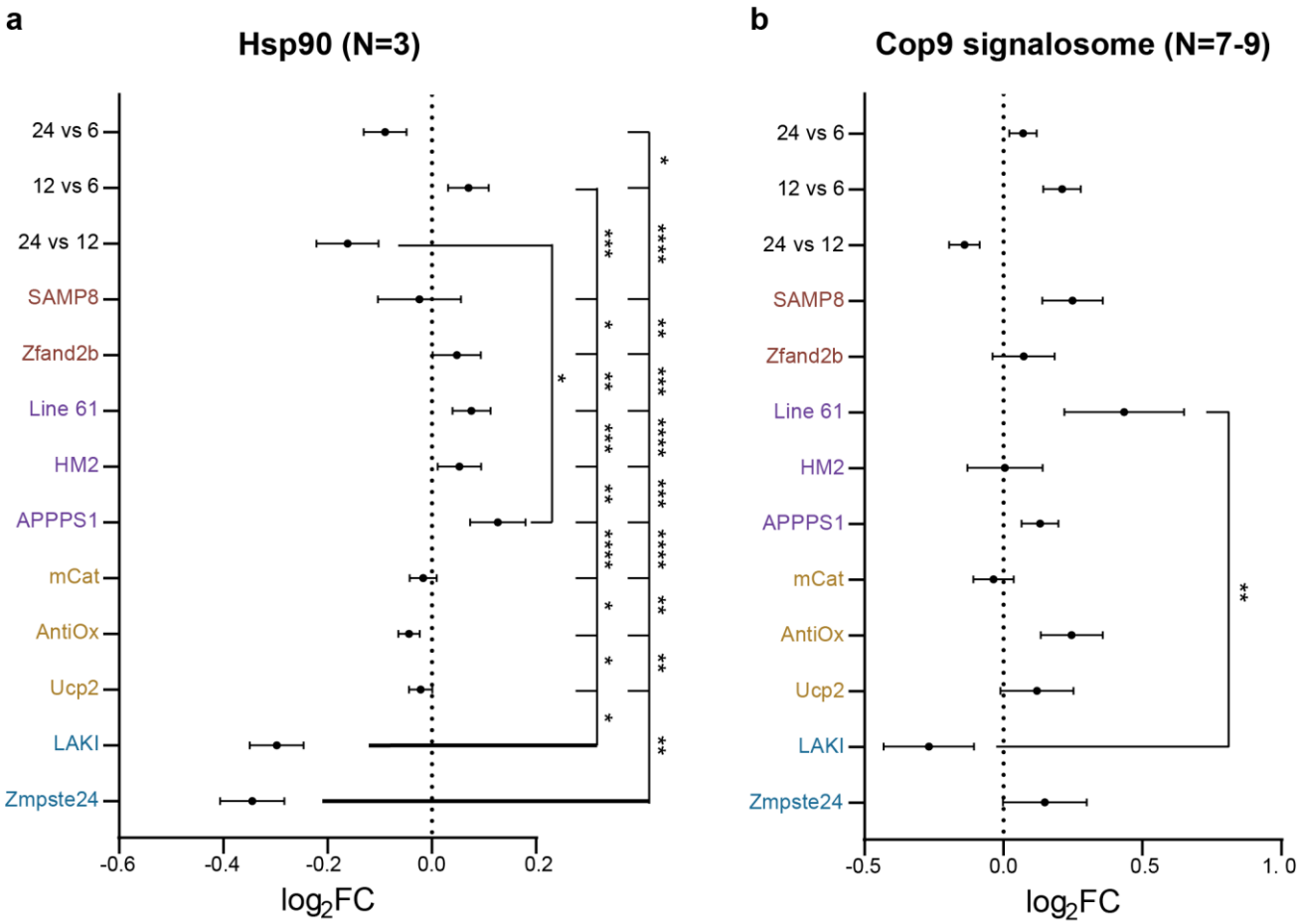

Figure 36 Across-cohort differences in protein abundance changes identify HSP90 and members of the COP9 signalosome as specifically downregulated in nuclear envelope defect models of HGPS. **a** Hsp90 proteins Hsp90aa1, HSP90ab1 and Hsp90b1 are downregulated in both LAKI and Zmpste24-KO mice. This downregulation is not found in physiological aging or any other cohort. **b** Cop9 signalosome proteins quantified in this study show marked downregulation in the LAKI-mice which is significantly different from upregulation in PD-modeling Line 61 mice. N indicates the number of proteins sorted into this functional category and compared here, not all corresponding proteins were quantified in all cohorts. ANOVA testing with Tukey correction for multiple comparison; thick lines indicate the cohort that is being tested against; * p<0.05, ** p<0.01, *** p<0.001, **** p<0.0001.

5 | Discussion

The aim of this work was to provide a systematic investigation of brain aging in the mouse brain. For this, RNA and protein abundances were measured with large-scale omics methods, next generation sequencing and LC-MS, respectively. After optimization of a streamlined sample preparation and analysis protocol, multiple sub-cellular fractions from the brains of physiologically aged mice as well as from mouse models of aging were prepared and investigated in paralell. This workflow provided an extensive databse and insights into the molecular mechanisms of brain aging, which will be discussed in the following sections.

5.1 | Gene expression changes are pronounced in early aging

In this study, I compared the transcriptomes of 6-, 12- and 24-months old mouse brains in a total and nuclear subcellular fraction. First, I show that my optimized, simple fractionation protocol delivers good separation of subcellular fractions 'total' and 'nuclear', which can be used for RNA isolation, and which contain the respectively localized transcripts (**Figure 4**). This allows the study of age-related alterations in the localization and distribution of RNAs, which likely affect translation rates and ultimately protein abundances. I found a higher number of DE genes in my early aging comparison, between 12 and 6 months, than in my late comparison, 24 vs 12 months (**Figure 5**). These results are in line with previous transcriptomic studies of brain aging with multiple compared timepoints, including a subregion study (Li et al., 2020a), single-cell data (Almanzar et al., 2020; Zhang et al., 2021) and transcriptomic profiling of microglia and astrocytes (Pan et al., 2020). However, I consider the differences between early and late aging as central and therefore examined these comparisons individually, rather than always calculating the ratios of the oldest to the younger groups. With this approach, I highlight the decreasing extent of transcriptomic changes with time until 24 months of age. Remarkably, this decrease is not observed in the nuclear fraction, where the number of DE genes is generally smaller, but less affected by aging. This observation could potentially also be explained by increasing transcriptional variability with age, reducing statistical power and thus lowering the number of DE genes. While increasing age-related variability in the brain and other tissues has been proposed by several studies (Bahar et al., 2006; Cellerino and Ori, 2017; Martinez-Jimenez et al., 2017), contradictory results exist (Warren et al., 2007; Ximerakis et al., 2019). Increasing sample number and/or a targeted analysis of inter-indiviual differences of my data could provide additional information on this topic.

Within the set of DE genes found in my study, an upregulation of immune reactions (e.g., increased levels of toll-like receptor 2, TNF- and INF-response genes) and a downregulation of mitochondrial genes (NADH dehydrogenase components and mitochondrial translocases) are found, both common signatures of aging (Lee et al., 2000; Yankner et al., 2008; Zahn et al., 2007) and both already found at 12 months (**Figure 6, 7**). Transcripts encoding structural components of synapses were found to be stable with age in humans, while transcripts regulating synaptic transmission are more likely to change (Loerch et al., 2008). Results on gene expression that regulates neuronal functions are varied, both between species as well as within, and likely specific for subgroups of proteins (Bishop et al., 2010; Loerch et al., 2008; Lu et al., 2004; Soreq et al., 2017; Wood et al., 2015; Zullo et al., 2019). While I found increasing levels of 'synaptic organization' transcripts (e.g., Shank2) both early (12 vs 6) and in the long comparison overall (24 vs 6), I also found their downregulation

specifically in the late comparison (24 vs 12) that is pronounced in the nucleus (e.g., decreased levels of Homer1 and neurexin-3) and possibly involves 'vesicle localization' (decreased levels of e.g. synaptotagmin 11 or syntaxin-binding protein 5-like).

5.2 | Nuclear transcription implicates specific rearrangements in synaptic, mitochondrial, and ribosomal processes

Combining the results from both subcellular fractions, a spatial redistribution of transcripts becomes apparent, that seems to preferentially affect synaptic, mitochondrial, and ribosomal genes (**Figure 8**). For synapse-related transcripts, the decreasing nuclear fraction (ratio of transcript abundance in the nucleus vs total) traces back to overall higher gene expression with age, while the nuclear-localized transcripts remain stable or show decreasing levels. The reverse is found for nuclear-transcribed mitochondrial transcripts, which decrease overall while being stable or slightly upregulated in the nucleus. Whereas these two functional groups of genes were already implicated by my GO analysis in both fractions, a pronounced increase in the nuclear fraction of ribosomal genes was not apparent before. I found a modest decline of ribosomal-associated genes in the total fraction, while the nuclear fraction of ribosomal transcripts remains stable or slightly upregulated with age. I can only speculate as to the underlying mechanisms and possible evolutionary factors that enable this nucleo-cytoplasmic redistribution. Transcripts might be either regulated by their rate of transcription within the nucleus, their rate of transport out of the nucleus, or by the rate of degradation in the cytoplasm. Additional experiments will be necessary to elucidate the primary mechanisms and their timeframes. Application of advanced RNA-sequencing methods (such as nanopore sequencing; Aw et al., 2021) and targeted measurements of non-coding RNAs, which influence neuronal function and change with age and NDD (Keihani et al., 2021; Keihani et al., 2019; Wood et al., 2013), combined with extensive bioinformatics would enable precise quantification of RNA species in both fractions, as well as better insights into nascent transcript formation and processing, taking place within the nucleus. Additionally, cytosolic RNA could be isolated to achieve better detection of splice junction detection (Zaghlool et al., 2013). Our group is currently in the process of setting up a pipeline that would allow to study these parameters thoroughly in the context of brain aging.

5.3 | Physiological aging shows modest, but relevant protein abundance changes

Transcriptomic datasets of (brain) aging dominate the field of 'omics' studies, although proteomic datasets actually show better conservation across species (Laurent et al., 2010) and are likely a better functional readout of age-related processes in the brain. It has been shown before how little proteomic and transcriptomic data of aging are correlated (Cellerino and Ori, 2017; Ori et al., 2015; Vogel and Marcotte, 2012), which I can confirm also in this work for both total and nuclear RNA (**Figure 16**). Protein and transcript abundance are likely separated by too many regulatory mechanisms between them, from RNA stability and binding, over translation efficiency, to protein stability and modifications to extract the one from the other. Very few proteins are well correlated with transcript abundance. Interestingly, Gfap, neurofilament light and heavy and several other

cytoskeleton (associated) proteins are among them, suggesting a tighter control or relationship in these cases. A similar finding has been made in a study comparing protein and RNA abundance in human cell lines (Gry et al., 2009), however, to my knowledge, this phenomenon has not been described or discussed in detail.

With protein and RNA levels being so poorly correlated, it is essential to expand our knowledge on brain aging beyond the existing transcriptomic studies and apply more proteomics. However, compared to next generation sequencing, proteomic studies using LC-MS suffer from increased technical difficulty, greater variability and considerably smaller numbers of identification and quantification. Especially the detection of small abundance changes, which are most prominent during aging, often do not pass the strict multiple comparison significance cutoffs that are commonly applied in transcriptomics. For proteomics, a standardized and unified analysis framework is missing, and studies use a wide range of statistical corrections.

We here used a method called DEqMS, that considers a specific feature of MS-data, the variation in identified peptides. With that, we identified 27-37 differentially abundant proteins in physiological aging, depending on the respective age-group comparison (**Figure 11**). The most significant protein that is age-upregulated is Gfap, with abundance increasing 85% from 6 to 24 months. This marker of astrogliosis and inflammation has been identified in aging contexts multiple times before (Boisvert et al., 2018; Jucker and Ingram, 1997; Savas et al., 2017), thus solidifying the validity of my other findings.

5.3.1 | Evidence for altered protein homeostasis in brain aging

I also found a strong upregulation of Ppt1 by 62%, a protein which removes thioester-linked fatty acyl groups during lysosomal degradation. Mutations in the gene encoding Ppt1 cause the neurodegenerative storage disorder neuronal ceroid lipofuscinois type 1, where progressive accumulation and aggregation of non-degraded proteins leads to gliosis, retinal degeneration, brain atrophy, mental and motor retardation and premature death (Vesa et al., 1995).

While lysosomal Ppt1 abundance is upregulated, its activity and efficiency are unknown. Upregulation of lysosomal components is observed in mice and humans, but their functionality might be compromised (Bäuerlein et al., 2017; Jinn et al., 2017; Zahn et al., 2007). Similarly, reduced proteasome activity is heavily implicated in aging (Chondrogianni et al., 2014; Kelmer Sacramento et al., 2020). Proteasome subunit beta type-6 (Psmb6) is a component of the 20S core proteasome and one of the relatively few proteins that are continuously downregulated (-39% and -29% from 6 to 12 and 12 to 24 months, respectively). Its decrease was also found in aging killifish (Kelmer Sacramento et al., 2020) and AD brains (Peng et al., 2020). Not continuously, but significantly decreased from 6 to 24 months (-30%), is proteolysis effector cullin-1 (Cul1), a core component of the cullin-RING E3 ubiquitin-protein ligase complex. Both efficiency as well as abundance of proteolysis proteins should therefore be evaluated in aging whenever possible.

Except for RNA-binding motif protein 3 (Rbm3), all chaperones that change significantly are downregulated after 12 months of age, including Hspa4, Hsph1, Hsp90ab1 and Hsp90 co-chaperones Ppid and stress-induced-phosphoprotein 1 (Stip1). Rbm3 is the only cold-shock protein (Danno et al., 1997) in this group and stimulates ribosomal assembly at low temperatures (Al-Astal et al., 2016), promotes neurogenesis after hypoxic-ischemic brain injury (Zhu et al., 2019) and regulates local synaptic translation (Sertel et al., 2021). One could speculate

that Rbm3 is less affected by or even tuned to a decrease in ATP-availability, which has been described to occur with age (Caldwell et al., 2015) and after hypoxic-ischemic injury (Perlman, 2007). Upregulation of ATP-independent chaperones is thus likely a neuroprotective mechanism employed by the brain during energy crisis, as suggested before (Brehme et al., 2014).

5.3.2 | Strong alterations in cytoskeleton and -associated proteins

The actin binding protein ermin (Ermn) is expressed exclusively in oligodendrocytes, where it regulates cytoskeletal arrangements, leading to myelin wrapping and compaction (Brockschnieder et al., 2006). Decreased expression of *Ermn* has been described in multiple sclerosis patients (Salek Esfahani et al., 2019) and Ermn KO mice exhibit aberrant myelin architecture and fractured myelin sheaths (Wang et al., 2020), features also found in physiological aging (Hill et al., 2018; Sim et al., 2002). However, I found Ermn levels increased by 98% in the aged brain. Both the upregulation of above described Ppt1 and Ermn could be protective mechanisms in the aging brain that prevent major neuronal damage but cause severe pathology when dysfunctional. Another protein associated with myelination is contactin-1 (Cntn1). Cntn1 is upregulated at 12 months (16% increase), but then its levels decline again at 24 months of age (-13%). Notably, the functions of Cntn1 extend to regulating neurogenesis and synaptic plasticity by mediating cell surface interactions (Chatterjee et al., 2019).

Neurofilaments and associated proteins show a very unique pattern of significant downregulation from 6 to 12 months (~-39%) and upregulation from 12 to 24 months (~58%). They are not significantly different between 6 and 24 months and would have been missed if only those two timepoints were compared. Neurofilaments build a compact and very long-lived structure and their content in axons expands axonal diameter and thus increases conduction velocity in myelinated fibers (Križ et al., 2000). The minor rearrangement and turnover of these cytoskeletal structures is believed to conserve energy in neurons with especially long axons (Fornasiero et al., 2018; Millecamps et al., 2007; Yuan et al., 2012). Functions in synaptic arrangement of receptor recycling and late-endosome/lysosome anchoring have also been suggested (Kim et al., 2002; Rao et al., 2011; Yuan et al., 2015). To my knowledge, neurofilaments and their largely phosphorylation dependent regulation, has not been studied extensively in physiological aging. They are however closely linked to axonal injury events and as such used as biomarkers for axonal loss and neuronal death. High levels of Nefl and Nefh, likely released from damaged and degenerating axons, are found in cerebrospinal fluid and blood in AD and frontotemporal dementia (Khalil et al., 2020; Petzold et al., 2007). Mutations in neurofilament genes, which lead to aggregation and transport failure of neurofilament components, are further considered primary pathogenic factors preceding axonal dysfunction and neurofilamental inclusion bodies. Such mutations have been identified in familial PD and AD (Lavedan et al., 2002; Yuan et al., 2017). In AD, hyperphosphorylated Nefm is associated with neurofibrillary tangles and amyloid plaques (Liao et al., 2004).

The group of intermediate filaments also include lamins, the major constituents of the nuclear lamina. Lamin-B1 (Lmnb1) and (to a lesser extend with just significant downregulation after 12 months) lamin-B2 (Lmnb2) show the same pattern of initial up- and late downregulation in my aging comparison. While prelamin-A/C (Lmna) is well known for its role in HGPS, Lamin-B reduction is emphasized in replicative senescence and physiological aging in human cell lines and simple model organisms (Freund et al., 2012; Tran et al., 2016).

Lamin-B further directs neuronal migration and neurodevelopment (Coffinier et al., 2011), possibly explaining its initial upregulation during ongoing network formation after 6, but not after 12 months of age.

Annexin 6 (Anx6) is one of the most abundant annexins in the brain, a family of calcium-binding proteins that is implicated in membrane trafficking and membrane-cytoskeleton interaction. In AD, Anx6 is associated with granulovacuolar bodies (Eberhard et al., 1994) and was found to be able to bind tau protein (Gauthier-Kemper et al., 2018). The observed reduction in Anx6 levels in aged brains (-14% from 12 to 24 months) might precede abnormal somatodendritic tau localization, when tau can no longer be bound and stabilized at the axon initial segment. However, no direct effect of aging on axon initial segment structure, protein levels and tau distribution was found in aged rats (Kneynsberg and Kanaan, 2017).

Neuronal and glial spectrin proteins are membrane-associated molecules which organize membrane formation, remodeling, and stabilization by interacting with the cell cytoskeleton. I found beta spectrin 2 and 4 (Sptbn2 and 4) to be significantly decreased already at 12 months of age (-12% and -34%, respectively). Spectrin degradation occurs via calcium-dependent proteases calpain and caspase-3, reacting to excitotoxicity and pro-apoptosis signals and thus potentially serves as early sign of neuronal pathology after traumatic and ischemic insult, but also in NDDs (Czogalla and Sikorski, 2005; Gafni and Ellerby, 2002; Masliah et al., 1990; Raynaud and Marcilhac, 2006). Increased abundance of spectrin degradation products was shown in rats by 16 months of age (Yan et al., 2012), fitting my observation of middle age decrease in intact spectrin. This means that spectrin and spectrin degradation products could serve as neurodegenerative markers also in physiological aging.

5.3.3 Neuron growth and network homeostasis

Limbic system-associated membrane protein (Lsamp) is known for its role in neuron guidance and growth during neurodevelopment (Singh et al., 2018). I found its abundance decreased at 24 months of age (-17%), possibly indicating a prolonged role of Lsamp in neuritogenesis into adulthood that ceases relatively late.

Immunoglobulin superfamily protein Igsf8, which is also found to be decreased in 24 months aged mice (-15%), has recently been identified as hippocampal CA3 microcircuit organizer. Its loss caused diminished feedforward inhibition, increasing excitability of CA3 pyramidal neurons (Apóstolo et al., 2020). As such, Igsf8 could be a contributing factor to the dysbalanced excitatory/inhibitory landscape found in aged neuronal networks (Rozycka and Liguz-Lecznar, 2017). Igsf8 protein levels were also found downregulated in AD tissues (Begcevic et al., 2013).

5.3.4 Altered energy metabolism and declining detoxification systems

I found adenylate kinase isoenzyme 1 (Ak1) upregulated early, from 6 to 12 months (27%), and then non-significantly changed later on. This protein plays an important role in energy homeostasis and ATP metabolic processes by catalyzing the transfer of the terminal phosphate group between ATP and AMP. It was further shown to link intracellular energy pathways via AMPK regulation and presence of amyloid beta species to tau

hyperphosphorylation (Park et al., 2012). As such, Ak1 protein expression is increased in AD models as well as human patients (Manavalan et al., 2013; Park et al., 2012).

Cytochrome c mediates the electron transfer to the cytochrome oxidase complex of the mitochondrial respiratory chain. As such, it is indispensable for energy production. Cytochrome c release from mitochondria also serves as apoptosis signal, though. The interim upregulation of Cycs in 12 months old mouse brains that I observed (increase of 31% followed by decrease of 22%) might be the brain's attempt to increase energy production via mitochondrial respiration. However, ultimate decline in cytochrome c oxidase function (Navarro et al., 2002) seems paralleled by decline of Cycs, possibly also protecting from overt cell apoptosis that is not observed in aging (Pollack and Leeuwenburgh, 2001).

Toxic byproducts of enzymatic reactions are cleared in healthy organisms by damage-control systems. The hydrated form of NADPH, NADPHX, is one such side product which can also arise spontaneously. NADPH-hydrate epimerase (Naxe) is essential to initiate subsequent dehydratase action and repair of the modified R-epimer of NADPHX. Without this safeguard mechanism, NADPH-based biochemical reactions and energy metabolism are disturbed. Abrogated function of Naxe has been described to be fatal in human patients due to rapidly progressing ataxia, spinal myelopathy, and cerebellar edema within the first three years of life (Kremer et al., 2016). Another reactive side product is formed during glycolysis: methylglyoxal, which further can elicit the formation of AGEs (Rabbani and Thornalley, 2012). Mitochondrial hydroxyacylglutathione hydrolase (Hagh), better known as glyoxalase 2, forms the detoxifying glyoxalase system together with glyoxalase 1 to neutralize methylglyoxal. Neuronal and especially astrocytic expression of glyoxalase thus confers neuroprotection (Bélanger et al., 2011). I show that protein abundance of both Naxe (-26%) and Hagh (-32%) decline in physiological aging after 12 months, indicative of failing detoxification mechanisms and energetic challenge.

Ferritin heavy chain (Fth1) is important for iron homeostasis as it stores iron in a soluble, readily available form. Iron progressively accumulates in the aging brain and extracellular iron deposits are present especially in the substantia nigra of individuals aged 80 years or more (Zecca et al., 2001). Ferritin, as iron storage structure composed of Fth and Ftl, shows increased iron load in PD. Upregulation of ferritin components is unclear in PD (Faucheux et al., 2002; Jellinger et al., 1990) and non-existent in AD (Connor et al., 1992). I find increased levels of both Fth1 (54%) and Ftl1 (24%) in 24 months aged mouse brains. Unbound iron may become cytotoxic and is linked to activation of microglia and inflammation in neurodegeneration (Zecca et al., 2004). Further, ferritin immunoreactivity is observed in and around senile plaques and neurofibrillary tangles (Jellinger et al., 1990). Correspondingly, I found that Fth1 and Ftl1 are also significantly increased in the insoluble fraction of aged mice and their relative insoluble enrichment increases significantly as well.

5.4 | Aging-specific enrichment of insoluble proteins

In line with increasing protein accumulation and aggregation in aged brains, I found ratios of protein enrichment in the insoluble fraction increasing continuously from 6 to 24 months (**Figure 17**). My results correspond well to previously published data on the aggregation propensity of proteins (determined after heat-induced stress; Määttä et al., 2020). Moreover, they show remarkable correlation to results from a recent study examining the SDS-insoluble protein fraction of aged mice (21-26 months of age; Kelmer Sacramento et al., 2020). Importantly, I here describe the changes within the insoluble fraction and its enrichment over time, instead of only considering

the single latest age timepoint (**Figure 18**). Strongly age-insoluble-enriched proteins, like collagens, are already enriched at 6 and 12 months of age in my study and their degree of enrichment does not significantly change with age. This is the case for several other proteins mentioned in the Kelmer Sacramento et al. study as well, e.g., ECM laminins.

5.4.1 | Aggregation of specific ribosomal proteins with age

Ribosomal protein stoichiometry has been described to undergo changes with age as components become upregulated and aggregation prone, thus more likely to be found in an insoluble fraction (Kelmer Sacramento et al., 2020), but invariable and decreasing ribosome component abundance have also been described in the mouse brain (Amirbeigiarab et al., 2019; Li et al., 2020b). I show here that only a specific subset of ribosomal proteins undergoes age-related insoluble upregulation by 24 months of age. Significantly, these are Rpl8, Rpl29, Rpl19 and Rps23. The fact that other ribosomal proteins, while found in the insoluble fraction, do not change their enrichment with age, firstly shows that my fractionation protocol does not generally enrich ribosomal proteins. Secondly, altered stoichiometry does not necessarily correlate with protein aggregation, as Kelmer Sacramento et al. also point out in their results for mitochondrial complexes. Specific roles for the assembly of ribosomes (La Cruz et al., 2015) and functions beyond ribosomal protein synthesis have been described for ribosomal proteins, in immune activation, cell cycle regulation and common cancers (Xie et al., 2018; Zhou et al., 2015). Without a more detailed examination of ribosome composition, efficiency and accumulation measures however, no clear picture of the role of ribosome proteins in the aging brain has emerged yet.

5.4.2 | Underlying mechanisms for age-related protein aggregation are diverse

Apart from ferritin and ribosomal proteins, 12 more proteins show significant solubility shifts in aging. Proteins found to significantly increase their insoluble enrichment with age are deubiquitinating enzyme 24 (Usp24), and heterochromatin protein 1-binding protein 3 (Hp1bp3). Both proteins have been connected to aging and NDDs: Elevated Usp24, negatively regulating autophagy, was found in PD (Thayer et al., 2020). Decreased levels of Hp1bp3 were sufficient to induce transcriptional changes reminiscent to those observed in aging and AD (Neuner et al., 2019). Histone reader zinc finger ZZ-type and EF-hand domain-containing protein 1 (Zzef1) is a histone H3 reader and transcriptional regulator (Yu et al., 2021). I found a strong insoluble enrichment increase from 6 to 24 months. Beyond a possible connection to DNA methylation in AD (Pellegrini et al., 2021), very little is known about this protein in the context of brain aging. As exemplified by these proteins, it is very difficult to draw conclusions as to whether protein enrichment in the insoluble fraction with age might be an active, potentially protective mechanism, a detrimental accumulation of material, or a byproduct of increasing aggregation load and binding of uninvolved proteins. More targeted experiments are needed to delineate some of these aspects. These could include more systematic descriptions of protein aggregation in mouse models of aging at different ages, in vitro aggregation assays or examination of organismal responses to exogenic stressors or seeding of aggregates. For some other proteins, when more functional or biochemical data is available, more educated guesses can be made.

For example, lipid droplets, recognized for their inflammatory role in peripheral myeloid cells, have recently been described within microglia. The lipid droplet protein Perilipin-3 (Plin3) is increasingly found within microglia in the aging mouse brain, likely causing the detrimental phenotype believed to underly inflammation and neurodegeneration (Marschallinger et al., 2020). The increased enrichment of Plin3 in the insoluble fraction of my physiologically aged mice fits well with an overall inflammatory environment and elevated concentrations of lipids, which might only be partially balanced by increased microglial uptake of such lipids.

Protein arginine N-methyltransferase 5 (Prmt5) catalyzes both protein and histone methylation. In oligodendrocytes, developmental myelination has been connected to Prmt5 action (Scaglione et al., 2018). Beyond that, interesting results come from kidney samples of 22-months aged mice (Yi et al., 2020): a cysteine residue of Prmt5 becomes glutathionylated in the increasingly oxidative environment of aging tissues. This modification disrupts the interaction with other proteins necessary for the formation of the functional methyltransferase complex, possibly leading to the aggregation of orphaned Prmt5, which could underly the increasing insoluble enrichment that I found in aged mouse brains.

5.4.3 | Altered aggregation status influences energy homeostasis across cellular networks, affecting neuronal activity

Monocarboxylate transporter 1 (Slc16a1, better known as Mct1) is the only protein to show the highest insoluble de-enrichment at 12 months, compared to positive enrichment at both 6 and 24 months. Monocarboxylates, such as lactate, pyruvate and ketone bodies are important energy substrates and their shuttling between cells, but also between blood and cells is enabled by Mcts (Bergersen, 2007). Mct1 is expressed by oligodendrocytes and lactate serves as metabolite to support lipid synthesis, especially when energy supply via glucose is limited (Philips et al., 2021; Rinholm and Bergersen, 2012). Lactate utilization changes depending on the myelination state, as was shown in adult mice where lactate from myelin was released to be used by axons (Fünfschilling et al., 2012; Lee et al., 2012). Abundant Mct1 that is freely available (and not detected in a possibly ‘bound’ state in the insoluble fraction) to transfer monocarboxylates between cells might thus be especially important in middle aged mice, when axons are myelinated but need to be maintained under increasingly challenging energy supply.

Possibly similar mechanisms to uphold energy and biosynthetic processes could be at play with ATPase family AAA domain-containing protein 3 (Atad3). This mitochondrial membrane ATPase is insoluble de-enriched in aged brains in my study. Atad3 is hypothesized to function as cholesterol transporter between ER and mitochondria, supporting mitochondrial biogenesis (Rone et al., 2012; Rousseau, 2019).

Glycogen synthase kinase-3 alpha (Gsk3a) is found enriched in the insoluble fraction already at 12 months. The protein kinase has a manifold of functions in bioenergetics, neuronal plasticity, neuronal survival and inflammation (Salcedo-Tello et al., 2011). Both increase and decrease of Gsk3a activity and abundance have been connected to altered lifespan and neuropathology (Beurel et al., 2015; Souder and Anderson, 2019). The complex networks linking Gsk3a, Gsk3b, insulin and AMPK-mTOR signaling, as well as tau phosphorylation and transcription regulation exceed the scope of this work. I speculate however that, as sustained activation of Gsk3 is associated with neurodegeneration (Hurtado et al., 2012), sequestration of Gsk3a into aggregates might be neuroprotective.

Brefeldin A-inhibited guanine nucleotide exchange protein 3 (Arfgef3) is strongly de-enriched in the insoluble fraction of 24 months aged mice. This guanine exchange factor is localized in lysosomes in hippocampal neurons, likely involved in intracellular vesicle trafficking and has been connected to GABA-A receptor organization, similar to Arfgef1 (Liu et al., 2016; Teoh et al., 2020). It is unclear at this point, why this protein is less abundant in the insoluble fraction of aged brains and whether this could contribute to the altered excitatory-inhibitory neurotransmission balance found in aging (Rozycka and Liguz-Lecznar, 2017). Little is also known about the role of vesicular trafficking protein transmembrane emp24 domain-containing protein 7 (Tmed7). Interestingly, a third vesicle organizing protein is changed in the same manner: Protein kinase C and casein kinase substrate in neurons protein 2 (Pacsin2, also known as Syndapin-2). Pacsin2 likely regulates AMPA receptor internalization (Anggono et al., 2013) and has been found with slightly increased levels in aging rat dentate gyrus (Smidak et al., 2017).

Myelin proteolipid protein (Plp1) is the major myelin protein in the brain. Assembly of stable Plp oligomers occurs slowly in the brain, forming SDS-resistant homooligomers (Smith et al., 1984; Swanton et al., 2005). Upon overexpression of Plp, detergent-insoluble accumulations build up in late endosomes/lysosomes (Simons et al., 2002), a process also observed during physiological aging (Safaiyan et al., 2016). Myelin fragment inclusions in microglia contribute to microglia senescence and immune dysregulation. In contrast, I found a relative de-enrichment of Plp1 in the insoluble fraction in aged 24 months old mice, meaning higher levels of Plp1 in the soluble fraction. Increasing levels of fragmented, still soluble, and not yet aggregated, myelin might explain this ratio-shift. Interestingly, another myelin protein, myelin-associated oligodendrocyte basic protein (Mobp) shows the highest abundance in the insoluble fraction at 12 months of age, its relative enrichment does not reach significance though. While a role of Mobp in myelin compaction or radial organization is assumed, KO mice display no overt phenotype or defect in myelination, leaving Mobp's function unclear (Montague et al., 2006; Raasakka and Kursula, 2020). My results might provide another piece of information for the still poorly characterized Mobp. However, my protein fractionation protocol is not specifically designed to separate myelin proteins or their aggregates and better suited extraction methods (Jahn et al., 2009) could be applied to shed light on myelin-specific redistributions with age.

5.5 | Aging signatures vary between different models of aging

The aging-implicated pathways described so far are modeled in the here-included mouse cohorts, but to varying degree. I will not discuss each model in detail, but rather touch upon some remarkable observations. Finally, I summarize which aspects of physiological aging can or cannot be studied by using one or the other mouse model.

5.5.1 | Core and accessory pathways of aging in mouse models

No inclusion bodies or amyloid plaques have been found in aged SAMP8 brains, but blood-brain-barrier dysfunction, abnormal glia responses and impaired glucose metabolism have been described (Akiguchi et al., 2017), the latter correlating with the severity of cognitive defects (Ohta et al., 1996). A metabolomic study of

SAMP8 mice additionally identified strong differences in the abundance of acetyl-CoA, a-ketoglutarate, succinate, citrate and aconitate (Currais et al., 2019), all pointing to a major defect of mitochondrial-associated energy balance in these animals. This is very much in line with my results showing an overrepresentation of metabolic and energy pathway proteins being upregulated in SAMP8 brains (**Figure 20**), such as insulin receptor, glucose-6-phosphate isomerase, or pyruvate dehydrogenase E1 component, which links glycolysis and TCA cycle. Combined, this allows the classification of SAMP8 as metabolic model of aging.

The Zfand2b mice are little described in an aging context. In *C. elegans,* inactivation of the *Zfand2b* ortholog impairs proteostasis and shortens lifespan (Yun et al., 2008). In mice, *Zfand2b* and its protein product, AIRAPL, link myeloid transformation and regulation of IGF1-receptor levels (Osorio et al., 2016). Recently, upregulation of *Zfand2b* was observed in a neuronal cell line exposed to autoantibodies from PD patients, potentially as neuroprotective effector (similar to the observed upregulation of glutathione peroxidase 1; Zimering et al., 2021). The basic function of AIRAPL seems to be regulation of ER translocation and thus quality control of secretory proteins (Glinka et al., 2014). The upregulation of chaperone complex proteins that I found in my GO analysis of Zfand2b-KO mice (**Figure 21**) could therefore be a response to impaired ER-functions. Additionally, with IGF1 receptor distribution being altered by absence or presence of AIRAPL, effects on the insulin-IGF-pathway are likely. I describe a brain-specific response to the KO of Zfand2b with upregulation of proteins belonging to the glycolytic process (e.g., fructose-bisphosphate aldolase C), cellular amino acid metabolism (e.g., cysteine--tRNA ligase) and glutathione metabolic process (e.g., glutathione S-transferase). These changes are paralleled by changes of synaptic vesicle cycle proteins and modulation of neurotransmission (increased levels of e.g., Snap25 or syntaxin-binding protein 1).

The models of NDDs, Line 61, HM2 and APPPS1 (**Figures 22-24**), have been described and discussed previously (Chesselet et al., 2012; Kahle et al., 2000; Li and Wei, 2015; Radde et al., 2006; Richfield et al., 2002; Sasaguri et al., 2017). Shared between them, I found the expected altered synaptic and neurotransmission-regulating proteins, e.g., synaptoporin, neuronal pentraxin receptor, sodium- and chloride-dependent GABA transporter 3 or postsynapse organizer disks large-associated protein 3. Declining neuronal protein levels and synaptic disarrangement are likely due to progressive neurodegeneration, the core process modeled in these animals. Interestingly, in Line 61 and APPPS1, I also observed an upregulation of glucose metabolic processes which is supported by findings of increased glucose uptake in relation to cerebral amyloidosis and α-synuclein levels (Poisnel et al., 2012; Rodriguez-Araujo et al., 2013). HM2 mice show the previously described dysfunction of proteasomal degradation (Chen et al., 2006), with decreased levels of proteasomal proteins. Interestingly, I found a high correlation of the abundance of α-synuclein and Cops4, a member of the Cop9 signalosome complex that is an essential regulator of ubiquitin conjugation. In the insoluble fraction of HM2 and APPPS1 mice, I found lower abundances of proteins related to respiration and the NADH dehydrogenase complex, possibly indicating a shift in energetic balance, with more glucose utilization and increased respiration, which keeps mitochondrial proteins from being orphaned and accumulating. Although α-synuclein aggregates are observed early on in Line 61 animals, my results show few significant changes in the insoluble fraction. It may be noted that the extent of protein aggregation in these animals differs between brain regions (Chesselet et al., 2012) and depends on the housing conditions of the mice, with fewer aggregates found in mice raised under germ-free conditions (Sampson et al., 2016). Additional experiments will be needed to determine the aggregation-load of the animals used here.

Interestingly, resembling HM2 and APPPS1 mice, the mCat mice show decreased abundance of mitochondrial respiration proteins in the insoluble fraction. Here, catalase might protect mitochondrial respiratory complexes and prevent their sequestration into insoluble aggregates, possibly in connection to the upregulated Fundc1, which mediates autophagic degradation. Recently, it was shown that Fundc1 interacts with Hsc70 to promote the degradation of unfolded proteins by sequestering them to mitochondria, establishing mitochondrion-associated protein aggregates (Li et al., 2019). Fundc1 is also required for autophagic degradation of these aggregates. Under proteostatic stress conditions, as observed in aging, this Fundc1-Hsc70 mediated translocation of unfolded proteins into mitochondria without subsequent aggregate sequestration and degradation can also cause senescence (Li et al., 2019). One could speculate that overexpression of catalase prevents such an overload of the mitochondrial proteostatic response, allowing Fundc1 to degrade unfolded proteins without risking mitochondrial malfunction and enabling the observed upregulation of Fundc1 in the mCat mice (**Figure 25**). Food supplementation of antioxidants could similarly enable and safeguard a higher mitochondrial and biosynthetic capacity. Along this line, the top two upregulated proteins in the AntiOx mice are complex I subunit Mtnd3 and eukaryotic translation initiation factor 4C (Eif1ax), which is required for maximal protein synthesis rate (**Figure 26**). While the AntiOx mice might not be a model of aging or anti-aging per se, observations like these are valuable to put findings from other models into a closer context.

In contrast to the increased capacities in mCat and AntiOx mice, Ucp2-KO mice are prone to suffer from energetic stress. Neurons have been shown to be less plastic in the absence of Ucp2, but the relative number of synapses was still increased (Hermes et al., 2016). The authors speculated that synaptic formation and maintenance are dysregulated as a consequence of altered mitochondrial support. I also observed varied protein abundance changes in protein categories relating to synaptic and mitochondrial functions which need to be dissected in more detail (**Figures 27, 28**). For example, the presynaptic scaffold bassoon is significantly downregulated in Ucp2 brains, while clathrin light chain A is upregulated. Some mitochondrial complex I (NADH-dehydrogenase complex) proteins are upregulated (e.g., Ndufab1), others are downregulated (e.g., Ndufb11). Many of those proteins show reverse patterns in mCat and Ucp2 mice, potentially identifying them as closely linked to cellular respiration and affected by ROS-levels in their immediate environment.

Nuclear lamina models are well-established in regard to modeling HGPS. Their relevance for mimicking brain aging is debated, though. Perturbed nuclear morphology strongly affects tissues under mechanical stress, but the central nervous system actually shows little to no signs of impairment (Baek et al., 2015; Jung et al., 2012; Yang et al., 2015). I still found significant upregulation of proteins regulating nuclear chromatin and the DNA packaging complex in LAKI mice and reductions in protein folding capabilities (surrounding Hsp90) in both LAKI and Zmpste24 brains (**Figures 29, 30**). Fatty acid and glutathione metabolism, as well as proteasomal degradation and splicing are additional functions that are altered in both models which are indicated in the aging process. Most notably though, the nuclear lamina models also show changes in both ribosomal and cytoskeleton components, two functional groups of proteins that are prominently affected in physiological aging. In an across cohort comparison, LAKI and Zmpste24 resemble late physiological aging in this regard the closest (**Figure 34**).

The paradigm of short-term environmental enrichment started at 19.5 months of age applied to the cohort of animals used here does not show major protein abundance rearrangements **(Figure 31**). The only significant change is the decrease of phospholigase A2 (Pla2g4e) in the insoluble fraction, which is involved in membrane structuring and phospholipid metabolism. In post ischemic brain injury, spinal cord injury and NDDs, reduction or KO of phospholipase A2 ameliorates many of the detrimental events (see Leslie, 2015). At the same time,

phospholipase A2 also regulates neuronal homeostasis, especially long-term potentiation and depression (Le et al., 2010). It will be interesting to study this protein in more detail to elucidate its potential in synaptic rewiring following environmental enrichment.

I included the comparison between female and male aged mice, as we, and many others, used both sexes in some experiments. Differences in brain structure, aging timelines and disease susceptibility between the sexes have been described (Coffey et al., 1998; Eliot et al., 2021; Goyal et al., 2019; Hanamsagar and Bilbo, 2016; Jäncke et al., 2015; McCarthy et al., 2012; Piscopo et al., 2021; Sherwin and Henry, 2008). For example. females have greater lifetime risk of AD (Alzheimer's Association, 2020) and seem to experience greater cognitive deterioration under amyloid burden (Buckley et al., 2018). In contrast, PD is more common in males, disease slope is steeper and cognitive decline is likely greater in males (Reekes et al., 2020). However, the published data on sex differences in cognition and aging is vast, controversial, and potentially biased (Eliot, 2019) and an extensive discussion is beyond the scope and aim of this work. My results (**Figure 32**) show very few significant differences, which are likely also mouse strain-specific, with possibly higher 'endpoint' abundance of Gfap and intermediate filaments in females and increased serine protease inhibitor A3K (Serpina3k) in males, which has been described as neuroprotective after traumatic brain injury (Jing et al., 2019). Nuclear receptor corepressor 2 (Ncor2), which I found female-upregulated, is a transcriptional corepressor, negatively regulating androgen receptor signaling and possibly linking endocrine signaling with synaptic plasticity and GABA signaling (Zhou et al., 2019). The only male-insoluble-upregulated protein is Rbfox1, a splicing factor that affects neurodevelopment and neuroexcitation and is linked to autism spectrum disorder, epilepsy, attention deficit hyperactivity and schizophrenia (Gehman et al., 2011; Hamada et al., 2016). Overall, I believe that these results could prompt further investigation of the significant proteins and their role in brain aging, but that no further correction of my data based on animal-sex is necessary, given the minor extent of differences in aged female and male brains.

5.5.2 | Composite modeling of physiological brain aging using mouse models

I present here an extensive resource of proteomic data for aging processes in the brain. Remarkably, I found no single protein being significantly altered in all studied cohorts. Gfap was most commonly found, with significant changes in 8 comparisons (**Figure 33**). Signatures of brain aging that can be derived from my results therefore remain unique for each model, or at least for groups of models. While single proteins that universally underlie aging might not exist, the comparison of aging patterns and identified influence of some pathways rather than others is invaluable (**Figures 34-36**). For example, altered ribosomal stoichiometry seems to play a role in physiological brain aging, but is badly modeled in SAMP8 and some NDD models. HGPS models might be better suited to study this specific aspect of aging biology. Further, energetic disbalance can be examined in SAMP8 mice and direct comparisons with mitochondrial models of aging has the potential to delineate directly mitochondrial vs overall metabolic adaptations. In the case of Cop9 signalosome proteins, Line 61 and LAKI mouse brain juxtaposition could elucidate molecular mechanisms that influence brain structure and function. Remarkably, the two HGPS models, whose usefulness for the study of brain aging was unclear up to now, seem to resemble physiological aging in regard to declining proteostatic mechanisms (with decreased chaperone abundance and proteasomal dysfunction), intermediate filament reorganization and altered ribosomal stoichiometry. Especially the latter two make them uniquely suited to model progressive brain aging. **Figure 37**

provides a summarizing overview of which pathways of aging were substantially altered in the mouse models used in this study. This overview is far from exhaustive and does not include the results from other works, which are discussed above, but it is the first large-scale comparison of its kind that will allow a better estimation of which model and which age of physiological aging to use for a specific pathway under investigation.

'aging signature' includes altered...	phys. aging early	phys. aging late	SAMP8	Zfand2b	Line 61	HM2	APPPS1	mCat	AntiOx	Ucp2	LAKI	Zmpste24
energy metabolism	✓	✓	✓	✓	✓		✓		✓		✓	✓
mitochondrial respiration		✓	✓			✓	✓	✓	✓	✓		
synapse organization and neuronal function	✓	✓		✓	✓	✓	✓		✓	✓	✓	
proteostasis		✓		✓	✓	✓	✓				✓	✓
gliosis		✓	✓	✓		✓	✓	✓		✓	✓	
splicing and mRNA processes	✓			✓		✓				✓	✓	✓
myelin components		✓	✓			✓	✓	✓	✓			
intermediate filament organization	✓	✓										✓
ribosome components		✓	✓									✓

Figure 37 Summary of 'aging signatures' of mouse brains analyzed in this work. Some of the pathways connected to the aging process are more prominently affected in some mouse models than others, tick marks represent the finding of substantial alterations in that respective category and cohort of mice.

5.6 | Conclusion and outlook

Overall, I present here an extensive set of data on brain aging, using RNA sequencing and LC-MS protein abundance measurements. My results lead to the formulation of the following six statements: **First**, gene expression, measured as transcript abundance levels, changes dramatically in early aging, from 6 to 12 months in mouse brains, but to a lesser extent in late aging, from 12 to 24 months of age. **Second**, transcription of synaptic organization related genes declines particularly in late aging and synaptic RNAs are depleted from the nucleus. Contrarily, mitochondrial, and ribosomal transcripts are upregulated specifically in the nucleus and increase their abundance ratio to the overall levels with age. **Third**, protein abundance changes in the aging brain are small, but implicate especially a decline of neurotransmission, a reorganization of neurofilamental structures, decreasing energetic capabilities and altered ribosomal stoichiometry. **Fourth**, ribosomal proteins undergo solubility transformations that are specific to age and protein, but not universal. Age-related accumulation of aggregates further includes ferritins and several proteins that influence neuronal network energy and activity homeostasis. **Fifth**, the mouse models of aging used here can be roughly grouped into modeling either metabolic, neurodegenerative, mitochondrial or proteostatic mechanisms. The proteomic alterations observed in each model are closely related to their main underlying modification, but accessory effects resemble physiological aging. Finally, **sixth**, it is important to differentiate between physiological aging and artificial models of it. No model analyzed here fully captures 'normal' brain aging, especially in terms of

ribosomal and neurofilamental alterations. Groups of models and the comparison between them can however be useful to delineate connections between pathways and to identify molecular adaptations that are specifically relevant in the brain, opposed to other tissues.

Several limitations and pitfalls of this work can be pointed out. First of all, the translation of mouse experiments into human applications is limited and always warrants caution. Whenever possible, I referred to available human studies of brain aging and their results, though most of them are acquired from NDD patients and lack a temporal dimension. With appropriate adjustments however, inferences from mouse experiments can be made to human physiology (see Kluever and Fornasiero, 2021). As ethical and practical reasons preclude most molecular examinations of human brain aging, the mouse remains the most promising model and tool that can help us to decipher the complex code of brain aging. Standardization and documentation of the exact breeding and housing conditions of all animals that are used is essential, though.

Further, I used whole brain homogenates for the acquisition of transcriptomic and proteomic data. While this was necessary to extract sufficient material for subsequent fractionation protocols and circumvent the need of pooling biological samples, it dilutes and possibly masks the different changes specific to subregions of the brain. The intricacies of structural composition and molecular functions of brain regions and their age-related transformations are immensely complex to study, but with advancing technologies, more details will be brought to light. Based on tissue dissection methods, fractionation protocols, laser capture microdissection or cell sorting (Drummond et al., 2015; García-Berrocoso et al., 2018; Hammond et al., 2019; Pan et al., 2020), this includes increasingly sensitive single-cell transcriptomics with the capacity to identify single base alterations (Gupta et al., 2018; Lebrigand et al., 2020; Philpott et al., 2021) and novel strategies to improve mass spectrometry based quantifications, compromising between robustness, multiplexing and sensitivity (Bian et al., 2020; Meier et al., 2020; Pappireddi et al., 2019; Stadlmann et al., 2019).

Fractionation and robust mass spectrometry quantification brings me to the next limitation of this study. As any manual preparation of samples, I cannot exclude variations in the efficiency of isolating nuclear and insoluble fractions from my samples. However, with all samples being prepared by the same person, meticulous quality controls before and after sample analysis and the fact that internal normalization and relative ratio calculation removes potential batch effects, a high quality standard of the presented data can be assumed. The good identification of proteins in the insoluble fraction also points to successful solubilization of proteins prior to mass spectrometric measurement. Very dense or compact aggregate structures which remain insoluble even in the harsh conditions that I used, might, however, not be digested properly and thus not be detectable in my data. Specialized protocols with vigorous solubilization methods using strong acids (Hosp et al., 2017) or similar could solve this issue, however compatibility with LC-MS needs to be kept in mind. Similarly, as touched upon previously, especially lipid and myelin protein quantification would likely improve by adjusting the preparatory protocol accordingly.

Statistic evaluation of LC-MS data lacks a unified framework and especially for the small changes observed in brain aging, strict analyses cut-offs and necessary normalizations across batches most likely mask small but impactful differences. The high variation between individual samples and between measurements that is very characteristic of both aging and LC-MS, respectively, further exacerbates this issue. Thus, the analyses presented here are limited by often small numbers of multiple-comparison corrected significant hits. The use of non-adjusted *p*-values allows more observations but increases the likelihood of false positive results. We are

therefore currently in the process of setting up a validation pipeline for some of the most prominent findings of this work. Parallel reaction monitoring (PRM) is a paradigm of targeted proteomics which provides excellent reproducibility and sensitivity over a wide dynamic range. We will use PRM and custom synthesized peptides to verify some of the protein abundance changes observed during aging.

The larger and more dimensional datasets become, the more important is a thorough analysis. My goal in this work was to describe effects from a biological point of view, relying on relatively simple analysis methods and linking back to existing knowledge whenever available. A purely bioinformatic approach could rely on more unsupervised and automated (clustering) methods and detect novel dependencies that are not apparent otherwise. However, similar to lacking a unified statistical framework, existing analysis methods and algorithms are not necessarily adjusted to the characteristic kind of data of brain aging (small changes with relatively large variations). Protein function and GO annotations also do not necessarily highlight the specific regulatory roles a protein might have in the brain, as they are often derived from findings in other tissues (which are studied more commonly). Established tools might therefore fail especially in large groups of proteins annotated under a common name and miss some of the relevant details of brain aging. Our group is actively working on establishing bioinformatic pipelines to solve some of these complex issues. I used custom, manually curated annotations in some analyses of this work to circumvent this issue. While being based on the specific function in the brain, whenever applicable, my own categorization will always carry some bias and can be contested. By using a combination of manual and official GO annotations though, I show that these two correspond well and that findings here are well based.

Further validations that will be useful are in part already set up by my myself and members of my lab. These include a modular CRISPR-Cas9 gene modification system, deliverable to primary hippocampal or cortical cell cultures via adeno-associated virus infection. With this, specific genes can be targeted for KO or overexpression and their molecular effects can be studied by basic neurophysiological assays (e.g., live calcium imaging or synaptic vesicle release monitoring using fluorescent dyes), imaging-based localization and interaction studies using super resolution microscopy techniques, or by biochemical evaluation of interaction partners (using pull-down assays) and metabolic state of the cells (using e.g., mitochondrial function and redox assays). Eventually though, these validations will need to be performed *in vivo*, in the context of aging in model animals. My results provide interesting new perspectives for the development of models, though. Ribosomal and intermediate filament-based alterations during brain aging for example are poorly characterized so far, which could be improved by specific targeting of these structures in aging mice.

Measurements taken here represent a single snapshot in time of abundance levels of transcripts and proteins. For the cohort of physiological aging, I have shown the value of analyzing at least three ages and two dimensions of functional biomolecules (RNA and protein). Ideally, multiple ages should be included in all aging studies and whenever possible, multiple levels of regulation should be assessed. Identification and cataloging of translation rates (Scheckel et al., 2020) and post-translational activity regulation by e.g. phosphorylation (Bai et al., 2020; Ori et al., 2015), as well as lipidomics (Fitzner et al., 2020) and metabolomics (Ivanisevic et al., 2016; Johnson et al., 2020; Zenobi, 2013) are adding to a comprehensive picture of brain aging. In our lab, we have begun the systematic study of two additional parameters that are particularly important in the context of protein homeostasis: ubiquitination pattern and protein turnover. For the former, in collaboration with Dr. Felipe Opazo and Nanotag, we have begun the characterization of nanobodies that specifically detect and bind different ubiquitin-linkage patterns. I started to optimize a pull-down assay to separate K48 and K63 linkage

poly-ubiquitin proteins from mouse brain homogenate. These proteins could then be analyzed with LC-MS, allowing both qualitative and quantitative readouts of proteins marked with one or the other pattern. As proteasomal degradation capacity likely declines with age, a redistribution of K48, K63 or other ubiquitinations could be both causative and consequential, making their study in aging brains highly valuable. Protein turnover calculation of proteins has been performed by feeding mice with food that contains heavy isotope (13C) labelled lysines in a pulse-chase experiment, causing a mass shift of 13C labelled proteins which can be measured by LC-MS (Alevra et al., 2019; Fornasiero et al., 2018). We have applied this method also to aged mice to identify the general turnover rate as well as age-related shifts in turnover prioritizations (publication currently under review). It will be interesting to combine the results of this study with the results obtained here, possibly revealing new links between RNA and protein abundance, aggregation-propensity, and protein lifetimes.

With all of the above-mentioned experimental measures, as well as advancing bioinformatic-based predictions and models of protein structures, functions and interactions (Voytik et al., 2021), we are getting closer to a thorough description of molecular aging processes occurring in the brain. It will be essential to continuously improve the existing annotations and classifications of protein functions, so that large scale combinatorial data and their analyses will be specific for the tissue or cell type under investigation. With that, and an open communication of results, our understanding of aging will broaden, which is essential to tackle the development of anti-aging strategies, to delay or rescue neurodegeneration and improve cognitive function in the elderly.

6 | References

Abdelmoez, M.N., Iida, K., Oguchi, Y., Nishikii, H., Yokokawa, R., Kotera, H., Uemura, S., Santiago, J.G., Shintaku, H., 2018. SINC-seq: correlation of transient gene expressions between nucleus and cytoplasm reflects single-cell physiology. Genome Biol 19, 66. https://doi.org/10.1186/s13059-018-1446-9.

Ackert-Bicknell, C.L., Anderson, L.C., Sheehan, S., Hill, W.G., Chang, B., Churchill, G.A., Chesler, E.J., Korstanje, R., Peters, L.L., 2015. Aging Research Using Mouse Models. Current protocols in mouse biology 5, 95–133. https://doi.org/10.1002/9780470942390.mo140195.

Adlard, P.A., Perreau, V.M., Engesser-Cesar, C., Cotman, C.W., 2004. The timecourse of induction of brain-derived neurotrophic factor mRNA and protein in the rat hippocampus following voluntary exercise. Neuroscience letters 363, 43–48. https://doi.org/10.1016/j.neulet.2004.03.058.

Afagh, A., Cummings, B.J., Cribbs, D.H., Cotman, C.W., Tenner, A.J., 1996. Localization and cell association of C1q in Alzheimer's disease brain. Experimental Neurology 138, 22–32. https://doi.org/10.1006/exnr.1996.0043.

Ain, Q., Schmeer, C., Penndorf, D., Fischer, M., Bondeva, T., Förster, M., Haenold, R., Witte, O.W., Kretz, A., 2018. Cell cycle-dependent and -independent telomere shortening accompanies murine brain aging. Aging 10, 3397–3420. https://doi.org/10.18632/aging.101655.

Akiguchi, I., Pallàs, M., Budka, H., Akiyama, H., Ueno, M., Han, J., Yagi, H., Nishikawa, T., Chiba, Y., Sugiyama, H., Takahashi, R., Unno, K., Higuchi, K., Hosokawa, M., 2017. SAMP8 mice as a neuropathological model of accelerated brain aging and dementia: Toshio Takeda's legacy and future directions. Neuropathology: official journal of the Japanese Society of Neuropathology. https://doi.org/10.1111/neup.12373.

Al-Astal, H.I.M., Massad, M., AlMatar, M., Ekal, H., 2016. Cellular Functions of RNA-Binding Motif Protein 3 (RBM3): Clues in Hypothermia, Cancer Biology and Apoptosis. Protein and peptide letters 23, 828–835. https://doi.org/10.2174/0929866523666160628090340.

Alevra, M., Mandad, S., Ischebeck, T., Urlaub, H., Rizzoli, S.O., Fornasiero, E.F., 2019. A mass spectrometry workflow for measuring protein turnover rates in vivo. Nature protocols 14, 3333–3365. https://doi.org/10.1038/s41596-019-0222-y.

Almanzar, N., Antony, J., Baghel, A.S., Bakerman, I., Bansal, I., Barres, B.A., Beachy, P.A., Berdnik, D., Bilen, B., Brownfield, D., Cain, C., Chan, C.K.F., Chen, M.B., Clarke, M.F., Conley, S.D., Darmanis, S., Demers, A., Demir, K., Morree, A. de, Divita, T., Du Bois, H., Ebadi, H., Espinoza, F.H., Fish, M., Gan, Q., George, B.M., Gillich, A., Gòmez-Sjöberg, R., Green, F., Genetiano, G., Gu, X., Gulati, G.S., Hahn, O., Haney, M.S., Hang, Y., Harris, L., He, M., Hosseinzadeh, S., Huang, A., Huang, K.C., Iram, T., Isobe, T., Ives, F., Jones, R.C., Kao, K.S., Karkanias, J., Karnam, G., Keller, A., Kershner, A.M., Khoury, N., Kim, S.K., Kiss, B.M., Kong, W., Krasnow, M.A., Kumar, M.E., Kuo, C.S., Lam, J., Lee, D.P., Lee, S.E., Lehallier, B., Leventhal, O., Li, G., Li, Q., Liu, L., Lo, A., Lu, W.-J., Lugo-Fagundo, M.F., Manjunath, A., May, A.P., Maynard, A., McGeever, A., McKay, M., McNerney, M.W., Merrill, B., Metzger, R.J., Mignardi, M., Min, D., Nabhan, A.N., Neff, N.F., Ng, K.M., Nguyen, P.K., Noh, J., Nusse, R., Pálovics, R., Patkar, R., Peng, W.C., Penland, L., Pisco, A.O., Pollard, K., Puccinelli, R., Qi, Z., Quake, S.R., Rando, T.A., Rulifson, E.J., Schaum, N., Segal, J.M., Sikandar, S.S., Sinha, R., Sit, R.V., Sonnenburg, J., Staehli, D., Szade, K., Tan, M., Tan, W., Tato, C., Tellez, K., Dulgeroff, L.B.T., Travaglini, K.J., Tropini, C., Tsui, M., Waldburger, L., Wang, B.M., van Weele, L.J., Weinberg, K., Weissman, I.L., Wosczyna, M.N., Wu, S.M., Wyss-Coray, T., Xiang, J., Xue, S., Yamauchi, K.A., Yang, A.C., Yerra, L.P., Youngyunpipatkul, J., Yu, B., Zanini, F., Zardeneta, M.E., Zee, A., Zhao, C., Zhang, F., Zhang, H., Zhang, M.J., Zhou, L., Zou, J., Consortium, T.T.M., 2020. A single-cell transcriptomic atlas characterizes ageing tissues in the mouse. Nature 583, 590–595. https://doi.org/10.1038/s41586-020-2496-1.

Alzheimer's Association, 2020. 2020 Alzheimer's disease facts and figures. Alzheimer's & Dementia. https://doi.org/10.1002/alz.12068.

Amigo, I., Menezes-Filho, S.L., Luevano-Martinez, L.A., Chausse, B., Kowaltowski, A.J., 2017. Caloric restriction increases brain mitochondrial calcium retention capacity and protects against excitotoxicity. Aging cell 16, 73–81. https://doi.org/10.1111/acel.12527.

Amirbeigiarab, S., Kiani, P., Velazquez Sanchez, A., Krisp, C., Kazantsev, A., Fester, L., Schlüter, H., Ignatova, Z., 2019. Invariable stoichiometry of ribosomal proteins in mouse brain tissues with aging. PNAS 116, 22567–22572. https://doi.org/10.1073/pnas.1912060116.

Andersen, B.B., Gundersen, H.J.G., Pakkenberg, B., 2003. Aging of the human cerebellum: a stereological study. The Journal of comparative neurology 466, 356–365. https://doi.org/10.1002/cne.10884.

Andrews, Z.B., Horvath, T.L., 2009. Uncoupling protein-2 regulates lifespan in mice. American journal of physiology. Endocrinology and metabolism 296, E621-7. https://doi.org/10.1152/ajpendo.90903.2008.

Anggono, V., Koç-Schmitz, Y., Widagdo, J., Kormann, J., Quan, A., Chen, C.-M., Robinson, P.J., Choi, S.-Y., Linden, D.J., Plomann, M., Huganir, R.L., 2013. PICK1 interacts with PACSIN to regulate AMPA receptor internalization and cerebellar long-term depression. PNAS 110, 13976–13981. https://doi.org/10.1073/pnas.1312467110.

Apóstolo, N., Smukowski, S.N., Vanderlinden, J., Condomitti, G., Rybakin, V., Bos, J. ten, Trobiani, L., Portegies, S., Vennekens, K.M., Gounko, N.V., Comoletti, D., Wierda, K.D., Savas, J.N., Wit, J. de, 2020. Synapse type-specific proteomic dissection identifies IgSF8 as a hippocampal CA3 microcircuit organizer. Nat Commun 11, 5171. https://doi.org/10.1038/s41467-020-18956-x.

Arranz, L., Castro, N.M. de, Baeza, I., Maté, I., Viveros, M.P., La Fuente, M. de, 2010. Environmental enrichment improves age-related immune system impairment: long-term exposure since adulthood increases life span in mice. Rejuvenation research 13, 415–428. https://doi.org/10.1089/rej.2009.0989.

Arsenijevic, D., Onuma, H., Pecqueur, C., Raimbault, S., Manning, B.S., Miroux, B., Couplan, E., Alves-Guerra, M.C., Goubern, M., Surwit, R., Bouillaud, F., Richard, D., Collins, S., Ricquier, D., 2000. Disruption of the uncoupling protein-2 gene in mice reveals a role in immunity and reactive oxygen species production. Nature genetics 26, 435–439. https://doi.org/10.1038/82565.

Aw, J.G.A., Lim, S.W., Wang, J.X., Lambert, F.R.P., Tan, W.T., Shen, Y., Zhang, Y., Kaewsapsak, P., Li, C., Ng, S.B., Vardy, L.A., Tan, M.H., Nagarajan, N., Wan, Y., 2021. Determination of isoform-specific RNA structure with nanopore long reads. Nat Biotechnol 39, 336–346. https://doi.org/10.1038/s41587-020-0712-z.

Baek, J.-H., Schmidt, E., Viceconte, N., Strandgren, C., Pernold, K., Richard, T.J.C., van Leeuwen, F.W., Dantuma, N.P., Damberg, P., Hultenby, K., Ulfhake, B., Mugnaini, E., Rozell, B., Eriksson, M., 2015. Expression of progerin in aging mouse brains reveals structural nuclear abnormalities without detectible significant alterations in gene expression, hippocampal stem cells or behavior. Human molecular genetics 24, 1305–1321. https://doi.org/10.1093/hmg/ddu541.

Bahar, R., Hartmann, C.H., Rodriguez, K.A., Denny, A.D., Busuttil, R.A., Dollé, M.E.T., Calder, R.B., Chisholm, G.B., Pollock, B.H., Klein, C.A., Vijg, J., 2006. Increased cell-to-cell variation in gene expression in ageing mouse heart. Nature 441, 1011–1014. https://doi.org/10.1038/nature04844.

Bahar Halpern, K., Caspi, I., Lemze, D., Levy, M., Landen, S., Elinav, E., Ulitsky, I., Itzkovitz, S., 2015. Nuclear Retention of mRNA in Mammalian Tissues. Cell reports 13, 2653–2662. https://doi.org/10.1016/j.celrep.2015.11.036.

Bai, B., Wang, X., Li, Y., Chen, P.-C., Yu, K., Dey, K.K., Yarbro, J.M., Han, X., Lutz, B.M., Rao, S., Jiao, Y., Sifford, J.M., Han, J., Wang, M., Tan, H., Shaw, T.I., Cho, J.-H., Zhou, S., Wang, H., Niu, M., Mancieri, A., Messler, K.A., Sun, X., Wu, Z., Pagala, V., High, A.A., Bi, W., Zhang, H., Chi, H., Haroutunian, V., Zhang, B., Beach, T.G., Yu, G., Peng, J., 2020. Deep Multilayer Brain Proteomics Identifies Molecular Networks in Alzheimer's Disease Progression. Neuron 105, 975-991.e7. https://doi.org/10.1016/j.neuron.2019.12.015.

Baker, D.J., Peleg, S., 2017. Biphasic Modeling of Mitochondrial Metabolism Dysregulation during Aging. Trends in biochemical sciences 42, 702–711. https://doi.org/10.1016/j.tibs.2017.06.005.

Bandopadhyay, R., 2016. Sequential Extraction of Soluble and Insoluble Alpha-Synuclein from Parkinsonian Brains. Journal of visualized experiments: JoVE. https://doi.org/10.3791/53415.

Barth, E., Srivastava, A., Stojiljkovic, M., Frahm, C., Axer, H., Witte, O.W., Marz, M., 2019. Conserved aging-related signatures of senescence and inflammation in different tissues and species. Aging 11, 8556–8572. https://doi.org/10.18632/aging.102345.

Bartke, A., Brown-Borg, H., 2004. Life extension in the dwarf mouse. Current topics in developmental biology 63, 189–225. https://doi.org/10.1016/S0070-2153(04)63006-7.

Basisty, N.B., Liu, Y., Reynolds, J., Karunadharma, P.P., Dai, D.-F., Fredrickson, J., Beyer, R.P., MacCoss, M.J., Rabinovitch, P.S., 2018. Stable Isotope Labeling Reveals Novel Insights Into Ubiquitin-Mediated Protein Aggregation With Age, Calorie Restriction, and Rapamycin Treatment. The journals of gerontology. Series A, Biological sciences and medical sciences 73, 561–570. https://doi.org/10.1093/gerona/glx047.

Bassil, F., Fernagut, P.-O., Bezard, E., Meissner, W.G., 2014. Insulin, IGF-1 and GLP-1 signaling in neurodegenerative disorders: targets for disease modification? Progress in neurobiology 118, 1–18. https://doi.org/10.1016/j.pneurobio.2014.02.005.

Bäuerlein, F.J.B., Saha, I., Mishra, A., Kalemanov, M., Martínez-Sánchez, A., Klein, R., Dudanova, I., Hipp, M.S., Hartl, F.U., Baumeister, W., Fernández-Busnadiego, R., 2017. In Situ Architecture and Cellular Interactions of PolyQ Inclusions. Cell 171, 179-187.e10. https://doi.org/10.1016/j.cell.2017.08.009.

Begcevic, I., Kosanam, H., Martínez-Morillo, E., Dimitromanolakis, A., Diamandis, P., Kuzmanov, U., Hazrati, L.-N., Diamandis, E.P., 2013. Semiquantitative proteomic analysis of human hippocampal tissues from

Alzheimer's disease and age-matched control brains. Clin Proteom 10, 5. https://doi.org/10.1186/1559-0275-10-5.
Bélanger, M., Yang, J., Petit, J.-M., Laroche, T., Magistretti, P.J., Allaman, I., 2011. Role of the glyoxalase system in astrocyte-mediated neuroprotection. J. Neurosci. 31, 18338–18352. https://doi.org/10.1523/JNEUROSCI.1249-11.2011.
Benito, E., Urbanke, H., Ramachandran, B., Barth, J., Halder, R., Awasthi, A., Jain, G., Capece, V., Burkhardt, S., Navarro-Sala, M., Nagarajan, S., Schütz, A.-L., Johnsen, S.A., Bonn, S., Lührmann, R., Dean, C., Fischer, A., 2015. HDAC inhibitor-dependent transcriptome and memory reinstatement in cognitive decline models. The Journal of clinical investigation 125, 3572–3584. https://doi.org/10.1172/JCI79942.
Berchtold, N.C., Castello, N., Cotman, C.W., 2010. Exercise and time-dependent benefits to learning and memory. Neuroscience 167, 588–597. https://doi.org/10.1016/j.neuroscience.2010.02.050.
Bergersen, L.H., 2007. Is lactate food for neurons? Comparison of monocarboxylate transporter subtypes in brain and muscle. Neuroscience 145, 11–19. https://doi.org/10.1016/j.neuroscience.2006.11.062.
Bernard, D., Prasanth, K.V., Tripathi, V., Colasse, S., Nakamura, T., Xuan, Z., Zhang, M.Q., Sedel, F., Jourdren, L., Coulpier, F., Triller, A., Spector, D.L., Bessis, A., 2010. A long nuclear-retained non-coding RNA regulates synaptogenesis by modulating gene expression. EMBO J 29, 3082–3093. https://doi.org/10.1038/emboj.2010.199.
Beurel, E., Grieco, S.F., Jope, R.S., 2015. Glycogen synthase kinase-3 (GSK3): regulation, actions, and diseases. Pharmacology & therapeutics 148, 114–131. https://doi.org/10.1016/j.pharmthera.2014.11.016.
Bian, Y., Zheng, R., Bayer, F.P., Wong, C., Chang, Y.-C., Meng, C., Zolg, D.P., Reinecke, M., Zecha, J., Wiechmann, S., Heinzlmeir, S., Scherr, J., Hemmer, B., Baynham, M., Gingras, A.-C., Boychenko, O., Kuster, B., 2020. Robust, reproducible and quantitative analysis of thousands of proteomes by micro-flow LC-MS/MS. Nat Commun 11, 157. https://doi.org/10.1038/s41467-019-13973-x.
Bilkei-Gorzo, A., 2014. Genetic mouse models of brain ageing and Alzheimer's disease. Pharmacology & therapeutics 142, 244–257. https://doi.org/10.1016/j.pharmthera.2013.12.009.
Bishop, N.A., Lu, T., Yankner, B.A., 2010. Neural mechanisms of ageing and cognitive decline. Nature 464, 529–535. https://doi.org/10.1038/nature08983.
Bjelakovic, G., Nikolova, D., Gluud, L.L., Simonetti, R.G., Gluud, C., 2012. Antioxidant supplements for prevention of mortality in healthy participants and patients with various diseases. The Cochrane database of systematic reviews, CD007176. https://doi.org/10.1002/14651858.CD007176.pub2.
Boisvert, M.M., Erikson, G.A., Shokhirev, M.N., Allen, N.J., 2018. The Aging Astrocyte Transcriptome from Multiple Regions of the Mouse Brain. Cell reports 22, 269–285. https://doi.org/10.1016/j.celrep.2017.12.039.
Bondy, C.A., Lee, W.H., 1993. Patterns of insulin-like growth factor and IGF receptor gene expression in the brain. Functional implications. Annals of the New York Academy of Sciences 692, 33–43. https://doi.org/10.1111/j.1749-6632.1993.tb26203.x.
Braak, H., Del Tredici, K., 2011. The pathological process underlying Alzheimer's disease in individuals under thirty. Acta neuropathologica 121, 171–181. https://doi.org/10.1007/s00401-010-0789-4.
de Brabander, Kramers, Uylings, 1998. Layer-specific dendritic regression of pyramidal cells with ageing in the human prefrontal cortex. European Journal of Neuroscience 10, 1261–1269. https://doi.org/10.1046/j.1460-9568.1998.00137.x.
Brandhorst, S., Choi, I.Y., Wei, M., Cheng, C.W., Sedrakyan, S., Navarrete, G., Dubeau, L., Yap, L.P., Park, R., Vinciguerra, M., Di Biase, S., Mirzaei, H., Mirisola, M.G., Childress, P., Ji, L., Groshen, S., Penna, F., Odetti, P., Perin, L., Conti, P.S., Ikeno, Y., Kennedy, B.K., Cohen, P., Morgan, T.E., Dorff, T.B., Longo, V.D., 2015. A Periodic Diet that Mimics Fasting Promotes Multi-System Regeneration, Enhanced Cognitive Performance, and Healthspan. Cell metabolism 22, 86–99. https://doi.org/10.1016/j.cmet.2015.05.012.
Brehme, M., Voisine, C., Rolland, T., Wachi, S., Soper, J.H., Zhu, Y., Orton, K., Villella, A., Garza, D., Vidal, M., Ge, H., Morimoto, R.I., 2014. A chaperome subnetwork safeguards proteostasis in aging and neurodegenerative disease. Cell reports 9, 1135–1150. https://doi.org/10.1016/j.celrep.2014.09.042.
Brockschnieder, D., Sabanay, H., Riethmacher, D., Peles, E., 2006. Ermin, a myelinating oligodendrocyte-specific protein that regulates cell morphology. J. Neurosci. 26, 757–762. https://doi.org/10.1523/JNEUROSCI.4317-05.2006.
Bronson, R.T., Lipman, R.D., Harrison, D.E., 1993. Age-related gliosis in the white matter of mice. Brain Research 609, 124–128.
Brown-Borg, H.M., Bartke, A., 2012. GH and IGF1: roles in energy metabolism of long-living GH mutant mice. The journals of gerontology. Series A, Biological sciences and medical sciences 67, 652–660. https://doi.org/10.1093/gerona/gls086.

Brunk, U., Ericsson, J.L., 1972. Electron microscopical studies on rat brain neurons. Localization of acid phosphatase and mode of formation of lipofuscin bodies. Journal of ultrastructure research 38, 1–15. https://doi.org/10.1016/s0022-5320(72)90080-9.

Bruss, M.D., Khambatta, C.F., Ruby, M.A., Aggarwal, I., Hellerstein, M.K., 2010. Calorie restriction increases fatty acid synthesis and whole body fat oxidation rates. American journal of physiology. Endocrinology and metabolism 298, E108-16. https://doi.org/10.1152/ajpendo.00524.2009.

Buckley, R.F., Mormino, E.C., Amariglio, R.E., Properzi, M.J., Rabin, J.S., Lim, Y.Y., Papp, K.V., Jacobs, H.I.L., Burnham, S., Hanseeuw, B.J., Doré, V., Dobson, A., Masters, C.L., Waller, M., Rowe, C.C., Maruff, P., Donohue, M.C., Rentz, D.M., Kirn, D., Hedden, T., Chhatwal, J., Schultz, A.P., Johnson, K.A., Villemagne, V.L., Sperling, R.A., 2018. Sex, amyloid, and APOE ε4 and risk of cognitive decline in preclinical Alzheimer's disease: Findings from three well-characterized cohorts. Alzheimer's & Dementia 14, 1193–1203. https://doi.org/10.1016/j.jalz.2018.04.010.

Buell, S., Coleman, P., 1979. Dendritic growth in the aged human brain and failure of growth in senile dementia. Science 206, 854–856. https://doi.org/10.1126/science.493989.

Burke, S.N., Barnes, C.A., 2006. Neural plasticity in the ageing brain. Nature reviews. Neuroscience 7, 30–40. https://doi.org/10.1038/nrn1809.

Cabral-Miranda, F., Tamburini, G., Martinez, G., Medinas, D., Gerakis, Y., Miedema, T., Duran-Aniotz, C., Ardiles, A.O., Gonzalez, C., Sabusap, C., Bermedo-Garcia, F., Adamson, S., Vitangcol, K., Huerta, H., Zhang, X., Nakamura, T., Sardi, S.P., Lipton, S.A., Kenedy, B.K., Cárdenas, J.C., Palacios, A.G., Plate, L., Henriquez, J.P., Hetz, C., 2020. Control of mammalian brain aging by the unfolded protein response (UPR). https://doi.org/10.1101/2020.04.13.039172.

Cahill, G.F., JR, 2006. Fuel metabolism in starvation. Annual review of nutrition 26, 1–22. https://doi.org/10.1146/annurev.nutr.26.061505.111258.

Caldwell, C.C., Yao, J., Brinton, R.D., 2015. Targeting the prodromal stage of Alzheimer's disease: bioenergetic and mitochondrial opportunities. Neurotherapeutics : the journal of the American Society for Experimental NeuroTherapeutics 12, 66–80. https://doi.org/10.1007/s13311-014-0324-8.

Camandola, S., Mattson, M.P., 2017. Brain metabolism in health, aging, and neurodegeneration. The EMBO journal 36, 1474–1492. https://doi.org/10.15252/embj.201695810.

Cellerino, A., Ori, A., 2017. What have we learned on aging from omics studies? Seminars in cell & developmental biology 70, 177–189. https://doi.org/10.1016/j.semcdb.2017.06.012.

Chatterjee, M., Schild, D., Teunissen, C.E., 2019. Contactins in the central nervous system: role in health and disease. Neural Regen Res 14, 206–216. https://doi.org/10.4103/1673-5374.244776.

Chen, L., Thiruchelvam, M.J., Madura, K., Richfield, E.K., 2006. Proteasome dysfunction in aged human alpha-synuclein transgenic mice. Neurobiology of disease 23, 120–126. https://doi.org/10.1016/j.nbd.2006.02.004.

Chesselet, M.-F., Richter, F., Zhu, C., Magen, I., Watson, M.B., Subramaniam, S.R., 2012. A progressive mouse model of Parkinson's disease: the Thy1-aSyn ("Line 61") mice. Neurotherapeutics : the journal of the American Society for Experimental NeuroTherapeutics 9, 297–314. https://doi.org/10.1007/s13311-012-0104-2.

Chiao, C., Botticello, A., Fuh, J.-L., 2014. Life-course socio-economic disadvantage and late-life cognitive functioning in Taiwan: results from a national cohort study. International health 6, 322–330. https://doi.org/10.1093/inthealth/ihu046.

Chinta, S.J., Woods, G., Rane, A., Demaria, M., Campisi, J., Andersen, J.K., 2015. Cellular senescence and the aging brain. Experimental gerontology 68, 3–7. https://doi.org/10.1016/j.exger.2014.09.018.

Chirles, T.J., Reiter, K., Weiss, L.R., Alfini, A.J., Nielson, K.A., Smith, J.C., 2017. Exercise Training and Functional Connectivity Changes in Mild Cognitive Impairment and Healthy Elders. Journal of Alzheimer's disease : JAD 57, 845–856. https://doi.org/10.3233/JAD-161151.

Cho, U.H., Hetzer, M.W., 2020. Nuclear Periphery Takes Center Stage: The Role of Nuclear Pore Complexes in Cell Identity and Aging. Neuron 106, 899–911. https://doi.org/10.1016/j.neuron.2020.05.031.

Choi, S.H., Bylykbashi, E., Chatila, Z.K., Lee, S.W., Pulli, B., Clemenson, G.D., Kim, E., Rompala, A., Oram, M.K., Asselin, C., Aronson, J., Zhang, C., Miller, S.J., Lesinski, A., Chen, J.W., Kim, D.Y., van Praag, H., Spiegelman, B.M., Gage, F.H., Tanzi, R.E., 2018. Combined adult neurogenesis and BDNF mimic exercise effects on cognition in an Alzheimer's mouse model. Science (New York, N.Y.) 361. https://doi.org/10.1126/science.aan8821.

Chondrogianni, N., Sakellari, M., Lefaki, M., Papaevgeniou, N., Gonos, E.S., 2014. Proteasome activation delays aging in vitro and in vivo. Free radical biology & medicine 71, 303–320. https://doi.org/10.1016/j.freeradbiomed.2014.03.031.

Coffey, C.E., Lucke, J.F., Saxton, J.A., Ratcliff, G., Unitas, L.J., Billig, B., Bryan, R.N., 1998. Sex differences in brain aging: a quantitative magnetic resonance imaging study. Arch Neurol 55, 169–179. https://doi.org/10.1001/archneur.55.2.169.

Coffinier, C., Jung, H.-J., Nobumori, C., Chang, S., Tu, Y., Barnes, R.H., Yoshinaga, Y., Jong, P.J. de, Vergnes, L., Reue, K., Fong, L.G., Young, S.G., 2011. Deficiencies in lamin B1 and lamin B2 cause neurodevelopmental defects and distinct nuclear shape abnormalities in neurons. MBoC 22, 4683–4693. https://doi.org/10.1091/mbc.e11-06-0504.

Connor, J.R., Snyder, B.S., Beard, J.L., Fine, R.E., Mufson, E.J., 1992. Regional distribution of iron and iron-regulatory proteins in the brain in aging and Alzheimer's disease. J. Neurosci. Res. 31, 327–335. https://doi.org/10.1002/jnr.490310214.

Cribbs, D.H., Berchtold, N.C., Perreau, V., Coleman, P.D., Rogers, J., Tenner, A.J., Cotman, C.W., 2012. Extensive innate immune gene activation accompanies brain aging, increasing vulnerability to cognitive decline and neurodegeneration: a microarray study. Journal of neuroinflammation 9, 179. https://doi.org/10.1186/1742-2094-9-179.

Cuervo, A.M., Dice, J.F., 2000. Age-related Decline in Chaperone-mediated Autophagy. J. Biol. Chem. 275, 31505–31513. https://doi.org/10.1074/jbc.M002102200.

Cui, H., Kong, Y., Zhang, H., 2012. Oxidative stress, mitochondrial dysfunction, and aging. Journal of signal transduction 2012, 646354. https://doi.org/10.1155/2012/646354.

Currais, A., Fischer, W., Maher, P., Schubert, D., 2017. Intraneuronal protein aggregation as a trigger for inflammation and neurodegeneration in the aging brain. FASEB journal: official publication of the Federation of American Societies for Experimental Biology 31, 5–10. https://doi.org/10.1096/fj.201601184.

Currais, A., Huang, L., Goldberg, J., Petrascheck, M., Ates, G., Pinto-Duarte, A., Shokhirev, M.N., Schubert, D., Maher, P., 2019. Elevating acetyl-CoA levels reduces aspects of brain aging. eLife 8. https://doi.org/10.7554/eLife.47866.

Czogalla, A., Sikorski, A.F., 2005. Spectrin and calpain: a 'target' and a 'sniper' in the pathology of neuronal cells. Cell. Mol. Life Sci. 62, 1913–1924. https://doi.org/10.1007/s00018-005-5097-0.

Dallagnol, K.M.C., Remor, A.P., da Silva, R.A., Prediger, R.D., Latini, A., Aguiar, A.S., 2017. Running for REST: Physical activity attenuates neuroinflammation in the hippocampus of aged mice. Brain, Behavior, and Immunity 61, 31–35. https://doi.org/10.1016/j.bbi.2016.07.159.

D'Angelo, M.A., Raices, M., Panowski, S.H., Hetzer, M.W., 2009. Age-dependent deterioration of nuclear pore complexes causes a loss of nuclear integrity in postmitotic cells. Cell 136, 284–295. https://doi.org/10.1016/j.cell.2008.11.037.

Danno, S., Nishiyama, H., Higashitsuji, H., Yokoi, H., Xue, J.H., Itoh, K., Matsuda, T., Fujita, J., 1997. Increased transcript level of RBM3, a member of the glycine-rich RNA-binding protein family, in human cells in response to cold stress. Biochemical and biophysical research communications 236, 804–807. https://doi.org/10.1006/bbrc.1997.7059.

Dechat, T., Pfleghaar, K., Sengupta, K., Shimi, T., Shumaker, D.K., Solimando, L., Goldman, R.D., 2008. Nuclear lamins: major factors in the structural organization and function of the nucleus and chromatin. Genes & development 22, 832–853. https://doi.org/10.1101/gad.1652708.

Ding, B., Sepehrimanesh, M., 2021. Nucleocytoplasmic Transport: Regulatory Mechanisms and the Implications in Neurodegeneration. International journal of molecular sciences 22. https://doi.org/10.3390/ijms22084165.

Dirks, A.J., Leeuwenburgh, C., 2006. Caloric restriction in humans: potential pitfalls and health concerns. Mechanisms of ageing and development 127, 1–7. https://doi.org/10.1016/j.mad.2005.09.001.

Dobarro, M., Orejana, L., Aguirre, N., Ramirez, M.J., 2013. Propranolol restores cognitive deficits and improves amyloid and Tau pathologies in a senescence-accelerated mouse model. Neuropharmacology 64, 137–144. https://doi.org/10.1016/j.neuropharm.2012.06.047.

Dong, J., Liu, Y., Zhan, Z., Wang, X., 2018. MicroRNA-132 is associated with the cognition improvement following voluntary exercise in SAMP8 mice. Brain research bulletin 140, 80–87. https://doi.org/10.1016/j.brainresbull.2018.04.007.

Drummond, E.S., Nayak, S., Ueberheide, B., Wisniewski, T., 2015. Proteomic analysis of neurons microdissected from formalin-fixed, paraffin-embedded Alzheimer's disease brain tissue. Scientific reports 5, 15456. https://doi.org/10.1038/srep15456.

Duning, K., Buck, F., Barnekow, A., Kremerskothen, J., 2008. SYNCRIP, a component of dendritically localized mRNPs, binds to the translation regulator BC200 RNA. Journal of neurochemistry 105, 351–359. https://doi.org/10.1111/j.1471-4159.2007.05138.x.

Eberhard, D.A., Brown, M.D., VandenBerg, S.R., 1994. Alterations of annexin expression in pathological neuronal and glial reactions. Immunohistochemical localization of annexins I, II (p36 and p11 subunits), IV, and VI in the human hippocampus. The American journal of pathology 145, 640–649.

Egan, D.F., Shackelford, D.B., Mihaylova, M.M., Gelino, S., Kohnz, R.A., Mair, W., Vasquez, D.S., Joshi, A., Gwinn, D.M., Taylor, R., Asara, J.M., Fitzpatrick, J., Dillin, A., Viollet, B., Kundu, M., Hansen, M., Shaw, R.J., 2011. Phosphorylation of ULK1 (hATG1) by AMP-activated protein kinase connects energy sensing to mitophagy. Science (New York, N.Y.) 331, 456–461. https://doi.org/10.1126/science.1196371.

Eliot, L., 2019. Neurosexism: the myth that men and women have different brains. Nature 566, 453–454. https://doi.org/10.1038/d41586-019-00677-x.

Eliot, L., Ahmed, A., Khan, H., Patel, J., 2021. Dump the "dimorphism": Comprehensive synthesis of human brain studies reveals few male-female differences beyond size. Neuroscience and biobehavioral reviews 125, 667–697. https://doi.org/10.1016/j.neubiorev.2021.02.026.

Elobeid, A., Libard, S., Leino, M., Popova, S.N., Alafuzoff, I., 2016. Altered Proteins in the Aging Brain. Journal of neuropathology and experimental neurology 75, 316–325. https://doi.org/10.1093/jnen/nlw002.

Encinas, J.M., Michurina, T.V., Peunova, N., Park, J.-H., Tordo, J., Peterson, D.A., Fishell, G., Koulakov, A., Enikolopov, G., 2011. Division-coupled astrocytic differentiation and age-related depletion of neural stem cells in the adult hippocampus. Cell stem cell 8, 566–579. https://doi.org/10.1016/j.stem.2011.03.010.

Erickson, M.A., Banks, W.A., 2019. Age-Associated Changes in the Immune System and Blood⁻Brain Barrier Functions. International journal of molecular sciences 20. https://doi.org/10.3390/ijms20071632.

Faucheux, B.A., Martin, M.-E., Beaumont, C., Hunot, S., Hauw, J.-J., Agid, Y., Hirsch, E.C., 2002. Lack of up-regulation of ferritin is associated with sustained iron regulatory protein-1 binding activity in the substantia nigra of patients with Parkinson's disease. J. Neurochem. 83, 320–330. https://doi.org/10.1046/j.1471-4159.2002.01118.x.

Felice, F.G.D., Lourenco, M.V., Ferreira, S.T., 2014. How does brain insulin resistance develop in Alzheimer's disease? Alzheimer's & Dementia: The Journal of the Alzheimer's Association 10, S26-S32. https://doi.org/10.1016/j.jalz.2013.12.004.

Fernández, Á.F., Sebti, S., Wei, Y., Zou, Z., Shi, M., McMillan, K.L., He, C., Ting, T., Liu, Y., Chiang, W.-C., Marciano, D.K., Schiattarella, G.G., Bhagat, G., Moe, O.W., Hu, M.C., Levine, B., 2018. Disruption of the beclin 1-BCL2 autophagy regulatory complex promotes longevity in mice. Nature 558, 136–140. https://doi.org/10.1038/s41586-018-0162-7.

Finch, C.E., Morgan, D.G., 1990. RNA and protein metabolism in the aging brain. Annual review of neuroscience 13, 75–88. https://doi.org/10.1146/annurev.ne.13.030190.000451.

Fitzner, D., Bader, J.M., Penkert, H., Bergner, C.G., Su, M., Weil, M.-T., Surma, M.A., Mann, M., Klose, C., Simons, M., 2020. Cell-Type- and Brain-Region-Resolved Mouse Brain Lipidome. Cell reports 32, 108132. https://doi.org/10.1016/j.celrep.2020.108132.

Flurkey, K., Currer, J., Harrison, D., 2007. Mouse Models in Aging Research: The Mouse in Biomedical Research; Volume 3 : normative biology, husbandry, and models III, 637–672. https://doi.org/10.1016/B978-012369454-6/50074-1.

Flurkey, K., Papaconstantinou, J., Harrison, D.E., 2002. The Snell dwarf mutation Pit1dw can increase life span in mice. Mechanisms of ageing and development 123, 121–130. https://doi.org/10.1016/S0047-6374(01)00339-6.

Folgueras, A.R., Freitas-Rodríguez, S., Velasco, G., López-Otín, C., 2018. Mouse Models to Disentangle the Hallmarks of Human Aging. Circulation research 123, 905–924. https://doi.org/10.1161/CIRCRESAHA.118.312204.

Fontana, L., Partridge, L., Longo, V.D., 2010. Extending healthy life span—from yeast to humans. Science (New York, N.Y.) 328, 321–326. https://doi.org/10.1126/science.1172539.

Fornasiero, E.F., Mandad, S., Wildhagen, H., Alevra, M., Rammner, B., Keihani, S., Opazo, F., Urban, I., Ischebeck, T., Sakib, M.S., Fard, M.K., Kirli, K., Centeno, T.P., Vidal, R.O., Rahman, R.-U., Benito, E., Fischer, A., Dennerlein, S., Rehling, P., Feussner, I., Bonn, S., Simons, M., Urlaub, H., Rizzoli, S.O., 2018. Precisely measured protein lifetimes in the mouse brain reveal differences across tissues and subcellular fractions. Nature communications 9, 4230. https://doi.org/10.1038/s41467-018-06519-0.

Franceschi, C., Campisi, J., 2014. Chronic inflammation (inflammaging) and its potential contribution to age-associated diseases. The journals of gerontology. Series A, Biological sciences and medical sciences 69 Suppl 1, S4-9. https://doi.org/10.1093/gerona/glu057.

French, M.E., Koehler, C.F., Hunter, T., 2021. Emerging functions of branched ubiquitin chains. Cell Discov 7, 6. https://doi.org/10.1038/s41421-020-00237-y.

Freund, A., Laberge, R.-M., Demaria, M., Campisi, J., 2012. Lamin B1 loss is a senescence-associated biomarker. MBoC 23, 2066–2075. https://doi.org/10.1091/mbc.e11-10-0884.

Fünfschilling, U., Supplie, L.M., Mahad, D., Boretius, S., Saab, A.S., Edgar, J., Brinkmann, B.G., Kassmann, C.M., Tzvetanova, I.D., Möbius, W., Diaz, F., Meijer, D., Suter, U., Hamprecht, B., Sereda, M.W., Moraes, C.T., Frahm, J., Goebbels, S., Nave, K.-A., 2012. Glycolytic oligodendrocytes maintain myelin and long-term axonal integrity. Nature 485, 517–521. https://doi.org/10.1038/nature11007.

Gafni, J., Ellerby, L.M., 2002. Calpain Activation in Huntington's Disease. J. Neurosci. 22, 4842–4849. https://doi.org/10.1523/JNEUROSCI.22-12-04842.2002.

Gagnon, K.T., Li, L., Janowski, B.A., Corey, D.R., 2014. Analysis of nuclear RNA interference in human cells by subcellular fractionation and Argonaute loading. Nat Protoc 9, 2045–2060. https://doi.org/10.1038/nprot.2014.135.

Garaschuk, O., Semchyshyn, H.M., Lushchak, V.I., 2018. Healthy brain aging: Interplay between reactive species, inflammation and energy supply. Ageing research reviews 43, 26–45. https://doi.org/10.1016/j.arr.2018.02.003.

García-Berrocoso, T., Llombart, V., Colàs-Campàs, L., Hainard, A., Licker, V., Penalba, A., Ramiro, L., Simats, A., Bustamante, A., Martínez-Saez, E., Canals, F., Sanchez, J.-C., Montaner, J., 2018. Single Cell Immuno-Laser Microdissection Coupled to Label-Free Proteomics to Reveal the Proteotypes of Human Brain Cells After Ischemia. Molecular & cellular proteomics: MCP 17, 175–189. https://doi.org/10.1074/mcp.RA117.000419.

Gauthier-Kemper, A., Suárez Alonso, M., Sündermann, F., Niewidok, B., Fernandez, M.-P., Bakota, L., Heinisch, J.J., Brandt, R., 2018. Annexins A2 and A6 interact with the extreme N terminus of tau and thereby contribute to tau's axonal localization. J. Biol. Chem. 293, 8065–8076. https://doi.org/10.1074/jbc.RA117.000490.

Gehman, L.T., Stoilov, P., Maguire, J., Damianov, A., Lin, C.-H., Shiue, L., Ares, M., Mody, I., Black, D.L., 2011. The splicing regulator Rbfox1 (A2BP1) controls neuronal excitation in the mammalian brain. Nat Genet 43, 706–711. https://doi.org/10.1038/ng.841.

Glinka, T., Alter, J., Braunstein, I., Tzach, L., Wei Sheng, C., Geifman, S., Edelmann, M.J., Kessler, B.M., Stanhill, A., 2014. Signal-peptide-mediated translocation is regulated by a p97-AIRAPL complex. The Biochemical journal 457, 253–261. https://doi.org/10.1042/BJ20130710.

Glisky, E.L., 2007. Brain Aging: Models, Methods, and Mechanisms: Changes in Cognitive Function in Human Aging. Boca Raton (FL).

Goyal, M.S., Blazey, T.M., Su, Y., Couture, L.E., Durbin, T.J., Bateman, R.J., Benzinger, T.L.-S., Morris, J.C., Raichle, M.E., Vlassenko, A.G., 2019. Persistent metabolic youth in the aging female brain. PNAS 116, 3251–3255. https://doi.org/10.1073/pnas.1815917116.

Graaf, E.L. de, Vermeij, W.P., Waard, M.C. de, Rijksen, Y., van der Pluijm, I., Hoogenraad, C.C., Hoeijmakers, J.H.J., Altelaar, A.F.M., Heck, A.J.R., 2013. Spatio-temporal analysis of molecular determinants of neuronal degeneration in the aging mouse cerebellum. Molecular & cellular proteomics: MCP 12, 1350–1362. https://doi.org/10.1074/mcp.M112.024950.

Gray, D.A., Tsirigotis, M., Woulfe, J., 2003. Ubiquitin, proteasomes, and the aging brain. Science of aging knowledge environment: SAGE KE 2003, RE6. https://doi.org/10.1126/sageke.2003.34.re6.

Green, D.R., Galluzzi, L., Kroemer, G., 2011. Mitochondria and the autophagy-inflammation-cell death axis in organismal aging. Science (New York, N.Y.) 333, 1109–1112. https://doi.org/10.1126/science.1201940.

Grillari, J., Katinger, H., Voglauer, R., 2006. Aging and the ubiquitinome: traditional and non-traditional functions of ubiquitin in aging cells and tissues. Experimental gerontology 41, 1067–1079. https://doi.org/10.1016/j.exger.2006.07.003.

Grinan-Ferre, C., Corpas, R., Puigoriol-Illamola, D., Palomera-Avalos, V., Sanfeliu, C., Pallas, M., 2018. Understanding Epigenetics in the Neurodegeneration of Alzheimer's Disease: SAMP8 Mouse Model. Journal of Alzheimer's disease: JAD 62, 943–963. https://doi.org/10.3233/JAD-170664.

Gry, M., Rimini, R., Strömberg, S., Asplund, A., Pontén, F., Uhlén, M., Nilsson, P., 2009. Correlations between RNA and protein expression profiles in 23 human cell lines. BMC genomics 10, 365. https://doi.org/10.1186/1471-2164-10-365.

Guan, J.-S., Haggarty, S.J., Giacometti, E., Dannenberg, J.-H., Joseph, N., Gao, J., Nieland, T.J.F., Zhou, Y., Wang, X., Mazitschek, R., Bradner, J.E., DePinho, R.A., Jaenisch, R., Tsai, L.-H., 2009. HDAC2 negatively regulates memory formation and synaptic plasticity. Nature 459, 55–60. https://doi.org/10.1038/nature07925.

Guarente, L., 2008. Mitochondria—A Nexus for Aging, Calorie Restriction, and Sirtuins? Cell 132, 171–176. https://doi.org/10.1016/j.cell.2008.01.007.

Gupta, I., Collier, P.G., Haase, B., Mahfouz, A., Joglekar, A., Floyd, T., Koopmans, F., Barres, B., Smit, A.B., Sloan, S.A., Luo, W., Fedrigo, O., Ross, M.E., Tilgner, H.U., 2018. Single-cell isoform RNA sequencing

characterizes isoforms in thousands of cerebellar cells. Nat Biotechnol 36, 1197–1202. https://doi.org/10.1038/nbt.4259.
Hamada, N., Ito, H., Nishijo, T., Iwamoto, I., Morishita, R., Tabata, H., Momiyama, T., Nagata, K.-I., 2016. Essential role of the nuclear isoform of RBFOX1, a candidate gene for autism spectrum disorders, in the brain development. Scientific reports 6, 30805. https://doi.org/10.1038/srep30805.
Hammond, T.R., Dufort, C., Dissing-Olesen, L., Giera, S., Young, A., Wysoker, A., Walker, A.J., Gergits, F., Segel, M., Nemesh, J., Marsh, S.E., Saunders, A., Macosko, E., Ginhoux, F., Chen, J., Franklin, R.J.M., Piao, X., McCarroll, S.A., Stevens, B., 2019. Single-Cell RNA Sequencing of Microglia throughout the Mouse Lifespan and in the Injured Brain Reveals Complex Cell-State Changes. Immunity 50, 253-271.e6. https://doi.org/10.1016/j.immuni.2018.11.004.
Hanamsagar, R., Bilbo, S.D., 2016. Sex differences in neurodevelopmental and neurodegenerative disorders: Focus on microglial function and neuroinflammation during development. The Journal of Steroid Biochemistry and Molecular Biology 160, 127–133. https://doi.org/10.1016/j.jsbmb.2015.09.039.
Harrison, D.E., Strong, R., Sharp, Z.D., Nelson, J.F., Astle, C.M., Flurkey, K., Nadon, N.L., Wilkinson, J.E., Frenkel, K., Carter, C.S., Pahor, M., Javors, M.A., Fernandez, E., Miller, R.A., 2009. Rapamycin fed late in life extends lifespan in genetically heterogeneous mice. Nature 460, 392–395. https://doi.org/10.1038/nature08221.
Harry, G.J., 2013. Microglia during development and aging. Pharmacology & therapeutics 139, 313–326. https://doi.org/10.1016/j.pharmthera.2013.04.013.
Hart, A.D., Wyttenbach, A., Hugh Perry, V., Teeling, J.L., 2012. Age related changes in microglial phenotype vary between CNS regions: Grey versus white matter differences. Brain, Behavior, and Immunity 26, 754–765. https://doi.org/10.1016/j.bbi.2011.11.006.
He, P., Xin, W., Schulz, P., Sierks, M.R., 2019. Bispecific Antibody Fragment Targeting APP and Inducing α-Site Cleavage Restores Neuronal Health in an Alzheimer's Mouse Model. Mol Neurobiol 56, 7420–7432. https://doi.org/10.1007/s12035-019-1597-z.
Heng, Y., Eggen, B.J., Boddeke, E.W., Kooistra, S.M., 2017. Mouse models of central nervous system ageing. Drug Discovery Today: Disease Models 25-26, 21–34. https://doi.org/10.1016/j.ddmod.2018.10.002.
Hennekam, R.C.M., 2006. Hutchinson-Gilford progeria syndrome: review of the phenotype. American journal of medical genetics. Part A 140, 2603–2624. https://doi.org/10.1002/ajmg.a.31346.
Hermes, G., Nagy, D., Waterson, M., Zsarnovszky, A., Varela, L., Hajos, M., Horvath, T.L., 2016. Role of mitochondrial uncoupling protein-2 (UCP2) in higher brain functions, neuronal plasticity and network oscillation. Molecular metabolism 5, 415–421. https://doi.org/10.1016/j.molmet.2016.04.002.
Hetz, C., Zhang, K., Kaufman, R.J., 2020. Mechanisms, regulation and functions of the unfolded protein response. Nature reviews. Molecular cell biology. https://doi.org/10.1038/s41580-020-0250-z.
Hill, R.A., Li, A.M., Grutzendler, J., 2018. Lifelong cortical myelin plasticity and age-related degeneration in the live mammalian brain. Nat Neurosci 21, 683–695. https://doi.org/10.1038/s41593-018-0120-6.
Hirose, M., Schilf, P., Lange, F., Mayer, J., Reichart, G., Maity, P., Jöhren, O., Schwaninger, M., Scharffetter-Kochanek, K., Sina, C., Sadik, C.D., Köhling, R., Miroux, B., Ibrahim, S.M., 2016. Uncoupling protein 2 protects mice from aging. Mitochondrion 30, 42–50. https://doi.org/10.1016/j.mito.2016.06.004.
Hoeijmakers, J.H., 2009. DNA Damage, Aging, and Cancer. New England Journal of Medicine 361, 1475–1485. https://doi.org/10.1056/NEJMra0804615.
Horie, K., Miyata, T., Yasuda, T., Takeda, A., Yasuda, Y., Maeda, K., Sobue, G., Kurokawa, K., 1997. Immunohistochemical localization of advanced glycation end products, pentosidine, and carboxymethyllysine in lipofuscin pigments of Alzheimer's disease and aged neurons. Biochemical and biophysical research communications 236, 327–332. https://doi.org/10.1006/bbrc.1997.6944.
Hosp, F., Gutiérrez-Ángel, S., Schaefer, M.H., Cox, J., Meissner, F., Hipp, M.S., Hartl, F.-U., Klein, R., Dudanova, I., Mann, M., 2017. Spatiotemporal Proteomic Profiling of Huntington's Disease Inclusions Reveals Widespread Loss of Protein Function. Cell reports 21, 2291–2303. https://doi.org/10.1016/j.celrep.2017.10.097.
Houtkooper, R.H., Argmann, C., Houten, S.M., Cantó, C., Jeninga, E.H., Andreux, P.A., Thomas, C., Doenlen, R., Schoonjans, K., Auwerx, J., 2011. The metabolic footprint of aging in mice. Scientific reports 1, 134. https://doi.org/10.1038/srep00134.
Huang, T.T., Carlson, E.J., Gillespie, A.M., Shi, Y., Epstein, C.J., 2000. Ubiquitous overexpression of CuZn superoxide dismutase does not extend life span in mice. The Journals of Gerontology Series A: Biological Sciences and Medical Sciences 55, B5-9. https://doi.org/10.1093/gerona/55.1.B5.

Hughes, C.S., Moggridge, S., Müller, T., Sorensen, P.H., Morin, G.B., Krijgsveld, J., 2019. Single-pot, solid-phase-enhanced sample preparation for proteomics experiments. Nature protocols 14, 68–85. https://doi.org/10.1038/s41596-018-0082-x.

Hurtado, D.E., Molina-Porcel, L., Carroll, J.C., Macdonald, C., Aboagye, A.K., Trojanowski, J.Q., Lee, V.M.-Y., 2012. Selectively silencing GSK-3 isoforms reduces plaques and tangles in mouse models of Alzheimer's disease. J. Neurosci. 32, 7392–7402. https://doi.org/10.1523/JNEUROSCI.0889-12.2012.

Ivanisevic, J., Stauch, K.L., Petrascheck, M., Benton, H.P., Epstein, A.A., Fang, M., Gorantla, S., Tran, M., Hoang, L., Kurczy, M.E., Boska, M.D., Gendelman, H.E., Fox, H.S., Siuzdak, G., 2016. Metabolic drift in the aging brain. Aging 8, 1000–1020. https://doi.org/10.18632/aging.100961.

Ivimey-Cook, E.R., Sales, K., Carlsson, H., Immler, S., Chapman, T., Maklakov, A.A., 2021. Transgenerational fitness effects of lifespan extension by dietary restriction in Caenorhabditis elegans. Proceedings. Biological sciences 288, 20210701. https://doi.org/10.1098/rspb.2021.0701.

Jahn, O., Tenzer, S., Werner, H.B., 2009. Myelin proteomics: molecular anatomy of an insulating sheath. Mol Neurobiol 40, 55–72. https://doi.org/10.1007/s12035-009-8071-2.

Jäncke, L., Mérillat, S., Liem, F., Hänggi, J., 2015. Brain size, sex, and the aging brain. Hum. Brain Mapp. 36, 150–169. https://doi.org/10.1002/hbm.22619.

Jellinger, K., Paulus, W., Grundke-Iqbal, I., Riederer, P., Youdim, M.B., 1990. Brain iron and ferritin in Parkinson's and Alzheimer's diseases. J Neural Transm Gen Sect 2, 327–340. https://doi.org/10.1007/BF02252926.

Jiang, C.H., Tsien, J.Z., Schultz, P.G., Hu, Y., 2001. The effects of aging on gene expression in the hypothalamus and cortex of mice. Proceedings of the National Academy of Sciences of the United States of America 98, 1930–1934. https://doi.org/10.1073/pnas.98.4.1930.

Jing, Y., Yang, D., Fu, Y., Wang, W., Yang, G., Yuan, F., Chen, H., Ding, J., Chen, S., Tian, H., 2019. Neuroprotective Effects of Serpina3k in Traumatic Brain Injury. Front. Neurol. 10, 1215, 1215. https://doi.org/10.3389/fneur.2019.01215.

Jinn, S., Drolet, R.E., Cramer, P.E., Wong, A.H.-K., Toolan, D.M., Gretzula, C.A., Voleti, B., Vassileva, G., Disa, J., Tadin-Strapps, M., Stone, D.J., 2017. TMEM175 deficiency impairs lysosomal and mitochondrial function and increases α-synuclein aggregation. Proceedings of the National Academy of Sciences of the United States of America 114, 2389–2394. https://doi.org/10.1073/pnas.1616332114.

Johnson, E.C.B., Dammer, E.B., Duong, D.M., Ping, L., Zhou, M., Yin, L., Higginbotham, L.A., Guajardo, A., White, B., Troncoso, J.C., Thambisetty, M., Montine, T.J., Lee, E.B., Trojanowski, J.Q., Beach, T.G., Reiman, E.M., Haroutunian, V., Wang, M., Schadt, E., Zhang, B., Dickson, D.W., Ertekin-Taner, N., Golde, T.E., Petyuk, V.A., Jager, P.L. de, Bennett, D.A., Wingo, T.S., Rangaraju, S., Hajjar, I., Shulman, J.M., Lah, J.J., Levey, A.I., Seyfried, N.T., 2020. Large-scale proteomic analysis of Alzheimer's disease brain and cerebrospinal fluid reveals early changes in energy metabolism associated with microglia and astrocyte activation. Nature medicine 26, 769–780. https://doi.org/10.1038/s41591-020-0815-6.

Jucker, M., Ingram, D.K., 1997. Murine models of brain aging and age-related neurodegenerative diseases. Behavioural Brain Research 85, 1–25. https://doi.org/10.1016/S0166-4328(96)02243-7.

Jucker, M., Walker, L.C., 2013. Self-propagation of pathogenic protein aggregates in neurodegenerative diseases. Nature 501, 45. https://doi.org/10.1038/nature12481.

Jung, H.-J., Coffinier, C., Choe, Y., Beigneux, A.P., Davies, B.S.J., Yang, S.H., Barnes, R.H., Hong, J., Sun, T., Pleasure, S.J., Young, S.G., Fong, L.G., 2012. Regulation of prelamin A but not lamin C by miR-9, a brain-specific microRNA. Proceedings of the National Academy of Sciences of the United States of America 109, E423-31. https://doi.org/10.1073/pnas.1111780109.

Jurk, D., Wang, C., Miwa, S., Maddick, M., Korolchuk, V., Tsolou, A., Gonos, E.S., Thrasivoulou, C., Saffrey, M.J., Cameron, K., Zglinicki, T. von, 2012. Postmitotic neurons develop a p21-dependent senescence-like phenotype driven by a DNA damage response. Aging cell 11, 996–1004. https://doi.org/10.1111/j.1474-9726.2012.00870.x.

Kahle, P.J., Neumann, M., Ozmen, L., Müller, V., Jacobsen, H., Schindzielorz, A., Okochi, M., Leimer, U., van der Putten, H., Probst, A., Kremmer, E., Kretzschmar, H.A., Haass, C., 2000. Subcellular Localization of Wild-Type and Parkinson's Disease-Associated Mutant α-Synuclein in Human and Transgenic Mouse Brain. J. Neurosci. 20, 6365–6373. https://doi.org/10.1523/JNEUROSCI.20-17-06365.2000.

Kappeler, L., Magalhaes Filho, C. de, Dupont, J., Leneuve, P., Cervera, P., Périn, L., Loudes, C., Blaise, A., Klein, R., Epelbaum, J., Le Bouc, Y., Holzenberger, M., 2008. Brain IGF-1 receptors control mammalian growth and lifespan through a neuroendocrine mechanism. PLoS biology 6, e254. https://doi.org/10.1371/journal.pbio.0060254.

Kaushik, S., Cuervo, A.M., 2015. Proteostasis and aging. Nature medicine 21, 1406–1415. https://doi.org/10.1038/nm.4001.

Ke, Z., Mallik, P., Johnson, A.B., Luna, F., Nevo, E., Zhang, Z.D., Gladyshev, V.N., Seluanov, A., Gorbunova, V., 2017. Translation fidelity coevolves with longevity. Aging cell 16, 988–993. https://doi.org/10.1111/acel.12628.

Keihani, S., Kluever, V., Fornasiero, E.F., 2021. Brain Long Noncoding RNAs: Multitask Regulators of Neuronal Differentiation and Function. Molecules 26, 3951. https://doi.org/10.3390/molecules26133951.

Keihani, S., Kluever, V., Mandad, S., Bansal, V., Rahman, R., Fritsch, E., Gomes, L.C., Gärtner, A., Kügler, S., Urlaub, H., Wren, J.D., Bonn, S., Rizzoli, S.O., Fornasiero, E.F., 2019. The long noncoding RNA neuroLNC regulates presynaptic activity by interacting with the neurodegeneration-associated protein TDP-43. Science advances 5, eaay2670. https://doi.org/10.1126/sciadv.aay2670.

Keller, J.N., Hanni, K.B., Markesbery, W.R., 2000. Possible involvement of proteasome inhibition in aging: implications for oxidative stress. Mechanisms of ageing and development 113, 61–70.

Kelmer Sacramento, E., Kirkpatrick, J.M., Mazzetto, M., Baumgart, M., Bartolome, A., Di Sanzo, S., Caterino, C., Sanguanini, M., Papaevgeniou, N., Lefaki, M., Childs, D., Bagnoli, S., Terzibasi Tozzini, E., Di Fraia, D., Romanov, N., Sudmant, P.H., Huber, W., Chondrogianni, N., Vendruscolo, M., Cellerino, A., Ori, A., 2020. Reduced proteasome activity in the aging brain results in ribosome stoichiometry loss and aggregation. Molecular systems biology 16, e9596. https://doi.org/10.15252/msb.20209596.

Kenyon, C., Chang, J., Gensch, E., Rudner, A., Tabtiang, R., 1993. A C. elegans mutant that lives twice as long as wild type. Nature 366, 461–464. https://doi.org/10.1038/366461a0.

Kenyon, C.J., 2010. The genetics of ageing. Nature 464, 504–512. https://doi.org/10.1038/nature08980.

Khalil, M., Pirpamer, L., Hofer, E., Voortman, M.M., Barro, C., Leppert, D., Benkert, P., Ropele, S., Enzinger, C., Fazekas, F., Schmidt, R., Kuhle, J., 2020. Serum neurofilament light levels in normal aging and their association with morphologic brain changes. Nat Commun 11, 812. https://doi.org/10.1038/s41467-020-14612-6.

Khrapko, K., Kraytsberg, Y., Grey, A.D.N.J. de, Vijg, J., Schon, E.A., 2006. Does premature aging of the mtDNA mutator mouse prove that mtDNA mutations are involved in natural aging? Aging cell 5, 279–282. https://doi.org/10.1111/j.1474-9726.2006.00209.x.

Kim, O.-J., Ariano, M.A., Lazzarini, R.A., Levine, M.S., Sibley, D.R., 2002. Neurofilament-M Interacts with the D 1 Dopamine Receptor to Regulate Cell Surface Expression and Desensitization. J. Neurosci. 22, 5920–5930. https://doi.org/10.1523/JNEUROSCI.22-14-05920.2002.

Kluever, V., Fornasiero, E.F., 2021. Principles of brain aging: Status and challenges of modeling human molecular changes in mice. Ageing research reviews, 101465. https://doi.org/10.1016/j.arr.2021.101465.

Kneynsberg, A., Kanaan, N.M., 2017. Aging Does Not Affect Axon Initial Segment Structure and Somatic Localization of Tau Protein in Hippocampal Neurons of Fischer 344 Rats. eNeuro 4, ENEURO.0043-17.2017. https://doi.org/10.1523/ENEURO.0043-17.2017.

Kõks, S., Dogan, S., Tuna, B.G., González-Navarro, H., Potter, P., Vandenbroucke, R.E., 2016. Mouse models of ageing and their relevance to disease. Mechanisms of ageing and development 160, 41–53. https://doi.org/10.1016/j.mad.2016.10.001.

Komatsu, M., Waguri, S., Chiba, T., Murata, S., Iwata, J., Tanida, I., Ueno, T., Koike, M., Uchiyama, Y., Kominami, E., Tanaka, K., 2006. Loss of autophagy in the central nervous system causes neurodegeneration in mice. Nature 441, 880–884. https://doi.org/10.1038/nature04723.

Kondo, C., Ito, K., Kai, W., Sato, K., Taki, Y., Fukuda, H., Aoki, T., 2015. An age estimation method using brain local features for T1-weighted images. Conference proceedings: … Annual International Conference of the IEEE Engineering in Medicine and Biology Society. IEEE Engineering in Medicine and Biology Society. Annual Conference 2015, 666–669. https://doi.org/10.1109/EMBC.2015.7318450.

Kremer, L.S., Danhauser, K., Herebian, D., Petkovic Ramadža, D., Piekutowska-Abramczuk, D., Seibt, A., Müller-Felber, W., Haack, T.B., Płoski, R., Lohmeier, K., Schneider, D., Klee, D., Rokicki, D., Mayatepek, E., Strom, T.M., Meitinger, T., Klopstock, T., Pronicka, E., Mayr, J.A., Baric, I., Distelmaier, F., Prokisch, H., 2016. NAXE Mutations Disrupt the Cellular NAD(P)HX Repair System and Cause a Lethal Neurometabolic Disorder of Early Childhood. American journal of human genetics 99, 894–902. https://doi.org/10.1016/j.ajhg.2016.07.018.

Križ, J., Zhu, Q., Julien, J.-P., Padjen, A.L., 2000. Electrophysiological properties of axons in mice lacking neurofilament subunit genes: disparity between conduction velocity and axon diameter in absence of NF-H. Brain Research 885, 32–44. https://doi.org/10.1016/S0006-8993(00)02899-7.

Kujoth, G.C., Hiona, A., Pugh, T.D., Someya, S., Panzer, K., Wohlgemuth, S.E., Hofer, T., Seo, A.Y., Sullivan, R., Jobling, W.A., Morrow, J.D., van Remmen, H., Sedivy, J.M., Yamasoba, T., Tanokura, M., Weindruch, R., Leeuwenburgh, C., Prolla, T.A., 2005. Mitochondrial DNA mutations, oxidative stress, and apoptosis in mammalian aging. Science 309, 481–484. https://doi.org/10.1126/science.1112125.

Kushnareva, Y., Murphy, A.N., Andreyev, A., 2002. Complex I-mediated reactive oxygen species generation: modulation by cytochrome c and NAD(P)+ oxidation-reduction state. The Biochemical journal 368, 545–553. https://doi.org/10.1042/BJ20021121.

Kuwabara, T., Kagalwala, M.N., Onuma, Y., Ito, Y., Warashina, M., Terashima, K., Sanosaka, T., Nakashima, K., Gage, F.H., Asashima, M., 2011. Insulin biosynthesis in neuronal progenitors derived from adult hippocampus and the olfactory bulb. EMBO molecular medicine 3, 742–754. https://doi.org/10.1002/emmm.201100177.

Kwon, D., Yoon, J.H., Shin, S.-Y., Jang, T.-H., Kim, H.-G., So, I., Jeon, J.-H., Park, H.H., 2012. A comprehensive manually curated protein-protein interaction database for the Death Domain superfamily. Nucleic acids research 40, D331-6. https://doi.org/10.1093/nar/gkr1149.

La Cruz, J. de, Karbstein, K., Woolford, J.L., 2015. Functions of ribosomal proteins in assembly of eukaryotic ribosomes in vivo. Annu. Rev. Biochem. 84, 93–129. https://doi.org/10.1146/annurev-biochem-060614-033917.

Lardenoije, R., Iatrou, A., Kenis, G., Kompotis, K., Steinbusch, H.W.M., Mastroeni, D., Coleman, P., Lemere, C.A., Hof, P.R., van den Hove, Daniel L A, Rutten, B.P.F., 2015. The epigenetics of aging and neurodegeneration. Progress in neurobiology 131, 21–64. https://doi.org/10.1016/j.pneurobio.2015.05.002.

Lau, Y.-S., Patki, G., Das-Panja, K., Le, W.-D., Ahmad, S.O., 2011. Neuroprotective effects and mechanisms of exercise in a chronic mouse model of Parkinson's disease with moderate neurodegeneration. European Journal of Neuroscience 33, 1264–1274. https://doi.org/10.1111/j.1460-9568.2011.07626.x.

Laurent, J.M., Vogel, C., Kwon, T., Craig, S.A., Boutz, D.R., Huse, H.K., Nozue, K., Walia, H., Whiteley, M., Ronald, P.C., Marcotte, E.M., 2010. Protein abundances are more conserved than mRNA abundances across diverse taxa. Proteomics 10, 4209–4212. https://doi.org/10.1002/pmic.201000327.

Lavedan, C., Buchholtz, S., Nussbaum, R.L., Albin, R.L., Polymeropoulos, M.H., 2002. A mutation in the human neurofilament M gene in Parkinson's disease that suggests a role for the cytoskeleton in neuronal degeneration. Neuroscience letters 322, 57–61. https://doi.org/10.1016/S0304-3940(01)02513-7.

Le, T.D., Shirai, Y., Okamoto, T., Tatsukawa, T., Nagao, S., Shimizu, T., Ito, M., 2010. Lipid signaling in cytosolic phospholipase A2alpha-cyclooxygenase-2 cascade mediates cerebellar long-term depression and motor learning. PNAS 107, 3198–3203. https://doi.org/10.1073/pnas.0915020107.

Lebrigand, K., Magnone, V., Barbry, P., Waldmann, R., 2020. High throughput error corrected Nanopore single cell transcriptome sequencing. Nat Commun 11, 4025. https://doi.org/10.1038/s41467-020-17800-6.

Lee, C.K., Klopp, R.G., Weindruch, R., Prolla, T.A., 1999. Gene expression profile of aging and its retardation by caloric restriction. Science (New York, N.Y.) 285, 1390–1393. https://doi.org/10.1126/science.285.5432.1390.

Lee, C.K., Weindruch, R., Prolla, T.A., 2000. Gene-expression profile of the ageing brain in mice. Nature genetics 25, 294–297. https://doi.org/10.1038/77046.

Lee, I.M., Skerrett, P.J., 2001. Physical activity and all-cause mortality: what is the dose-response relation? Medicine and Science in Sports and Exercise 33, S459-71; discussion S493-4. https://doi.org/10.1097/00005768-200106001-00016.

Lee, Y., Morrison, B.M., Li, Y., Lengacher, S., Farah, M.H., Hoffman, P.N., Liu, Y., Tsingalia, A., Jin, L., Zhang, P.-W., Pellerin, L., Magistretti, P.J., Rothstein, J.D., 2012. Oligodendroglia metabolically support axons and contribute to neurodegeneration. Nature 487, 443–448. https://doi.org/10.1038/nature11314.

Leslie, C.C., 2015. Cytosolic phospholipase A_2: physiological function and role in disease. Journal of Lipid Research 56, 1386–1402. https://doi.org/10.1194/jlr.R057588.

Li, H., Wei, Y., 2015. Application of APP/PS1 Transgenic Mouse Model for AlzheimerÃ¢Â□Â™s Disease. J Alzheimers Dis Parkinsonism 05. https://doi.org/10.4172/2161-0460.1000201.

Li, M., Su, S., Cai, W., Cao, J., Miao, X., Zang, W., Gao, S., Xu, Y., Yang, J., Tao, Y.-X., Ai, Y., 2020a. Differentially Expressed Genes in the Brain of Aging Mice With Cognitive Alteration and Depression- and Anxiety-Like Behaviors. Front. Cell Dev. Biol. 8, 814, 814. https://doi.org/10.3389/fcell.2020.00814.

Li, N., Bates, D.J., An, J., Terry, D.A., Wang, E., 2011. Up-regulation of key microRNAs, and inverse down-regulation of their predicted oxidative phosphorylation target genes, during aging in mouse brain. Neurobiology of aging 32, 944–955. https://doi.org/10.1016/j.neurobiolaging.2009.04.020.

Li, N., Lagier-Tourenne, C., 2018. Nuclear pores: the gate to neurodegeneration. Nat Neurosci 21, 156–158. https://doi.org/10.1038/s41593-017-0066-0.

Li, Y., Xue, Y., Xu, X., Wang, G., Liu, Y., Wu, H., Li, W., Wang, Y., Chen, Z., Zhang, W., Zhu, Y., Ji, W., Xu, T., Liu, L., Chen, Q., 2019. A mitochondrial FUNDC1/HSC70 interaction organizes the proteostatic stress response at the risk of cell morbidity. The EMBO journal 38. https://doi.org/10.15252/embj.201798786.

Li, Y., Yu, H., Chen, C., Li, S., Zhang, Z., Xu, H., Zhu, F., Liu, J., Spencer, P.S., Dai, Z., Yang, X., 2020b. Proteomic Profile of Mouse Brain Aging Contributions to Mitochondrial Dysfunction, DNA Oxidative Damage, Loss of Neurotrophic Factor, and Synaptic and Ribosomal Proteins. Oxidative medicine and cellular longevity 2020, 5408452. https://doi.org/10.1155/2020/5408452.

Liao, C.-Y., Rikke, B.A., Johnson, T.E., Diaz, V., Nelson, J.F., 2010. Genetic variation in the murine lifespan response to dietary restriction: From life extension to life shortening. Aging cell 9, 92–95. https://doi.org/10.1111/j.1474-9726.2009.00533.x.

Liao, L., Cheng, D., Wang, J., Duong, D.M., Losik, T.G., Gearing, M., Rees, H.D., Lah, J.J., Levey, A.I., Peng, J., 2004. Proteomic characterization of postmortem amyloid plaques isolated by laser capture microdissection. The Journal of biological chemistry 279, 37061–37068. https://doi.org/10.1074/jbc.M403672200.

Liao, Y., Wang, J., Jaehnig, E.J., Shi, Z., Zhang, B., 2019. WebGestalt 2019: gene set analysis toolkit with revamped UIs and APIs. Nucleic acids research 47, W199-W205. https://doi.org/10.1093/nar/gkz401.

Lindner, A.B., Demarez, A., 2009. Protein aggregation as a paradigm of aging. Biochimica et biophysica acta 1790, 980–996. https://doi.org/10.1016/j.bbagen.2009.06.005.

Liu, B., Huang, B., Liu, J., Shi, J.-S., 2020. Dendrobium nobile Lindl alkaloid and metformin ameliorate cognitive dysfunction in senescence-accelerated mice via suppression of endoplasmic reticulum stress. Brain Research 1741, 146871. https://doi.org/10.1016/j.brainres.2020.146871.

Liu, J., Head, E., Gharib, A.M., Yuan, W., Ingersoll, R.T., Hagen, T.M., Cotman, C.W., Ames, B.N., 2002. Memory loss in old rats is associated with brain mitochondrial decay and RNA/DNA oxidation: partial reversal by feeding acetyl-L-carnitine and/or R-alpha -lipoic acid. Proceedings of the National Academy of Sciences of the United States of America 99, 2356–2361. https://doi.org/10.1073/pnas.261709299.

Liu, T., Li, H., Hong, W., Han, W., 2016. Brefeldin A-inhibited guanine nucleotide exchange protein 3 is localized in lysosomes and regulates GABA signaling in hippocampal neurons. Journal of neurochemistry 139, 748–756. https://doi.org/10.1111/jnc.13859.

Lodato, M.A., Rodin, R.E., Bohrson, C.L., Coulter, M.E., Barton, A.R., Kwon, M., Sherman, M.A., Vitzthum, C.M., Luquette, L.J., Yandava, C.N., Yang, P., Chittenden, T.W., Hatem, N.E., Ryu, S.C., Woodworth, M.B., Park, P.J., Walsh, C.A., 2018. Aging and neurodegeneration are associated with increased mutations in single human neurons. Science (New York, N.Y.) 359, 555–559. https://doi.org/10.1126/science.aao4426.

Loerch, P.M., Lu, T., Dakin, K.A., Vann, J.M., Isaacs, A., Geula, C., Wang, J., Pan, Y., Gabuzda, D.H., Li, C., Prolla, T.A., Yankner, B.A., 2008. Evolution of the aging brain transcriptome and synaptic regulation. PloS one 3, e3329. https://doi.org/10.1371/journal.pone.0003329.

López-Erauskin, J., Fourcade, S., Galino, J., Ruiz, M., Schlüter, A., Naudi, A., Jove, M., Portero-Otin, M., Pamplona, R., Ferrer, I., Pujol, A., 2011. Antioxidants halt axonal degeneration in a mouse model of X-adrenoleukodystrophy. Annals of neurology 70, 84–92. https://doi.org/10.1002/ana.22363.

Lu, T., Pan, Y., Kao, S.-Y., Li, C., Kohane, I., Chan, J., Yankner, B.A., 2004. Gene regulation and DNA damage in the ageing human brain. Nature 429, 883–891. https://doi.org/10.1038/nature02661.

Lucking, C.B., Durr, A., Bonifati, V., Vaughan, J., Michele, G. de, Gasser, T., Harhangi, B.S., Meco, G., Denefle, P., Wood, N.W., Agid, Y., Brice, A., 2000. Association between early-onset Parkinson's disease and mutations in the parkin gene. The New England journal of medicine 342, 1560–1567. https://doi.org/10.1056/NEJM200005253422103.

Lupo, G., Gioia, R., Nisi, P.S., Biagioni, S., Cacci, E., 2019. Molecular Mechanisms of Neurogenic Aging in the Adult Mouse Subventricular Zone. Journal of experimental neuroscience 13, 1179069519829040. https://doi.org/10.1177/1179069519829040.

Määttä, T.A., Rettel, M., Sridharan, S., Helm, D., Kurzawa, N., Stein, F., Savitski, M.M., 2020. Aggregation and disaggregation features of the human proteome. Molecular systems biology 16, e9500. https://doi.org/10.15252/msb.20209500.

Malm, T.M., Iivonen, H., Goldsteins, G., Keksa-Goldsteine, V., Ahtoniemi, T., Kanninen, K., Salminen, A., Auriola, S., van Groen, T., Tanila, H., Koistinaho, J., 2007. Pyrrolidine dithiocarbamate activates Akt and improves spatial learning in APP/PS1 mice without affecting beta-amyloid burden. J. Neurosci. 27, 3712–3721. https://doi.org/10.1523/JNEUROSCI.0059-07.2007.

Manavalan, A., Mishra, M., Feng, L., Sze, S.K., Akatsu, H., Heese, K., 2013. Brain site-specific proteome changes in aging-related dementia. Experimental & molecular medicine 45, e39. https://doi.org/10.1038/emm.2013.76.

Mao, L., Römer, I., Nebrich, G., Klein, O., Koppelstätter, A., Hin, S.C., Hartl, D., Zabel, C., 2010. Aging in mouse brain is a cell/tissue-level phenomenon exacerbated by proteasome loss. Journal of proteome research 9, 3551–3560. https://doi.org/10.1021/pr100059j.

Mao, P., Manczak, M., Calkins, M.J., Truong, Q., Reddy, T.P., Reddy, A.P., Shirendeb, U., Lo, H.-H., Rabinovitch, P.S., Reddy, P.H., 2012. Mitochondria-targeted catalase reduces abnormal APP processing, amyloid β production and BACE1 in a mouse model of Alzheimer's disease: implications for neuroprotection and lifespan extension. Human molecular genetics 21, 2973–2990. https://doi.org/10.1093/hmg/dds128.

Marschallinger, J., Iram, T., Zardeneta, M., Lee, S.E., Lehallier, B., Haney, M.S., Pluvinage, J.V., Mathur, V., Hahn, O., Morgens, D.W., Kim, J., Tevini, J., Felder, T.K., Wolinski, H., Bertozzi, C.R., Bassik, M.C., Aigner, L., Wyss-Coray, T., 2020. Lipid-droplet-accumulating microglia represent a dysfunctional and proinflammatory state in the aging brain. Nat Neurosci 23, 194–208. https://doi.org/10.1038/s41593-019-0566-1.

Martinez-Jimenez, C.P., Eling, N., Chen, H.-C., Vallejos, C.A., Kolodziejczyk, A.A., Connor, F., Stojic, L., Rayner, T.F., Stubbington, M.J.T., Teichmann, S.A., La Roche, M. de, Marioni, J.C., Odom, D.T., 2017. Aging increases cell-to-cell transcriptional variability upon immune stimulation. Science 355, 1433–1436. https://doi.org/10.1126/science.aah4115.

Martin-Montalvo, A., Mercken, E.M., Mitchell, S.J., Palacios, H.H., Mote, P.L., Scheibye-Knudsen, M., Gomes, A.P., Ward, T.M., Minor, R.K., Blouin, M.-J., Schwab, M., Pollak, M., Zhang, Y., Yu, Y., Becker, K.G., Bohr, V.A., Ingram, D.K., Sinclair, D.A., Wolf, N.S., Spindler, S.R., Bernier, M., Cabo, R. de, 2013. Metformin improves healthspan and lifespan in mice. Nature communications 4, 2192. https://doi.org/10.1038/ncomms3192.

Masliah, E., Iimoto, D.S., Saitoh, T., Hansen, L.A., Terry, R.D., 1990. Increased immunoreactivity of brain spectrin in Alzheimer disease: a marker for synapse loss? Brain Research 531, 36–44. https://doi.org/10.1016/0006-8993(90)90755-Z.

Masoro, E.J., 2005. Overview of caloric restriction and ageing. Mechanisms of ageing and development 126, 913–922. https://doi.org/10.1016/j.mad.2005.03.012.

Mautz, B.S., Lind, M.I., Maklakov, A.A., 2020. Dietary Restriction Improves Fitness of Aging Parents But Reduces Fitness of Their Offspring in Nematodes. The Journals of Gerontology Series A: Biological Sciences and Medical Sciences 75, 843–848. https://doi.org/10.1093/gerona/glz276.

McCarthy, M.M., Arnold, A.P., Ball, G.F., Blaustein, J.D., Vries, G.J. de, 2012. Sex differences in the brain: the not so inconvenient truth. J. Neurosci. 32, 2241–2247. https://doi.org/10.1523/JNEUROSCI.5372-11.2012.

McCay, C.M., Crowell, M.F., Maynard, L.A., 1935. The Effect of Retarded Growth Upon the Length of Life Span and Upon the Ultimate Body Size. The Journal of Nutrition 10, 63–79. https://doi.org/10.1093/jn/10.1.63.

McMurphy, T., Huang, W., Queen, N.J., Ali, S., Widstrom, K.J., Liu, X., Xiao, R., Siu, J.J., Cao, L., 2018. Implementation of environmental enrichment after middle age promotes healthy aging. Aging (Albany NY) 10, 1698–1721. https://doi.org/10.18632/aging.101502.

Meier, F., Brunner, A.-D., Frank, M., Ha, A., Bludau, I., Voytik, E., Kaspar-Schoenefeld, S., Lubeck, M., Raether, O., Bache, N., Aebersold, R., Collins, B.C., Röst, H.L., Mann, M., 2020. diaPASEF: parallel accumulation-serial fragmentation combined with data-independent acquisition. Nature Methods 17, 1229–1236. https://doi.org/10.1038/s41592-020-00998-0.

Meier, F., Geyer, P.E., Winter, S.V., Cox, J., Mann, M., 2018. BoxCar acquisition method enables single-shot proteomics at a depth of 10,000 proteins in 100 minutes. Nature Methods 15, 440. https://doi.org/10.1038/s41592-018-0003-5.

Millecamps, S., Gowing, G., Corti, O., Mallet, J., Julien, J.-P., 2007. Conditional NF-L transgene expression in mice for in vivo analysis of turnover and transport rate of neurofilaments. J. Neurosci. 27, 4947–4956. https://doi.org/10.1523/JNEUROSCI.5299-06.2007.

Min, J.-N., Whaley, R.A., Sharpless, N.E., Lockyer, P., Portbury, A.L., Patterson, C., 2008. CHIP deficiency decreases longevity, with accelerated aging phenotypes accompanied by altered protein quality control. Molecular and cellular biology 28, 4018–4025. https://doi.org/10.1128/MCB.00296-08.

Miyamoto, M., 1997. Characteristics of age-related behavioral changes in senescence-accelerated mouse SAMP8 and SAMP10. Experimental gerontology 32, 139–148.

Molofsky, A.V., Slutsky, S.G., Joseph, N.M., He, S., Pardal, R., Krishnamurthy, J., Sharpless, N.E., Morrison, S.J., 2006. Increasing p16INK4a expression decreases forebrain progenitors and neurogenesis during ageing. Nature 443, 448–452. https://doi.org/10.1038/nature05091.

Montagne, A., Barnes, S.R., Sweeney, M.D., Halliday, M.R., Sagare, A.P., Zhao, Z., Toga, A.W., Jacobs, R.E., Liu, C.Y., Amezcua, L., Harrington, M.G., Chui, H.C., Law, M., Zlokovic, B.V., 2015. Blood-brain barrier breakdown in the aging human hippocampus. Neuron 85, 296–302. https://doi.org/10.1016/j.neuron.2014.12.032.

Montague, P., McCallion, A.S., Davies, R.W., Griffiths, I.R., 2006. Myelin-associated oligodendrocytic basic protein: a family of abundant CNS myelin proteins in search of a function. Dev Neurosci 28, 479–487. https://doi.org/10.1159/000095110.

Most, J., Tosti, V., Redman, L.M., Fontana, L., 2017. Calorie restriction in humans: an update. Ageing research reviews 39, 36–45. https://doi.org/10.1016/j.arr.2016.08.005.

Munch, G., Westcott, B., Menini, T., Gugliucci, A., 2012. Advanced glycation endproducts and their pathogenic roles in neurological disorders. Amino acids 42, 1221–1236. https://doi.org/10.1007/s00726-010-0777-y.

Naidoo, N., Ferber, M., Master, M., Zhu, Y., Pack, A.I., 2008. Aging impairs the unfolded protein response to sleep deprivation and leads to proapoptotic signaling. The Journal of neuroscience: the official journal of the Society for Neuroscience 28, 6539–6548. https://doi.org/10.1523/JNEUROSCI.5685-07.2008.

Navarro, A., Del Sánchez Pino, M.J., Gómez, C., Peralta, J.L., Boveris, A., 2002. Behavioral dysfunction, brain oxidative stress, and impaired mitochondrial electron transfer in aging mice. American Journal of Physiology-Regulatory, Integrative and Comparative Physiology 282, R985-92. https://doi.org/10.1152/ajpregu.00537.2001.

Neuner, S.M., Ding, S., Kaczorowski, C.C., 2019. Knockdown of heterochromatin protein 1 binding protein 3 recapitulates phenotypic, cellular, and molecular features of aging. Aging cell 18, e12886. https://doi.org/10.1111/acel.12886.

Niccoli, T., Partridge, L., 2012. Ageing as a risk factor for disease. Current biology: CB 22, R741-52. https://doi.org/10.1016/j.cub.2012.07.024.

Nithianantharajah, J., Hannan, A.J., 2006. Enriched environments, experience-dependent plasticity and disorders of the nervous system. Nature reviews. Neuroscience 7, 697–709. https://doi.org/10.1038/nrn1970.

Nowotny, K., Jung, T., Grune, T., Höhn, A., 2014. Accumulation of modified proteins and aggregate formation in aging. Experimental gerontology 57, 122–131. https://doi.org/10.1016/j.exger.2014.05.016.

Nuss, J.E., Choksi, K.B., DeFord, J.H., Papaconstantinou, J., 2008. Decreased enzyme activities of chaperones PDI and BiP in aged mouse livers. Biochemical and biophysical research communications 365, 355–361. https://doi.org/10.1016/j.bbrc.2007.10.194.

Oh, G., Ebrahimi, S., Wang, S.-C., Cortese, R., Kaminsky, Z.A., Gottesman, I.I., Burke, J.R., Plassman, B.L., Petronis, A., 2016. Epigenetic assimilation in the aging human brain. Genome biology 17, 76. https://doi.org/10.1186/s13059-016-0946-8.

Ohta, H., Nishikawa, H., Hirai, K., Kato, K., Miyamoto, M., 1996. Relationship of impaired brain glucose metabolism to learning deficit in the senescence-accelerated mouse. Neuroscience letters 217, 37–40. https://doi.org/10.1016/0304-3940(96)13064-0.

Ori, A., Toyama, B.H., Harris, M.S., Bock, T., Iskar, M., Bork, P., Ingolia, N.T., Hetzer, M.W., Beck, M., 2015. Integrated Transcriptome and Proteome Analyses Reveal Organ-Specific Proteome Deterioration in Old Rats. Cell systems 1, 224–237. https://doi.org/10.1016/j.cels.2015.08.012.

Osorio, F.G., Navarro, C.L., Cadiñanos, J., López-Mejía, I.C., Quirós, P.M., Bartoli, C., Rivera, J., Tazi, J., Guzmán, G., Varela, I., Depetris, D., Carlos, F. de, Cobo, J., Andrés, V., Sandre-Giovannoli, A. de, Freije, J.M.P., Lévy, N., López-Otín, C., 2011. Splicing-directed therapy in a new mouse model of human accelerated aging. Science translational medicine 3, 106ra107. https://doi.org/10.1126/scitranslmed.3002847.

Osorio, F.G., Soria-Valles, C., Santiago-Fernández, O., Bernal, T., Mittelbrunn, M., Colado, E., Rodríguez, F., Bonzon-Kulichenko, E., Vázquez, J., Porta-de-la-Riva, M., Cerón, J., Fueyo, A., Li, J., Green, A.R., Freije, J.M.P., López-Otín, C., 2016. Loss of the proteostasis factor AIRAPL causes myeloid transformation by deregulating IGF-1 signaling. Nature medicine 22, 91–96. https://doi.org/10.1038/nm.4013.

Oughtred, R., Rust, J., Chang, C., Breitkreutz, B.-J., Stark, C., Willems, A., Boucher, L., Leung, G., Kolas, N., Zhang, F., Dolma, S., Coulombe-Huntington, J., Chatr-Aryamontri, A., Dolinski, K., Tyers, M., 2021. The BioGRID database: A comprehensive biomedical resource of curated protein, genetic, and chemical interactions. Protein Science 30, 187–200. https://doi.org/10.1002/pro.3978.

Pan, J., Ma, N., Yu, B., Zhang, W., Wan, J., 2020. Transcriptomic profiling of microglia and astrocytes throughout aging. J Neuroinflammation 17, 97. https://doi.org/10.1186/s12974-020-01774-9.

Pannese, E., 2011. Morphological changes in nerve cells during normal aging. Brain structure & function 216, 85–89. https://doi.org/10.1007/s00429-011-0308-y.

Panov, A., Orynbayeva, Z., Vavilin, V., Lyakhovich, V., 2014. Fatty acids in energy metabolism of the central nervous system. BioMed research international 2014, 472459. https://doi.org/10.1155/2014/472459.

Pappireddi, N., Martin, L., Wühr, M., 2019. A Review on Quantitative Multiplexed Proteomics. ChemBioChem 20, 1210–1224. https://doi.org/10.1002/cbic.201800650.

Park, H., Kam, T.-I., Kim, Y., Choi, H., Gwon, Y., Kim, C., Koh, J.-Y., Jung, Y.-K., 2012. Neuropathogenic role of adenylate kinase-1 in Aβ-mediated tau phosphorylation via AMPK and GSK3β. Human molecular genetics 21, 2725–2737. https://doi.org/10.1093/hmg/dds100.

Park, S.-K., Kim, K., Page, G.P., Allison, D.B., Weindruch, R., Prolla, T.A., 2009. Gene expression profiling of aging in multiple mouse strains: identification of aging biomarkers and impact of dietary antioxidants. Aging cell 8, 484–495. https://doi.org/10.1111/j.1474-9726.2009.00496.x.

Paz Gavilán, M., Vela, J., Castaño, A., Ramos, B., del Río, J.C., Vitorica, J., Ruano, D., 2006. Cellular environment facilitates protein accumulation in aged rat hippocampus. Neurobiology of aging 27, 973–982. https://doi.org/10.1016/j.neurobiolaging.2005.05.010.

Pellegrini, C., Pirazzini, C., Sala, C., Sambati, L., Yusipov, I., Kalyakulina, A., Ravaioli, F., Kwiatkowska, K.M., Durso, D.F., Ivanchenko, M., Monti, D., Lodi, R., Franceschi, C., Cortelli, P., Garagnani, P., Bacalini, M.G., 2021. A Meta-Analysis of Brain DNA Methylation Across Sex, Age, and Alzheimer's Disease Points for Accelerated Epigenetic Aging in Neurodegeneration. Frontiers in aging neuroscience 13, 639428, 639428. https://doi.org/10.3389/fnagi.2021.639428.

Pendás, A.M., Zhou, Z., Cadiñanos, J., Freije, J.M.P., Wang, J., Hultenby, K., Astudillo, A., Wernerson, A., Rodríguez, F., Tryggvason, K., López-Otín, C., 2002. Defective prelamin A processing and muscular and adipocyte alterations in Zmpste24 metalloproteinase-deficient mice. Nature genetics 31, 94–99. https://doi.org/10.1038/ng871.

Peng, Y.-S., Tang, C.-W., Peng, Y.-Y., Chang, H., Chen, C.-L., Guo, S.-L., Wu, L.-C., Huang, M.-C., Lee, H.-C., 2020. Comparative functional genomic analysis of Alzheimer's affected and naturally aging brains. PeerJ 8, e8682. https://doi.org/10.7717/peerj.8682.

Pérez, V.I., Buffenstein, R., Masamsetti, V., Leonard, S., Salmon, A.B., Mele, J., Andziak, B., Yang, T., Edrey, Y., Friguet, B., Ward, W., Richardson, A., Chaudhuri, A., 2009a. Protein stability and resistance to oxidative stress are determinants of longevity in the longest-living rodent, the naked mole-rat. Proceedings of the National Academy of Sciences of the United States of America 106, 3059–3064. https://doi.org/10.1073/pnas.0809620106.

Pérez, V.I., van Remmen, H., Bokov, A., Epstein, C.J., Vijg, J., Richardson, A., 2009b. The overexpression of major antioxidant enzymes does not extend the lifespan of mice. Aging cell 8, 73–75. https://doi.org/10.1111/j.1474-9726.2008.00449.x.

Perlman, J.M., 2007. Pathogenesis of hypoxic-ischemic brain injury. J Perinatol 27, S39-S46. https://doi.org/10.1038/sj.jp.7211716.

Peters, A., 2002. The effects of normal aging on myelin and nerve fibers: a review. Journal of neurocytology 31, 581–593.

Petzold, A., Keir, G., Warren, J., Fox, N., Rossor, M.N., 2007. A systematic review and meta-analysis of CSF neurofilament protein levels as biomarkers in dementia. Neurodegener Dis 4, 185–194. https://doi.org/10.1159/000101843.

Philips, T., Mironova, Y.A., Jouroukhin, Y., Chew, J., Vidensky, S., Farah, M.H., Pletnikov, M.V., Bergles, D.E., Morrison, B.M., Rothstein, J.D., 2021. MCT1 Deletion in Oligodendrocyte Lineage Cells Causes Late-Onset Hypomyelination and Axonal Degeneration. Cell reports 34, 108610. https://doi.org/10.1016/j.celrep.2020.108610.

Philpott, M., Watson, J., Thakurta, A., Brown, T., Oppermann, U., Cribbs, A.P., 2021. Nanopore sequencing of single-cell transcriptomes with scCOLOR-seq. Nat Biotechnol. https://doi.org/10.1038/s41587-021-00965-w.

Piscopo, P., Bellenghi, M., Manzini, V., Crestini, A., Pontecorvi, G., Corbo, M., Ortona, E., Carè, A., Confaloni, A., 2021. A Sex Perspective in Neurodegenerative Diseases: microRNAs as Possible Peripheral Biomarkers. International journal of molecular sciences 22, 4423. https://doi.org/10.3390/ijms22094423.

Podtelezhnikov, A.A., Tanis, K.Q., Nebozhyn, M., Ray, W.J., Stone, D.J., Loboda, A.P., 2011. Molecular insights into the pathogenesis of Alzheimer's disease and its relationship to normal aging. PloS one 6, e29610. https://doi.org/10.1371/journal.pone.0029610.

Poisnel, G., Hérard, A.-S., El Tannir El Tayara, N., Bourrin, E., Volk, A., Kober, F., Delatour, B., Delzescaux, T., Debeir, T., Rooney, T., Benavides, J., Hantraye, P., Dhenain, M., 2012. Increased regional cerebral glucose uptake in an APP/PS1 model of Alzheimer's disease. Neurobiology of aging 33, 1995–2005. https://doi.org/10.1016/j.neurobiolaging.2011.09.026.

Pollack, M., Leeuwenburgh, C., 2001. Apoptosis and aging: role of the mitochondria. The Journals of Gerontology Series A: Biological Sciences and Medical Sciences 56, B475-82. https://doi.org/10.1093/gerona/56.11.B475.

Prince, M., Ali, G.-C., Guerchet, M., Prina, A.M., Albanese, E., Wu, Y.-T., 2016. Recent global trends in the prevalence and incidence of dementia, and survival with dementia. Alzheimer's research & therapy 8. https://doi.org/10.1186/s13195-016-0188-8.
Princz, A., Tavernarakis, N., 2017. The role of SUMOylation in ageing and senescent decline. Mechanisms of ageing and development 162, 85–90. https://doi.org/10.1016/j.mad.2017.01.002.
Raasakka, A., Kursula, P., 2020. Flexible Players within the Sheaths: The Intrinsically Disordered Proteins of Myelin in Health and Disease. Cells 9, 470. https://doi.org/10.3390/cells9020470.
Rabbani, N., Thornalley, P.J., 2012. Methylglyoxal, glyoxalase 1 and the dicarbonyl proteome. Amino acids 42, 1133–1142. https://doi.org/10.1007/s00726-010-0783-0.
Radde, R., Bolmont, T., Kaeser, S.A., Coomaraswamy, J., Lindau, D., Stoltze, L., Calhoun, M.E., Jäggi, F., Wolburg, H., Gengler, S., Haass, C., Ghetti, B., Czech, C., Hölscher, C., Mathews, P.M., Jucker, M., 2006. Abeta42-driven cerebral amyloidosis in transgenic mice reveals early and robust pathology. EMBO reports 7, 940–946. https://doi.org/10.1038/sj.embor.7400784.
Rao, M.V., Mohan, P.S., Kumar, A., Yuan, A., Montagna, L., Campbell, J., Veeranna, Espreafico, E.M., Julien, J.P., Nixon, R.A., 2011. The myosin Va head domain binds to the neurofilament-L rod and modulates endoplasmic reticulum (ER) content and distribution within axons. PloS one 6, e17087. https://doi.org/10.1371/journal.pone.0017087.
Rath, S., Sharma, R., Gupta, R., Ast, T., Chan, C., Durham, T.J., Goodman, R.P., Grabarek, Z., Haas, M.E., Hung, W.H.W., Joshi, P.R., Jourdain, A.A., Kim, S.H., Kotrys, A.V., Lam, S.S., McCoy, J.G., Meisel, J.D., Miranda, M., Panda, A., Patgiri, A., Rogers, R., Sadre, S., Shah, H., Skinner, O.S., To, T.-L., Walker, M.A., Wang, H., Ward, P.S., Wengrod, J., Yuan, C.-C., Calvo, S.E., Mootha, V.K., 2021. MitoCarta3.0: an updated mitochondrial proteome now with sub-organelle localization and pathway annotations. Nucleic acids research 49, D1541-D1547. https://doi.org/10.1093/nar/gkaa1011.
Raynaud, F., Marcilhac, A., 2006. Implication of calpain in neuronal apoptosis. A possible regulation of Alzheimer's disease. FEBS Journal 273, 3437–3443. https://doi.org/10.1111/j.1742-4658.2006.05352.x.
Reekes, T.H., Higginson, C.I., Ledbetter, C.R., Sathivadivel, N., Zweig, R.M., Disbrow, E.A., 2020. Sex specific cognitive differences in Parkinson disease. NPJ Parkinson's disease 6, 7. https://doi.org/10.1038/s41531-020-0109-1.
Reis-Rodrigues, P., Czerwieniec, G., Peters, T.W., Evani, U.S., Alavez, S., Gaman, E.A., Vantipalli, M., Mooney, S.D., Gibson, B.W., Lithgow, G.J., Hughes, R.E., 2012. Proteomic analysis of age-dependent changes in protein solubility identifies genes that modulate lifespan. Aging cell 11, 120–127. https://doi.org/10.1111/j.1474-9726.2011.00765.x.
Rhyu, I.J., Bytheway, J.A., Kohler, S.J., Lange, H., Lee, K.J., Boklewski, J., McCormick, K., Williams, N.I., Stanton, G.B., Greenough, W.T., Cameron, J.L., 2010. Effects of aerobic exercise training on cognitive function and cortical vascularity in monkeys. Neuroscience 167, 1239–1248. https://doi.org/10.1016/j.neuroscience.2010.03.003.
Richfield, E.K., Thiruchelvam, M.J., Cory-Slechta, D.A., Wuertzer, C., Gainetdinov, R.R., Caron, M.G., Di Monte, D.A., Federoff, H.J., 2002. Behavioral and neurochemical effects of wild-type and mutated human alpha-synuclein in transgenic mice. Experimental Neurology 175, 35–48. https://doi.org/10.1006/exnr.2002.7882.
Rinholm, J.E., Bergersen, L.H., 2012. Neuroscience: The wrap that feeds neurons. Nature 487, 435–436. https://doi.org/10.1038/487435a.
Ristow, M., Zarse, K., 2010. How increased oxidative stress promotes longevity and metabolic health: The concept of mitochondrial hormesis (mitohormesis). Experimental gerontology 45, 410–418. https://doi.org/10.1016/j.exger.2010.03.014.
Ritchie, M.E., Phipson, B., Di Wu, Hu, Y., Law, C.W., Shi, W., Smyth, G.K., 2015. limma powers differential expression analyses for RNA-sequencing and microarray studies. Nucleic acids research 43, e47. https://doi.org/10.1093/nar/gkv007.
Roberts, M.N., Wallace, M.A., Tomilov, A.A., Zhou, Z., Marcotte, G.R., Tran, D., Perez, G., Gutierrez-Casado, E., Koike, S., Knotts, T.A., Imai, D.M., Griffey, S.M., Kim, K., Hagopian, K., Haj, F.G., Baar, K., Cortopassi, G.A., Ramsey, J.J., Lopez-Dominguez, J.A., 2017. A Ketogenic Diet Extends Longevity and Healthspan in Adult Mice. Cell metabolism 26, 539-546.e5. https://doi.org/10.1016/j.cmet.2017.08.005.
Rockenstein, E., Mallory, M., Hashimoto, M., Song, D., Shults, C.W., Lang, I., Masliah, E., 2002. Differential neuropathological alterations in transgenic mice expressing alpha-synuclein from the platelet-derived growth factor and Thy-1 promoters. J. Neurosci. Res. 68, 568–578. https://doi.org/10.1002/jnr.10231.
Rodriguez-Araujo, G., Nakagami, H., Hayashi, H., Mori, M., Shiuchi, T., Minokoshi, Y., Nakaoka, Y., Takami, Y., Komuro, I., Morishita, R., Kaneda, Y., 2013. Alpha-synuclein elicits glucose uptake and utilization in

adipocytes through the Gab1/PI3K/Akt transduction pathway. Cell. Mol. Life Sci. 70, 1123–1133. https://doi.org/10.1007/s00018-012-1198-8.
Romano, A., Koczwara, J.B., Gallelli, C.A., Vergara, D., Di Micioni Bonaventura, M.V., Gaetani, S., Giudetti, A.M., 2017. Fats for thoughts: An update on brain fatty acid metabolism. The international journal of biochemistry & cell biology 84, 40–45. https://doi.org/10.1016/j.biocel.2016.12.015.
Rone, M.B., Midzak, A.S., Issop, L., Rammouz, G., Jagannathan, S., Fan, J., Ye, X., Blonder, J., Veenstra, T., Papadopoulos, V., 2012. Identification of a dynamic mitochondrial protein complex driving cholesterol import, trafficking, and metabolism to steroid hormones. Molecular Endocrinology 26, 1868–1882. https://doi.org/10.1210/me.2012-1159.
Ross, J.M., Coppotelli, G., Branca, R.M., Kim, K.M., Lehtiö, J., Sinclair, D.A., Olson, L., 2019. Voluntary exercise normalizes the proteomic landscape in muscle and brain and improves the phenotype of progeroid mice. Aging cell, e13029. https://doi.org/10.1111/acel.13029.
Rousseau, D., 2019. ATAD3 and endoplasmic reticulum to mitochondria connection: a main actor and interaction regarding pathogenesis. J Med Therap 3. https://doi.org/10.15761/JMT.1000139.
Rozycka, A., Liguz-Lecznar, M., 2017. The space where aging acts: focus on the GABAergic synapse. Aging cell 16, 634–643. https://doi.org/10.1111/acel.12605.
Safaiyan, S., Kannaiyan, N., Snaidero, N., Brioschi, S., Biber, K., Yona, S., Edinger, A.L., Jung, S., Rossner, M.J., Simons, M., 2016. Age-related myelin degradation burdens the clearance function of microglia during aging. Nat Neurosci 19, 995–998. https://doi.org/10.1038/nn.4325.
Safdar, A., Khrapko, K., Flynn, J.M., Saleem, A., Lisio, M., Johnston, A.P.W., Kratysberg, Y., Samjoo, I.A., Kitaoka, Y., Ogborn, D.I., Little, J.P., Raha, S., Parise, G., Akhtar, M., Hettinga, B.P., Rowe, G.C., Arany, Z., Prolla, T.A., Tarnopolsky, M.A., 2015. Exercise-induced mitochondrial p53 repairs mtDNA mutations in mutator mice. Skeletal Muscle 6, 7. https://doi.org/10.1186/s13395-016-0075-9.
Salcedo-Tello, P., Ortiz-Matamoros, A., Arias, C., 2011. GSK3 Function in the Brain during Development, Neuronal Plasticity, and Neurodegeneration. International journal of Alzheimer's disease 2011, 189728. https://doi.org/10.4061/2011/189728.
Salek Esfahani, B., Gharesouran, J., Ghafouri-Fard, S., Talebian, S., Arsang-Jang, S., Omrani, M.D., Taheri, M., Rezazadeh, M., 2019. Down-regulation of ERMN expression in relapsing remitting multiple sclerosis. Metab Brain Dis 34, 1261–1266. https://doi.org/10.1007/s11011-019-00429-w.
Salminen, A., Kaarniranta, K., 2012. AMP-activated protein kinase (AMPK) controls the aging process via an integrated signaling network. Ageing research reviews 11, 230–241. https://doi.org/10.1016/j.arr.2011.12.005.
Salthouse, T.A., 2010. Selective review of cognitive aging. Journal of the International Neuropsychological Society : JINS 16, 754–760. https://doi.org/10.1017/S1355617710000706.
Sampson, T.R., Debelius, J.W., Thron, T., Janssen, S., Shastri, G.G., Ilhan, Z.E., Challis, C., Schretter, C.E., Rocha, S., Gradinaru, V., Chesselet, M.-F., Keshavarzian, A., Shannon, K.M., Krajmalnik-Brown, R., Wittung-Stafshede, P., Knight, R., Mazmanian, S.K., 2016. Gut Microbiota Regulate Motor Deficits and Neuroinflammation in a Model of Parkinson's Disease. Cell 167, 1469-1480.e12. https://doi.org/10.1016/j.cell.2016.11.018.
Santoro, A., Spinelli, C.C., Martucciello, S., Nori, S.L., Capunzo, M., Puca, A.A., Ciaglia, E., 2018. Innate immunity and cellular senescence: The good and the bad in the developmental and aged brain. Journal of leukocyte biology. https://doi.org/10.1002/JLB.3MR0118-003R.
Santos, C.L., Roppa, P.H.A., Truccolo, P., Fontella, F.U., Souza, D.O., Bobermin, L.D., Quincozes-Santos, A., 2018. Age-Dependent Neurochemical Remodeling of Hypothalamic Astrocytes. Molecular neurobiology 55, 5565–5579. https://doi.org/10.1007/s12035-017-0786-x.
Sasaguri, H., Nilsson, P., Hashimoto, S., Nagata, K., Saito, T., Strooper, B. de, Hardy, J., Vassar, R., Winblad, B., Saido, T.C., 2017. APP mouse models for Alzheimer's disease preclinical studies. The EMBO journal 36, 2473–2487. https://doi.org/10.15252/embj.201797397.
Savas, J.N., Toyama, B.H., Xu, T., Yates, J.R., Hetzer, M.W., 2012. Extremely long-lived nuclear pore proteins in the rat brain. Science 335, 942. https://doi.org/10.1126/science.1217421.
Savas, J.N., Wang, Y.-Z., DeNardo, L.A., Martinez-Bartolome, S., McClatchy, D.B., Hark, T.J., Shanks, N.F., Cozzolino, K.A., Lavallée-Adam, M., Smukowski, S.N., Park, S.K., Kelly, J.W., Koo, E.H., Nakagawa, T., Masliah, E., Ghosh, A., Yates, J.R., 2017. Amyloid Accumulation Drives Proteome-wide Alterations in Mouse Models of Alzheimer's Disease-like Pathology. Cell reports 21, 2614–2627. https://doi.org/10.1016/j.celrep.2017.11.009.
Scaglione, A., Patzig, J., Liang, J., Frawley, R., Bok, J., Mela, A., Yattah, C., Zhang, J., Teo, S.X., Zhou, T., Chen, S., Bernstein, E., Canoll, P., Guccione, E., Casaccia, P., 2018. PRMT5-mediated regulation of developmental myelination. Nat Commun 9, 2840. https://doi.org/10.1038/s41467-018-04863-9.

Scheckel, C., Imeri, M., Schwarz, P., Aguzzi, A., 2020. Ribosomal profiling during prion disease uncovers progressive translational derangement in glia but not in neurons. eLife 9. https://doi.org/10.7554/eLife.62911.
Schimanski, L.A., Barnes, C.A., 2010. Neural Protein Synthesis during Aging: Effects on Plasticity and Memory. Frontiers in aging neuroscience 2. https://doi.org/10.3389/fnagi.2010.00026.
Schriner, S.E., Linford, N.J., Martin, G.M., Treuting, P., Ogburn, C.E., Emond, M., Coskun, P.E., Ladiges, W., Wolf, N., van Remmen, H., Wallace, D.C., Rabinovitch, P.S., 2005. Extension of murine life span by overexpression of catalase targeted to mitochondria. Science (New York, N.Y.) 308, 1909–1911. https://doi.org/10.1126/science.1106653.
Schuitemaker, A., van der Doef, T.F., Boellaard, R., van der Flier, W.M., Yaqub, M., Windhorst, A.D., Barkhof, F., Jonker, C., Kloet, R.W., Lammertsma, A.A., Scheltens, P., van Berckel, B.N.M., 2012. Microglial activation in healthy aging. Neurobiology of aging 33, 1067–1072. https://doi.org/10.1016/j.neurobiolaging.2010.09.016.
Schulz, T.J., Zarse, K., Voigt, A., Urban, N., Birringer, M., Ristow, M., 2007. Glucose restriction extends Caenorhabditis elegans life span by inducing mitochondrial respiration and increasing oxidative stress. Cell Metabolism 6, 280–293. https://doi.org/10.1016/j.cmet.2007.08.011.
Sepe, S., Milanese, C., Gabriels, S., Derks, K.W.J., Payan-Gomez, C., van IJcken, W.F.J., Rijksen, Y.M.A., Nigg, A.L., Moreno, S., Cerri, S., Blandini, F., Hoeijmakers, J.H.J., Mastroberardino, P.G., 2016. Inefficient DNA Repair Is an Aging-Related Modifier of Parkinson's Disease. Cell reports 15, 1866–1875. https://doi.org/10.1016/j.celrep.2016.04.071.
Sertel, S.M., Elling-Tammen, M.S. von, Rizzoli, S.O., 2021. The mRNA-Binding Protein RBM3 Regulates Activity Patterns and Local Synaptic Translation in Cultured Hippocampal Neurons. J. Neurosci. 41, 1157–1173. https://doi.org/10.1523/JNEUROSCI.0921-20.2020.
Shang, F., Deng, G., Liu, Q., Guo, W., Haas, A.L., Crosas, B., Finley, D., Taylor, A., 2005. Lys6-modified ubiquitin inhibits ubiquitin-dependent protein degradation. The Journal of biological chemistry 280, 20365–20374. https://doi.org/10.1074/jbc.M414356200.
Sharma, K., Schmitt, S., Bergner, C.G., Tyanova, S., Kannaiyan, N., Manrique-Hoyos, N., Kongi, K., Cantuti, L., Hanisch, U.-K., Philips, M.-A., Rossner, M.J., Mann, M., Simons, M., 2015. Cell type- and brain region-resolved mouse brain proteome. Nat Neurosci 18, 1819–1831. https://doi.org/10.1038/nn.4160.
Shen, C., Honda, H., Suzuki, S.O., Maeda, N., Shijo, M., Hamasaki, H., Sasagasako, N., Fujii, N., Iwaki, T., 2018. Dynactin is involved in Lewy body pathology. Neuropathology : official journal of the Japanese Society of Neuropathology 38, 583–590. https://doi.org/10.1111/neup.12512.
Sherwin, B.B., Henry, J.F., 2008. Brain aging modulates the neuroprotective effects of estrogen on selective aspects of cognition in women: a critical review. Frontiers in Neuroendocrinology 29, 88–113. https://doi.org/10.1016/j.yfrne.2007.08.002.
Shimada, A., Hasegawa-Ishii, S., 2011. Senescence-accelerated Mice (SAMs) as a Model for Brain Aging and Immunosenescence. Aging and disease 2, 414–435.
Shimada, A., Keino, H., Satoh, M., Kishikawa, M., Hosokawa, M., 2003. Age-related loss of synapses in the frontal cortex of SAMP10 mouse: a model of cerebral degeneration. Synapse (New York, N.Y.) 48, 198–204. https://doi.org/10.1002/syn.10209.
Shimura, H., Schlossmacher, M.G., Hattori, N., Frosch, M.P., Trockenbacher, A., Schneider, R., Mizuno, Y., Kosik, K.S., Selkoe, D.J., 2001. Ubiquitination of a new form of alpha-synuclein by parkin from human brain: implications for Parkinson's disease. Science (New York, N.Y.) 293, 263–269. https://doi.org/10.1126/science.1060627.
Shinitzky, M., 1987. Patterns of lipid changes in membranes of the aged brain. Gerontology 33, 149–154. https://doi.org/10.1159/000212868.
Sierra, A., Gottfried-Blackmore, A.C., McEwen, B.S., Bulloch, K., 2007. Microglia derived from aging mice exhibit an altered inflammatory profile. Glia 55, 412–424. https://doi.org/10.1002/glia.20468.
Sim, F.J., Zhao, C., Penderis, J., Franklin, R.J.M., 2002. The age-related decrease in CNS remyelination efficiency is attributable to an impairment of both oligodendrocyte progenitor recruitment and differentiation. The Journal of neuroscience: the official journal of the Society for Neuroscience 22, 2451–2459.
Simons, M., Kramer, E.-M., Macchi, P., Rathke-Hartlieb, S., Trotter, J., Nave, K.-A., Schulz, J.B., 2002. Overexpression of the myelin proteolipid protein leads to accumulation of cholesterol and proteolipid protein in endosomes/lysosomes: implications for Pelizaeus-Merzbacher disease. Journal of Cell Biology 157, 327–336. https://doi.org/10.1083/jcb.200110138.
Singh, K., Lilleväli, K., Gilbert, S.F., Bregin, A., Narvik, J., Jayaram, M., Rahi, M., Innos, J., Kaasik, A., Vasar, E., Philips, M.-A., 2018. The combined impact of IgLON family proteins Lsamp and Neurotrimin on

developing neurons and behavioral profiles in mouse. Brain research bulletin 140, 5–18. https://doi.org/10.1016/j.brainresbull.2018.03.013.
Smidak, R., Sialana, F.J., Kristofova, M., Stojanovic, T., Rajcic, D., Malikovic, J., Feyissa, D.D., Korz, V., Hoeger, H., Wackerlig, J., Mechtcheriakova, D., Lubec, G., 2017. Reduced Levels of the Synaptic Functional Regulator FMRP in Dentate Gyrus of the Aging Sprague-Dawley Rat. Frontiers in aging neuroscience 9, 384, 384. https://doi.org/10.3389/fnagi.2017.00384.
Smith, D.L., Elam, C.F., Mattison, J.A., Lane, M.A., Roth, G.S., Ingram, D.K., Allison, D.B., 2010. Metformin supplementation and life span in Fischer-344 rats. The Journals of Gerontology Series A: Biological Sciences and Medical Sciences 65, 468–474. https://doi.org/10.1093/gerona/glq033.
Smith, R., Cook, J., Dickens, P.A., 1984. Structure of the proteolipid protein extracted from bovine central nervous system myelin with nondenaturing detergents. J. Neurochem. 42, 306–313. https://doi.org/10.1111/j.1471-4159.1984.tb02679.x.
Snell, G.D., 1929. DWARF, A NEW MENDELIAN RECESSIVE CHARACTER OF THE HOUSE MOUSE. Proceedings of the National Academy of Sciences of the United States of America 15, 733–734. https://doi.org/10.1073/pnas.15.9.733.
Song, Y., Hao, Y., Sun, A., Li, T., Li, W., Guo, L., Yan, Y., Geng, C., Chen, N., Zhong, F., Wei, H., Jiang, Y., He, F., 2006. Sample preparation project for the subcellular proteome of mouse liver. Proteomics 6, 5269–5277. https://doi.org/10.1002/pmic.200500893.
Sörensen, L., Ekstrand, M., Silva, J.P., Lindqvist, E., Xu, B., Rustin, P., Olson, L., Larsson, N.G., 2001. Late-onset corticohippocampal neurodepletion attributable to catastrophic failure of oxidative phosphorylation in MILON mice. The Journal of neuroscience: the official journal of the Society for Neuroscience 21, 8082–8090.
Soreq, L., Rose, J., Soreq, E., Hardy, J., Trabzuni, D., Cookson, M.R., Smith, C., Ryten, M., Patani, R., Ule, J., 2017. Major Shifts in Glial Regional Identity Are a Transcriptional Hallmark of Human Brain Aging. Cell reports 18, 557–570. https://doi.org/10.1016/j.celrep.2016.12.011.
Souder, D.C., Anderson, R.M., 2019. An expanding GSK3 network: implications for aging research. GeroScience 41, 369–382. https://doi.org/10.1007/s11357-019-00085-z.
Souza, M.M. de, Zerlotini, A., Geistlinger, L., Tizioto, P.C., Taylor, J.F., Rocha, M.I.P., Diniz, W.J.S., Coutinho, L.L., Regitano, L.C.A., 2018. A comprehensive manually-curated compendium of bovine transcription factors. Scientific reports 8, 13747. https://doi.org/10.1038/s41598-018-32146-2.
Speisman, R.B., Kumar, A., Rani, A., Foster, T.C., Ormerod, B.K., 2013. Daily exercise improves memory, stimulates hippocampal neurogenesis and modulates immune and neuroimmune cytokines in aging rats. Brain, Behavior, and Immunity 28, 25–43. https://doi.org/10.1016/j.bbi.2012.09.013.
Sperling, R., Mormino, E., Johnson, K., 2014. The Evolution of Preclinical Alzheimer's Disease: Implications for Prevention Trials. Neuron 84, 608–622. https://doi.org/10.1016/j.neuron.2014.10.038.
Stadlmann, J., Hudecz, O., Krššáková, G., Ctortecka, C., van Raemdonck, G., Beeck, J. op de, Desmet, G., Penninger, J.M., Jacobs, P., Mechtler, K., 2019. Improved Sensitivity in Low-Input Proteomics Using Micropillar Array-Based Chromatography. Anal. Chem. 91, 14203–14207. https://doi.org/10.1021/acs.analchem.9b02899.
Steiner, J.L., Murphy, E.A., McClellan, J.L., Carmichael, M.D., Davis, J.M., 2011. Exercise training increases mitochondrial biogenesis in the brain. Journal of applied physiology (Bethesda, Md. : 1985) 111, 1066–1071. https://doi.org/10.1152/japplphysiol.00343.2011.
Stichel, C.C., Luebbert, H., 2007. Inflammatory processes in the aging mouse brain: participation of dendritic cells and T-cells. Neurobiology of aging 28, 1507–1521. https://doi.org/10.1016/j.neurobiolaging.2006.07.022.
Stranahan, A.M., Lee, K., Becker, K.G., Zhang, Y., Maudsley, S., Martin, B., Cutler, R.G., Mattson, M.P., 2010. Hippocampal gene expression patterns underlying the enhancement of memory by running in aged mice. Neurobiology of aging 31, 1937–1949. https://doi.org/10.1016/j.neurobiolaging.2008.10.016.
Sulzer, D., Mosharov, E., Talloczy, Z., Zucca, F.A., Simon, J.D., Zecca, L., 2008. Neuronal pigmented autophagic vacuoles: lipofuscin, neuromelanin, and ceroid as macroautophagic responses during aging and disease. Journal of neurochemistry 106, 24–36. https://doi.org/10.1111/j.1471-4159.2008.05385.x.
Swanton, E., Holland, A., High, S., Woodman, P., 2005. Disease-associated mutations cause premature oligomerization of myelin proteolipid protein in the endoplasmic reticulum. Proceedings of the National Academy of Sciences of the United States of America 102, 4342–4347. https://doi.org/10.1073/pnas.0407287102.
Szklarczyk, D., Gable, A.L., Lyon, D., Junge, A., Wyder, S., Huerta-Cepas, J., Simonovic, M., Doncheva, N.T., Morris, J.H., Bork, P., Jensen, L.J., Mering, C.v., 2019. STRING v11: protein-protein association networks

with increased coverage, supporting functional discovery in genome-wide experimental datasets. Nucleic acids research 47, D607-D613. https://doi.org/10.1093/nar/gky1131.
Takeda, T., 2009. Senescence-accelerated mouse (SAM) with special references to neurodegeneration models, SAMP8 and SAMP10 mice. Neurochemical research 34, 639–659. https://doi.org/10.1007/s11064-009-9922-y.
Takeda, T., Hosokawa, M., Takeshita, S., Irino, M., Higuchi, K., Matsushita, T., Tomita, Y., Yasuhira, K., Hamamoto, H., Shimizu, K., Ishii, M., Yamamuro, T., 1981. A new murine model of accelerated senescence. Mechanisms of ageing and development 17, 183–194.
Teoh, J., Subramanian, N., Pero, M.E., Bartolini, F., Amador, A., Kanber, A., Williams, D., Petri, S., Yang, M., Allen, A.S., Beal, J., Haut, S.R., Frankel, W.N., 2020. Arfgef1 haploinsufficiency in mice alters neuronal endosome composition and decreases membrane surface postsynaptic GABAA receptors. Neurobiology of disease 134, 104632. https://doi.org/10.1016/j.nbd.2019.104632.
Terman, A., Brunk, U.T., 1998. Lipofuscin: mechanisms of formation and increase with age. APMIS : acta pathologica, microbiologica, et immunologica Scandinavica 106, 265–276.
Thayer, J.A., Awad, O., Hegdekar, N., Sarkar, C., Tesfay, H., Burt, C., Zeng, X., Feldman, R.A., Lipinski, M.M., 2020. The PARK10 gene USP24 is a negative regulator of autophagy and ULK1 protein stability. Autophagy 16, 140–153. https://doi.org/10.1080/15548627.2019.1598754.
Tran, J.R., Chen, H., Zheng, X., Zheng, Y., 2016. Lamin in inflammation and aging. Current Opinion in Cell Biology 40, 124–130. https://doi.org/10.1016/j.ceb.2016.03.004.
Treaster, S.B., Ridgway, I.D., Richardson, C.A., Gaspar, M.B., Chaudhuri, A.R., Austad, S.N., 2014. Superior proteome stability in the longest lived animal. Age (Dordrecht, Netherlands) 36, 9597. https://doi.org/10.1007/s11357-013-9597-9.
Trifunovic, A., Wredenberg, A., Falkenberg, M., Spelbrink, J.N., Rovio, A.T., Bruder, C.E., Bohlooly-Y, M., Gidlöf, S., Oldfors, A., Wibom, R., Törnell, J., Jacobs, H.T., Larsson, N.-G., 2004. Premature ageing in mice expressing defective mitochondrial DNA polymerase. Nature 429, 417–423. https://doi.org/10.1038/nature02517.
Uylings, H.B.M., Brabander, J.M. de, 2002. Neuronal changes in normal human aging and Alzheimer's disease. Brain and cognition 49, 268–276.
Varela, I., Cadiñanos, J., Pendás, A.M., Gutiérrez-Fernández, A., Folgueras, A.R., Sánchez, L.M., Zhou, Z., Rodríguez, F.J., Stewart, C.L., Vega, J.A., Tryggvason, K., Freije, J.M.P., López-Otín, C., 2005. Accelerated ageing in mice deficient in Zmpste24 protease is linked to p53 signalling activation. Nature 437, 564–568. https://doi.org/10.1038/nature04019.
Vermeij, W.P., Hoeijmakers, J.H.J., Pothof, J., 2016. Genome Integrity in Aging: Human Syndromes, Mouse Models, and Therapeutic Options. Annual review of pharmacology and toxicology 56, 427–445. https://doi.org/10.1146/annurev-pharmtox-010814-124316.
Vesa, J., Hellsten, E., Verkruyse, L.A., Camp, L.A., Rapola, J., Santavuori, P., Hofmann, S.L., Peltonen, L., 1995. Mutations in the palmitoyl protein thioesterase gene causing infantile neuronal ceroid lipofuscinosis. Nature 376, 584–587. https://doi.org/10.1038/376584a0.
Vijayakumaran, S., Pountney, D.L., 2018. SUMOylation, aging and autophagy in neurodegeneration. Neurotoxicology 66, 53–57. https://doi.org/10.1016/j.neuro.2018.02.015.
Vilchez, D., Boyer, L., Morantte, I., Lutz, M., Merkwirth, C., Joyce, D., Spencer, B., Page, L., Masliah, E., Berggren, W.T., Gage, F.H., Dillin, A., 2012. Increased proteasome activity in human embryonic stem cells is regulated by PSMD11. Nature 489, 304. https://doi.org/10.1038/nature11468.
Virok, D.P., Simon, D., Bozsó, Z., Rajkó, R., Datki, Z., Bálint, É., Szegedi, V., Janáky, T., Penke, B., Fülöp, L., 2011. Protein array based interactome analysis of amyloid-β indicates an inhibition of protein translation. J. Proteome Res. 10, 1538–1547. https://doi.org/10.1021/pr1009096.
Vogel, C., Marcotte, E.M., 2012. Insights into the regulation of protein abundance from proteomic and transcriptomic analyses. Nat Rev Genet 13, 227–232. https://doi.org/10.1038/nrg3185.
Voytik, E., Bludau, I., Willems, S., Hansen, F.M., Brunner, A.-D., Strauss, M.T., Mann, M., 2021. AlphaMap: an open-source python package for the visual annotation of proteomics data with sequence specific knowledge. Bioinformatics (Oxford, England), btab674. https://doi.org/10.1093/bioinformatics/btab674.
Waard, M.C. de, van der Pluijm, I., Zuiderveen Borgesius, N., Comley, L.H., Haasdijk, E.D., Rijksen, Y., Ridwan, Y., Zondag, G., Hoeijmakers, J.H.J., Elgersma, Y., Gillingwater, T.H., Jaarsma, D., 2010. Age-related motor neuron degeneration in DNA repair-deficient Ercc1 mice. Acta neuropathologica 120, 461–475. https://doi.org/10.1007/s00401-010-0715-9.
Walther, D.M., Mann, M., 2011. Accurate quantification of more than 4000 mouse tissue proteins reveals minimal proteome changes during aging. Molecular & cellular proteomics : MCP 10, M110.004523. https://doi.org/10.1074/mcp.M110.004523.

Wang, S., Wang, T., Liu, T., Xie, R.-G., Zhao, X.-H., Wang, L., Yang, Q., Jia, L.-T., Han, J., 2020. Ermin is a p116RIP -interacting protein promoting oligodendroglial differentiation and myelin maintenance. Glia 68, 2264–2276. https://doi.org/10.1002/glia.23838.

Ward, W.F., 2000. The relentless effects of the aging process on protein turnover. Biogerontology 1, 195–199. https://doi.org/10.1023/a:1010076818119.

Warren, L.A., Rossi, D.J., Schiebinger, G.R., Weissman, I.L., Kim, S.K., Quake, S.R., 2007. Transcriptional instability is not a universal attribute of aging. Aging cell 6, 775–782. https://doi.org/10.1111/j.1474-9726.2007.00337.x.

Whittemore, K., Derevyanko, A., Martinez, P., Serrano, R., Pumarola, M., Bosch, F., Blasco, M.A., 2019. Telomerase gene therapy ameliorates the effects of neurodegeneration associated to short telomeres in mice. Aging 11, 2916–2948. https://doi.org/10.18632/aging.101982.

Wood, S.H., Craig, T., Li, Y., Merry, B., Magalhães, J.P. de, 2013. Whole transcriptome sequencing of the aging rat brain reveals dynamic RNA changes in the dark matter of the genome. Age (Dordrecht, Netherlands) 35, 763–776. https://doi.org/10.1007/s11357-012-9410-1.

Wood, S.H., van Dam, S., Craig, T., Tacutu, R., O'Toole, A., Merry, B.J., Magalhães, J.P. de, 2015. Transcriptome analysis in calorie-restricted rats implicates epigenetic and post-translational mechanisms in neuroprotection and aging. Genome biology 16, 285. https://doi.org/10.1186/s13059-015-0847-2.

Woodruff-Pak, D.S., 2006. Stereological estimation of Purkinje neuron number in C57BL/6 mice and its relation to associative learning. Neuroscience 141, 233–243. https://doi.org/10.1016/j.neuroscience.2006.03.070.

Woodruff-Pak, D.S., Foy, M.R., Akopian, G.G., Lee, K.H., Zach, J., Nguyen, K.P.T., Comalli, D.M., Kennard, J.A., Agelan, A., Thompson, R.F., 2010. Differential effects and rates of normal aging in cerebellum and hippocampus. Proceedings of the National Academy of Sciences of the United States of America 107, 1624–1629. https://doi.org/10.1073/pnas.0914207107.

Xiao, H., Jedrychowski, M.P., Schweppe, D.K., Huttlin, E.L., Yu, Q., Heppner, D.E., Li, J., Long, J., Mills, E.L., Szpyt, J., He, Z., Du, G., Garrity, R., Reddy, A., Vaites, L.P., Paulo, J.A., Zhang, T., Gray, N.S., Gygi, S.P., Chouchani, E.T., 2020. A Quantitative Tissue-Specific Landscape of Protein Redox Regulation during Aging. Cell 180, 968-983.e24. https://doi.org/10.1016/j.cell.2020.02.012.

Xie, X., Guo, P., Yu, H., Wang, Y., Chen, G., 2018. Ribosomal proteins: insight into molecular roles and functions in hepatocellular carcinoma. Oncogene 37, 277–285. https://doi.org/10.1038/onc.2017.343.

Ximerakis, M., Lipnick, S.L., Innes, B.T., Simmons, S.K., Adiconis, X., Dionne, D., Mayweather, B.A., Nguyen, L., Niziolek, Z., Ozek, C., Butty, V.L., Isserlin, R., Buchanan, S.M., Levine, S.S., Regev, A., Bader, G.D., Levin, J.Z., Rubin, L.L., 2019. Single-cell transcriptomic profiling of the aging mouse brain. Nat Neurosci 22, 1696–1708. https://doi.org/10.1038/s41593-019-0491-3.

Yan, J., Zhang, P., Jiao, F., Wang, Q., He, F., Zhang, Q., Zhang, Z., Lv, Z., Peng, X., Cai, H., Tian, B., 2017. Quantitative proteomics in A30P*A53T α-synuclein transgenic mice reveals upregulation of Sel1l. PloS one 12, e0182092. https://doi.org/10.1371/journal.pone.0182092.

Yan, X.-X., Jeromin, A., Jeromin, A., 2012. Spectrin Breakdown Products (SBDPs) as Potential Biomarkers for Neurodegenerative Diseases. Curr Tran Geriatr Exp Gerontol Rep 1, 85–93. https://doi.org/10.1007/s13670-012-0009-2.

Yang, S.H., Procaccia, S., Jung, H.-J., Nobumori, C., Tatar, A., Tu, Y., Bayguinov, Y.R., Hwang, S.J., Tran, D., Ward, S.M., Fong, L.G., Young, S.G., 2015. Mice that express farnesylated versions of prelamin A in neurons develop achalasia. Human molecular genetics 24, 2826–2840. https://doi.org/10.1093/hmg/ddv043.

Yankner, B.A., Lu, T., Loerch, P., 2008. The aging brain. Annual review of pathology 3, 41–66. https://doi.org/10.1146/annurev.pathmechdis.2.010506.092044.

Yi, M., Ma, Y., Chen, Y., Liu, C., Wang, Q., Deng, H., 2020. Glutathionylation Decreases Methyltransferase Activity of PRMT5 and Inhibits Cell Proliferation. Molecular & cellular proteomics: MCP 19, 1910–1920. https://doi.org/10.1074/mcp.RA120.002132.

Ypsilanti, A.R., Girão da Cruz, M.T., Burgess, A., Aubert, I., 2008. The length of hippocampal cholinergic fibers is reduced in the aging brain. Neurobiology of aging 29, 1666–1679. https://doi.org/10.1016/j.neurobiolaging.2007.04.001.

Yu, Q., Xiao, H., Jedrychowski, M.P., Schweppe, D.K., Navarrete-Perea, J., Knott, J., Rogers, J., Chouchani, E.T., Gygi, S.P., 2020. Sample multiplexing for targeted pathway proteomics in aging mice. Proceedings of the National Academy of Sciences of the United States of America 117, 9723–9732. https://doi.org/10.1073/pnas.1919410117.

Yu, Y., Tencer, A., Xuan, H., Kutateladze, T.G., Shi, X., 2021. ZZEF1 is a Histone Reader and Transcriptional Coregulator of Krüppel-Like Factors. Journal of molecular biology 433, 166722. https://doi.org/10.1016/j.jmb.2020.11.021.

Yu, Z.F., Mattson, M.P., 1999. Dietary restriction and 2-deoxyglucose administration reduce focal ischemic brain damage and improve behavioral outcome: evidence for a preconditioning mechanism. Journal of neuroscience research 57, 830–839.

Yuan, A., Rao, M.V., Veeranna, Nixon, R.A., 2017. Neurofilaments and Neurofilament Proteins in Health and Disease. Cold Spring Harb Perspect Biol 9, a018309. https://doi.org/10.1101/cshperspect.a018309.

Yuan, A., Sasaki, T., Kumar, A., Peterhoff, C.M., Rao, M.V., Liem, R.K., Julien, J.-P., Nixon, R.A., 2012. Peripherin is a subunit of peripheral nerve neurofilaments: implications for differential vulnerability of CNS and peripheral nervous system axons. J. Neurosci. 32, 8501–8508. https://doi.org/10.1523/JNEUROSCI.1081-12.2012.

Yuan, A., Sershen, H., Veeranna, Basavarajappa, B.S., Kumar, A., Hashim, A., Berg, M., Lee, J.-H., Sato, Y., Rao, M.V., Mohan, P.S., Dyakin, V., Julien, J.-P., Lee, V.M.-Y., Nixon, R.A., 2015. Neurofilament subunits are integral components of synapses and modulate neurotransmission and behavior in vivo. Molecular psychiatry 20, 986–994. https://doi.org/10.1038/mp.2015.45.

Yuan, R., Tsaih, S.-W., Petkova, S.B., Marin de Evsikova, C., Xing, S., Marion, M.A., Bogue, M.A., Mills, K.D., Peters, L.L., Bult, C.J., Rosen, C.J., Sundberg, J.P., Harrison, D.E., Churchill, G.A., Paigen, B., 2009. Aging in inbred strains of mice: Study design and interim report on median lifespans and circulating IGF1 levels. Aging cell 8, 277–287. https://doi.org/10.1111/j.1474-9726.2009.00478.x.

Yun, C., Stanhill, A., Yang, Y., Zhang, Y., Haynes, C.M., Xu, C.-F., Neubert, T.A., Mor, A., Philips, M.R., Ron, D., 2008. Proteasomal adaptation to environmental stress links resistance to proteotoxicity with longevity in Caenorhabditis elegans. PNAS 105, 7094–7099. https://doi.org/10.1073/pnas.0707025105.

Zaghlool, A., Ameur, A., Nyberg, L., Halvardson, J., Grabherr, M., Cavelier, L., Feuk, L., 2013. Efficient cellular fractionation improves RNA sequencing analysis of mature and nascent transcripts from human tissues. BMC biotechnology 13, 99. https://doi.org/10.1186/1472-6750-13-99.

Zahn, J.M., Poosala, S., Owen, A.B., Ingram, D.K., Lustig, A., Carter, A., Weeraratna, A.T., Taub, D.D., Gorospe, M., Mazan-Mamczarz, K., Lakatta, E.G., Boheler, K.R., Xu, X., Mattson, M.P., Falco, G., Ko, M.S.H., Schlessinger, D., Firman, J., Kummerfeld, S.K., Wood, W.H., Zonderman, A.B., Kim, S.K., Becker, K.G., 2007. AGEMAP: A gene expression database for aging in mice. PLoS genetics 3, e201. https://doi.org/10.1371/journal.pgen.0030201.

Zaia, A., Piantanelli, L., 2000. Insulin receptors in the brain cortex of aging mice. Mechanisms of ageing and development 113, 227–232.

Zatorre, R.J., Fields, R.D., Johansen-Berg, H., 2012. Plasticity in gray and white: neuroimaging changes in brain structure during learning. neuro 15, 528–536. https://doi.org/10.1038/nn.3045.

Zecca, L., Gallorini, M., Schünemann, V., Trautwein, A.X., Gerlach, M., Riederer, P., Vezzoni, P., Tampellini, D., 2001. Iron, neuromelanin and ferritin content in the substantia nigra of normal subjects at different ages: consequences for iron storage and neurodegenerative processes. J. Neurochem. 76, 1766–1773. https://doi.org/10.1046/j.1471-4159.2001.00186.x.

Zecca, L., Youdim, M.B.H., Riederer, P., Connor, J.R., Crichton, R.R., 2004. Iron, brain ageing and neurodegenerative disorders. Nature reviews. Neuroscience 5, 863–873. https://doi.org/10.1038/nrn1537.

Zenobi, R., 2013. Single-Cell Metabolomics: Analytical and Biological Perspectives. Science 342, 1243259. https://doi.org/10.1126/science.1243259.

Zhang, M.J., Pisco, A.O., Darmanis, S., Zou, J., 2021. Mouse aging cell atlas analysis reveals global and cell type-specific aging signatures. eLife 10, e62293. https://doi.org/10.7554/eLife.62293.

Zhang, T., Tan, P., Wang, L., Jin, N., Li, Y., Zhang, L., Yang, H., Hu, Z., Zhang, L., Hu, C., Li, C., Qian, K., Zhang, C., Huang, Y., Li, K., Lin, H., Wang, D., 2017a. RNALocate: a resource for RNA subcellular localizations. Nucleic acids research 45, D135-D138. https://doi.org/10.1093/nar/gkw728.

Zhang, Y., Kim, M.S., Jia, B., Yan, J., Zuniga-Hertz, J.P., Han, C., Cai, D., 2017b. Hypothalamic stem cells control ageing speed partly through exosomal miRNAs. Nature 548, 52–57. https://doi.org/10.1038/nature23282.

Zhou, Q.-G., Liu, M.-Y., Lee, H.-W., Ishikawa, F., Devkota, S., Shen, X.-R., Jin, X., Wu, H.-Y., Liu, Z., Liu, X., Jin, X., Zhou, H.-H., Ro, E.J., Zhang, J., Zhang, Y., Lin, Y.-H., Suh, H., Zhu, D.-Y., 2017. Hippocampal TERT Regulates Spatial Memory Formation through Modulation of Neural Development. Stem cell reports 9, 543–556. https://doi.org/10.1016/j.stemcr.2017.06.014.

Zhou, W., He, Y., Rehman, A.U., Kong, Y., Hong, S., Ding, G., Yalamanchili, H.K., Wan, Y.-W., Paul, B., Wang, C., Gong, Y., Zhou, W., Liu, H., Dean, J., Scalais, E., O'Driscoll, M., Morton, J.E.V., Hou, X., Wu, Q., Tong, Q., Liu, Z., Liu, P., Xu, Y., Sun, Z., 2019. Loss of function of NCOR1 and NCOR2 impairs

memory through a novel GABAergic hypothalamus-CA3 projection. Nat Neurosci 22, 205–217. https://doi.org/10.1038/s41593-018-0311-1.
Zhou, X., Liao, W.-J., Liao, J.-M., Liao, P., Lu, H., 2015. Ribosomal proteins: functions beyond the ribosome. Journal of Molecular Cell Biology 7, 92–104. https://doi.org/10.1093/jmcb/mjv014.
Zhu, X., Yan, J., Bregere, C., Zelmer, A., Goerne, T., Kapfhammer, J.P., Guzman, R., Wellmann, S., 2019. RBM3 promotes neurogenesis in a niche-dependent manner via IMP2-IGF2 signaling pathway after hypoxic-ischemic brain injury. Nat Commun 10, 3983. https://doi.org/10.1038/s41467-019-11870-x.
Zhu, Y., Orre, L.M., Zhou Tran, Y., Mermelekas, G., Johansson, H.J., Malyutina, A., Anders, S., Lehtiö, J., 2020. DEqMS: A Method for Accurate Variance Estimation in Differential Protein Expression Analysis. Molecular & cellular proteomics: MCP 19, 1047–1057. https://doi.org/10.1074/mcp.TIR119.001646.
Ziegler, D.R., Ribeiro, L.C., Hagenn, M., Siqueira, I.R., Araujo, E., Torres, I.L.S., Gottfried, C., Netto, C.A., Goncalves, C.-A., 2003. Ketogenic diet increases glutathione peroxidase activity in rat hippocampus. Neurochemical research 28, 1793–1797.
Zimering, M.B., Delic, V., Citron, B.A., 2021. Gene Expression Changes in a Model Neuron Cell Line Exposed to Autoantibodies from Patients with Traumatic Brain Injury and/or Type 2 Diabetes. Mol Neurobiol 58, 4365–4375. https://doi.org/10.1007/s12035-021-02428-4.
Zullo, J.M., Drake, D., Aron, L., O'Hern, P., Dhamne, S.C., Davidsohn, N., Mao, C.-A., Klein, W.H., Rotenberg, A., Bennett, D.A., Church, G.M., Colaiácovo, M.P., Yankner, B.A., 2019. Regulation of lifespan by neural excitation and REST. Nature 574, 359–364. https://doi.org/10.1038/s41586-019-1647-8.

7 | List of abbreviations

AD	Alzheimer's Disease
AGE	advanced glycation end product
AIRAPL	arsenite-inducible RNA-associated protein-like
AMPK	5' adenosine monophosphate-activated protein kinase
APP	amyloid precursor protein
Aβ (42)	amyloid beta
BACE1	beta-secretase1
BDNF	brain-derived neurotrophic factor
BP	biological process
CAMK	calcium/calmodulin-dependent protein kinase
CC	cellular component
DDA	data dependent acquisition
DR	dietary restriction
ER	endoplasmic reticulum
FC	fold change
GABA	gamma-aminobutyric acid
GFAP	glial fibrillary protein
GH	growth hormone
GO	gene ontology
GWAS	genome-wide association study
HLB	hypotonic lysis buffer
HD	Huntington's Disease
HDAC	histone deacetylase
HGPS	Hutchinson-Gilford Progeria Syndrome
IGF(R)	insulin-like growth factor (receptor)
IL	interleukin
INF	interferon
IR	insulin receptor
KD	knock-down
KI	knock-in
KO	knock-out
LC-MS	liquid chromatography mass spectrometry
Lmna	prelamin-A/C
mCat	mitochondrial catalase
mtDNA	mitochondrial DNA
mTOR	mechanistic/mammalian target of rapamycin
NDD	neurodegenerative disease
ORA	overrepresentation analysis
padj	adjusted *p*-value
PD	Parkinson's Disease
PI3-K	phosphoinositide 3-kinase
PS(EN)1	presenilin-1
ROS	reactive oxygen species
SB	sucrose buffer
SAMP	senescence-accelerated mouse prone
SAMR	senescence-accelerated mouse resistant
SDS	sodium dodecyl sulfate
SP3	single-pot, solid-phase-enhanced sample-preparation
SUMO	small ubiquitin-like modifier
TCA	tricarboxylic acid cycle
Tg	transgenic
TGF	transforming growth factor
TNFα	tumor necrosis factor alpha
UCP2	uncoupling protein 2
UPR	unfolded protein response
WT	wildtype
ZFAND2B	zinc finger AN1-type containing 2b
ZMPSTE24	zinc metalloproteinase Ste24 homolog